Inaugural dissertation

for

obtaining the doctoral degree

of the

Combined Faculty of Mathematics, Engineering and Natural Sciences

of the

Ruprecht - Karls - University

Heidelberg

Presented by

M.Sc. Anna Hübenthal

born in: Tübingen, Germany

Oral examination: 08.05.2024

Influence of antimicrobial compounds and the RNA-binding protein RibR on the activity of B vitamin-responsive bacterial riboswitches

Referees: Prof. Dr. Matthias Mayer
Prof. Dr. Matthias Mack

Abstract

Riboswitches are RNA elements that modulate the expression of genes involved in essential metabolic pathways and occur mainly in the bacterial world. Binding of a specific small ligand to the aptamer domain of the riboswitch typically results in repression of the downstream genes, either by transcriptional termination or inhibition of translation. As riboswitches constitute widespread genetic control elements, they are auspicious novel targets for antibiotic substances. The fact that hardly any new, effective antibiotic groups have been discovered in recent decades poses a significant problem, especially regarding the spread of multi-resistant pathogens, such as those from the so called ESKAPE group (*Enterococcus faecium*, *Staphylococcus aureus*, *Klebsiella pneumoniae*, *Acinetobacter baumannii*, *Pseudomonas aeruginosa* and *Enterobacter* species).

In the first part of this study, thiamine pyrophosphate (TPP) riboswitches from relevant pathogenic strains were identified using a newly adapted dual-luciferase reporter gene assay. TPP riboswitches from the ESKAPE pathogens *Enterobacter* spp., *A. baumannii*, *P. aeruginosa*, *K. pneumoniae* and *E. faecium* as well as from the pathogens *Streptococcus pneumoniae* and *Mammaliicoccus sciuri* were experimentally validated. The experimental outcome shows that the functionality of some of these riboswitches is dependent on the upstream promoter region. In addition to the affirmation of their function as regulators of gene expression, the riboswitches were characterized by their mode of action using translational and transcriptional reporter gene fusions. The *thiE* TPP riboswitch from *M. sciuri* and the *thiBPQ* riboswitch from *Enterobacter* spp. exhibit translational regulation, while the *thiC* riboswitches from *P. aeruginosa* and *Enterobacter* spp. mainly operate *via* termination of transcription. For the *thiC* riboswitches from *A. baumannii*, *E. faecium* and *K. pneumoniae* a combined function of translation inhibition and transcriptional termination was found. Interestingly, none of the riboswitches examined in this study were affected by the antibiotic pyrithiamine, which is known to block the *E. coli thiC* riboswitch. The study of the *K. pneumoniae thiC* riboswitch identified several key nucleotides in the extended P3 stem region of the aptamer that are responsible for the non-responsiveness of the riboswitch to pyrithiamine pyrophosphate.

The second chapter of this study addresses the riboswitch-binding protein RibR. This protein was first described in *Bacillus subtilis* as a regulatory element of flavin mononucleotide (FMN) riboswitches and has two different functional parts. While the N-terminal part has flavokinase activity, the RNA-binding activity could be assigned to the C-terminal part of the protein. Expression of *ribR* in *B. subtilis* is induced by the presence of the sulfur sources methionine and taurine. The RibR protein of *B. subtilis* ($RibR_{sub}$) counteracts the effect of the ligand FMN

on FMN riboswitch activity, allowing expression of the downstream genes involved in riboflavin biosynthesis even in the presence of high FMN levels.

In *Bacillus amyloliquefaciens*, a truncated RibR-variant ($RibR_{amy}$) has been identified, which only consists of a putative RNA-binding domain. Electrophoretic mobility shift assays showed that $RibR_{amy}$, just like $RibR_{sub}$, binds both *ribD* FMN riboswitch aptamers from *B. subtilis* and *B. amyloliquefaciens*. CRISPR-Cas9 genome editing was used to generate *B. subtilis ribR* mutants expressing different versions of $ribR_{sub}$ and $ribR_{amy}$. Enzyme assays with cell-free extracts from these strains which allowed monitoring of the FMN riboswitch activity confirmed that $RibR_{amy}$ derepressed the FMN riboswitch even in the presence of FMN. This effect depends on two conserved arginine residues in the primary structures of the *B. subtilis* and *B. amyloliquefaciens* RibR proteins as shown by site directed mutagenesis experiments. Further results suggest a link between $RibR_{amy}$ and the response to oxidative stress in *B. amyloliquefaciens*.

Zusammenfassung

Sogenannte *riboswitches* sind RNA-Elemente, die die Expression von Genen modulieren, welche an wichtigen Stoffwechselwegen beteiligt sind und vor allem in Bakterien vorkommen. Die Bindung eines spezifischen Liganden an die Aptamer-Domäne des RNA-Schalters führt in der Regel zu einer Herunterregulierung der nachgeschalteten Gene, entweder durch Beendigung der Transkription oder durch Hemmung der Translation. Da diese RNA-Schalter weitverbreitete genetische Steuerungselemente darstellen, sind sie vielversprechende neue Ziele für antibiotische Substanzen. Die Tatsache, dass in den letzten Jahrzehnten kaum neue, wirksame Antibiotikagruppen entdeckt wurden, stellt ein erhebliches Problem dar, insbesondere im Hinblick auf die Ausbreitung multiresistenter Erreger, z. B. aus der sogenannten ESKAPE-Gruppe (*Enterococcus faecium*, *Staphylococcus aureus*, *Klebsiella pneumoniae*, *Acinetobacter baumannii*, *Pseudomonas aeruginosa* und *Enterobacter*-Spezies).

Im ersten Teil dieser Arbeit wurden Thiaminpyrophosphat (TPP)-Schalter von relevanten pathogenen Stämmen mit Hilfe eines neu angepassten *Dual-Luciferase* Reportergen-Assays identifiziert. Dabei wurden TPP abhängige RNA-Schalter der ESKAPE-Pathogene *Enterobacter* spp., *A. baumannii*, *P. aeruginosa*, *K. pneumoniae* und *E. faecium*, sowie der Pathogene *Streptococcus pneumoniae* und *Mammaliicoccus sciuri*, experimentell validiert. Die Ergebnisse der durchgeführten Experimente zeigen, dass die Funktionalität einiger dieser RNA-Schalter abhängig ist von der davorliegenden Promotorregion. Neben der Bestätigung ihrer Funktion als Regulatoren der Genexpression wurden die jeweiligen Wirkmechanismen dieser Schalter mit Hilfe von translationalen und transkriptionalen Reportergenfusionen charakterisiert. Der *thiE*-TPP-Schalter aus *M. sciuri* und der *thiBPQ*-Schalter aus *Enterobacter* spp. zeigen eine translationale Regulation, während die *thiC*-Schalter aus *P. aeruginosa* und *Enterobacter* spp. hauptsächlich über eine transkriptionale Termination wirken. Bei den *thiC*-RNA-Schaltern aus *A. baumannii, E. faecium* und *K. pneumoniae* wurde eine kombinierte Funktionsweise aus Translationshemmung und Termination der Transkription festgestellt. Interessanterweise wurde keiner der hier untersuchten RNA-Schalter durch die antibiotische Substanz Pyrithiamin beeinträchtigt, von der bekannt ist, dass sie den *thiC* RNA-Schalter aus *E. coli* blockiert. Bei der Untersuchung des *thiC*-RNA-Schalters aus *K. pneumoniae* wurden bestimmte Nukleotide im verlängerten P3-Arm der Aptamer-Region identifiziert, die für die fehlende Reaktion dieses RNA-Schalters auf Pyrithiaminpyrophosphat verantwortlich sind.

Der zweite Teil dieser Arbeit beschäftigt sich mit dem *riboswitch*-bindenden Protein RibR. Dieses Protein wurde in *Bacillus subtilis* als regulierender Faktor von FMN Riboschaltern beschrieben und besitzt zwei unterschiedlich funktionale Teile. Während der N-terminale Teil Flavokinase-Aktivität aufweist, konnte die RNA-Bindungsaktivität dem C-terminalen Teil des Proteins zugeordnet werden. Die Expression von *ribR* in *B. subtilis* wird durch die Anwesenheit

der Schwefelquellen Methionin und Taurin induziert. Das RibR-Protein aus *B. subtilis* ($RibR_{sub}$) wirkt dem Effekt des Liganden FMN auf die Aktivität des FMN-RNA-Schalters entgegen und ermöglicht die Expression der an der Riboflavin-Biosynthese beteiligten nachgeschalteten Gene auch in Gegenwart hoher FMN-Konzentrationen.

In *Bacillus amyloliquefaciens* wurde eine verkürzte RibR-Variante ($RibR_{amy}$) identifiziert, die nur aus einer mutmaßlichen RNA-Bindungsdomäne besteht. *Electrophoretic Mobility Shift Assays* zeigten, dass $RibR_{amy}$, genau wie $RibR_{sub}$, an die Aptamerregion der *ribD*-RNA-Schalter, sowohl aus *B. subtilis* als auch aus *B. amyloliquefaciens* bindet. Mithilfe von CRISPR-Cas9-Genom-Editierung wurden *B. subtilis ribR*-Mutanten erzeugt, die verschiedene Versionen von $ribR_{sub}$ und $ribR_{amy}$ exprimieren. Enzymtests mit zellfreien Extrakten dieser Stämme, die eine Messung der Aktivität der FMN-RNA-Schalter ermöglichten, bestätigten, dass $RibR_{amy}$ den FMN-RNA-Schalter auch in Gegenwart von FMN dereguliert.

Dieser Effekt hängt von zwei konservierte Arginin-Resten in den Primärstrukturen der RibR-Proteine von *B. subtilis* und *B. amyloliquefaciens* ab, wie durch gezielte Mutagenese-Experimente gezeigt wurde. Weitere Ergebnisse deuten auf einen Zusammenhang zwischen $RibR_{amy}$ und der Reaktion auf oxidativen Stress in *B. amyloliquefaciens* hin.

Table of content

List of Figures

Supplementary figures

List of Tables

Supplementary Tables

1 Introduction

1.1 Riboswitches

The regulatory mechanisms inside a bacterial cell are manifold. Speculations of messenger RNA (mRNA) acting as an active control element of gene expression, aside of its function as a transmission element for genetic information, came up more than 20 years ago (Gelfand *et al.*, 1999; Nahvi *et al.*, 2002). Soon, the first experimental evidence of RNA elements, so called riboswitches, which regulate the expression of genes involved in the synthesis of vitamin B_{12}, cobalamin, and vitamin B_1, thiamine, was provided (Nahvi *et al.*, 2002; Winkler, Nahvi, *et al.*, 2002). Riboswitches are noncoding RNA elements, mostly located in the 5'-untranslated region of some mRNAs. They consist of a 5'-sided aptamer domain and a downstream expression platform (Mandal and Breaker, 2004). The aptamer domain is highly conserved and carries a selective binding site for a specific small molecule. Binding of the respective ligand to the aptamer domain leads to a conformational change in the expression platform which then modulates the expression of the downstream gene (Barrick and Breaker, 2007).

To date, more than 55 different classes of riboswitches are known, of which nearly 40 have been experimentally validated (Kavita and Breaker, 2023). They are mostly found in bacteria but have also been reported to exist in plants (Sudarsan *et al.*, 2003), fungi (Kubodera *et al.*, 2003; Cheah *et al.*, 2007), algae (Croft *et al.*, 2007) and archaea (Speed *et al.*, 2018). The riboswitches identified so far can be divided into seven groups based on the respective ligand they bind. The biggest group comprises cofactors like thiamine pyrophosphate (TPP), flavin mononucleotide (FMN) or adenosylcobalamin (AdoCbl). Other ligand groups include RNA precursors and RNA derivatives, signaling molecules like c-di-GMP, amino acids, sugars, and elemental ions such as Mg^{2+} and fluoride (Salvail and Breaker, 2023).

Although the most abundant riboswitch classes have probably been discovered by now, it is believed that a large number of less common classes of riboswitches are still unidentified to date. However, the search for small noncoding RNAs is apparently quite difficult, especially in eukaryotes, and it is suspected that many classes will remain undiscovered (McCown *et al.*, 2017; Salvail and Breaker, 2023).

1.1.1 Control mechanisms of riboswitches

Upon binding of their respective ligand, most riboswitches act as OFF switches, meaning that they downregulate downstream gene expression (Panchal and Brenk, 2021; Salvail and Breaker, 2023). In these cases, riboswitches function as part of a negative feedback control mechanism. If the concentration of the specific metabolite reaches a certain threshold level

inside the cell, binding of the metabolite to the riboswitch represses genes involved in the synthesis or transport of this ligand (Serganov and Patel, 2012; Panchal and Brenk, 2021). Examples of this type of regulation include the TPP and FMN riboswitches in *Bacillus subtilis* (Mironov *et al.*, 2002). However, there are also several examples of riboswitches that act as ON switches, where ligand binding results in upregulation of the downstream genes. This mechanism was observed for guanidine (Nelson *et al.*, 2017), as well as fluoride riboswitches (Ren *et al.*, 2012).

In all cases, the ligand-binding domain of the respective riboswitch is highly conserved, which allows discrimination of the respective ligand against other molecules with similar structures and therefore ensures a tight regulation (Winkler and Breaker, 2003; Breaker, 2011). The high degree of conservation in riboswitch nucleotide sequences (Gelfand *et al.*, 1999) is complemented by various important motifs at the structural level (Xu *et al.*, 2023). These include, for example, pseudoknots (McDaniel *et al.*, 2005), K-turn motifs (Heppell and Lafontaine, 2008; Batey, 2011) and kissing-loop interactions (Blouin and Lafontaine, 2007; Lussier *et al.*, 2015).

Riboswitch aptamers typically bind their ligand with high affinities, with dissociation constants (K_D) in the nanomolar range (Garst *et al.*, 2011; Panchal and Brenk, 2021). However, regulation of gene expression in the actual cellular environment often appears to require ligand concentrations higher than the equilibrium K_D to achieve a half-maximal transcription termination (Garst *et al.*, 2011), for example for FMN, S-adenosyl methionine (SAM-I) and lysine riboswitches (Wickiser *et al.*, 2005; Blouin and Lafontaine, 2007; Tomšič *et al.*, 2008).

While most reported riboswitches consist of one aptamer domain and the accompanying expression platform, aptamer regions have also been reported to exist in tandem, which allows an even more fine-tuned regulation (Salvail and Breaker, 2023), observed for example for glycine riboswitches that contain two adjacent aptamers, which function cooperatively (Mandal *et al.*, 2004).

The expression platform of the riboswitch typically partly overlaps with the aptamer and is ultimately responsible for transferring the ligand-binding event into an actual change of downstream gene expression. Upon binding of the ligand, the changes in the RNA structure of the aptamer domain result in a conformational change of the expression platform (Garst *et al.*, 2011). In contrast to the highly conserved aptamer region, the expression platform exhibits greater diversity in sequence and structure, corresponding with the variety of regulatory mechanisms identified (Barrick and Breaker, 2007; Breaker, 2011).

Nevertheless, two general mechanisms are described by which the regulation of gene expression is achieved: termination of transcription and inhibition of translation (Serganov and Nudler, 2013) (Figure 1). For an OFF switch using a translational control mechanism, ligand binding to the aptamer domain causes an alternative folding of the expression platform that

sequesters the ribosomal binding site. This renders the binding site inaccessible to the ribosomal complex, thus preventing translation of downstream genes (Figure 1B). In case of the transcriptional regulation, binding of a ligand will lead to formation of a terminator stem, which prevents transcription by the RNA polymerase (Figure 1A).

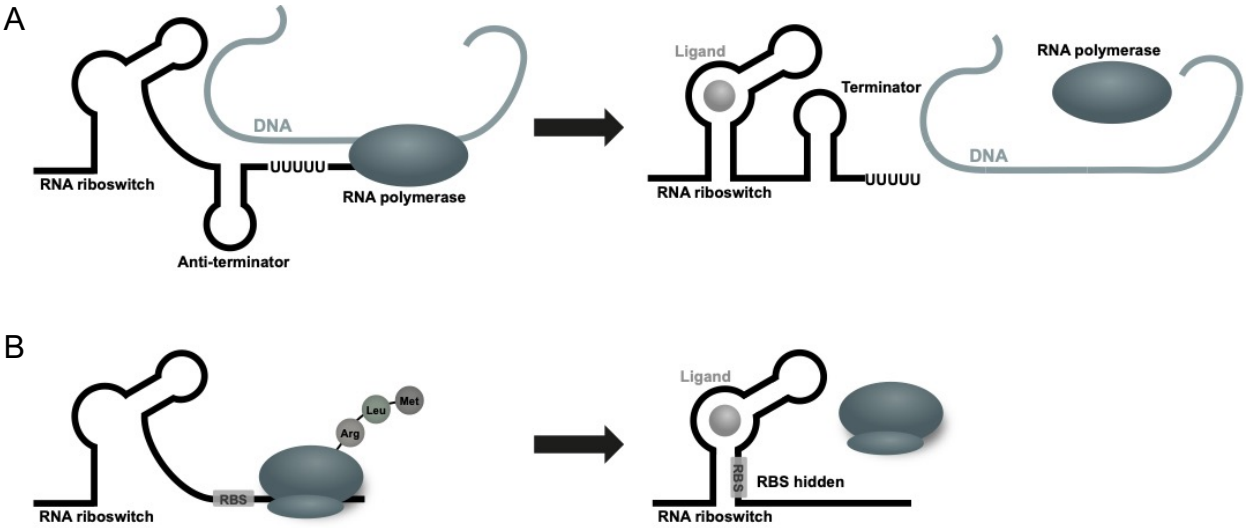

Figure 1: Riboswitch regulation of downstream gene expression upon ligand binding. (A) Via formation of a transcriptional terminator and (B) via sequestration of the ribosomal binding site (RBS). The figures were adapted from https://2015.igem.org/Team:Exeter/RNA_Riboswitches.

For some riboswitches like the FMN riboswitch of *E. coli*, also a combined mechanism of transcriptional and translational control was observed (Pedrolli, Langer, *et al.*, 2015). Additionally, transcriptional pause sites within the riboswitch sequence were discussed to play an important role in gene regulation by riboswitches (Lemay *et al.*, 2011; Larson *et al.*, 2014; Chauvier *et al.*, 2017).

Furthermore, other mechanisms of riboswitch regulation have been reported. These include Rho-dependent transcription termination, where binding of a ligand to the aptamer provides access to a Rho-binding sequence (rut site) located in the riboswitch region (Hollands *et al.*, 2012; Bastet *et al.*, 2017; Chauvier *et al.*, 2017), self-cleavage of RNA (Winkler *et al.*, 2004; Lee *et al.*, 2010) and RNA destabilization (Richards 2021). While most riboswitches were described as *cis*-acting elements, some examples of riboswitches acting in *trans* have been reported as well (DebRoy *et al.*, 2014; Mellin *et al.*, 2014).

1.2 The thiamine pyrophosphate riboswitch

1.2.1 The riboswitch ligand thiamine pyrophosphate

One of the well-studied riboswitches is the TPP riboswitch, which binds thiamine pyrophosphate, the active form of vitamin B_1. Thiamine is an essential nutrient for animals and

humans. The vitamin is synthesized not only by microorganisms but also by fungi and plants (Jurgenson *et al.*, 2009; Rapala-Kozik, 2011). Thiamine pyrophosphate (TPP) was identified as a cocarboxylase and is an important cofactor for various enzymes involved in the carbohydrate and amino acid metabolism of a cell, including the transketolase, pyruvate dehydrogenase, and α-ketoglutarate dehydrogenase (Panchal and Brenk, 2021). TPP consists of an aminopyrimidine ring linked by a methylene bridge to a thiazole ring with two phosphate groups attached to it (Bunik *et al.*, 2013). In all organisms producing thiamine, first thiamine monophosphate is synthesized from two precursors, the thiazole moiety 4-methyl-5-(ß-hydroxyethyl) thiazole monophosphate (THZ-P) and the pyrimidine moiety 4-amino-5-hydroxymethyl-2-methylpyrimidine pyrophosphate (HMP-PP) (Begley *et al.*, 1999). The monophosphate is then further phosphorylated to thiamine pyrophosphate, either by direct phosphorylation or by dephosphorylation to thiamine and subsequent pyrophosphorylation (Spenser, White, 1997).

Figure 3 shows the essential steps of thiamine biosynthesis in *E. coli* and the most important enzymes involved. When thiamine itself is taken up by the bacterial cell, it is phosphorylated to TPP by the thiamine pyrophosphokinase ThiN (McCulloch *et al.*, 2008).

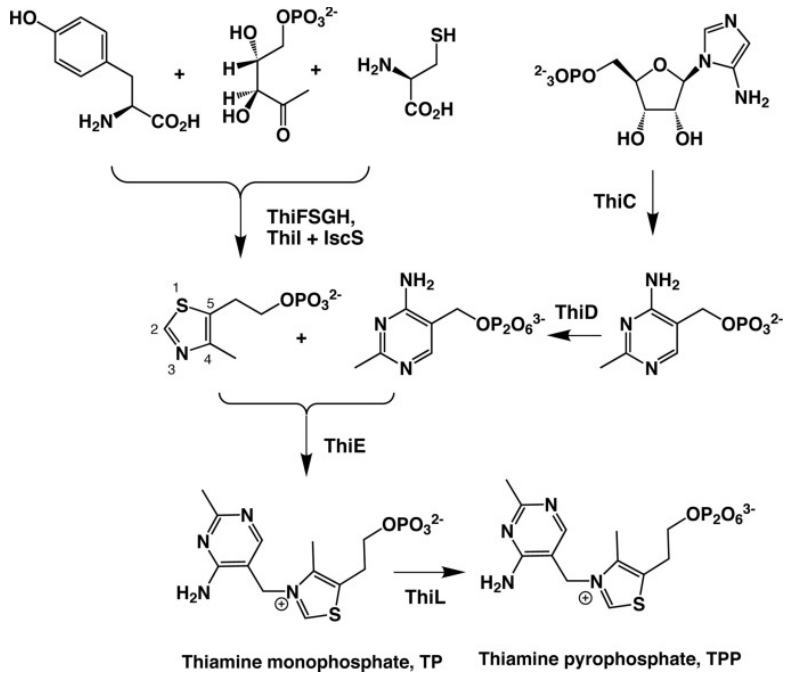

Figure 2: Essential steps of thiamine biosynthesis in *E. coli*. The figure was taken from Leonardi and Roach, 2004.

Most of the thiamine related genes in *E. coli* are organized in operons. Two operons exist with genes coding for thiamine synthesis proteins, the *thiC* operon *thiCEFGH* and the *thiM* operon *thiMD*. Additionally, one operon is built of three genes coding for a thiamine transport system,

thiBPQ (Begley *et al.*, 1999). The *E. coli thiC* and *thiM* riboswitches were two of the first TPP riboswitches experimentally validated (Winkler, Nahvi, *et al.*, 2002).

1.2.2 Distribution and conservation of TPP riboswitch sequences

The TPP riboswitch is the most widespread riboswitch known to date (Pavlova *et al.*, 2019; Kavita and Breaker, 2023). The initially so called *thi* box was identified in various bacterial species as a highly conserved, untranslated RNA leader in the 5' region of genes associated with thiamine synthesis and transport (Miranda-Ríos *et al.*, 1997). Miranda-Ríos *et al.* showed that the *thi* box of *Rhizobium etli* was involved in thiamine-dependent gene regulation. Furthermore, they already compared possible structures of the *thi* box regions and found them to be conserved among several bacterial species (Miranda-Ríos *et al.*, 2001). However, TPP riboswitches are not only found in bacteria, but are also present in various eukaryotic organisms like plants and fungi (Sudarsan *et al.*, 2003; Cheah *et al.*, 2007; Croft *et al.*, 2007). Especially the already mentioned *thiC* and *thiM* riboswitches of *E. coli* have been extensively studied, including detailed analyses of their structure and the ligand recognition (Winkler, Cohen-Chalamish, *et al.*, 2002; Edwards and Ferré-D'Amaré, 2006; Miranda-Ríos, 2007; Chen *et al.*, 2012; Bastet *et al.*, 2017).

1.2.3 Structure and ligand-binding of the TPP riboswitch

Structural analyses of the TPP riboswitch have revealed a complex, specifically folded structure with five double helical stems, P1-P5, junctions J2/4, J3/2, J4/5, J5/4 and the terminal loops L3 and L5 (Edwards and Ferré-D'Amaré, 2006; Serganov *et al.*, 2006) (Figure 3A). This secondary structure is very conserved (Edwards and Ferré-D'Amaré, 2006) and a similar folding is also observed for the eukaryotic TPP riboswitch from *Arabidopsis thaliana* (Thore *et al.*, 2006). Mainly, the helical domains are responsible for the binding of TPP by forming two binding pockets (Edwards and Ferré-D'Amaré, 2006; Serganov *et al.*, 2006). The P2 and P3 stems form a structure for sensing of the pyrimidine moiety and the P4/P5 regions bind the pyrophosphate groups (Figure 3B). Thereby, the TPP molecule is encapsulated and positioned vertically to the two helices, forming a bridge between the two domains. Several conserved nucleotides are most important for ligand binding. The HMP moiety intercalates between nucleotides G42 and A43 of the J3/2 region and forms additional hydrogen bonds with the polar parts of G19 and G40 (Serganov *et al.*, 2006).

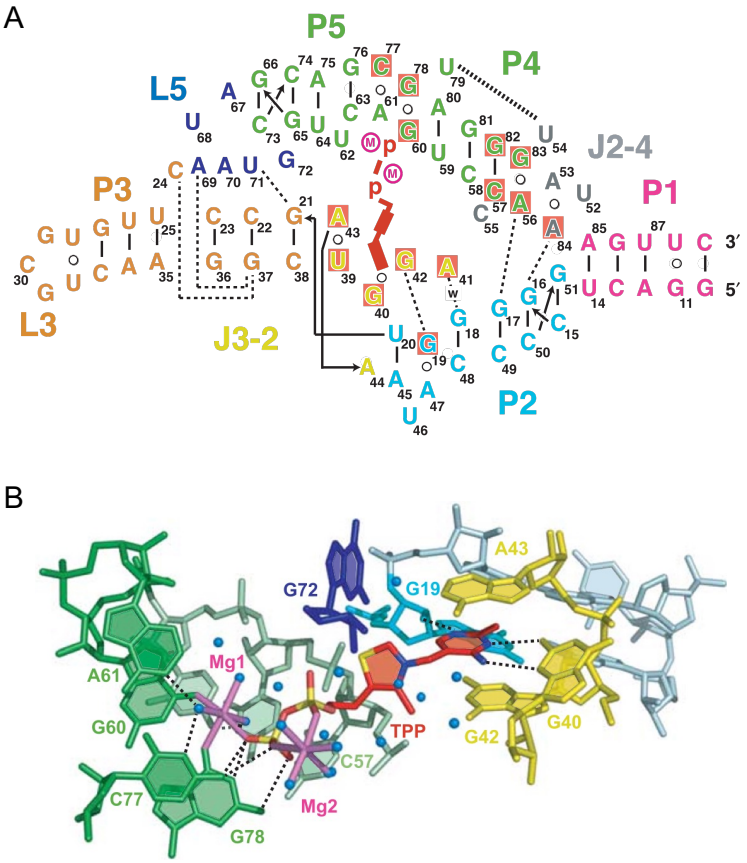

Figure 3: Structural model of (A) a TPP riboswitch and (B) the central region of the TPP-binding pocket. (A) The riboswitch bound TPP with its two phosphate groups (p) is shown in red. The tertiary contacts formed by hydrogen bonds between bases (thin dashed lines) and stacking interactions (thick dashed lines) are depicted. A 'w' represents a water-mediated bond. An encircled M represents a magnesium ion. Conserved nucleotides are highlighted in red. **(B)** The bound TPP is depicted together with the important nucleotides of the TPP-binding pocket. Mg1 and Mg2 are the coordinated magnesium ions, water is displayed as blue spheres. The figures and respective descriptions are adapted from Serganov *et al.*, 2006.

The pyrophosphate on the other hand is positioned in a pocket where it is coordinated to two magnesium ions. The oxygen of the terminal phosphate group forms direct and water-mediated hydrogen bonds with nucleotides C77 and G78 of the riboswitch (Ontiveros-Palacios *et al.*, 2008; Kulshina *et al.*, 2010). Additionally, one of the Mg^{2+} ions forms a bond with the O^6 carbonyls of the conserved nucleotide G60 (Serganov *et al.*, 2006). Some studies have also emphasized the importance of more distant conserved substructures for the overall folding and ligand binding, namely the P3-L5 interaction, which is not part of the actual TPP binding site (Lang *et al.*, 2007; Kulshina *et al.*, 2010).

The thiazole ring at the core of the TPP molecule appears to play a minor role in ligand recognition. It seems that this part of the molecule is only in hydrophobic contact with G72. However, a structural study with TPP, thiamine and several thiamine-analogues has shown that the G72 nucleotide plays an important role in the overall structural arrangement of the riboswitch (Deigan Warner *et al.*, 2014). An Rfam analysis of 115 TPP riboswitches showed a 99 % conservation rate of this residue (Burge *et al.*, 2013), underlying its relevance for the riboswitch.

The TPP riboswitch aptamer binds its specific ligand thiamine pyrophosphate with a dissociation constant in the low nanomolar range (Winkler, Nahvi, *et al.*, 2002; Aghdam *et al.*, 2017), but can also bind thiamine monophosphate (TMP) with lower affinity (Edwards and Ferré-D'Amaré, 2006). Several studies have also further examined the specificity of the riboswitch for its ligand and its binding to other structurally similar molecules (Cressina *et al.*, 2011; Chen *et al.*, 2012; Deigan Warner *et al.*, 2014; Lünse *et al.*, 2014)

1.3 Antimicrobial resistance and new antibiotic compounds

1.3.1 The increasing problem of antimicrobial resistance

The problem of increasing antibiotic resistance among pathogenic bacteria is well known and has been discussed intensively in the past years (González-Zorn and Escudero, 2012; Lee Ventola, 2015; Petchiappan and Chatterji, 2017; Uddin *et al.*, 2021; Aljeldah, 2022; Murray *et al.*, 2022). Antimicrobial resistance is considered a leading cause of human death worldwide. In 2019, 4.95 million deaths were associated with bacterial resistance, of which 1.27 million were attributable to it. The six leading pathogens responsible for these deaths were *E. coli*, *Staphylococcus aureus*, *Klebsiella pneumoniae*, *Streptococcus pneumoniae*, *Acinetobacter baumannii* and *Pseudo-monas aeruginosa*. Additional pathogens that are responsible for a considerable amount of deaths around the world and are listed by the World Health Organization (WHO) as critical or high priority are *Enterobacter* spp. and *Enterococcus faecium* (Murray *et al.*, 2022; World Health Organization, 2022). Special focus has been placed on a group of six of these potentially multiresistant species, the so called ESKAPE group of pathogens, namely comprising *E. faecium*, *S. aureus*, *K. pneumoniae*, *A. baumannii*, *P. aeruginosa* and *Enterobacter* spp. (Rice, 2008).

The main causes for the resistance of many pathogenic strains to the currently known antibiotics are over-prescription, misuse by patients and the common use in agricultural livestock farming (González-Zorn and Escudero, 2012). In addition to the improper use of existing antibiotics, the core of the problem is that no new classes of antibiotics have been discovered for a long time (Durand *et al.*, 2019; Aljeldah, 2022). Most of the newly approved antibiotic substances are derivatives of established classes like cephalosporins, fluoroquinolones or tetracyclines, against which multiple resistance mechanisms already exist (World Health Organization, 2022).

There are mainly five mechanisms how antibacterial agents target the cell. These include the interference with cell wall synthesis, disruption of the membrane structure, suppression of nucleic acid or protein synthesis, especially by targeting the bacterial ribosome, and inhibition of specific metabolic pathways and enzymes (Abushaheen *et al.*, 2020; Ellinger *et al.*, 2023). Bacteria have developed various resistance mechanisms against these modes of action.

These can be broadly grouped in reduced permeability or increased efflux of the substance, modification or inactivation of the molecule or a modulation of the target site of the antibiotic (Abushaheen *et al.*, 2020). All this underscores the urgent need to identify new targets for novel antibiotic substances.

1.4 Riboswitches as new antibiotic targets

Soon after the first riboswitches had been experimentally validated, their suitability as antibiotic targets was reviewed (Kaempfer, 2003; Winkler and Breaker, 2003; Zaman *et al.*, 2003). Several factors are discussed, which qualify them as potential drug targets. First, it is essential that riboswitches are important regulatory elements, involved in main metabolic pathways of bacteria, so that targeting of these RNA elements would interfere with crucial biochemical processes of the cell (Kaempfer, 2003; Blount and Breaker, 2006; Giarimoglou *et al.*, 2022). Furthermore, even though TPP riboswitches have been found in some eukaryotic genomes, so far, no riboswitches have been identified in mammals, thus not in humans, which should allow a specific targeting of the bacterial cells only and minimize the risk of side effects of the antibiotic compound on human cells (Ellinger *et al.*, 2023).

Generally, riboswitches are widely distributed amongst bacteria and the aptamer regions of the classes are highly conserved (Blount and Breaker, 2006; Pavlova and Penchovsky, 2019). The sequence conservation allows a rather straightforward *in silico* search for riboswitch aptamers in genomic databases and several classes of riboswitches have been identified in many human pathogens. Some of the most common riboswitches in human pathogenic bacteria are binding the ligands TPP, FMN and cobalamin, but also lysine, glucosamine-6-phosphate and glycine riboswitches are often found in various pathogenic species. Other riboswitch classes, however, seem to be more specific for certain bacterial groups (Pavlova and Penchovsky, 2019, 2022). This would provide the opportunity to, on the one hand, develop broad-spectrum antibiotics, targeting the widespread riboswitches, and narrow-spectrum antibiotics on the other hand, targeting the less distributed classes (Panchal and Brenk, 2021). Additional to the presence in relevant pathogens and the control of essential genes, to be pharmacologically relevant, a riboswitch must act as an OFF switch and possess a ligand pocket that has the necessary characteristics to bind potential drug molecules (Panchal and Brenk, 2021).

Generally, riboswitches constitute very selective ligand-receptors with a distinct secondary structure, which should make it possible to design highly selective antibiotic compounds (Blount and Breaker, 2006). To identify such compounds, the establishment of reliable high-throughput screenings that allow a fast screening of big molecule libraries would be necessary (Penchovsky and Stoilova, 2013). For the glucosamine-6-phosphate riboswitch from

S. aureus, for example, a high-throughput assay was developed for potential ligands, based on fluorescence resonance energy transfer (FRET) (Blount *et al.*, 2006) and a fluorescent ligand displacement assay was designed and validated for a high-throughput screening of compounds targeting SAM-I riboswitches (Hickey and Hammond, 2014).

1.4.1 Challenges for riboswitches as antibacterial targets

However, there are also some more aspects to consider regarding the development of riboswitch ligands with antimicrobial activity. It is possible that resistance to a new drug could evolve rather quickly (Panchal and Brenk, 2021), since a single mutation in the riboswitch sequence can disrupt ligand binding, as it has been shown for TPP and FMN riboswitches, for example (Serganov *et al.*, 2006, 2009). On the other hand, it has been argued that single mutations at one riboswitch site would not be enough to gain complete resistance against an antibiotic compound, especially when different riboswitches of the same class are present in the cell. In any case, the mutations in the riboswitch region are expected to also interfere with binding of the natural ligand and thereby the natural riboswitch regulation (Blount and Breaker, 2006; Pavlova and Penchovsky, 2022).

Since most of the riboswitch-targeting compounds known so far are structural analogs of the actual ligand, they all bear a higher risk of undesired off-target effects in human cells by interfering with other metabolic processes where they substitute the natural ligand (Panchal and Brenk, 2021; Giarimoglou *et al.*, 2022). So, the capability of the drug molecule to substitute the natural ligand should also be considered, when new ligands are developed (Matzner and Mayer, 2015). Furthermore, potential ligands must be able to either penetrate the cell or to use the transport system of the actual ligand to get to the inside of the cell (Giarimoglou *et al.*, 2022; Pavlova and Penchovsky, 2022).

1.4.2 The TPP riboswitch as an antibiotic target

One of the riboswitches that has been focused on as an antibacterial drug target is the thiamine pyrophosphate riboswitch (Cressina *et al.*, 2011; Chen *et al.*, 2012; Lünse *et al.*, 2014; Traykovska *et al.*, 2022). Especially its wide distribution, its presence in genomes of important pathogens and the high sequence conservation make it an interesting object of study (Panchal and Brenk, 2021). Pavlova *et al.* have considered it a suitable target for antibiotic research, due to its control of important biosynthetic pathways, its regulation of thiamine transport proteins and the fact that no alternative pathway, which is not controlled by a TPP riboswitch, for the synthesis of its metabolite is known (Pavlova and Penchovsky, 2019). So far, different

alternative ligands for the TPP riboswitch have already been reported, some of which have also been tested for their antibiotic activity (Giarimoglou *et al.*, 2022).

Among the first thiamine analogs studied for their binding affinity to the TPP riboswitch was oxythiamine, a molecule very similar to thiamine, but with a hydroxyl group in place of the exocyclic amino group of the pyrimidine ring of thiamine. In *E. coli*, this molecule failed to induce the structural rearrangement of the *thiM* riboswitch and exhibited a strongly decreased binding affinity (Winkler, Nahvi, *et al.*, 2002). However, for a eukaryotic TPP riboswitch, a comparison of the TPP-bound structure and the structure of the riboswitch bound to the pyrophosphorylated form of oxythiamine revealed only small differences, underlining the relevance of the pyrophosphate group of the ligand (Thore *et al.*, 2008).

Another more extensively studied thiamine analog is pyrithiamine (PT). Here, a pyridine ring replaces the central thiazole ring of thiamine. Pyrithiamine has initially been synthesized to study thiamine metabolism (Sudarsan *et al.*, 2005), but had shown antimicrobial activity against bacterial species and fungi (Robbins, 1941; Woolley and White, 1943). Addition of pyrithiamine to the cultures resulted in growth inhibition of *B. subtilis* and *E. coli*. This could be attributed to its effect on TPP riboswitch activity. It was concluded that pyrithiamine was intracellularly phosphorylated to pyrithiamine pyrophosphate (PTPP) and in this form was able to bind the TPP riboswitch with high affinity. For the *B. subtilis tenA* riboswitch, a binding affinity of 160 nM was determined, compared to 50 nM for the natural ligand TPP (Sudarsan *et al.*, 2005). From the 23 PT-resistant mutants of *B. subtilis* generated in this study, all had acquired mutations in the *tenA* riboswitch region, while for *E. coli* only 8 out of 23 PT-resistant mutants showed mutations in either the *thiC* or *thiM* riboswitch region, with the remaining mutants having gained resistance through some other mechanism.

The high affinity of PTPP to the TPP riboswitch is consistent with the observation that the thiazolium ring of thiamine is not essential for binding of the molecule to the riboswitch. A study by Chen *et al.* has tested different TPP and PTPP analogs, where the distinct rings or group have been replaced individually. A replacement of the aminopyrimidine ring with different heterocyclic rings strongly reduced binding affinities. The thiazolium ring, on the other hand, even though this was not observed for open-chain structures, could be replaced with other positively charged heterocyclic rings without a significant effect on binding. Consistent with observations from other studies mentioned before, the removal of the pyrophosphate group was again found to strongly decrease the affinity of the ligand to the riboswitch (Chen *et al.*, 2012).

Another promising compound that was described as a potential ligand for the TPP riboswitch is triazolethiamine (TT), in which the central thiazole ring is replaced by 1,2,3-triazole. While triazolethiamine led to a significant decrease in reporter activity, its effect on the riboswitch was shown to be dependent on intracellular phosphorylation by the thiamine kinase ThiK.

However, in this context it was stated that pyrithiamine was acting independently of ThiK, leading to the assumption that it was either converted to TPP through salvage pathways or that it can be phosphorylated by other enzymes. To bypass the ThiK-dependency of triazolethiamine, different derivatives with groups that mimic the pyrophosphate moiety were tested as riboswitch ligands. One compound, triazolethiamine methanesulfonate, indeed exhibited strong reporter gene repression even in a Δ*thiK* strain (Lünse *et al.*, 2014).

Further attempts to find a suitable ligand for the TPP riboswitch were undertaken by screening of fragment library of 1300 molecules with a combination of biophysical methods. The most promising hits were then tested in an *in vitro* transcription/translation (IVTT) assay (Cressina *et al.*, 2011). However, of the 17 chosen compounds that had shown the best binding affinities to the *E. coli thiM* riboswitch aptamer with K_D values of 22 to 670 µM, none was able to significantly decrease gene expression in the IVTT assay. In the following, some of the hits from this study were tested in a folding study that confirmed that they only induced partial folding of some regions, with the G72 of the riboswitch found in a new conformation (Deigan Warner *et al.*, 2014).

A very recent study further examined two more potential ligands with docking studies and well-tempered metadynamics (Wakchaure and Ganguly, 2021). These two ligands CH_2-TPP and CF_2-TPP contain different pyrophosphate analogues and in both structures the thiazole is replaced by a triazole ring. These compounds had already been described before in the study by Chen *et al.* In their *in vitro* reporter assay, the CF_2-TPP compound significantly repressed gene expression of the reporter gene, while CH_2-TPP even led to a decrease in gene expression that was comparable to the effect of TPP (Chen *et al.*, 2012). The computational method from the new study found a slightly lower binding affinity to the riboswitch of CH_2-TPP compared to TPP with a structural rearrangement of the G72 occurring upon binding. This rearrangement is assumed to stabilize the pyrophosphate binding helix and is not observed for the second compound CF_2-TPP (Wakchaure and Ganguly, 2021).

Taken together, the studies mentioned above provide a solid background for the continued search for thiamine analogs that target the TPP riboswitch and thereby exhibit antibiotic activity.

1.5 The FMN riboswitch

Another widespread riboswitch is the flavin mononucleotide (FMN) riboswitch, which is also found in a large number of bacteria, including important pathogenic species (Pavlova *et al.*, 2019). Like the TPP riboswitch, it regulates the expression of genes involved in the synthesis and transport of an important vitamin, in this case riboflavin (vitamin B_2). Riboflavin is synthesized by plants and fungi, but also by many microorganisms from guanosine-5'-

triphosphate and ribulose-5-phosphate (Bacher *et al.*, 2000; Vitreschak *et al.*, 2002, see Figure 4). It is the precursor of FMN and flavin adenine dinucleotide (FAD), important cofactors for flavoenzymes and involved in many biological processes (Joosten and van Berkel, 2007). In *B. subtilis*, 1.4 % of the genes are predicted to depend on these two cofactors (Macheroux *et al.*, 2011).

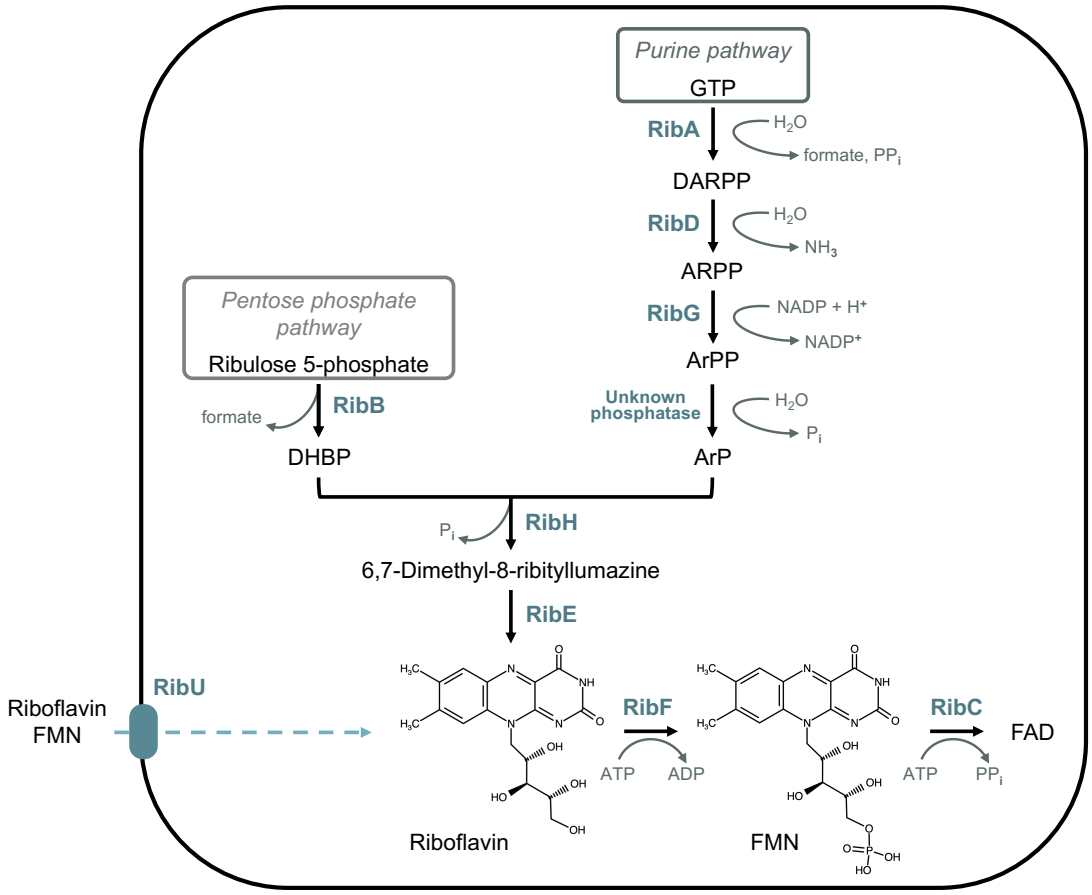

Figure 4: Schematic pathways of riboflavin biosynthesis in *B. subtilis*. Enzymes involved in the pathway are the bifunctional GTP cyclohydrolase II/3,4-DHBP synthase RibAB, the bifunctional deaminase/reductase RibDG, the lumazine synthase RibH, the riboflavin synthase RibE and the bifunctional flavokinase/FAD synthetase RibFC. The phosphatase, which converts ArPP to ArP, is unknown. RibU (formerly YpaA) is a riboflavin transmembrane transporter, able to transport FMN and riboflavin. Abbreviated compounds are: guanosine triphosphate (GTP), 2,5-diamino-6-ribosyl-amino-4(3H)pyrimidinedione 5'-phosphate (DARPP), 5-amino-6-ribosyl-amino-2,4(1H,3H) pyrimidinedione 5'-phosphate (ARPP), 5-amino-6-ribityl-amino-2,4(1H,3H)pyrimidinedione 5'-phosphate (ArPP), 5-amino-6-ribityl-amino-2,4(1H,3H)pyrimidinedione (ArP), 3,4-dihydroxy-2-butanone-4-phosphate (DHBP), flavin mononucleotide (FMN) and flavin adenine dinucleotide (FAD). Figure and description were adapted from Averianova *et al.*, 2020.

The FMN riboswitch was first described as the so called RFN element, a conserved sequence in the untranslated, upstream region of riboflavin biosynthesis genes (Gelfand *et al.*, 1999; Mironov *et al.*, 2002; Vitreschak *et al.*, 2002). In *B. subtilis* most of the riboflavin synthesis genes are organized in an operon, comprising the genes *ribDG* (coding for a bifunctional deaminase/reductase), *ribE* (riboflavin synthase), *ribAB* (bifunctional GTP cyclohydrolase II/ 3,4-DHBP synthase), *ribH* (lumazine synthase) and *ribT* (putative N-acetyltransferase)

(Averianova *et al.*, 2020, see Figure 5). It was observed that mutations in the leader sequence of this *ribD* operon, named *ribO* mutations, led to elevated riboflavin synthase activity. In this context it was already described that the *ribD* leader sequence seems to fold into a “clover-like structure” (Kil *et al.*, 1992). Some years later, it was shown that in the presence of FMN, secretion of riboflavin from *B. subtilis* was strongly downregulated, an effect, which could not be observed for a strain with a mutation in the *ribD* leader sequence (Mack *et al.*, 1998). The presence of an FMN-dependent riboswitch upstream of the *ribD* operon, with the previously described RFN element constituting the aptamer domain, was then experimentally validated, and it was demonstrated that it regulates gene expression by transcription attenuation (Mironov *et al.*, 2002; Winkler, Cohen-Chalamish, *et al.*, 2002). A second FMN riboswitch regulating at the translational level was discovered upstream of the *ribU* gene (formerly *ypaA*) in *B. subtilis* (Winkler, Cohen-Chalamish, *et al.*, 2002; Sklyarova and Mironov, 2014), which codes for a riboflavin transporter (Vogl *et al.*, 2007) (see Figure 4, Figure 5).

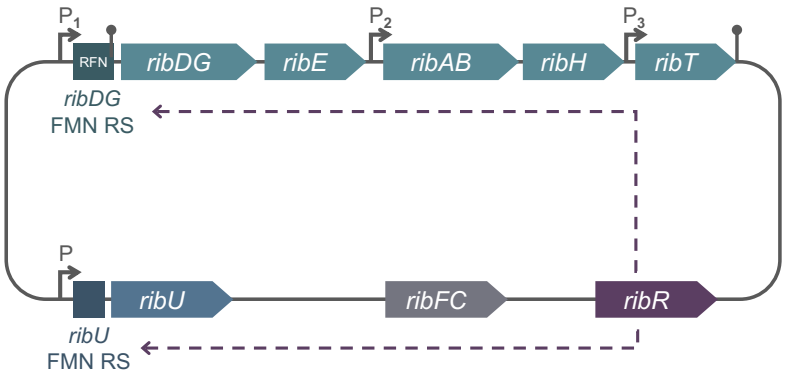

Figure 5: Schematic representation of riboflavin synthesis and transport genes in *B. subtilis*. The *rib* operon *ribDG-E-AB-H-T* is regulated by the *ribDG* FMN riboswitch (RS), also referred to as the RFN element. Expression of the *ribU* gene coding for a riboflavin transporter is regulated by a second FMN riboswitch (*ribU* FMN RS) The gene *ribFC* encodes a bifunctional flavokinase/FAD synthetase. The gene *ribR* codes for a two-domain protein with the C-terminus affecting the FMN riboswitch regulation (indicated by dashed arrows). The promoters P1, P2, and P3 (arrows) are confirmed. The *ribU* promoter P is predicted. Hairpin symbols represent confirmed transcription terminators. Figure and description were adapted from Averianova *et al.* 2020.

Structurally, the FMN riboswitch consists of six helices, which form a butterfly-like structure. The FMN molecule is bound asymmetrically by base-specific interactions of the isoalloxazine ring chromophore and Mg^{2+}-mediated bonds of the phosphate group (Serganov *et al.*, 2009). While the *ribD* FMN riboswitch aptamer of *B. subtilis* binds FMN with high affinity of approximately 5 nM, it discriminates strongly against the FMN precursor riboflavin, which it binds with a K_D value of around 3 µM, as well as against FAD (Winkler, Cohen-Chalamish, *et al.*, 2002).

Several other ligands with antibiotic activity have been discovered that can bind to the FMN riboswitch and regulate downstream gene expression. One of them is the naturally occurring riboflavin analog roseoflavin. This compound is produced by *Streptomyces davaonensis* and

its phosphorylated form RoFMN inhibits growth of several, mainly Gram-positive bacteria (Ott *et al.*, 2009; Mansjö and Johansson, 2011; Wang *et al.*, 2017). Another compound that targets the FMN riboswitch and exhibits antibiotic activity is the synthetically constructed ribocil (Howe *et al.*, 2015). All riboswitch-resistant *E. coli* mutants found had mutations in the *ribB* FMN riboswitch sequence, demonstrating the selective targeting of the riboswitch by ribocil-B. In the following, a ribocil derivative ribocil-C was found, which exhibited eight-fold higher antimicrobial activity compared to ribocil-B (Howe *et al.*, 2016; Wang *et al.*, 2017). Since ribocil-C was mostly active against Gram-positive bacteria, a further derivative was constructed, called ribocil-C-PA. This compound was able to inhibit several resistant strains of the Gram-negative *E. coli* and *K. pneumoniae* and was even found to be effective in a mouse model against *E. coli* infections. However, a high frequency of target-based resistance was observed for both ribocil-C and ribocil-C-PA (Motika *et al.*, 2020).

1.6 The riboswitch-binding protein RibR in *Bacillus subtilis*

1.6.1 RNA-binding proteins

Different types of RNA-binding enzymes have been discovered so far. For example, CsrA was shown to repress glycogen synthesis in *E. coli* by binding to the *glgCAP* mRNA and destabilizing it (Romeo, 1998). In two *Vibrio* species, Hfq was described as a mediator of interactions between small, regulatory RNAs (sRNAs) and messenger RNAs (mRNAs), thereby altering stability of the transcribed RNA. Together with the sRNAs, Hfq seems to form a sensitive regulator of gene expression (Lenz *et al.*, 2004).

In *B. subtilis* more examples for RNA-binding regulatory proteins were discovered. PyrR can bind to three binding loops in the leader sequence in the 5'-untranslated end of the *pyr* mRNA. Binding of the protein leads to a stabilization of an anti-antiterminator structure and repression of the downstream genes (Bonner *et al.*, 2001; Hobl and Mack, 2007). A similar mechanism was observed for the *trp* RNA-binding attenuation protein (TRAP) and the GlcT protein. While GlcT, a member of the BglG family, is involved in the regulation of the *ptsGHI* operon (Stülke *et al.*, 1997), TRAP binds to the leader sequence of the *trp* operon and promotes formation of a transcriptional terminator by blocking the anti-terminator structure (Babitzke, 1997). Furthermore, binding of TRAP to the mRNA can also induce translocation of the RNA polymerase, which is required for the transcription attenuation mechanism (Potter *et al.*, 2011).

1.6.2 Riboswitch-binding proteins

While all these are examples for the involvement of protein factors in regulating gene expression by binding to mRNAs, there are also some examples of proteins which directly

interact with more complex RNA structures like riboswitches. Firstly, these can be RNases, involved in the mRNA decay like the RNases E and Y (Bédard *et al.*, 2020). RNase E, for example, targets the *mgtA* riboswitch, which regulates expression of a magnesium transporter, to degradation. This constitutes an additional mechanism for downregulation of gene expression, next to the transcription termination by the riboswitch (Spinelli *et al.*, 2008).
Also, the K-turn elements found in many riboswitches were suspected to represent binding sites for regulatory proteins. It was shown that interaction with K-turn binding proteins leads to a stabilization of the K-turn motif structure (Turner *et al.*, 2005), and the archaeal L7Ae protein was shown to facilitate ligand binding to the *B. subtilis* SAM riboswitch (Heppell and Lafontaine, 2008). These observations suggest that K-turn elements in riboswitch sequences are anchor sites for proteins, which facilitate folding of the riboswitch RNA (Bédard *et al.*, 2020).

1.6.3 The riboswitch-regulator RibR in *Bacillus subtilis*

In *B. subtilis*, a more complex mechanism of regulation, involving another protein, has been discovered for the FMN riboswitch. The protein RibR was first described as a flavokinase or riboflavin kinase with cryptic cellular function (Solovieva *et al.*, 1999, 2005; Perkins and Pero, 2001). The gene coding for *ribR* is part of a large operon, consisting of the twelve genes *snaA, tcyJ, tcyK, tcyL, tcyM, tcyN, cmoO, cmoI, cmoJ, ribR, sndA* and *ytnM* (Solovieva *et al.*, 1999; Burguière *et al.*, 2005a). Except for *ribR*, the other genes of this operon code for enzymes and transport proteins involved in sulfur metabolism. Most of the gene products are part of a cysteine salvage pathway. The proteins TcyJLKMN constitute a high-affinity transporter for the uptake of sulfur compounds like L-cystein, cystathionine and S-methylcysteine (Burguière *et al.*, 2005a). *SnaA* codes for an acetyltranferase, *cmoI* for glutaredoxin and *sndA* for an amidohydrolase, while CmoO and CmoJ were identified as two flavin-dependent monooxygenases. The exact function of YtnM is still unknown (Hazra *et al.*, 2022). RibR itself is a small protein consisting of 230 amino acids. The flavokinase activity that was first attributed to the protein, is actually restricted to its N-terminal domain. The C-terminal domain, on the other hand, does not exhibit close similarity to any other protein class. However, by using a yeast three-hybrid system it was shown that RibR *in vivo* interacts with the *ribD* FMN riboswitch of *B. subtilis* and this function could be located to the C-terminal part of the protein. Mutations in the *ribD* operon leader sequence resulted in less efficient binding (Higashitsuji *et al.*, 2007). It was confirmed that RibR interacts with both FMN riboswitches of *B. subtilis* and that it allows expression of the riboflavin-related genes, even at high levels of FMN (Pedrolli, Kühm, *et al.*, 2015).
Expression of *ribR* and the other genes of the transcription unit is regulated by the presence of certain sulfur compounds. Methionine and taurine (2-aminoethanesulfonic acid) were found

to strongly induce the operon, while in the presence of $MgSO_4$ the genes were repressed (Coppée *et al.*, 2001; Chan *et al.*, 2014). When methionine and taurine were added to cultures of *B. subtilis*, *ribR* was induced, which counteracted the repressive effect of high FMN levels on expression of the *ribD* operon genes. Compared to cultures grown with $MgSO_4$, this resulted in elevated levels of riboflavin and FMN/FAD production. The increased amount of these cofactors might in turn be required by the two encoded flavoenzymes of the induced *snaA* operon, CmoO and CmoJ. In the light of these findings, it was suggested that the regulatory function of the RibR C-terminal domain is of physiological relevance to the cell, rather than the N-terminal flavokinase activity. Still, the exact nature of the link between riboflavin and sulfur metabolism remains unclear (Pedrolli, Kühm, *et al.*, 2015).

1.6.3.1 A RibR-like protein in *Bacillus amyloliquefaciens*

In *Bacillus amyloliquefaciens*, a close relative of *B. subtilis*, a RibR-like protein was identified, which only consists of a homolog of the RNA-binding domain (see result chapter 6.2). Although the genomes of the two *Bacillus* strains show a high similarity, this *ribR* coding region of *B. amyloliquefaciens* is not located in the same operon of sulfur-related genes as in *B. subtilis*. The *ribR*-like gene of *B. amyloliquefaciens* (hereafter referred to as $ribR_{amy}$) is found at a different position in the genome, downstream of the gene *yezD*, which codes for a small protein with unknown function.

1.6.3.2 Oxidative stress by diamide and induction of *yezD* in *B. subtilis*

However, a homologue of *yezD* is also found in *B. subtilis* and transcription studies have suggested that expression of this gene is induced by diamide (Zhu and Stülke, 2018a). Diamide (tetramethylazodicarboxamide, Figure 6) is a thiol-specific oxidant, which induces cell stress by formation of intra- and intermolecular disulfide bonds and S thiolation (Kosower and Kosower, 1995; Pöther *et al.*, 2009).

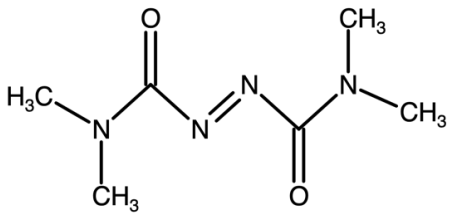

Figure 6: Chemical structure of tetramethylazodicarboxamide (diamide).

Among other effects, the thiol-specific stress caused by diamide leads to a derepression of the CymR regulon (Pöther *et al.*, 2009). CymR (cysteine metabolism repressor) is a master regulator of sulfur metabolism and in *B. subtilis* it not only represses *yezD* (Choi *et al.*, 2006),

but also controls the expression of *ribR* via the YtlI activator (Burguière *et al.*, 2005a; Even *et al.*, 2006). Furthermore, the transcriptional regulator Spx, involved in the maintenance of redox homeostasis of *B. subtilis* under diamide-induced disulfide stress, represses the *yezD* gene (Rochat *et al.*, 2012).

Due to the close relation of *B. subtilis* to *B. amyloliquefaciens*, similar regulatory mechanisms could be assumed for this organism. And since *yezD* and $ribR_{amy}$ seem to be co-transcribed in *B. amyloliquefaciens*, this would again hint to a complex interdependence of oxidative stress, sulfur metabolism and the riboswitch-dependent regulation of riboflavin synthesis.

1.7 Aim of the study

1.7.1 TPP riboswitches as potential targets for new antibiotics

The aim of this PhD project is to identify and characterize TPP riboswitches from important ESKAPE pathogens and to study their response to thiamine analogues. *In vivo* reporter gene assays with thiamine using a newly adapted dual-luciferase system for detection and quantification are used to identify and characterize the riboswitches. The mode of action of the riboswitches is determined by transcriptional and translational gene fusions in this system. The same reporter gene assays are then employed to test the effect of TPP analogues on riboswitch activity. To compare the effect of thiamine analogues on TPP riboswitches from different organisms, the compound pyrithiamine is used as a representative of the group of thiamine analogues with previously described antibiotic properties.

1.7.2 Influence of the RNA-binding protein RibR on FMN riboswitches

In addition, the RNA-binding protein RibR and its influence on FMN riboswitch activity is investigated. First, the *B. subtilis* RibR and its function are further characterized. Different *B. subtilis ribR* mutant strains are generated with the CRISPR/Cas9 system to analyze the important RNA-binding residues and the flavokinase function of the RibR protein. By monitoring an enzymatic reaction within the riboflavin synthesis pathway, the influence of different RibR versions on the FMN riboswitches and downstream gene expression can be observed. The RibR-like protein from *Bacillus amyloliquefaci*ens ($RibR_{amy}$), which lacks the flavokinase domain, is studied in more detail. Here, the same reporter system is employed in the *B. subtilis* host. Thereby, its effect on both the *B. amyloliquefaciens* and *B. subtilis* FMN riboswitches is examined. Furthermore, the goal is to shed more light on the connection of diamide-induced stress and expression of $ribR_{amy}$ in *B. amyloliquefaciens*.

2 Materials

2.1 Laboratory equipment

All laboratory devices used for performing the described experiments are listed in Table 1.

Table 1: List of the used laboratory equipment and the respective manufacturers.

Instrument	Model	Manufacturer
Autoclave	Varioklav® Dampfsterilisator 175	H+P Labortechnik, Habermoos, Germany
Basic power supply	Power Pac 200, Power Pac 300	Bio-Rad Laboratories GmbH, Feldkirchen, Germany
Bead lysis system	FastPrep-24 5G	MP Biomedicals, Santa Ana, CA, USA
Cell disruptor	Constant Cell Disruption System	Constant Systems Lt., Northants, UK
Centrifuge	Heraeus Multifuge X1R	Thermo Fisher Scientific, Waltham, MA, USA
FPLC System	Äkta Purifier P-900 with fraction collector Frac-920 and a 50 mL	GE Healthcare GmbH, Solingen, Germany
Gel imager	Molecular Imager® GelDoc™ XR, Quantity One 1D-Analysis software	Bio-Rad Laboratories GmbH, Feldkirchen, Germany
Incubators	TS 606-G/2, Heraeus B20	WTW, Weilheim, Germany, Thermo Fisher Scientific, Waltham, MA,
Incubation shaker	Certomat IS	Sartorius Lab Instruments GmbH & Co. KG, Göttingen, Germany
HPLC System	1260 Infinity System with DAD/FLD	Agilent Technologies, Waldbronn, Germany
Laminar flow hood	Variolab Mobilien W 90	Waldner Laboreinrichtungen GmbH & Co KG, Wangen, Germany
Microplate reader	Spark®	Tecan Group, Männedorf, Schweiz
Phosphorimager	Typhoon® 9100	GE Healthcare GmbH, Solingen, Germany
Scintillation counter	Wallac 1409 Liquid Scintillation Counter	Wallac, Monza
Semi-dry blotting system	Trans-Blot® SD Semi-Dry Transfer Cell	Bio-Rad Laboratories GmbH, Feldkirchen, Germany
Spectrophotometer	Ultrospec 3100 pro	Amersham Biosciences, Amersham, UK (now GE Healthcare)
Tabletop centrifuge	Eppendorf 5415 R	Eppendorf, Hamburg, Germany
Thermocycler	C1000™ Thermal Cycler, dual	Bio-Rad Laboratories GmbH, Feldkirchen, Germany
Thermomixer	Thermomixer comfort	Eppendorf, Hamburg, Germany
Ultracentrifuge	Avanti J-30I	Beckmann Coulter, Brea, CA, USA
Water bath	IKA® HBR4 digital	IKA GmbH, Staufen im Breisgau, Germany
Water Purification System	Milli-Q® Gradient	Millipore GmbH, Schwalbach, Germany

2.2 Chemicals, reagents, and consumables

2.2.1 Chemicals and reagents

For all buffers and reagents, standard laboratory-grade chemicals from the following suppliers were used, if not stated otherwise:

- AppliChem GmbH, Darmstadt, Germany
- Carl Roth GmbH & Co. KG, Karlsruhe, Germany
- Caymen Chemical, Ann Arbor, MI, USA
- Merck KGaA, Darmstadt, Germany
- Thermo Fisher Scientific, Darmstadt, Germany
- VWR International GmbH, Darmstadt, Germany

The 6,7-dimethyl-8-ribityllumazine used as a substrate in the riboflavin synthase assay was a gift from Dr. Boris Illarionov from the group of Dr. Markus Fischer (Universität Hamburg, Germany).

2.3 Media and buffers

All media and buffers listed below were prepared with ultrapure water (Milli-Q® water purification system), except for the Lysogeny broth (LB) medium, which was prepared with distilled water. All heat-stable media and components were sterilized by autoclaving at 120 °C for 20 minutes. Heat-sensitive components like sugar solutions were filter sterilized using a 0.22 µm cellulose-acetate filter.

2.3.1 Growth media

Table 2: Media composition for Lysogeny broth (LB).

Component	Mass conc.
Tryptone	10 g/L
Yeast extract	5 g/L
NaCl	10 g/L

LB medium was prepared from a premix (Carl Roth GmbH + Co. KG, Karlsruhe, Germany), using 25 g of the compound mixture per liter of medium.

Table 3: Media composition for M9 minimal medium.

Component	Mass conc.	Vol. fraction	Final conc.
5 x M9 salt solution		**200 mL/ L**	
Na_2HPO_4 x 2 H_2O	33.79 g/L		33.7 mM
KH_2PO_4	14.97 g/L		22 mM
NaCl	2.51 g/L		8.5 mM
NH_4Cl	4.97 g/L		18.6 mM
		2 mL/ L	
1 M $MgSO_4$ solution			
$MgSO_4$ x 7 H_2O	246.48 g/ L		2 mM
0.5 M $CaCl_2$ solution		**0.2 mL/ L**	0.1 mM
$CaCl_2$ x 2 H_2O	73.5 g/L		
100 x Trace metal solution		**10 mL/ L**	
$FeCl_3$ x 6 H_2O	135.147 g/L		5 µM
$MnCl_2$ x 4 H_2O	19.790 g/L		2 µM
$ZnSO_4$ x 7 H_2O	28.754 g/L		1 µM
$CoCl_2$ x 6 H_2O	4.758 g/L		1 µM
$CuCl_2$ x 2 H_2O	3.409 g/L		0.2 µM
$NiCl_2$ x 6 H_2O	4.753 g/L		0.2 µM
Na_2MoO_4 x 2 H_2O	4.839 g/L		0.2 µM
Na_2SeO_3 x 5 H_2O	5.260 g/L		0.2 µM
H_3BO_3	1.23 g/L		0.2 µM

Table 4: Media composition for *Bacillus* minimal medium.

Component	Vol. conc.	Final conc.
1 M K_2HPO_4	6 mL/L	6 mM
1 M KH_2PO_4	4.5 mL/L	4.5 mM
1 M Trisodium citrate	0.3 mL/L	0.3 mM
1 M $MgCl_2$	5 mL/L	5 mM
2.2 % (w/v) Ferric ammonium citrate	1 mL/L	84 µM
20% (w/v) glucose	25 mL/L	0.5% (w/v)
2.5% (w/v) glutamine	40 mL/L	0.1% (w/v)

Table 5: Media composition for T base, SpC medium and SpII medium.

Component	Mass conc.	Vol. fraction
T base		
$(NH_4)_2SO_4$	2 g/L	
K_2HPO_4 x 3 H_2O	18.3 g/L	
KH_2PO_4	6 g/L	
Trisodium citrate x 2 H_2O	1 g/L	
SpC medium		
T base		20 mL
50% (w/v) glucose		0.2 mL
1.2% (w/v) $MgSO_4$ x 3 H_2O		0.3 mL
10% (w/v) Bacto yeast extract		0.4 mL
1% (w/v) casamino acids		0.5 mL
SpII medium		
T base		200 mL
50% (w/v) glucose		2 mL
1.2% (w/v) $MgSO_4$ x 3 H_2O		14 mL
10% (w/v) Bacto yeast extract		2 mL
1% (w/v) casamino acids		2 mL
0.1 M $CaCl_2$		1 mL

2.3.2 Buffers

The tables below list the compositions of all buffers and solutions used in this study, which are not part of a commercially available kit. The usage of the individual buffers is explained in the respective method sections.

Table 6: Media for generating competent cells with the RbCl-method.

RF1 (pH 5.8)	Mass conc.	RF2 (pH 6.5)	Mass conc.
RbCl	12.08 g/L	RbCl	1.2 g/L
$CaCl_2$ x 2 H_2O	1.48 g/L	$CaCl_2$ x 2 H_2O	11 g/L
Glycerol (100 %)	150 mL/L	Glycerol (100 %)	150 mL/L
MnCl x 4 H_2O	9.92 g/L	MOPS	2.12 g/L
Potassium acetate	2.96 g/L		

Table 7: Z buffer for the β-galactosidase reporter gene assay.

Component	Mass conc.	Final conc.
Na_2HPO_4 x 7 H_2O	16.08 g/L	60 mM
NaH_2PO_4	5.52 g/L	40 mM
KCl	0.746 g/L	10 mM
$MgSO_4$	0.247 g/L	1 mM

Table 8: 1x Tris-Acetate-EDTA (TAE) buffer

Component	Mass conc.	Final conc.
Tris	4.85 g/L	40 mM
Acetic acid (100%)	1.14 mL/L	20 mM
0.5 M EDTA (pH 8)	2 mL/L	1 mM

Table 9: 1x Tris-Borate-EDTA (TBE) buffer

Component	Mass conc.	Final conc.
Tris	10.8 g/L	89 mM
Boric acid	5.5 g/L	89 mM
0.5 M EDTA (pH 8.3)	4 mL/L	2 mM

Table 10: Polyacrylamide (PAA) mix for RNA gels. Urea was only added for denaturing gels.

Component	6 % PAA	8 % PAA
10x TBE	100 mL/L	10x TBE
40 % acrylamide	150 mL/L	200 mL/L
8 M urea	480 g/L	480 g/L

Table 11: Composition of Column Buffer used for purification of MBP-fusion proteins.

Component	Mass conc.	Final conc.
1 M Tris-HCl (pH 7.5)	20 mL/L	20 mM
NaCl	11.7 g/L	200 mM
0.5 M EDTA (pH 8.3)	2 mL/L	1 mM
DTT	154 mg	1 mM

Table 12: Composition of Elution Buffer used for purification of MBP-fusion proteins.

Component	Mass conc.	Final conc.
1 M Tris-HCl (pH 7.5)	20 mL/L	20 mM
NaCl	11.7 g/L	200 mM
0.5 M EDTA (pH 8.3)	2 mL/L	1 mM
D(+)-Maltose x H_2O	3.6 g/L	10 mM

Table 13: Composition of the 5x protein loading dye.

Component	Mass conc.	Final conc.
1 M Tris-HCl (pH 6.8)	2.5 mL/10 mL	250 mM
SDS	800 mg/10 mL	8%
Bromophenol blue	10 mg/10 mL	0.1%
Glycerol (80%, v/v)	5 mL/10 mL	10 mM
1 M DTT	1 mL/10 mL	100 mM

Table 14: 1x Phosphate Buffered Saline (PBS) (pH 7.2).

Component	Mass conc.	Final conc.
NaCl	8.2 g/L	140 mM
KCl	0.1 g/L	3 mM
Na_2HPO_4 x 2 H_2O	0.89 g/L	10 mM
KH_2PO_4	0.12 g/L	1.8 mM

Table 15: Composition of the Towbin transfer buffer (pH 8.3).

Component	Mass conc.	Final conc.
Tris	3 g/L	25 mM
Glycine	14.33 g/L	192 mM
Methanol	200 mL/L	20 % (v/v)

Table 16: 3,3'-Diaminobenzidine (DAB) staining solution in 1x PBS.

Component	Amount
1x PBS	10 mL
Solution A: 140 mM DAB in dimethylformamide	40 µL
H_2O_2 (35%)	1.7 µL
Solution B: 10 % (w/v) CuSo4 in ddH_2O	10 µL
Solution C: 5% (w/v) NiSO4 in ddH_2O	1 µL

Solutions A, B and C were prepared individually and stored at -20 °C. The final DAB staining solution was always prepared freshly before usage and the components were added in the indicated order.

2.4 Bacterial strains

Table 17: List of bacterial strains used in this study.

Strain		Characteristics & usage	Origin or reference
E. coli	DH5α	F- Φ80*lac*ZΔM15 Δ(*lac*ZYA-*arg*F) U169 *rec*A1 *end*A1 *hsd*R17(rk-, mk+) *pho*A *sup*E44 *thi*-1 *gyr*A96 *rel*A1 λ-, used for cloning and plasmid multiplication	Hanahan, 1983
	Top10	*mcrA, Δ(mrr-hsdRMS-mcrBC), Phi80lacZ(del)M15, ΔlacX74, deoR, recA1, araD139, Δ(ara-leu)7697, galU, galK, rpsL(SmR), endA1, nupG*, used for plasmid multiplication	Invitrogen
	BL21 (DE3)	F–, *omp*T, *hsd*SB (rB-, mB-), *dcm*, *gal*, λ(DE3), used for protein overproduction	Merck KGaA
	BL21 (DE3) pLysS	F–, *omp*T, *hsd*SB (rB-, mB-), *dcm*, *gal*, λ(DE3), the plasmid pLysS allows the suppression of basal expression from the T7 promoter by producing T7 lysozyme, a natural inhibitor of the T7 RNA polymerase, used for protein overproduction of potentially toxic proteins	Novagen
	NEBExpress	*fhuA2 [lon] ompT gal sulA11 R(mcr-73:: miniTn10--TetS)2 [dcm] R(zgb-210::Tn10--TetS) endA1 Δ(mcrC-mrr)114::IS10,* used for overproduction of MBP-tagged proteins	New England Biolabs GmbH
K. pneumoniae	WT	Risk group 2	DSMZ
B. subtilis	WT 168	*trpC2*	Bacillus Genetic Stock Center
	Δ*ribR*	*trpC2*, complete deletion of the *ribR* gene (nucleotides 4-687)	This study
	ΔC-*ribR*	*trpC2*, deletion of the 5'-part of *ribR* (nucleotides 4-117), coding for the N-terminal riboflavin kinase domain	This study
	ΔN-*ribR*	*trpC2*, deletion of the 3'-part of *ribR* (nucleotides 118-687), coding for the N-terminal riboflavin kinase domain	This study

Strain		Characteristics & usage	Origin or reference
B. subtilis	$ribR^{m}_{sub}$	*trpC2*, mutation of *ribR* gene generating the RibR R179A R180A mutant	This study
	$ribR_{amy}$	*trpC2,* exchange of the coding sequence for RibR by the coding sequence for the RibR-like protein $RibR_{amy}$ from *B. amyloliquefaciens*	This study
	$ribR^{m}_{amy}$	*trpC2,* exchange of $ribR_{sub}$ by $ribR^{m}_{amy}$ carrying a mutation of the $ribR_{amy}$ gene generating the $RibR_{amy}$ R54A R55A mutant	This study
	$ribR_{amy}$-his_6	*trpC2,* exchange of the coding sequence for RibR by the coding sequence for the RibR-like protein $RibR_{amy}$ from *B. amyloliquefaciens* including a His_6-tag coding sequence	This study
B. amyloliquefaciens	WT DSM7	type strain	DSMZ

2.5 Plasmids

All general plasmids used in this study are listed in Table 18. All other plasmids with the respective inserts are found in the supplementary list of strains (Table S2).

Table 18: Plasmids used in this study.

Plasmid	Characteristics	Reference
pHAt191	Plasmid originating from pUC19, carrying the *lacZ* reporter gene for a translational fusion with a promoter/riboswitch sequence; Amp^R	This work, Figure S1
pDluc	Plasmid originating from pT7Luc (Promega), carrying the firefly (*Photinus pyralis*) luciferase luc^F gene for a translational fusion with a promoter/riboswitch and POXB15 for constitutive expression of *Renilla reniformis* luciferase gene luc^R, Amp^R	This work, Figure S2
pDlucTC	Plasmid originating from pT7Luc (Promega), carrying the firefly (*Photinus pyralis*) luciferase luc^F gene + RBS for a transcriptional fusion with a promoter/riboswitch and pOXB15 for constitutive expression of *Renilla reniformis* luciferase gene luc^R, Amp^R	This work, Figure S3
pJOE8999.1	Temperature sensitive CRISPR/Cas9 plasmid for *B. subtilis,* replicable in *E. coli*, $pE194^{ts}$, P*manP cas9,* P*vanP lacPOZ'*-gRNA, Kan^R *(E. coli* & *B. subtilis)*	Altenbuchner, 2016, Figure S4

Plasmid	Characteristics	Reference
pMAL-c6T	Vector to produce maltose-binding protein (MBP) fusions, N-terminal his_6-tagged *malE*, TEV protease recognition site, Amp^R	New England Biolabs, Figure S5
pMAL-c5X	Older version of the pMAL-c5X plasmid, no N-terminal his_6-tag on *malE*	New England Biolabs
pSP64	Standard cloning vector for creation of *in vitro* transcripts, Amp^R	Promega, Figure S6

2.6 Oligonucleotides

All relevant oligonucleotides used in this study as primers for DNA amplifications and sequencing are listed in Table 19.

Table 19: Oligonucleotides used in this study for PCR amplification and sequencing. Overhangs are underlined, recognition sites for restriction enzymes are depicted in bold. Lower-case letters indicate insertions/nucleotide changes for site-directed mutagenesis.

#	Oligonucleotides	Sequence (5'-3')	Usage
P1	ΔPlac_fwd	GCGCAACGCAATCACACAGGAAACAGCT	Amplification of pUC19 for deletion of lac promoter
P2	ΔPlac_rev	GTTTCCTGTGTGATTGCGTTGCGCTCAC	
P3	lacZ_TL_fwd	TACAT**TCTAGA**CGGGTCGACCGGGAAAAC	Amplification of lacZ from plasmid pDG268
P4	lacZ_rev	TACAT**GAATTC**GAAATACGGCAGACATGG	
P5	lac_term_fwd	TACTA**GAATTC**GCCTGATACGCTGCGCTTA	Amplification of lac terminator
P6	lac_term_rev	TACTA**GAATTC**AAGAGGCATGATGCGACG	
P7	*rrnB*T1_term_fwd	TATAAAGCG**GAAGAGC**TAGGGAACTGCCAGGCAT	Amplification of *rrnB*T1 terminator
P8	*rrnB*T1_term_rev	TACAT**AAGCTT**TACTCAGGAGAGCGTTCA	
P9	Ec01_pHA_fwd	TCACT**AAGCTTG**CTGGAAGATAAGCTGATT	Amplification of *E. coli thiC* RS region Ec01
P10	Ec01_pHA_rev	TATAT**TCTAGA**GCGTTGTTCGCGGCGGGT	
P11	pEc01_rev	TCACT**CTGCAG**GGGGCATTGAATGTAAAT	Rev primer for *E. coli thiC* promoter
P12	Ec01_RBS_fwd	TACAT**CTGCAG**TTTTGGAATGAGCTATG	Fwd primer for *E. coli thiC* RBS
P13	Kp04_pHA_fwd	ATCAT**AAGCTT**GATAATATTGCGCCGACC	Amplification of *K. pneumoniae thiC* RS Kp04 & control region
P14	Kp04_pHA_rev	TACTT**TCTAGA**ACGGGTTAGTTTGGTAGT	
P15	Kp01_gen_fwd	GCTGGTTCGATTTTAAATCC	Amplification of the Kp01 RS region of *K. pneumoniae*
P16	Kp01_gen_rev	CATAGGTATAGACGGTAAGA	
P17	Kp04_gen_fwd	ATAACCTGAGCAATGACGTG	Amplification of the Kp04 RS region of *K. pneumoniae*
P18	Kp04_gen_rev	GTGAATTAGGAAAAGCGGTA	
P19	Kp10_gen_fwd	CGCCGACAAAGAAACTATTG	Amplification of the Kp10 RS region of *K. pneumoniae*
P20	Kp10_gen_rev	TCAGATAGCGACGAAAGGC	

P21	Kp11_gen_fwd	AATGCAATCCCGTCCGGTC	Amplification of the Kp11 RS region of *K. pneumoniae*
P22	Kp11_gen_rev	CAGAACATTGGCGGTAAAGG	
P23	pUC19del_seq	TGTTCTTTCCTGCGTTATCCCC	Sequencing/ Colony PCR for pUC19del and pHA plasmids
P24	M13_fw_(-43)	AGGGTTTTCCCAGTCACGACGTT	
P25	lacZ_in_fwd	AGGGTTTTCCCAGTCACGACGTT	
P26	lacZ_in_rev	TCAGGCAGTTCAATCAAC	
P27	pHA_lacZ_rev	GTTTTCCCGGTCGACCCGTC	
P28	pHA_lacZ_rev2	GTCACGTTGGTGTAGATGG	
P29	pRib-luc_fwd	AGCTATTGTAATCCTCCGAG	Sequencing/Colony PCR for OXB15-*luc*^{F} in pluc plasmid
P30	pRib-luc_rev	GGTGATGCCAATTCGGTT	
P31	pluc_seq	GAGTCAGTGAGCGAGGAA	Sequencing/Colony PCR for pDluc/pDlucTC plasmids
P32	pluc_rev	TTTGGCGTCTTCTGCTTG	
P33	pluc_TC_rev	CCAGGGCGTATCTCTTCA	
P34	pJOE_HTseq_fwd	TCTGGATTTGTTCAGACGC	Sequencing/Colony PCR for pJOE8999 vector
P35	pJOE_HTseq_rev	AACACGCATTGATTTGAGTC	
P36	pSP64_seq_fwd	CCAGGCTTTACACTTTATGC	Sequencing/Colony PCR for pSP64 vector
P37	pSP64_seq_rev	CATATTGTCGTTAGAACGCG	
P38	T7_prom	TAATACGACTCACTATAGGG	Sequencing/Colony PCR for pET28a vector
P39	T7_term	CTAGTTATTGCTCAGCGGT	
P40	pMAL_seq_fwd	GGTCGTCAGACTGTCGATGAAGCC	Sequencing/Colony PCR for pMAL vectors
P41	pMAL_seq_rev	TGTCCTACTCAGGAGAGCGTTCAC	
P42	*rrnB*T1_*Sac*I_fwd	TACAT**GAGCT**CTAGGGAACTGCCAGGCATCA	Amplification of *rrnB*T1 for pPrib-RFN-luc.t at *Sac*I site, additionally inserting *Xho*I site
P43	*rrnB*T1_*Sac*I_*Xho*I_rev	TACAT**GAGCTC**CAGAA**CTCGAG**TACTCAGGAGAGCGTT	

P44	Pluc_*Kpn*I-ins_fwd	ATAGGTC**GGTACC**GAGCTCCCAAAAAAAAAA	Insertion of *Kpn*I site between *Xho*I and *Sac*I site
P45	Pluc_*Kpn*I-ins_rev	**GGTACC**GACCTATCAGAACTCGAGTACTCAG	
P46	OXB15-luc^R_fwd	TCAGA**CTCGAG**TACTTGT	Amplification of OXB15-luc^R fragment with *Xho*I & *Kpn*I restriction sites
P47	OXB15-luc^R_*Kpn*I_rev	TCGTA**GGTACC**TGTCA**CTGCAG**TTACTGTT	
P48	*Nco*I_ins_fwd	GCTAATCATTAGCGTTATAGTGAATCCGCT**CCATGG**TTTAAGG ACAAATGAATAAAGATTGTATCC	Replacing the *Hin*dIII restriction site of pPrib-Dluc with an *Nco*I site
P49	*Nco*I_ins_rev	GGATACAATCTTTATTCATTTGTCCTTAAA**CCATGG**AGCGGATT CACTATAACGCTAATGATTAGC	
P50	pDluc_RS-del_fwd	CATGGGGGAGGGAAACAAATGTG	Deletion of FMN riboswitch from pPrib-RFN-Dluc
P51	pDluc_RS-del_rev	GATCCACATTTGTTTCCCTCCCC	
P52	pDluc_Δprom_fwd	CTGTGCTGCCCAAGGTATATCTCC	Deletion of T7 promoter in pT7Dluc
P53	pDluc_Δprom_rev	CATGGGAGATATACCTTGGGCAGCACAG	
P54	pDluc_RBSins_fwd	AAACAAATGTGGATCCAATAGAGGGCCCGCATCCAAATGGAAG ACGCCAAAAAC	Insertion of RBS for luc^F to create transcriptional fusion plasmid pDlucTC
P55	pDluc_RBSins_rev	GTTTTTGGCGTCTTCCATTTGGATGCGGGCCCTCTATTGGATC CACATTTGTTT	
P56	Ec01_fwd	TCACT**CAGCTG**GCTGGAAGATAAGCTGATT	Amplification of *E. coli thiC* RS region
P57	Ec01_rev	ACTTCGTCTC**GGATCC**AGCGTTGTTCGCGGCGGGT	
P58	pEc01_pluc_rev	TCACT**CCATGG**GGGGCATTGAATGTAAAT	Amplification of *E. coli thiC* promoter region
P59	Ab01_fwd	TACAT**CCATGG**TTAAATCGCTTGACGGAG	Amplification of *A. baumannii thiC* RS region
P60	Ab01_rev	AACAT**GGATCC**AAGAGAGATTCGTTAATTG	
P61	Ab01_prom_fwd	TCACT**CAGCTG**GTATAGATACAAATTGAC	Amplification of *A. baumannii thiC* prom+RS region
P62	Ef02_prom_fwd	TAT**CAGCTG**CCAGTTAGTCCATTGTTTG	Amplification of *E. faecium* ABC transp. prom+RS region
P63	Ef02_rev	TACAT**GGATCC**GTTCTACCCAAACTCTATT	

P64	Kp04_fwd	TACAT**CCATGG**TTTCATCTTGTCGGAGTG	Amplification of *K. pneumoniae thiC* RS region
P65	Kp04_rev	ACTTCGTCTC**GGATCC**AACGGGTTAGTTTGGTAGT	
P66	Kp04_prom_fwd	ATCAT**CAGCTG**GATAATATTGCGCCGACC	Amplification of *K. pneumoniae thiC* prom+RS region
P67	Eb01_fwd	TACAT**CCATGG**AAATTTCTTGTCGGAGTGC	Amplification of *Enterobacter* spp. *thiC* RS region
P68	Eb01_rev	ATCGTCTC**GGATCC**AGCGGCGGGTCAATTTTGC	
P69	Eb03_fwd	TACAT**CCATGG**GCTGTTCTCAACGGGGTG	Amplification of *Enterobacter* spp. *thiBPQ* RS region
P70	Eb03_rev	TACAT**GGATCC**TCGCCAGCAGGGGGAGAAC	
P71	Ms01_fwd	GAGA**CCATGG**TTAAACCACTGGAAGTGC	Amplification of *M. sciuri tenA* RS region
P72	Ms01_rev	CACA**GGATCC**GTTATAATTAAAAAAACGC	Amplification of *M. sciuri tenA* prom+RS region
P73	Ms01_prom_fwd	CGT**CAGCTG**ATTTTATTTGCAATCCTAG	
P74	Ms02_fwd	TATA**CCATGG**AATGTCCACTGGAAGTGC	Amplification of *M. sciuri thiE* RS region
P75	Ms02_rev	GACGA**GGATCC**ATTTATACGGTGTAACAGC	Amplification of *M. sciuri thiE* prom+RS region
P76	Ms02_prom_fwd	TTCAT**CAGCTG**TTCTGCAATCATCTGAGC	
P77	Pa01_fwd	TATA**CCATGG**GGGTTCTTGTCGGGGTGC	Amplification of *P. aeruginosa thiC* RS region
P78	Pa01_rev	TACGTCTC**GGATCC**CGCGGATGTCCGGGCGCGA	
P79	Sa02_fwd	TATA**CCATGG**AAATCGCACACACTAGGG	Amplification of *S. aureus thiBPQ* RS region
P80	Sa02_rev	TATA**GGATCC**GTTCAGATAGCTTTAAACC	
P81	Sp06_prom_fwd	TAT**CAGCTG**AATCATTTGAAAAACGAT	Amplification of *S. pneumoniae thiD* prom+RS region
P82	Sp06_rev	TATA**GGATCC**TTAAATCTGCCATAATGCC	
P83	Kp01_prom_fwd	TAT**CAGCTG**CATGGTTTGCGC	Amplification of *K. pneumoniae thiBPQ* prom+RS region
P84	Kp01_rev	TATA**GGATCC**ACGCCAGCA	

P85	Kp10_prom_fwd	ATA**CAGCTG**TTCTTGCGC	Amplification of *K. pneumoniae tenA* prom+RS region
P86	Kp10_rev	ATA**GGATCC**AGTAAAGACCTTG	
P87	Kp11_prom_fwd	CAT**CAGCTG**GGCCGCGAA	Amplification of *K. pneumoniae thiM* prom+RS region
P88	Kp11_rev	TATA**GGATCC**AGACAGGCGC	
P89	Kp04_A63U_fwd	AGGCTGAGACCGTTtATTCGGGATCCGCG	Site-directed mutagenesis of *K. pneumoniae thiC* RS (change A63 to T)
P90	Kp04_A63U_rev	CGCGGATCCCGAATaAACGGTCTCAGCCT	
P91	Kp04_del21-37_fwd	ATCTTGTCGGAGTGCCTTAACGTGGAAAAGGCTG	Site-directed mutagenesis of *K. pneumoniae thiC* RS (deletion of nucleotides 21-37)
P92	Kp04_del21-37_rev	CAGCCTTTTCCACGTTAAGGCACTCCGACAAGAT	
P93	Kp04_del42-48_fwd	CATGCGCAGGCTAACAGGCTGAGACCGTTA	Site-directed mutagenesis of *K. pneumoniae thiC* RS (deletion of nucleotides 42-48)
P94	Kp04_del42-48_rev	TAACGGTCTCAGCCTGTTAGCCTGCGCATG	
P95	Kp04_del42G_fwd	CCATGCGCAGGCTAACTGGAAAAGGCTGAG	Site-directed mutagenesis of *K. pneumoniae thiC* RS (deletion of 42G)
P96	Kp04_del42G_rev	CTCAGCCTTTTCCAGTTAGCCTGCGCATGG	
P97	Kp04_del43U_fwd	ATGCGCAGGCTAACGGGAAAAGGCTGAGAC	Site-directed mutagenesis of *K. pneumoniae thiC* RS (deletion of 43U)
P98	Kp04_del43U_rev	GTCTCAGCCTTTTCCCGTTAGCCTGCGCAT	
P99	Kp04_del44G_fwd	TGCGCAGGCTAACGTGAAAAGGCTGAGACC	Site-directed mutagenesis of *K. pneumoniae thiC* RS (deletion of 44G)
P100	Kp04_del44G_rev	GGTCTCAGCCTTTTCACGTTAGCCTGCGCA	
P101	Kp04_del46A_fwd	GCAGGCTAACGTGGAAAGGCTGAGACCG	Site-directed mutagenesis of *K. pneumoniae thiC* RS (deletion of 46A)
P102	Kp04_del46A_rev	CGGTCTCAGCCTTTCCACGTTAGCCTGC	
P103	spacer1_ribR_fwd	TACGCATTTAGGGGTTATGAATAT	Spacer sequence for targeting the *ribR* gene of *B. subtilis*
P104	spacer1_ribR_rev	AAACATATTCATAACCCCTAAATG	
P105	spacer2_ribR_fwd	TACGCGGAAGATTTAACTCCTGAT	2nd spacer sequence for targeting the *ribR* gene of *B. subtilis*
P106	spacer2_ribR_rev	AAACATCAGGAGTTAAATCTTCCG	

P107	spacer3_ribD-RS_fwd	TACGACATCACCCTTCGATCCGAA	Spacer sequence for targeting the *ribD* RS of *B. subtilis*
P108	spacer3_ribD-RS_rev	AAACTTCGGATCGAAGGGTGATGT	
P109	HRT-ΔribR_fwd	TACAA**GTCGAC**TTGCTGCTAAAA	Amplification of homology repair template for *ribR* deletion
P110	HRT-ΔribR_rev	TAGTA**TCTAGA**TTATGCGGCAATG	
P111	HRT-ΔN-ribR_fwd	TACAA**GTCGAC**TTGCTGCTAAAA	Amplification of homology repair template for deletion of N-terminal coding sequence of *ribR*
P112	HRT-ΔN-ribR_rev	TAGTA**TCTAGA**AACACACCCGTT	
P113	HRT-ΔC-ribR_fwd	TACAA**GTCGAC**ACCCGTTGGATG	Amplification of homology repair template for deletion of C-terminal coding sequence of *ribR*
P114	HRT-ΔC-ribR_rev	TAGTA**TCTAGA**TTATGCGGCAATG	
P115	HRT-ribR_RR>AA_fwd	TACAA**GTCGAC**ATTCCGATTCTTC	Amplification of homology repair template for changing of *ribR* RR motif coding sequence to AA
P116	HRT-ribR_RR>AA_rev	TAGTA**TCTAGA**TGGCCGTCCTCT	
P117	HRT-ribR$_{amy}$_fwd	TACAA**GTCGAC**TTGCTGCTAAAA	Amplification of homology repair template to replace *ribR$_{sub}$* with *ribR$_{amy}$*
P118	HRT-ribR$_{amy}$_rev	TAGTA**TCTAGA**TTATGCGGCAATG	
P119	HRT-ribD-RS$_{amy}$_fwd	TCAT**GTCGAC**GATTCATATTGGCTGGAG	Amplification of homology repair template to replace *ribD*-RS$_{sub}$ with *ribD*-RS$_{amy}$
P120	HRT-ribD-RS$_{amy}$_rev	TACT**TCTAGA**ATCCATTTGCTGTCACCC	
P121	RibR$_{amy}$_His1_fwd	CGCAGCAAAACGCCAGGCTcatcaccatTGAGGAAAGGAGC	Site-directed mutagenesis for addition of his$_6$-tag to *ribR$_{amy}$* gene in HRT-ribR$_{amy}$
P122	RibR$_{amy}$_His1_rev	GCTCCTTTCCTCAatggtgatgAGCCTGGCGTTTTGCTGCG	
P123	RibR$_{amy}$_His2_fwd	AACGCCAGGCTCATCACCATCACCATCACTGAGGAAAGGAGC	Site-directed mutagenesis for addition of his$_6$-tag to *ribR$_{amy}$* gene in HRT-ribR$_{amy}$
P124	RibR$_{amy}$_His2_rev	GCTCCTTTCCTCAGTGATGGTGATGGTGATGAGCCTGGCGTT	
P125	ribR_gen_fwd	ATTTTCAAGTAGAGGGGC	Sequencing/Colony PCR of *B. subtilis ribR* genomic region
P126	ribR_gen_rev	ATGACATTCCAAGTGCTG	
P127	ribD-RS_gen_fwd	CAAAGTTTGTTTTCTACCCG	Sequencing/Colony PCR of *B. subtilis ribD*-RS genomic region
P128	ribD-RS_gen_rev	TCGTAAAAATCCATGTCGGC	

P129	T7_ribDRSapt_sub_fwd	GACT**GAATTC**TAATACGACTCACTATAGGGCAGATTGTATCCTTCGG	Amplification of the *B. subtilis ribD* RS aptamer with addition of a T7 promoter sequence
P130	T7_ribDRSapt_sub_rev	TAGC**AAGCTT**CATCATCCTTCTCCCATCC	
P131	T7_ribDRSapt_amy_fwd	GACT**GAATTC**TAATACGACTCACTATAGGGCTGATTGTATCCTTCGG	Amplification of the *B. amyloliquefaciens ribD* RS aptamer with addition of a T7 promoter sequence
P132	T7_ribDRSapt_amy_rev	TAGC**AAGCTT**TCTCATCCTTCTCCCATCC	
P133	$ribR_{amy}$_pET_fwd	GACTGC**ATAT**GATGAAGCAT	Amplification of $ribR_{amy}$ for insertion into pET28a
P134	$ribR_{amy}$_pET_rev	ATGTT**CTCGAG**TCAAGCC	
P135	$ribR_{amy}$_pMAL_fwd	GCAG**GTCGAC**ATGAAGCATTCAACTGTCCC	Amplification of $ribR_{amy}$ for insertion into pMAL vectors
P136	$ribR_{amy}$_pMAL_rev	TACA**CTGCAG**TCAAGCCTGGCGTTTTGC	
P137	$ribR_{sub}$_RR-AA_fwd	AACTGGTTTTTTGAGTACGGAATTACACAAGTAGCTTACgcagcgATTTATATTTTATCTTTTTTAAGCTTTTTGAAAGAAGATA	Site-directed mutagenesis, change coding sequence of RR motif in $ribR_{sub}$ to AA
P138	$ribR_{sub}$_RR-AA_rev	TATCTTCTTTCAAAAAGCTTAAAAAAGATAAAATATAAATcgctgcGTAAGCTACTTGTGTAATTCCGTACTCAAAAAACCAGTT	
P139	$ribR_{amy}$_RR-AA_fwd	GGGCATCATTCCCATTCCCGTCgcagcgCTTTATGTGCTGGCGTTTCTCG	Site-directed mutagenesis, change coding sequence of RR motif in $ribR_{amy}$ to AA
P140	$ribR_{amy}$_RR-AA_rev	CGAGAAACGCCAGCACATAAAGcgctgcGACGGGAATGGGAATGATGCCC	
P141	ribR_RTout_fwd	CAGGAGGCGGTACATATGAA	Reverse transcription *B. subtilis ribR* gene
P142	ribR_RTout_rev	TTCAAGCCTGGCGTTTTGC	
P143	ribR_RTin_fwd	GCATTCAACTGTCCCTTTCCG	Amplification of *B. subtilis ribR* cDNA
P144	ribR_RTin_rev	GTTTTGCTGCGCACTCCTG	
P145	citZ_RTout_fwd	GGTCTTGAAGGGGTTGTAG	Reverse transcription of *B. subtilis citZ* gene
P146	citZ_RTout_rev	CGTACTCTTCCTTCGGTTC	
P147	citZ_RTin_fwd	CAACAACATCATCTGTAAGC	Amplification of *B. subtilis citZ* cDNA
P148	citZ_RTin_rev	GCCCTTTACGGATTCTTGAG	

2.7 Programs and databases

The programs, software and databases used in the current study are listed in Table 20.

Table 20: Programs and databases used in this study.

Software/ Database	Use	Reference
AlphaFold	Protein structure database	https://alphafold.ebi.ac.uk/
BLASTn/BLASTp	Search for and comparison of specific nucleotide or amino acid sequences	https://blast.ncbi.nlm.nih.gov/Blast.cgi
Cas-OFFinder	Search for potential off-target sites of Cas9 guide RNAs	Bae *et al.*, 2014
CLC Main Workbench	DNA and protein sequence analysis and design	QIAGEN GmbH, Hilden, Germany
Clustal Omega	Creation of multiple sequence alignments	https://www.ebi.ac.uk/Tools/msa/clustalo/
CRISPick	Design of CRISPRko single guide RNAs (sgRNA)	Doench *et al.*, 2016
GraphPad Prism 9	Statistical analysis and presentation of data	GraphPad Software Inc., Boston, MA, USA
ImageJ, Fiji	Gel image processing and analysis	https://imagej.net/ij/
Image Lab	Agarose gel visualization and analysis	Bio-Rad Laboratories GmbH, Feldkirchen, Germany
InterPro	Protein domain classification and analysis database	https://www.ebi.ac.uk/interpro/
MEGA 11	Generation of phylogenetic trees	Tamura *et al.*, 2021
Microsoft Excel	Data preparation and processing	Microsoft, Redmond, WA, USA
NEBio Calculator	Calculation of ligation	https://nebiocalculator.neb.com/#!/ligation
NEB Tm Calculator	Calculation of annealing	https://tmcalculator.neb.com/#!/main
PASIFIC	Structure prediction and identification of *cis* regulation	https://www.weizmann.ac.il/molgen/Sorek/PASIFIC/
PyMOL	Visualization of protein structures	DeLano, 2002
QuikChange Primer Design Tool	Primer design for site-directed mutagenesis	https://www.agilent.com/store/primerDesignProgram.jsp
RNAfold	RNA structure prediction	http://rna.tbi.univie.ac.at/cgi-bin/RNAWebSuite/RNAfold.cgi
SubtiWiki	Database for genes and proteins from *B. subtilis*	http://subtiwiki.uni-goettingen.de/
VARNA	Visualization of RNA secondary structures	https://varna.lisn.upsaclay.fr

3 Methods

3.1 Microbiological methods

3.1.1 Cultivation of bacterial strains

All bacterial strains used were either grown in LB medium (Table 2) or in a minimal medium. The LB medium was generally used for protein production, plasmid and gDNA extractions and cryoconservation. For the β-galactosidase and luciferase assays, *E. coli* strains were grown in M9 medium (Table 3) with 0.4% (w/v) glucose as a carbon source and 0.1% (w/v) casamino acids. Cultures of *E. coli* DH5α were additionally supplemented with 20 nM of thiamine. *K. pneumoniae* was also grown in M9 medium with 0.4% glucose and 0.1% casamino acids. For *B. subtilis* and *B. amyloliquefaciens*, a specific *Bacillus* minimal medium (Table 4) according to Coppée *et al.* (2001) was used for cultivation. Either 4 mM of $MgSO_4$ or 1 mM methionine/5 mM taurine was added as a sulfur source. For the *B. subtilis* 168 strains, the medium was supplemented with 20 µg/mL of tryptophane. When required, antibiotics were added to the media for selection. All antibiotics and the respective concentrations used for the different bacterial strains are listed in Table 21.

Pre-cultures were grown in test tubes in 6-10 mL of medium or in a 24-well plate with a culture volume of 1 mL per well, while cultures with a larger volume were grown in baffled shake flasks. Generally, *E. coli* and *K. pneumoniae* cultures were incubated in a shaking incubator at 180 rpm and 37 °C, while *B. subtilis* cultures were grown at 30 °C with shaking at 150-180 rpm. When incubation parameters for certain assays differed from the general conditions described above, it is stated in the respective method section.

Table 21: Antibiotics used for selection of recombinant *E. coli* and *B. subtilis*.

Antibiotic compound	Stock conc. (1000x) mg/mL	Final conc. *E. coli* µg/mL	Final conc. *B. subtilis* µg/mL
Ampicillin (in H_2O)	100	100	-
Kanamycin (in H_2O)	50	50	15

3.1.2 Conservation of bacterial strains

All newly generated bacterial strains were conserved as glycerol stocks at -80 °C. The stocks were prepared by mixing 700 µL of a fresh LB overnight culture with 300 µL of 80% (v/v) glycerol in a cryo tube on ice. The tubes were then immediately frozen in a -80 °C freezer. To recover cells from the stocks, a small amount of the frozen bacteria was scraped off with a

sterile pipette tip or inoculation loop and streaked onto a fresh LB agar plate containing the respective antibiotics.

3.1.3 Growth experiments

Growth experiments of *K. pneumoniae* were performed in M9 medium supplemented with 0.1 % casamino acids. 200-300 µM of either thiamine or pyrithiamine were added to the medium. The cultures grew in a 12-well plate with a culture volume of 2 mL. Plates were placed in a humidity cassette and incubated in a plate reader (Tecan Spark) at 37 °C, with a double-orbital shaking movement and an amplitude of 6. OD_{600} measurements were taken automatically every 45 minutes.

3.1.4 Selection of pyrithiamine-resistant *K. pneumoniae*

For selection of pyrithiamine-resistant *K. pneumoniae* strains, a similar approach was used as previously described for *E. coli* and *B. subtilis* (Sudarsan *et al.*, 2005). Pre-cultures of *K. pneumoniae* grown in M9 minimal medium with 0.4% glucose were diluted 1/100 in 100 µL M9 medium cultures in a transparent 96-well plate (Greiner Bio-One GmbH, Frickenhausen, Germany). The cultures were either supplemented with 1 mM of pyrithiamine or an equal volume of H_2O as a control. The plate was incubated at 37 °C and shaking at 180 rpm in a humidity cassette to avoid evaporation. The growth of the strains was monitored by regular absorption measurements at 600 nm in a microplate reader (Tecan Spark). When the cultures reached the stationary phase, 1 µL of each culture was used to inoculate a fresh 100 µL M9 culture containing 1 mM of pyrithiamine. The passaging was continued until the cultures containing pyrithiamine showed approximately the same growth curve as the *K. pneumoniae* WT in a culture without pyrithiamine. The cultures were then diluted and plated on M9 minimal agar containing 1 mM pf pyrithiamine to obtain single colonies.
From these colonies, 13 resistant clones from 13 individually selected cultures were picked and used for a colony PCR (see section 3.2.4.1) to amplify the four different TPP riboswitch regions Kp01 (Table 19, primers 15/16), Kp04 (primers 17/18), Kp10 (primers 19/20) and Kp11 (primers 21/22). The riboswitch regions were sequenced using the same primer pairs and compared to the *K. pneumoniae* WT sequences.

3.1.5 Generation of competent cells and bacterial transformation

3.1.5.1 Competent cells and transformation of *E. coli*

To generate competent cells of *E. coli* strains, 100 mL of LB medium in a 300 mL Erlenmeyer flask with baffles were inoculated from an overnight culture to an OD_{600} of approximately 0.1. The culture was incubated at 37 °C and 180 rpm until an optical density of 0.6 was reached. The total culture volume was transferred to two 50 mL conical centrifugation tubes and from now on, all steps were performed on ice. The tubes were centrifuged at 5000 rpm for 15 minutes at 4 °C. After the supernatant was discarded, each cell pellet was resuspended in 16 mL of RF1 (Table 6), followed by an incubation on ice for 15 minutes. The cell suspensions were centrifuged again under the same conditions as before. Each cell pellet was then resuspended in 4 mL of RF2 (Table 6), the suspended cells were reunited. Following a final incubation on ice for 15 minutes, the suspension was divided in aliquots of 100 µL and immediately stored at -80 °C.

For the transformation, 50 µL of competent *E. coli* cells were thawed on ice and were added to a 1.5 mL microcentrifuge tube containing 50-100 ng of plasmid DNA in a small volume of water (1-2 µL) or a ligation mixture containing 50-100 ng of ligated plasmid. The competent cells and the DNA were mixed very carefully. The mixture was incubated for 30 minutes on ice. The cells were then subjected to a heat shock of 42°C for one minute, either in a thermoblock or in a water bath. The mixture was immediately placed back on ice for 5 minutes. Then 500 µL of sterile LB medium were added to the transformation mix and the tube was incubated at 200 rpm for one hour at 37 °C. After the regeneration time, the *E. coli* cells were centrifuged for 3 minutes at 6000 x *g*, concentrated in 100 µL of the supernatant and plated on LB agar supplemented with the appropriate antibiotics and the plates were incubated overnight at 37 °C.

3.1.5.2 Competent cells and transformation of *B. subtilis*

Fresh *B. subtilis* cell material was scraped off an agar plate and used to inoculate 20 mL of freshly prepared, prewarmed SpC medium (Table 5) supplemented with 20 µg/mL of tryptophane in a 100 mL baffled shake flask to obtain an initial OD_{600} of ~0.5. The culture was incubated at 37 °C with vigorous aeration and cell growth was monitored by periodic OD_{600} readings. When the cells had just entered the stationary phase, 2 mL of the culture were used to inoculate 200 mL of fresh, prewarmed SpII medium (Table 5) with tryptophane in a 500 mL baffled shake flask. After an incubation time of 1.5 hours at 37 °C with slower aeration, the cells were harvested by centrifugation at 8000 x *g* for 5 minutes at room temperature. The supernatant was carefully decanted and saved in a sterile container. The remaining cell pellets were resuspended in 18 mL of the saved supernatant and mixed gently with 2 mL of glycerol.

This suspension was divided into aliquots of 500 µL in sterile microcentrifuge tubes and frozen immediately at -80 °C.
For the transformation, competent cells were rapidly thawed in a 37 °C water bath. One volume of SpII (without $CaCl_2$) + 2% EGTA (0.1 M, pH 8) was immediately added to the defrosted cells and mixed gently. 500 µL of the cell suspension were added to ~1000 ng of plasmid DNA in a microcentrifuge tube. The tube was incubated at 37 °C with shaking at 180 rpm for one hour. After the regeneration time, the *B. subtilis* cells were centrifuged for 3 minutes at 6000 x *g*, concentrated in 100 µL of the supernatant and plated on LB agar supplemented with the appropriate antibiotics (Table 21). The plates were incubated overnight at 30 °C.

3.1.6 Overproduction of proteins in *E. coli*

To overproduce proteins, the *E. coli* expression strains BL21 and BL21 pLysS were transformed with the pET28a vector carrying the $ribR_{amy}$ gene under control of an IPTG-inducible T7 promoter. For the overproduction of the MBP-tagged RibR versions, *E. coli* ER2523 (NEBExpress, New England Biolabs GmbH, Frankfurt a. M., Germany) were transformed with the pMAL-c6T or pMAL-c5X expression vectors (New England Biolabs GmbH, Table 18), carrying the *malE* gene, coding for the maltose-binding protein (MBP6), fused to the different *ribR* versions under control of the IPTG-inducible tac promoter (see section 3.2.11.6).
For all *E. coli* expression strains, pre-cultures were grown in 10 mL of LB medium with 100 µg/mL ampicillin in test tubes. The next day, main cultures of 300 mL of LB with 100 µg/mL of ampicillin were prepared in a 1 L shake flask with baffles and inoculated from the pre-cultures to an OD of 0.1. For strains with the pMAL-c6T or pMAL-c5X plasmid the medium was additionally supplemented with 0.2 % of glucose to repress the *E. coli* maltose genes. All cultures were grown at 37 °C and 180 rpm. *E. coli* BL21 and BL21pLysS cultures were induced with 0.1 mM of IPTG when they had reached an OD_{600} of 0.6 and *E. coli* ER2535 cultures were induced with 0.3 mM of IPTG at an OD_{600} of 0.5. After induction the BL21 strains were grown for another two hours, while the ER2535 cultures were incubated for 2-3 hours more at 30 °C. For each strain, an uninduced culture was grown in parallel as a control. After this time, cultures were harvested in centrifuge bottles at 4000 x *g* for 20 minutes. For a subsequent FPLC purification the cell pellets of three 300 mL cultures were united upon harvesting. The supernatant was discarded, and the cell pellets were kept at -20 °C until cell lysis.

3.2 Molecular biological methods

3.2.1 Plasmid preparation

Plasmids were isolated using the GeneJET Plasmid Miniprep Kit (Thermo Fisher Scientific, Waltham, USA) according to the instructions of the manufacturer. Pre-cultures of *E. coli* strains harboring the respective plasmid were grown overnight in LB medium supplemented with the appropriate antibiotics. 1- 2 mL of the culture volume were transferred to a microcentrifuge tube and centrifuged at 6000 x *g* for 3 minutes at room temperature (Microcentrifuge 5415 R, Eppendorf, Hamburg, Germany). The supernatant was discarded, and plasmid extraction was performed from the cell pellets. For preparation of the plasmids used for *in vitro* transcription of riboswitch aptamers, the GeneJET Plasmid Maxiprep Kit was used with adjusted cell culture volumes, according to the recommendations of the manufacturer. Plasmids were always eluted with 30-40 µL of ultrapure H_2O for the Miniprep kit and 700 µL of H_2O for the Maxiprep kit.

3.2.2 Preparation of genomic DNA

Genomic DNA from *E. coli* and *B. subtilis* was extracted using the Genomic DNA Purification Kit (Thermo Fisher Scientific, Waltham, USA), according to the instructions of the manufacturer for either Gram-negative or Gram-positive bacteria. The DNA was eluted with ultrapure H_2O.

3.2.3 Preparation of total RNA

Total RNA from *B. subtilis* strains grown under varying conditions was extracted using the Quick-RNA Miniprep Plus Kit (Zymo Research Europe GmbH, Freiburg, Germany), according to the instructions of the manufacturer. The on-column DNase I treatment was included in the protocol. An additional in-tube DNaseI treatment was performed to ensure that no residual DNA was present in the RNA samples, followed by a second clean-up using the RNA Clean & Concentrator-5 kit (Zymo Research Europe GmbH, Freiburg, Germany), according to the instructions of the manufacturer. The RNA was eluted with the provided nuclease-free water and the samples were stored at -80 °C until further usage.

3.2.4 Polymerase chain reactions

For amplification of specific DNA sequences and identification of transformants and mutants, polymerase chain reactions (PCR) were performed using Phusion Hot Start II DNA Polymerase (Thermo Fisher Scientific, Waltham, USA). Reaction mixtures were prepared according to the recipe in Table 22.

Table 22: Reaction mixtures for PCR amplifications with the Phusion HS II DNA Polymerase.

Component	Volume/ µL
Template DNA	20-50 ng
5x High GC buffer	10
Reverse primer (10 µM)	2.5
Forward primer (10 µM)	2.5
dNTP mix (10 mM)	2
Phusion HS II DNA polymerase (2 U/µL)	0.5
ddH_2O	*ad* 50 µL

The general thermocycler settings for all PCR reactions using different polymerases are given in Table 23. The annealing temperatures for all primer pairs used were calculated using the New England Biolabs Tm calculator. For Phusion polymerase reactions, the actual annealing temperature was set two degrees lower than the calculated annealing temperature.

Table 23: Thermocycler settings for PCR amplifications with the Phusion HS II and the DreamTaq DNA polymerases.

Reaction step	Phusion HS II			DreamTaq		
	Temp./ °C	Duration	Cycles	Temp./ °C	Duration	Cycles
Initial Denaturation	98	30 s	x 1	95	3 min	x 1
Denaturation	98	10 s	x 30	95	30 s	x 25
Annealing	primer specific	15 s		primer specific	30 s	
Elongation	72	15-30 s/kb		72	30-60 s/kb	
Final Elongation	72	5 min	x 1	72	10 min	x 1
Cooling	12	∞		12	∞	

3.2.4.1 Colony PCRs

PCR reactions with bacterial colonies as a template were used to identify positive transformants of *E. coli* and *B. subtilis* and to amplify the TPP riboswitch regions of pyrithiamine-resistant mutants of *K. pneumoniae*. For the latter, the Phusion polymerase was used to decrease the risk of amplification-based errors in the sequence, while the colony PCRs for *E. coli* and *B. subtilis* were performed with the DreamTaq DNA polymerase (Thermo Fisher Scientific, Waltham, MA, USA). The respective thermocycler settings are listed in Table 23.
For colony PCRs of *E. coli* colonies, reaction mixtures for the DreamTaq DNA polymerase with a final volume of 10 µL and a small amount of the respective bacterial colony as a template were set up (Table 24). *B. subtilis* colonies of 2-3 mm in diameter were each suspended in

40 µL of ultrapure H_2O. The cell suspensions were incubated at -80 °C for 20 minutes followed by a 10-minute incubation at 99 °C. The samples were then briefly vortexed and spun down. The freeze/boil cycle was repeated three times before the tubes were centrifuged at 6000 x *g* for 10 minutes and 5 µL of the supernatant were used as a template for a 40 µL PCR reaction with the DreamTaq DNA polymerase (Table 24).
For colony PCRs of *K. pneumoniae*, the respective colony was suspended in 10 µL of ultrapure H_2O and incubated at 99 °C for 10 minutes. 1 µL of the cell suspension was used as the template for a 10 µL PCR reaction with the Phusion Hot Start II DNA Polymerase (Table 22).

Table 24: Reaction mixtures for PCR amplifications with the DreamTaq DNA Polymerase.

Component	Volume/ µL
Template DNA	colony
10x DreamTaq Green buffer	1
rev primer (10 µM)	0.2
fwd primer (10 µM)	0.2
dNTP mix (10 mM)	0.2
DMSO	0.5
DreamTaq DNA polymerase (5 U/µL)	0.1
ddH_2O	*ad* 10 µL

3.2.5 Restriction and ligation of DNA fragments and plasmids

DNA fragments and plasmids were digested for cloning with Fast Digest Restriction Enzymes (Thermo Fisher Scientific, Waltham, MA, USA), listed in Table 25. For a 10 µL reaction 1 µL of total restriction enzyme were used. To prevent religation, the FastAP Thermosensitive Alkaline Phosphatase (Thermo Fisher Scientific, Waltham, MA, USA) was added to the restriction reaction of plasmids, according to the instructions of the manufacturer. For DNA fragments, 200-300 ng per 10 µL reaction were digested, for plasmids 1000 ng per 10 µL were used. Either the 10x FastDigest buffer or the 10x FastDigest Green buffer (Thermo Fisher Scientific, Waltham, MA, USA) were used in the restriction reactions. Reaction mixtures were incubated at 37 °C for a specified time, depending on the required duration indicated for each restriction enzyme (Table 25). If necessary, reactions were stopped with an incubation at 80 °C for 10-20 minutes.

Table 25: Restriction endonucleases used in this study with respective restriction sites and required incubation times. The digestion times and the maximum incubation times were taken from the table "Reaction Conditions for FastDigest Enzymes" on the website of the manufacturer (https://www.thermofisher.com/).

Restriction enzyme	Restriction site	Digestion time in min with 1 µL of restriction enzyme		Max. incubation time without star activity
		Plasmid DNA (1 µg/20 µL)	DNA fragments (200 ng/30 µL)	
FastDigest *Bam*HI	G|GATCC	5	5	1 h
FastDigest *Bgl*I	GCCNNNN|NGGC	5	5	2 h
FastDigest *Eco*RI	G|AATTC	5	20	0.5 h
FastDigest *Eco*31I	$GGTCTC(N)_1$	5	5	16 h
FastDigest *Dpn*I	GA^{CH_3}|TC	5	not applicable	16 h
FastDigest *Hin*dIII	A|AGCTT	5	20	16 h
FastDigest *Kpn*I	G|GTACC	5	5	16 h
FastDigest *Nco*I	C|CATGG	10	10	16 h
FastDigest *Nde*I	C|ATATG	5	60	6 h
FastDigest *Pst*I	C|TGCAG	5	30	16 h
FastDigest *Pvu*II	CAG|CTG	5	5	0.5 h
FastDigest *Sac*I	GAGCT|C	15	30	16 h
FastDigest *Sal*I	G|TCGAC	5	60	16 h
FastDigest *Xba*I	T|CTAGA	5	5	16 h
FastDigest *Xho*I	C|TCGAG	5	5	16 h

For ligation of the restriction products, the linearized vector and the respective restricted DNA insert were mixed in a 5:1 ratio. Typically, 50 ng of vector was used per reaction. The insert quantities required were calculated using the New England Biolabs ligation calculator. Ligations were performed using T4 DNA ligase and the related T4 DNA ligase buffer (Thermo Fisher Scientific, Waltham, MA, USA), according to the instructions of the manufacturer.

3.2.6 Agarose gel electrophoresis of DNA

Agarose gel electrophoresis was used to verify the correct amplification of DNA fragments and restriction of plasmids. DNA samples were mixed with 6x DNA Gel Loading Dye (Thermo Fisher Scientific Inc., Waltham, MA, USA) and loaded onto the gel. 1-2 % (w/v) agarose gels were prepared and run at 120-130 V with Tris-Acetate-EDTA (TAE) buffer (Table 8) for 30-45 minutes. For colony PCR reactions performed with the DreamTaq Green buffer, no loading dye had to be added to the samples. Either the GeneRuler™ 1 kb or the 100 bp DNA Ladder (Thermo Fisher Scientific) were included in every run to allow comparison of fragment lengths. Following the electrophoretic separation, agarose gels were incubated in an ethidium bromide solution (0.01 µg/mL) for 20 minutes and destained in distilled H_2O for 5 minutes.

Subsequently, DNA bands were visualized with an UV-light imager (GelDoc™ XR Imaging System, Bio-Rad Laboratories GmbH, Feldkirchen, Germany).

3.2.7 Polyacrylamide gel electrophoresis of RNA

For analyzation of RNA transcription, an 8 % (w/v) denaturing polyacrylamide urea gel (Table 10) was loaded with RNA samples mixed with a 2x RNA loading dye (formamide with 25 mM EDTA, pH 8 + bromophenol blue). RNA gels were run with 1x Tris-Borate-EDTA (TBE) buffer (Table 9) in a Mini-Vertical Electrophoresis System (CBS Systems, San Diego, CA, USA) at 180 V for 20-30 minutes. The gels were stained in an ethidium bromide solution (0.01 µg/mL) for 5 minutes and the RNA bands were visualized with an UV-light imaging system. The conditions used for preparative RNA gels are described in section 3.2.15.

3.2.8 DNA purification

Linear DNA from polymerase chain reactions or restriction reactions was normally purified with the GeneJET PCR Purification Kit (Thermo Fisher Scientific, Waltham, MA, USA), according to the instructions of the manufacturer. The DNA was eluted from the column with 20-40 µL of ultrapure H_2O.

The *Hin*dIII-linearized plasmid pSP64 was purified from the 5 mL restriction reaction via phenol-chloroform extraction. 5 mL of a phenol/chloroform/isoamyl alcohol mix (25:24:1, v/v) (Carl Roth GmbH + Co. KG, Karlsruhe, Germany) were added to the restriction reaction in a 50 mL conical tube. The tube was centrifuged at 4 °C and maximum speed for 20 minutes. The aqueous phase was then carefully transferred to a fresh tube and mixed with one volume of a chloroform/isoamyl alcohol mixture (24:1, v/v). the tube was vortexed and again centrifuged at 4 °C and maximum speed for 20 minutes. The aqueous phase was transferred to a fresh tube and mixed with 1.2 volumes of ice-cold isopropanol (100 %). After the mixture was incubated at -20 °C for 20 minutes, a third centrifugation was performed under the same conditions as before. The supernatant was carefully discarded, and the DNA pellet was washed with 2 mL of 70 % ethanol. The tube was centrifuged again at 4 °C and maximum speed for 15 minutes. The ethanol was carefully removed, and the DNA pellet was dissolved in 200 µL of ultrapure H_2O.

3.2.8.1 Gel extraction of linear DNA

DNA fragments or linearized plasmids used for cloning were usually purified from an agarose gel to ensure that there were as little contaminations with unwanted DNA or unrestricted vector as possible. The gel purification was performed with the Monarch DNA Gel Extraction Kit (New

England Biolabs GmbH, Frankfurt a. M., Germany), following the instructions of the manufacturer. Elution was performed in 10-15 µL of prewarmed, ultrapure H_2O.

3.2.9 Concentration measurements of nucleic acids and DNA sequencing

3.2.9.1 Measuring DNA and RNA concentrations

Concentrations of DNA and RNA solutions were determined by absorption measurement. For this purpose, 2 µL of the respective nucleic acid solution were applied to a NanoQuant plate (Tecan, Männedorf, Switzerland) and the absorption at 260 nm was measured in a plate reader (Tecan Spark). Additionally, the ratios of the absorptions at 230/260 nm and 260/280 nm were determined to check for DNA/RNA purity.

3.2.9.2 DNA sequencing

Sequencing of PCR products and plasmids was performed by LGC Genomics GmbH (Berlin, Germany). In accordance with the suggestions of the service company, plasmids were diluted to a concentration of 100 µg/µL, while linear DNA fragments were diluted to a concentration of 10-40 µg/µL, depending on the fragment size. 2 µL of the respective sequencing primer (10 µM) were added to 10 µL of the DNA solution and the total volume of the sequencing mixture was adjusted to 14 µL with ddH_2O. Sequencing was performed according to the Sanger sequencing method (Sanger *et al.*, 1977). The obtained sequencing results were analyzed using the software CLC Main Workbench 20.

3.2.10 Reverse Transcriptase (RT) -PCR

Reverse transcription of specific regions of total RNA was used to determine the presence of certain mRNAs and, to some extent, the quantity of these transcripts. Total RNA was extracted according to the protocol in section 3.2.3. from *B. subtilis* strains grown in *Bacillus* minimal medium supplemented with either $MgSO_4$ or methionine/ taurine as a sulfur source. The cultures were either grown without diamide (-dia), or with 0.5 mM of diamide (+dia) and harvested at an OD_{600} of 0.8**.** Additionally, cultures were included where diamide was added at an OD_{600} of 0.8 and cells were harvested 2 hours later (2h ind.) together with cells from the diamide-free control culture.

The total extracted RNA was used as a template for a PCR reaction with the reverse transcriptase, an enzyme that transcribes mRNA back into cDNA. For the reaction, random hexamer oligonucleotides, as well as specific primers for the regions of interest were used. In addition to the *ribR* gene, the transcription of the *citZ* gene of *B. subtilis* was examined. This gene should be expressed constitutively, independently of the different growth conditions, and

was therefore used as a housekeeping gene and positive control of the reverse transcription. The respective primer pairs used for the reverse transcription of the *ribR* (P141/P142) and *citZ* (P145/P146) mRNA are listed in Table 19.

The RT-reaction was performed using the Maxima First Strand cDNA synthesis kit for RT-qPCR (Thermo Fisher Scientific, Waltham, MA, USA). The composition of the RT-PCR reaction mixture is shown in Table 26. Negative control reactions without any RNA template (RT nc) were included for both specific primer pairs for *ribR* and *citZ*. Additionally, a control reaction without the reverse transcriptase (RT-) was included for all RNA templates to check for possible DNA contaminations.

Table 26: Reaction mixture for the RT-PCR reactions performed with the Maxima First Strand cDNA synthesis kit.

Component	Volume/ µL
Template RNA	3-4 µg
5x reaction mix	4 µL
Rev primer (10 µM)	3 µL
Fwd primer (10 µM)	3 µL
Maxima enzyme mix	2 µL
ddH_2O	*ad* 20 µL

The reaction mixtures were gently mixed and incubated for 10 minutes at 25 °C, followed by 30 minutes at 50 °C. The reaction was terminated with a 5-minute incubation at 85 °C.

Subsequently, 2.5 µL of each reverse transcription reaction were used as a template for a PCR reaction with the Phusion DNA polymerase (see chapter 3.2.4). For a specific amplification of the regions of interest, the internal primers for the cDNA of the *ribR* P143/P144 and the *citZ* P147/P148 gene were used.

3.2.11 Plasmid and strain construction

The construction of all plasmids used in this study is described in the following paragraphs. All basic plasmids used and created in this study are listed in Table 18. All oligonucleotides used for plasmid construction, amplifications and sequencing are listed in Table 19. The specifically designed insert sequences including riboswitch regions, riboswitch promoter control regions, promoters, terminators and homology repair templates are provided in the supplementary material (Table S3, Table S4, Table S5).

3.2.11.1 β-galactosidase reporter plasmid pHAt191l

For construction of the β-galactosidase reporter gene plasmid, the pUC19 vector backbone was used. To delete the *lac* promoter, the whole plasmid was amplified with the overlapping oligonucleotides P1 and P2 (Table 19) and the resulting sequence with complementary overhangs was ligated again to create the plasmid pUC19del. The *lacZ* reporter gene for a translational fusion was amplified from the plasmid pDG268, using the primer pair P3/P4 and inserted into a *Xba*I/*Eco*RI restricted pUC19del plasmid, creating the plasmid pHA191. The terminator sequences for the *lac* terminator and the *rrnB* T1 terminator (Table S3) were both amplified from genomic DNA of *E. coli* MG1655 with the modifying primer pairs P5/P6 and P7/P8, respectively. The *rrnB* T1 terminator was inserted between the *Sap*I and *Hin*dIII restriction sites upstream of *lacZ*, while the *lac* terminator was inserted downstream of *lacZ* at the *Eco*RI restriction site, creating the plasmid pHAt191l.

The TPP riboswitch region Ec01 from *E. coli*, including the respective promoter, ribosomal binding site and the first few codons of the downstream gene *thiC* was amplified from genomic DNA with the oligonucleotide pair P9/P10 and inserted between the *Hin*dIII and *Xba*I restriction sites of the plasmid to generate the reporter plasmid pHAt191l::Ec01. To create the promoter control plasmid pHAt191l::pEc01, the *E. coli thiC* promoter region was individually amplified with the oligonucleotides P9 and P11 and inserted between the *Hin*dIII and *Pst*I restriction sites of pHAt191l. Subsequently, the ribosomal binding site together with the start of the coding sequence of *thiC* was amplified with the primer pair P10/P12 and inserted downstream of the promoter region between the *Pst*I and the *Xba*I restriction site. The reporter plasmid pHAt191l::Kp04 and control vector pHAt191l::pKp04 for the *thiC* riboswitch from *K. pneumoniae* were generated in a similar way. Both, the riboswitch region and the control insert were designed and obtained as custom DNA constructs cloned into the GeneArt pMA plasmid (Thermo Fisher Scientific, Waltham, MA, USA). This eliminated the intermediate cloning step for the promoter control construct. The two inserts were amplified from the pMA plasmid using the oligonucleotide pair P13/P14 and cloned into *Hin*dIII/*Xba*I restricted pHAt191l. All cloning steps described were individually verified by sequencing of the generated plasmids (P23-P28). The plasmids were propagated using *E. coli* DH5α.

3.2.11.2 Dual-luciferase plasmid pDluc

The dual-luciferase plasmid was constructed based on the plasmid pPrib-RibDG-RFN-luc (Pedrolli, Kühm, *et al.*, 2015), which originated from the single-luciferase reporter plasmid pT7luc (Promega, Mannheim, Germany). To generate a dual-luciferase plasmid, a second luciferase gene with a codon-optimized sequence coding for the *Renilla reniformis* luciferase (luc^R) was inserted downstream of the firefly luciferase gene (luc^F) on the pPrib-RibDG-RFN-luc plasmid. This luc^R gene was placed under control of the strong constitutive promoter

OXB15 (derived from the *recA* promoter by random mutagenesis, Oxford Genetics Limited, Oxford, UK), which, and was used as an internal control reporter.

The *rrnB* T1 terminator sequence (Table S3) was produced by PCR from *E. coli* gDNA with the primer pair P42/P43 (Table 19), introducing *Sac*I restriction sites at each end of the fragment and an additional *Xho*I restriction site at the 3'-end of the terminator sequence. The *rrnB* T1 fragment was ligated to the *Sac*I restricted pPrib-RibDG-RFN-luc plasmid, downstream of luc^F to generate the plasmid pPrib-RFN-luc-t. A *Kpn*I restriction site was introduced into the plasmid 12 base pairs downstream of the new *Xho*I site by amplifying the whole plasmid using the overlapping primers P44 and P45 and religation of the resulting sequence.

The DNA sequence comprising the OXB15 promoter and the codon-optimized luc^R gene (Table S3) was obtained as a custom DNA string (Thermo Fisher Scientific, Waltham, MA, USA), amplified using the modifying oligonucleotide pair P46/P47 and ligated to the *Xho*I/*Kpn*I restricted pPrib-luc.t, creating the plasmid pPrib-RFN-Dluc. Since the luc^R sequence contains a *Hin*dIII restriction site, the *Hin*dIII binding site upstream of luc^R in pPrib-RFN-Dluc was replaced with an *Nco*I site by a site-directed mutagenesis reaction (see 3.2.12) using the overlapping oligonucleotides P48 and P49. To delete the FMN riboswitch sequence from the plasmid, the complementary oligonucleotides P50 and P51, containing an RBS sequence and an ATG start codon, were used. The two oligonucleotides (10 µM each) were mixed in 1x NEBuffer™ 2 (New England Biolabs GmbH, Frankfurt a. M., Germany) and annealed by heating the mixture to 98 °C for 5 minutes before slowly cooling it down to room temperature. Thereby, a linker with sticky ends was generated to be ligated into the *Nco*I/*Bam*HI restricted pPrib-RFN-Dluc, creating the plasmid pPrib-Dluc. To remove the *rib* promoter sequence from this plasmid, the complementary oligonucleotides P52 and P53 were annealed to create a second linker with a blunt end and a sticky end to be inserted into the *Pvu*II/*Nco*I restricted pPrib-Dluc. The generated double-strand linker was ligated to pPrib-Dluc to create the translational fusion plasmid pDluc (Figure 10A). Another site-directed mutagenesis reaction with the primer pair P53/P54 was used to insert a stop codon and a ribosomal binding site upstream of luc^F, as well as a start codon for the luc^F gene to generate the transcriptional fusion plasmid pDlucTC (Figure 10B). For testing the TPP riboswitch function, the *thiC* promoter of *E. coli* (Table S3) was amplified with the primers P56 and P58 and the promoter region was ligated into the *Pvu*II/*Nco*I restricted pDluc and pDlucTC plasmid respectively, creating plasmids pDluc::pEc01 and pDlucTC::pEc01.

The TPP riboswitch regions from different bacterial species including the promoter, riboswitch, RBS together with the first few codons of the downstream gene (Table S4) were obtained as custom DNA constructs cloned into the GeneArt pMA plasmid (Thermo Fisher Scientific, Waltham, MA, USA). The riboswitches Ab01, Kp04, Eb01, Eb03, Ms01, Ms02, Pa01 and Sa02 were amplified from these templates using the respective primer pairs P59/P60, P64/P65,

P67/P68, P69/P70, P71/P72, P74/P75, P77/P78 and P79/P80 (Table 19), creating inserts with sticky ends for ligation with the *Nco*I/*Bam*HI restricted pDluc::pEc01 plasmid and (except for Sa02) the pDlucTC::pEc01 plasmid. For the TPP riboswitches Ec01, Ab01, Ef02, Kp04, Ms01, Ms02, Sp06, Kp01, Kp10 and Kp11 the whole regions including the native riboswitch promoter were amplified from the custom templates using the respective primer pairs P56/P57, P60/P61, P62/P63, P65/P66, P72/P73, P75/P76, P81/P82, P83/P84, P85/P86 and P87/P88. The amplified riboswitch inserts were cloned between the *Pvu*II/*Bam*HI restriction sites of the pDluc and pDlucTC reporter plasmids. The respective promoter control regions consist of the native riboswitch promoter and the RBS together with the first codons of the downstream gene but lack the riboswitch sequence itself. These sequences were also obtained as custom DNA constructs and amplified using the same primer pairs.

To generate the reporter plasmids for the mutated Kp04 riboswitch versions, site-directed mutagenesis was performed (section 3.2.12) on the pDluc::Kp04 plasmid, using the respective mutagenic primer pairs (P89-P102, Table 19). All cloning steps described were individually verified by sequencing of the generated plasmids (P29-P33). The plasmids were propagated using *E. coli* DH5α and final plasmids were used to transform *E. coli* DH5α and *E. coli* MG1655.

3.2.11.3 CRISPR-Cas9 plasmids for *B. subtilis* genome editing

For the CRISPR-Cas9 genome editing, the vector pJOE8999.1 carrying the coding gene for the Cas9 enzyme was used. Spacer DNA sequences for the Cas9 guide RNA were designed using the CRISPick sgRNA design tool (Doench *et al.*, 2016) and candidates were tested for target specificity in *B. subtilis* with the Cas-OFFinder (Bae *et al.*, 2014). The double stranded spacer linkers were generated by annealing the complementary oligonucleotide pairs P103/P104 to target the *B. subtilis ribR* gene for complete deletion and deletion of the N-terminal domain (s1), P105/P106 for other modifications of the *ribR* sequence (s2) and P107/P108 for targeting the *ribD* FMN riboswitch sequence. (s3) The respective oligonucleotide pairs (10 µM each) were mixed in 1x NEBuffer™ 2 (New England Biolabs GmbH, Frankfurt a.M., Germany) and annealed by heating the mixture to 98 °C for 5 minutes before slowly cooling it down to room temperature. The dsDNA spacer sequences were then ligated into *Eco*31I-digested pJOE8999.1 in a Golden Gate assembly reaction (Table 27), generating the plasmids pJOEs1, pJOEs2 and pJOEs3.

The resulting plasmids were digested with *Sal*I and *Xba*I. The homology repair templates (HRT) for the different modifications of the *ribR* gene of *B. subtilis* and for the replacement of *ribR* and the *ribD* FMN riboswitch with the homologous sequences from *B. amyloliquefaciens* were obtained as custom DNA sequences cloned into the GeneArt pMA plasmid (Thermo Fisher Scientific, Waltham, MA, USA).

Table 27: Golden Gate assembly reaction for insertion of spacer sequences into pJOE8999.1.

Component	Volume/ µL
Vector (100 ng/µL)	1 µL
dsDNA spacer	1 µL
10x FastDigest buffer	2 µL
*Eco*31I	1 µL
T4 DNA ligase	0.5 µL
ddH_2O	*ad* 20 µL

All HRT sequences used (Table S5) were amplified using the respective primer pair (P109-P120, Table 19), thereby adding a *Sal*I restriction site at the 5'-end and an *Xba*I site at the 3'-end. Following the restriction digest, the HRT sequences were cloned into the *Sal*I/*Xba*I restricted pJOE8999 vector, carrying the appropriate spacer sequence. This created the final CRISPR-Cas9 plasmids pJOEs1::HRT-Δ*ribR*, pJOEs1::HRT-ΔN-*ribR*, pJOEs2::HRT-ΔC-*ribR*, pJOEs2::HRT-*ribR*^{m}_RR>AA, pJOEs2::HRT-*ribR*$_{amy}$ and pJOEs3::HRT-*ribD*-RS$_{amy}$. Site-directed mutagenesis (section 3.2.12) with the modifying primers P139/P140 was used to generate the plasmid pJOEs2::HRT-*ribR*$^m_{amy}$*_RR>AA* from pJOEs2::HRT-*ribR*$_{amy}$. The resulting pJOEs2::HRT-*ribR*$^m_{amy}$*_RR>AA* was used to replace the *ribR* gene in *B. subtilis* by a mutated version of *ribR*$_{amy}$, coding for the protein RibR$^m_{amy}$ (R54A/R55A).
Two rounds of site-directed mutagenesis (section 3.2.12) with the respective modifying primer pairs P121/P122 and P123/P124 were used to add a His$_6$-coding sequence to the 5'-end of the *ribR*$_{amy}$ gene on pJOEs2::HRT-*ribR*$_{amy}$. The resulting CRISPR plasmid pJOEs2::HRT-his$_6$-*ribR*$_{amy}$ was used to replace the *ribR* gene in *B. subtilis* by a *his*$_6$-tagged version of *ribR*$_{amy}$. All plasmids were propagated using *E. coli* DH5α and all cloning steps described were individually verified by sequencing of the generated plasmids (P34/P35).

3.2.11.4 *In vitro* transcription plasmids for FMN riboswitch aptamers

The plasmids used for the *in vitro* transcription of FMN riboswitch aptamers for the RibR binding assays were constructed based on the vector backbone of pSP64 (Promega, Mannheim, Germany), a gift from Dr. Michael Vockenhuber from the group of Prof. Dr. Beatrix Süß, Technische Universität Darmstadt. The *ribD* FMN riboswitch aptamers from *B. subtilis* and *B. amyloliquefaciens* were amplified from gDNA of these organisms, using the modifying oligonucleotide pairs P129/P130 and P131/P132 (Table 19), respectively. The forward primers introduced an *Eco*RI restriction site, as well as the T7 promoter sequence (Table S3), while the reverse primers added a *Hin*dIII restriction site at the 3'-end of the fragment. The restricted fragments were then cloned into the *Eco*RI/*Hin*dIII digested pSP64 plasmid, creating pSP64::*ribD*RSapt$_{sub}$ and pSP64::*ribD*RSapt$_{amy}$. The plasmids were propagated using *E. coli*

DH5α and all cloning steps described were individually verified by sequencing of the generated plasmids with primers P36 and P37.

3.2.11.5 pET28a expression vector

To overproduce and test the solubility of the RibR protein from *B. amyloliquefaciens*, the *ribR*$_{amy}$ gene was cloned into the expression vector pET28a. The *ribR*$_{amy}$ insert was obtained as a custom DNA string (Thermo Fisher Scientific, Waltham, MA, USA) and amplified using the primer pair P133/P134. After digestion, the fragment was ligated into the *Nde*I/*Xho*I restricted pET28a backbone, downstream of the T7 promoter sequence. The plasmid was propagated using *E. coli* DH5α and the insertion was verified by sequencing of the plasmid region, using the primer pair P38/P39. The final plasmids were used to transform the *E. coli* expression strains BL21 and BL21 pLysS.

3.2.11.6 pMAL expression vectors for generating MBP-tagged RibR proteins

The plasmids pMAL-c6T and pMAL-c5X (New England Biolabs GmbH) were used to generate N-terminal maltose binding protein (MBP) fusions of RibR proteins. The coding sequence of the RibR protein from *B. amyloliquefaciens ribR*$_{amy}$ was PCR amplified using the modifying primers P135 and P136 and cloned between the *Sal*I and *Pst*I restriction sites of pMAL-c6T, resulting in pMAL-c6T::*ribR*$_{amy}$. The pMAL-c5X::*ribR*$_{sub}$ plasmid was already generated in a previous study (Pedrolli, Kühm, *et al.*, 2015). The production plasmids for the mutated RibR versions RibR$^{m}_{sub}$ (R179A/R180A) and RibR$^{m}_{amy}$ (R54A/R55A) were generated via site-directed mutagenesis (section 3.2.12) of the plasmids pMAL-c5X::*ribR*$_{sub}$ and pMAL-c6T::*ribR*$_{amy}$ using the mutating primer pairs P137/P138 and P139/P140, respectively. The plasmids were propagated using *E. coli* DH5α and the insertion of the correct sequences was verified using the primer pair P40/P41 for sequencing. The final plasmids were used to transform the *E. coli* expression strain ER2535 (NEBExpress, New England Biolabs GmbH).

3.2.12 Plasmid site-directed mutagenesis

Plasmid mutagenesis was performed using the QuikChange Lightning Site-Directed Mutagenesis Kit (Agilent, Santa Clara, CA, USA). The complementary oligonucleotides for integration of the respective insertions, deletions or nucleotide changes were designed with the Agilent QuikChange Primer Design tool. The primer pairs are listed in Table 19 and the specific changes introduced are described in the respective method sections for plasmid construction. Table 28 gives the composition of a standard reaction for the site-directed mutagenesis using the QuikChange Lightning Kit. The 50 µL reaction mix was divided into two

aliquots of 25 µL. 0.5 µL of the QuikChange Lightning enzyme were added to one of the aliquots, while the other served as a negative control.

Table 28: Standard reaction for plasmid site-directed mutagenesis using the QuikChange Lightning Kit.

Component	Amount
Plasmid DNA	100 ng
10x QuikChange reaction buffer	5 µL
Forward Primer (10 µM)	0.8 µL
Reverse Primer (10 µM)	0.8 µL
dNTP mix (10 mM)	1 µL
QuikSolution	1.5 µL
ddH_2O	*ad* 50 µL

The thermocycler program for the QuikChange reaction is shown below (Table 29). After the amplification of the plasmids with the respective mutagenesis primers, the reaction mix as well as the negative control reaction were again split into two aliquots of 12.5 µL each. To one aliquot of each mixture, 0.5 µL of the restriction enzyme *Dpn*I were added. All four tubes were incubated at 37 °C for 5 minutes to allow digestion of the methylated DNA of the original plasmid template. After the *Dpn*I digestion, 2 µL from each reaction mix were used to transform 50 µL of competent *E. coli* DH5α cells according to the heat shock protocol in section 3.1.5.1.

Table 29: Thermocycler settings for the site-directed mutagenesis using the QuikChange Lightning Kit.

Reaction step	Temperature/ °C	Duration	No. of cycles
Initial Denaturation	95	2 min	x 1
Denaturation	95	20 s	
Annealing	60	10 s	x 18
Elongation	68	30 s/kb	
Final Elongation	68	5 min	x 1
Cooling	12	∞	

3.2.13 CRISPR-Cas9 genome editing of *B. subtilis*

The CRISPR-Cas9 genome editing of *B. subtilis* was performed according to a previously established protocol (Altenbuchner, 2016) with slight modifications. The CRISPR-Cas9 plasmids based on the pJOE8999.1 vector (see section 3.2.11.3) were generated using *E. coli* DH5α. The plasmids were isolated from the strain and used for transformation of *B. subtilis*,

according to the protocol described (section 3.1.5.2). Following transformation with the pJOE8999.1 derivatives, *B. subtilis* strains were streaked on LB agar containing 0.2% mannose for promoter induction and 15 µg/mL kanamycin for selection.
The plates were incubated for 24 hours at 30 °C. Single colonies were then transferred to a fresh LB plate without any supplements and incubated overnight at 50 °C for plasmid curing. The next day, colonies were streaked onto a fresh LB agar plate and the plates were again incubated at 50 °C overnight. After this second heat treatment, single colonies were picked and transferred to plain LB agar plates and incubated at 30 °C. Simultaneously, the same colonies were streaked on LB agar containing 15 µg/mL kanamycin and incubated at 30 °C to test for plasmid loss. Colonies that did not grow on kanamycin anymore were used as templates in a colony PCR (section 3.2.4.1) to amplify the region of interest, either the *ribR* region, using primers P125 and P126 (Table 19), or the *ribD* riboswitch region with the primer pair P127/P128. The amplified regions were sequenced to identify positive mutants.

3.2.14 *In vitro* transcription

In vitro transcription of the riboswitch aptamer DNA was performed using the T7 RNA polymerase. The composition of the reaction mixture can be found in Table 30. All components were combined in a 50 mL conical centrifugation tube and incubated overnight at 28 °C. Initially, different concentrations of DMSO and magnesium acetate ($Mg(Ac)_2$) were tested. For the *in vitro* transcription of the *B. subtilis ribD* aptamer, 10 % of DMSO and 30 mM of $Mg(Ac)_2$ were used, while for the *B. amyloliquefaciens* aptamer, the concentration of $Mg(Ac)_2$ was increased to 40 mM.

Table 30: Reaction mixture for an *in vitro* transcription reaction.

Component	Amount
Plasmid DNA (linear)	1 mg
250 mM $Mg(Ac)_2$	600 µL /800 µL
1M Tris-HCl, pH 8	1000 µL
1M DTT	100 µL
200 mM spermidine	100 µL
NTP mix (100 mM ATP, UTP, GTP, CTP)	800 µL
DMSO	500 µL
Triton X-100 (1:100)	500 µL
T7 RNA Polymerase	50 µL
ddH_2O	*ad* 5 mL

3.2.15 RNA precipitation and gel purification

The RNA of the riboswitch aptamers from *B. subtilis* and *B. amyloliquefaciens* was purified from the *in vitro* transcription reactions by isopropanol/ethanol precipitation. The 5 mL transcription reaction mix was shaken and centrifuged for 1 min at 8500 rpm. The supernatant was transferred to a new 50 mL conical centrifugation tube and 1 mL of EDTA, 670 µL of 3 M sodium acetate and 23.75 µL of 100% ice-cold isopropanol were added to the mixture. The tube was then incubated for one hour at -20 °C and subsequently centrifuged for one hour at 4 °C and 8500 rpm. The supernatant was carefully removed, and 5 mL of ethanol were added 8500 rpm. The supernatant was carefully taken off with a pipette and the remaining pellet was dissolved in 500 µL of ultrapure, nuclease free water.

The dissolved aptamer RNA was mixed with 2x RNA loading dye (formamide with 25 mM EDTA, pH 8 + bromophenol blue) applied to a large format 8% polyacrylamide (PAA) urea gel (Table 10) in 1x TBE buffer (Table 9). The gel was pre-run at 10 W for 30 minutes in a Large Format Adjustable Vertical System (CBS Scientific Company, San Diego, CA, USA) before the power was increased to 30 W for the actual run. Again, 1x TBE was used as a running buffer. When the loading dye indicated sufficient resolution, the run was stopped, and bands were visualized under UV light. The gel area containing one band was excised and the gel slice was cut into pieces of approximately 0.5 cm, which were transferred to a 50 mL conical tube. The tubes containing the gel slices were frozen in liquid nitrogen and defrosted quickly in a 40 °C water bath. This freeze-defrost cycle was repeated three times, before 5 mL of 300 mM sodium acetate were added to each tube. Tubes were placed on a roller shaker and incubated at 4°C overnight for elution of the RNA.

The next day, the liquid phase from the tube was filtered with a 0.2 µm cellulose-acetate filter. 100% isopropanol were added in a 1:1 ratio (v/v) and the RNA was incubated at 4°C for 20 minutes. The tubes were centrifuged at 4°C and 8000 rpm for 30 minutes and the supernatant was carefully decanted. The remaining RNA pellet was carefully washed with 700 µL of 70% ethanol, followed by a second centrifugation at 4°C and 8000 rpm for 30 minutes. The ethanol was carefully taken off and the pellet was dried at room temperature for 5 minutes. The RNA pellet was resuspended in 250 µL of ultrapure nuclease-free water and the RNA concentration was determined via spectrophotometric measurement (NanoPhotometer® N50, Implen GmbH, Munich, Germany). Purity of the resulting RNA was checked by applying a sample of approximately 500 ng to a small format 8% PAA gel and performing gel electrophoresis with 1x TBE as a running buffer.

3.2.16 Radioactive labeling of RNA

3.2.16.1 Dephosphorylation of RNA

To be able to perform radioactive end-labeling, the gel-purified RNA has to be dephosphorylated first. Dephosphorylation was performed with a calf-intestine alkaline phosphatase (Roche Diagnostics, Mannheim, Germany). All components of the reaction mixture (Table 31) were combined in a microcentrifuge tube.

Table 31: Reaction mixture for the dephosphorylation reaction using alkaline phosphatase.

Component	Amount
10x phosphatase buffer	2 µL
RNA (10 µM)	2 µL
Calf-intestine alkaline phosphatase	2 µL
ddH_2O	*ad* 20 µL

The reaction was incubated for 30 minutes at 50 °C. The enzyme was inactivated at 96 °C for 2 minutes and the reaction was immediately put on ice. The tube was then centrifuged briefly.

3.2.16.2 5'-labeling of RNA with [γ-^{32}P]ATP

For the radioactive end-labeling 10 µL of the dephosphorylation reaction were used. Table 32 shows the composition of the reaction mixture with the T4 polynucleotide kinase (PNK) (New England Biolabs GmbH, Frankfurt a. M., Germany).

Table 32: Reaction mixture for the 5'-labeling of RNA with [γ-^{32}P]ATP.

Component	Amount
10x PNK buffer	2 µL
RNA, dephosphorylated	10 µL
PNK	2 µL
[γ-^{32}P]ATP	4 µL
ddH_2O	*ad* 20 µL

The reaction mixture was incubated at 37 °C for 30 minutes. Subsequently, 40 µL of ultrapure water were added to the reaction mix and the 5'-labeled RNA was purified with a Microspin G-25 column (Merck KGaA, Darmstadt, Germany), according to the instructions of the manufacturer.

3.3 Biochemical methods

3.3.1 Preparation of cell-free extracts and total protein measurement

Cell-free extracts from bacterial cultures were either prepared in a small-scale or large-scale cell lysis approach as described below. The passive lysis methods used for *E. coli* cells in the β-galactosidase and luciferase reporter gene assays are described in the method section of the assays in chapter 3.3.4 and 3.3.5, respectively. For all cell-free extracts, the total protein concentration of the samples was determined by the method of Bradford (Bradford, 1976) and compared to a standard curve prepared for concentrations of 0-2000 µg/mL of bovine serum albumin (BSA). 10 µL of each protein sample were diluted in 150 µL of ultrapure water and mixed with 40 µL of protein assay dye reagent concentrate (Bio-Rad Laboratories GmbH, Feldkirchen, Germany) in a transparent, flat-bottom 96-well plate (Greiner Bio-One GmbH, Frickenhausen, Germany). The samples were incubated in the dark at room temperature for 10 minutes and the absorption at 595 nm was measured in a microplate reader (Tecan Spark).

3.3.1.1 Small-scale cell lysis

For cell suspensions with a volume up to 2 mL cells were lysed using a FastPrep-24T M 5G bead lysis system (MP Biomedicals, Santa Ana, CA, USA). Cell pellets of *B. subtilis* or *B. amyloliquefaciens* were resuspended in 1-1.5 mL of 100 mM potassium phosphate buffer (pH 7.4) and the cell suspensions were transferred to 2 mL screw cap tubes with 200 µL of glass beads (∅ 0.2-0.3 mm). Cells lysis was performed with 8 cycles of 30 seconds at 6.5 m/s in the FastPrep instrument. After every other cycle, the tubes were incubated on ice for 2 minutes. After completion of all cycles, the tubes were centrifuged at 13,000 rpm and 4 °C for 10 minutes and the supernatant was transferred to a fresh tube and stored on ice until further usage.

3.3.1.2 Large-scale cell lysis

Frozen cell pellets of *E. coli* ER2535 used for protein overproduction of MBP-RibR fusions were defrosted on ice and resuspended in Column Buffer (Table 11, 5 mL/g of cells), which contained the cOmplete EDTA-free protease inhibitor cocktail (Merck KGaA, Darmstadt, Germany). The cells were disrupted by 3-5 cycles in a Constant Cell Disruption System at 10 °C and at a pressure of 1.3 kbar. After each cycle, the cells were cooled on ice for 5 minutes. Cell debris was removed by centrifugation at 10,000 rpm and 4 °C for 10 minutes, followed by an ultracentrifugation step at 75,600 x *g* and 4 °C for 20 minutes. The lysate was stored on ice until protein purification via Fast Protein Liquid Chromatography was performed (see chapter 3.3.3).

3.3.2 SDS polyacrylamide gel electrophoresis and Coomassie staining of proteins

To separate proteins and to examine protein expression and purification, a sodium dodecyl sulfate polyacrylamide gel electrophoresis (SDS-PAGE) was performed. Cell-free extracts and other protein samples were diluted with ultrapure water if necessary and mixed with 5x protein loading buffer (Table 13). Usually, 8-20 µg of total protein were used. The samples were denatured by an incubation at 98 °C for 10 minutes and subsequently kept on ice for 5 minutes. The samples were then loaded onto a Novex™ WedgeWell™ 4-20% Tris-Glycine Mini Protein Gel (Thermo Fisher Scientific, Waltham, MA, USA) and the gel run was performed with 1x Tris-Glycine buffer (25 mM Tris-HCl; 192 mM Glycine; 0.1 % (w/v) SDS; pH 8.3). The PageRuler™ Plus Prestained Protein Ladder (Thermo Fisher Scientific) was included in every run to allow size comparison. The proteins were separated in the gel at 100-110 V for 1.5-2 hours. After the run, the gel was rinsed with distilled water and incubated overnight in PageBlue Protein Staining Solution (Thermo Fisher Scientific) with gentle shaking. The next day, the gel was destained in distilled water for at least 1 hour and pictures of the gel were taken.

3.3.3 Fast Protein Liquid Chromatography for protein purification

The Fast Protein Liquid Chromatography (FPLC) for purification of MBP-tagged RibR proteins was performed with an ÄKTApurifier system (GE Healthcare GmbH, Solingen, Germany) and the resulting data was analyzed with the software Unicorn 5.1.
For the specific purification of MBP-tagged proteins a 5 mL MBPTrap™ HP column with a dextrin sepharose resin (Merck KGaA, Darmstadt, Germany) was used. First, the column was equilibrated with 5 column volumes (CV) of Column Buffer (Table 11) at a flow rate of 1 mL/min after which the crude protein extract (see section 3.3.1.2) was loaded onto the column at a flow rate of 0.5-1 mL/min via a 50 mL superloop (GE Healthcare GmbH, Solingen, Germany). When the loading of the protein extract was completed, the column was washed again with 12 CV of Column Buffer at a flow rate of 1-1.5 mL/min. Subsequently, the MBP-tagged protein bound to the column was eluted with a linear gradient of Elution Buffer (Table 12), increasing to 100% of Elution Buffer over 2 hours, at a flow rate of 1 mL/min. Around 20 elution fractions of 1 mL were collected in each run, while elution of the protein was detected by UV absorbance at 280 nm. The protein concentration was determined for the fractions that corresponded to the observed protein peak and the purity of the collected protein was examined with an SDS-PAGE. The purest fractions were united and the protein solutions were stored at 4 °C until further usage.

3.3.4 β-galactosidase assay

To analyze the activity of TPP riboswitches and their response to thiamine-analogs, at first a β-galactosidase reporter gene assay was employed. For the assay, *E. coli* DH5α strains carrying the plasmid pHAt191l with a translational fusion of the promoter and TPP riboswitch region with the *lacZ* reporter gene were used. Pre-cultures of the strains were grown in 1 mL of M9 medium with 100 µg/mL ampicillin, supplemented with 20 nM of thiamine. The cultures were incubated overnight in a 24-well plate at 37 °C and shaking at 160 rpm. The OD_{600} of each overnight culture was determined and the culture volume was transferred to a 1.5 mL microcentrifuge tube. The cells were pelleted by centrifugation at 6000 x *g* for 5 minutes and washed once with fresh M9 medium without supplements. The cell pellets were then resuspended in fresh M9 medium and 10 µL of the cell suspension were used to inoculate 200 µL of fresh M9 medium in a transparent, flat-bottom 96-well plate (Greiner Bio-One GmbH, Frickenhausen, Germany) to an initial OD_{600} of 0.1. Thiamine and different thiamine analogs dissolved in DMSO were added to the cultures to a concentration of 1 mM and the plate was incubated for 4 hours at 37 °C with shaking at 180 rpm. After the incubation time, 100 µL of each culture were transferred to a new 96-well plate and the OD_{600} was determined in a plate reader. 10 µL of a 1:1 mixture of PopCulture reagent (Merck KGaA, Darmstadt, Germany) and lysozyme solution (50 mg in 1 mL of Z buffer (Table 7)) were added to each well. The plate was incubated at room temperature for 15 minutes to enable cell lysis. Afterwards, 15 µL of each cell lysate were mixed with 155 µL of Z buffer containing 0.135 % of dithiothreitol (DTT). 30 µL of the enzyme substrate *ortho*-Nitrophenyl-β-galactoside (ONPG) (4 mg in 1 mL of Z buffer) were added to each well. After addition of the substrate, the β-galactosidase activity was determined by following the conversion of ONPG to *ortho*-Nitrophenol (ONP). To do so, absorption at 420 nm was measured at 30 °C for up to 1 hour. The specific activity of the β-galactosidase in Miller units was calculated with the following formula:

$$Specific\ Activity\ = \frac{OD_{420}}{\Delta t\ \times\ V \times OD_{600}} \times 1000$$

3.3.5 Dual-luciferase assay

The dual luciferase assay was used as a more sensitive reporter gene assay to test putative TPP riboswitches and their response to thiamine and thiamine analogs. Pre-cultures of *E. coli* DH5α or MG1655 containing the pDluc or pDlucTC reporter plasmids with the different TPP riboswitches were inoculated in M9 minimal medium with 100 µg/mL ampicillin. Pre-cultures of *E. coli* DH5α were additionally supplemented with 20 nM of thiamine. The overnight cultures were incubated in a 24-well plate at 37°C with shaking at 160 rpm. The OD_{600} of each overnight

culture was measured, and the corresponding culture volume was transferred to a 1.5 mL microcentrifuge tube. The cells were then pelleted by centrifugation at 6000 x g for 5 minutes and washed once with fresh M9 medium without supplements. Finally, the cell pellets were resuspended in fresh M9 medium to the same OD_{600}. 10 µL of the resulting cell suspension were used to inoculate the 2 mL main cultures in triplicates in a non-treated 12-well plate (VWR International GmbH, Darmstadt, Germany) to an initial OD_{600} of 0.1. The M9 minimal medium for the main cultures was supplemented with 10 µM of either thiamine, pyrithiamine or bacimethrin, or the equivalent volume of water as a control. The 12-well plates were incubated at 37 °C and 180 rpm for four hours. The whole culture volume was then transferred to a 2 mL microcentrifuge tube and cells were harvested by centrifugation at 4000 x *g* and 10 °C for 10 minutes. After discarding the supernatant, the cell pellets were washed once with 500 µL of 1x Phosphate Buffered Saline (PBS,). The centrifugation step was repeated and the supernatant discarded again. The cell pellets were resuspended in 100-200 µL of 1x Passive Lysis Buffer (PLB, Dual Luciferase Reporter Assay System, Promega, Mannheim, Germany), depending on the pellet size. This was followed by an incubation on ice for 15 minutes.

To determine the amount of total protein in the samples, a standard Bradford assay was performed (see section 3.3.1). The cell extracts were diluted to a total protein amount of 20 µg/mL with 1x PLB buffer. 20 µL of each diluted sample were transferred to one well of a white, flat-bottom 96-well microplate (Greiner). The plate was incubated inside a microplate reader (Tecan Spark) for 10 minutes at room temperature to decrease self-luminescence during the measurement. Meanwhile, the connected injectors were flushed three times with dH_2O. Injector A was primed with 1000 µL of LARII and injector B with 1000 µL of Stop& Glo reagent (Dual Luciferase Reporter Assay System, Promega). The dual-luciferase measurement was performed using the well-wise luminescence measurement. Per well, 100 µL of LARII were injected, followed by a three-second waiting period, before the luminescence measurement was performed with automatic attenuation, an integration time of 10,000 milliseconds and a settling time of 0 milliseconds. Subsequently, 100 µL of Stop & Glo reagent were injected per well and luminescence was measured using the same parameters as before. The output was given in counts per second.

3.3.6 Riboflavin synthase activity assay

To determine the effect of RibR on gene expression, the riboflavin synthase of *B. subtilis* and *B. amyloliquefaciens* was used as a natural reporter gene and its activity was measured with an *in vitro* enzyme activity assay. *B. amyloliquefaciens, B. subtilis* and different *B. subtilis* RibR-mutant strains were inoculated from overnight cultures to an initial OD_{600} of 0.05 and grown in shake flasks in 20 mL of *Bacillus* minimal medium, containing either 4 mM of $MgSO_4$ or 1 mM

methionine/5 mM taurine as a sulfur source. For *B. amyloliquefaciens*, 0.5 mM of diamide were additionally added to some cultures to induce oxidative stress. The cultures were grown until they reached an OD_{600} of 1.4-1.5 and cells were harvested by centrifugation at 4000 x *g* for 10 minutes at 4 °C. The supernatant was discarded, and the cell pellets were washed three times with 100 mM potassium phosphate buffer (pH 7.4). Cell-free extracts were prepared according to the protocol in section 3.3.1.1 and the total protein content of the samples was determined. Table 33 specifies the composition of the reaction mix. All components except for the cell-free extracts were united in a dark reaction tube and pre-warmed at 37 °C for 5 minutes.

Table 33: Reaction composition of the *in vitro* riboflavin synthase activity assay.

Component	Concentration
Potassium phosphate (pH 7.4)	100 mM
EDTA	10 mM
DTT	7.5 mM
6,7-dimethyl-8-ribityllumazine	0.5 mM
Cell-free extract (total protein)	50-200 µg/mL

The reaction was started by the addition of the cell-free extracts. Samples for HPLC analysis (section 3.3.7) were taken after 0, 30, 60, 90 and 120 minutes. In some cases, an additional sample was taken after 180 minutes. All samples were immediately mixed with 5% trichloroacetic acid (TCA) to stop the reaction and stored on ice until further preparation for analysis.

3.3.7 High-performance liquid chromatography

The samples collected from the riboflavin synthase assay were analyzed for riboflavin production via high-performance liquid chromatography (HPLC) using an Agilent 1260 Infinity System with a 1260 Diode Array Detector (DAD) and a 1260 Fluorescence Detector (FLD).
All samples used for HPLC analysis were centrifuged at 14,000 rpm and 4 °C for 10 minutes. The supernatant was filtered through a 0.22 µm cellulose-acetate membrane into a dark HPLC vial and stored at 14 °C until analysis.

3.3.7.1 HPLC analysis of riboflavin samples

The detection and quantification of riboflavin in the samples was performed using a reverse-phase biphenyl column (2.6 µm particle size, 150 mm x 2.1 mm; Phenomenex, Aschaffenburg, Germany) at a flow rate of 0.2 ml/min. For the run, the column was heated to 50 °C and equilibrated in 85% of buffer A (40 mM formic acid, 40 mM ammonium formate, pH 3.7) and

15% of buffer B (ultrapure methanol) at a flow rate of 0.1 mL/min. For each run, 10-15 µL of sample were loaded onto the column. For the separation of flavins, an increasing methanol gradient was used. The exact gradient protocol is given in Table 34.

Table 34: HPLC protocol used for flavin separation and analysis of riboflavin production.

Step	Time/ min	% buffer A	% buffer B
Gradient	0	85	15
	3	77	23
	3.1	73	27
	5	70	30
	6.5	68	32
	13.5	68	32
	20	5	95
Wash	20.1	0	100
	24.1	0	100
	24.5	100	0
	29.5	100	0
Equilibration	30	85	15

Riboflavin was detected via DAD at a wavelength of 445 nm. Additionally, it was analyzed with the fluorescence detector (excitation 450 nm, emission 525 nm). Standardized flavin solutions were used to generate calibration curves with concentrations ranging from 0.2-50 µM to allow quantification of the riboflavin produced.

3.3.1 Western blot

For the Western blot analysis of *ribR*$_{amy}$ expression in *B. subtilis*, cell-free extracts from *B. subtilis ribR*$_{amy}$*-his*$_6$ cultures grown with either $MgSO_4$ or methionine/taurine as a sulfur source (according to the growth conditions described in section 3.3.6) were used. Samples were prepared according to the protocol described by Pedrolli *et al.* (2015) with small adjustments. After harvesting, cells were suspended in 1 mL of pre-warmed TMS buffer (50 mM Tris-HCl pH 8.0, 16 mM $MgCl_2$, 33% (w/v) sucrose), containing 300 µg/mL lysozyme and the cOmplete EDTA-free protease inhibitor cocktail (Merck KGaA, Darmstadt, Germany), and incubated at 37 °C for 30 minutes. The samples were cooled to 4 °C and the protoplasts were harvested by centrifugation at 7,500 x *g* for 1 minute. They were resuspended in 1 mL of lysis buffer (50 mM Tris-HCl pH 8, 5 mM $MgSO_4$), again containing the protease inhibitor cocktail. Membranes were disrupted by bead beating (see section 3.3.1.1) and harvested by centrifugation at 25,000 x *g* for 30 minutes. Following a wash step with 50 mM Tris-HCl (pH 8),

membranes were resuspended in 50 µL of 50 mM Tris-HCl (pH 8). Samples with a total protein content of 20 µg were separated by SDS-PAGE (see section 3.3.2). Instead of the Coomassie staining, a protein transfer to a 0.45 µm nitrocellulose membrane was performed. The membrane was first soaked in cold transfer buffer (Towbin, Table 15) before the SDS gel was carefully placed on top. Two layers of Whatman® filter paper soaked in transfer buffer were placed on the top and bottom. The proteins were transferred to the membrane in a Trans-Blot® SD Semi-Dry Transfer Cell (Bio-Rad) at 0.04 A for 60 minutes. Following the transfer, the gel was removed and stained with Coomassie to detect any remaining protein. The nitrocellulose membrane was incubated in the blocking solution (1x PBS with 0.05% (v/v) Tween20 and 1% (w/v) BSA) for 1 hour at 4°C with gentle shaking. Afterwards, the membrane was transferred to a tightly sealed plastic bag containing a 1:700 dilution of a horseradish peroxidase (HRP)-conjugated 6x-His tag monoclonal antibody (MA1-21315-HRP, Invitrogen) in blocking solution and incubated at 4°C with slight agitation overnight. The membrane was then washed three times for 8 minutes in 1x PBS with 0.05 % (w/v) Tween20. Addition of the staining solution to the membrane allowed protein band detection by horseradish peroxidase (HRP) driven conversion of DAB. After the appearance of dark bands, the reaction was stopped by rinsing the membrane with dH_2O.

3.3.2 Electrophoretic mobility shift assay

The electrophoretic mobility shift assay was used to examine interactions of the RibR-proteins from *B. subtilis* and *B. amyloliquefaciens* with the RNA-sequences of the *ribD* FMN-riboswitches from these two organisms. For this purpose, 5'-[γ-^{32}P]ATP-labeled riboswitch RNA (see section 3.2.16) was incubated with FPLC-purified MBP-tagged RibR proteins (see section 3.3.3) from *B. subtilis* or *B. amyloliquefaciens,* including the respective RibR mutants $RibR^{m}_{sub}$ (R179A/R180A) and $RibR^{m}_{amy}$ (R54A/R55A). The reactions were set up in 1x Structure Buffer (10 mM Tris-HCl, pH 7; 100 mM KCl; 10 mM MgCl). An RNA master mix was prepared for the riboswitch aptamers of the ribD FMN riboswitch from *B. subtilis* and *B. amyloliquefaciens* (Table 35).

Table 35: Composition of a 50 µL RNA master mix for EMSA.

Component	Amount
10 x Structure Buffer	5 µL
Unlabeled RNA (1 µM)	5 µL
[γ-^{32}P]ATP-labeled RNA (100.000 counts/µL)	1 µL
tRNA (1 µg/µL)	10 µL
ddH_2O	*ad* 50 µL

The RNA master mix was divided into aliquots of 5 µL. Each aliquot was mixed with 5 µL of a RibR protein solution in 1x Structure Buffer for a final protein concentration of 5.25 µM. A “no protein” control with an equal volume of protein elution buffer was included. Either FMN or $FMNH_2$ was added to the protein samples to a final concentration of 5 µM in the 10 µL EMSA reaction. The reaction mixtures were incubated for 15 minutes at 20 °C. Subsequently, the samples were mixed with EMSA loading buffer (50% (v/v) glycerol; 0.2% bromophenol blue in 0.5x Tris-borate buffer) and loaded onto a running 6% native polyacrylamide gel, which was pre-cooled to 4°C and had been pre-run for 30 minutes. The running buffer was 0.5x Tris-borate containing 1 mM of $MgCl_2$. To achieve good separation of the RNA bands, the gel was run for ~1.5 hours. After the run, the gel was transferred to a cellulose paper and dried at 80 °C for 30 minutes on a pre-heated gel dryer. The signal was detected overnight on a storage phosphor screen and analyzed the next day with a phosphorimager (Typhoon® 9100, GE Healthcare).

3.4 Statistical analysis

All statistics were either performed in Microsoft Excel 2016 or with the GraphPad Prism 9 software. A two-tailed Students T-test was performed for all data sets. First, an F-test was performed to examine standard deviation equality. When the p-value of the F-test was ≤ 0.05, a heteroscedastic T-test was performed, otherwise a homoscedastic T-test was performed. When the p-value of the T-test was less than 0.05, the data sets were considered significantly different. A value below 0.05 was marked with one asterisk, a value below 0.01 with two asterisks and a value below 0.001 with three asterisks.

CHAPTER I –

The thiamine pyrophosphate riboswitch as a target for new antimicrobial compounds

4 Results – Chapter I

4.1 Identification of a TPP riboswitch in *Klebsiella pneumoniae* with a β-galactosidase reporter gene assay

The overall objective of the present study was to investigate the suitability of TPP riboswitches as targets for a new class of antibiotics. The focus was on TPP riboswitches from the group of ESKAPE pathogens, which comprise multiresistant bacteria, responsible for severe human infections. Prior to testing compounds which potentially affect riboswitch activity, functional riboswitches had to be identified in these bacterial strains. *E. coli* was used as a host to test riboswitch activity *in vivo* and, accordingly, a plasmid was constructed which allowed coupling of a range of riboswitches under control of different promoters to a reporter gene.

Initially, β-galactosidase (LacZ) was employed as a reporter. The first riboswitch sequence that was examined was the *thiC* riboswitch from *K. pneumoniae* (Kp04), which was predicted by Rfam. To validate riboswitch activity, a translational fusion plasmid with the *lacZ* reporter gene fused to the first few codons of the native downstream gene *thiC* was used. For the assay, thiamine was added to the growth medium, which is expected to be taken up by the *E. coli* cells and phosphorylated to its active form thiamine pyrophosphate. When the reporter was fused to the complete riboswitch sequence including the native promoter a decrease in *lacZ* expression was observed when thiamine was present in the cultures (Figure 7). This effect was absent when only the Kp04 promoter (pKp04) was regulating reporter gene expression.

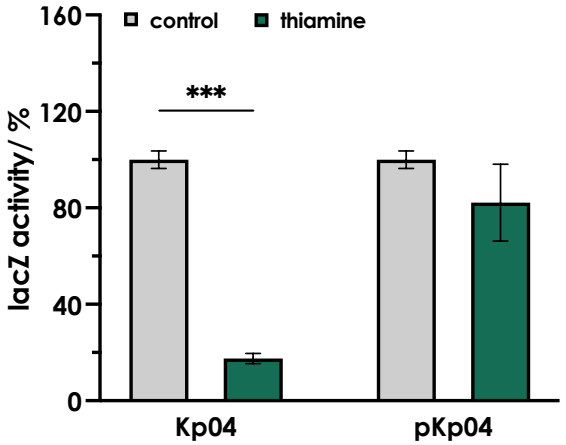

Figure 7: Thiamine decreases β-galactosidase (LacZ) activity in an *Escherichia coli* strain containing a translational fusion of the *Klebsiella pneumoniae thiC* riboswitch Kp04 with the reporter gene, but not in the respective promoter control strain pKp04. *E. coli* strains transformed with the reporter plasmids were grown in M9 minimal medium in the absence (control) or presence of 10 µM thiamine. LacZ activity was measured using *o*-nitrophenyl-β-D-galactopyranoside as a substrate. In strain Kp04 the native *K. pneumoniae* promoter *thiC* is coupled to the riboswitch *thiC* and thus expression of the reporter gene is controlled by this riboswitch. Accordingly, the reduced gene expression upon addition of thiamine indicates that thiamine turns the riboswitch off. In strain pKp04 the reporter gene is constitutively expressed from the *K. pneumoniae thiC* promoter as no riboswitch is present. LacZ activity is given as relative activity compared to the control. Cultures were grown in triplicates in a plate reader in a 12-well plate. Depicted are the mean values ± standard deviations of the data obtained from the triplicates. Asterisks indicate statistically significant differences (*** $p \leq 0.001$).

4.2 Testing the effect of 18 small compounds on the *thiC* riboswitch of *K. pneumoniae*

Following validation of the *K. pneumoniae thiC* riboswitch, 18 small compounds were tested for their effect on this riboswitch. The initial idea was to test potential ligands from a novel substance library that had been synthesized and successfully tested in an *in vitro* high-throughput assay by the research project partners (Ruth Brenk, University of Bergen, Norway; Petr Bartunek, Institute of Molecular Genetics of the ASCR, Czech Republic; Gints Smits, Latvian Institute of Organic Synthesis, Latvia; Daniel Lafontaine, Université de Sherbrooke, Canada). However, synthesis of the compounds and the performance of the *in vitro* high-throughput assay turned out to be more complicated than expected, and thus, no pre-screened substances were available to be examined in the *in vivo* experiments. Therefore, commercially available candidates (selected by Prof. Dr. Ruth Brenk, University of Bergen, Norway) were tested in the *in vivo* assay for their effect on riboswitch activity. Table 36 lists the selected compounds that were chosen as the most promising candidates.

Table 36: List of substances 1-18, tested for their effect on riboswitch activity in the β-galactosidase reporter gene assay.

Substance 1	1-[4-(1H-imidazol-2-yl)phenyl] methanamine
Substance 2	1-[4-(1H-pyrazol-5-yl)phenyl] methanamine
Substance 3	1-[4-(1,3-Thiazol-2-yl)phenyl] methanamine hydrochloride
Substance 4	2-(1H-imidazol-2-yl) pyridine
Substance 5	1-[4-(1H-pyrazol-1-yl)phenyl] methanamine
Substance 6	4-(2H-tetrazol-5-yl) pyridine
Substance 7	1-[4-(1H-1,2,4-triazol-1-yl)phenyl] methanamine dihydrochloride
Substance 8	1-[4-(5-Methyl-1H-1,2,4-triazol-3-yl)phenyl] methanamine hydrochloride
Substance 9	4-(1H-1,2,4-triazol-3-yl)phenyl] methanamine hydrochloride
Substance 10	4-(2H-tetrazol-5-yl)-benzenemethanamine hydrochloride
Substance 11	1-[4-(1H-imidazol-4-yl)phenyl] methanamine dihydrochloride
Substance 12	4-(1,2,3-Thiadizol-4-yl) benzylamine hydrochloride
Substance 13	Thieno [2,3-b]pyrazin-7-amine
Substance 14	1-[4-(1H-Pyrazol-4-yl)-2-thienyl] methanamine
Substance 15	1-[4-(1H-Pyrazol-3-yl)-2-thienyl] methanamine
Substance 16	1-[5-fluoro-2-methyl-4-(1H-1,2,3-triazol-5-yl)phenyl] methanamine
Substance 17	1-[5-(4H-1,2,4-Triazol-3-yl)-2-pyrimidinyl] methanamine
Substance 18	6-(pyrazin-2-yl)-1,2,3,4-tetrahydroisoquinoline

The respective molecular structures are depicted in the following (Figure 8). All substances used were dissolvable in DMSO.

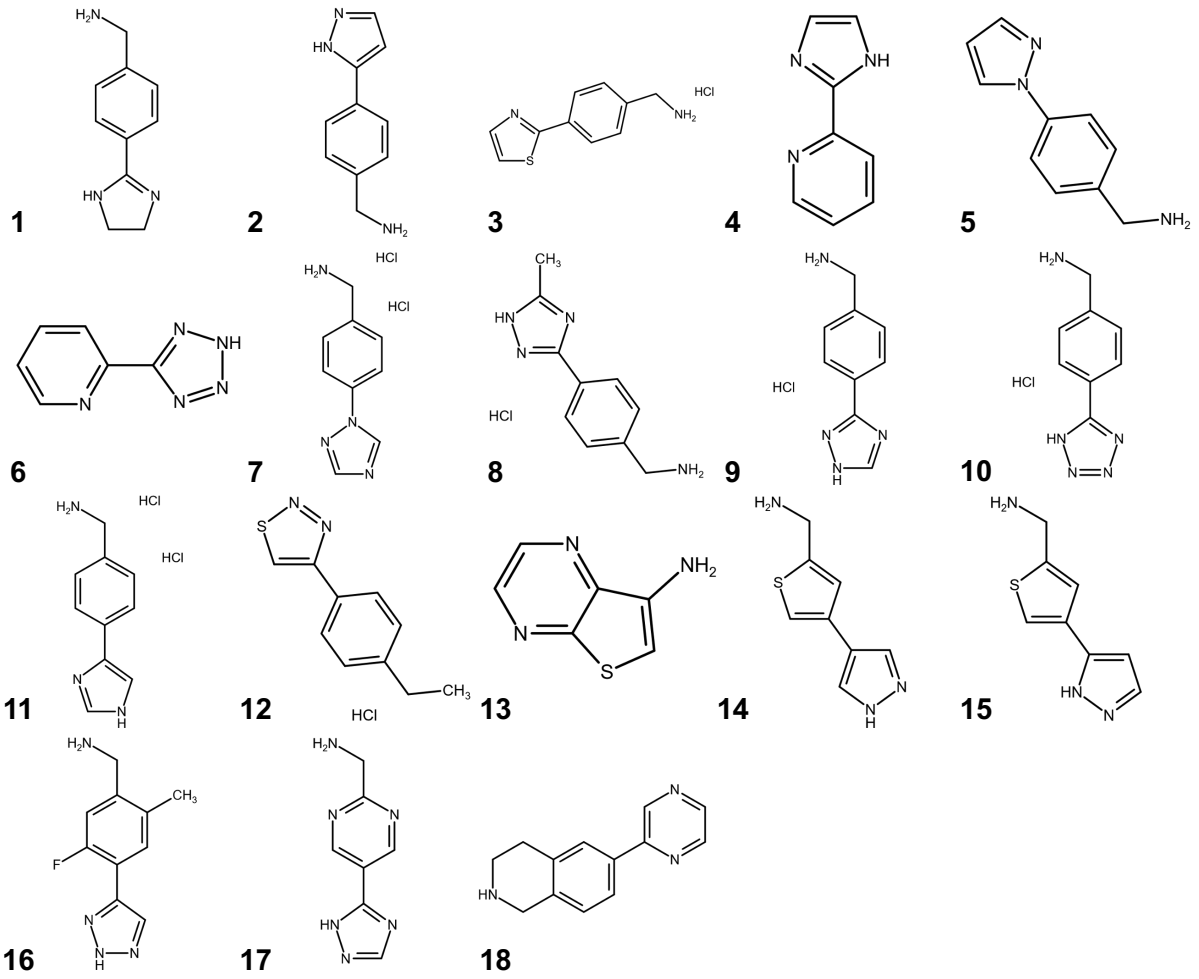

Figure 8: Chemical structures of the compounds listed in Table 36.

All substances, including thiamine, were first tested in a comparably high final concentration of 1 mM. Since no previous *in vitro* tests could be run with these substances, the high concentration was used to ensure that the binding affinity was met.

Addition of none of the 18 small compounds to the medium resulted in a significant decrease in beta-galactosidase expression, as would be expected if a substance regulated riboswitch activity comparable to thiamine pyrophosphate (Figure 9A). On the contrary, some substances even led to an increase of β-galactosidase activity, thus even had an opposite effect on the expression of the downstream gene (see e.g., substance 11 and 17). However, the effect of these compounds on reporter gene activity in the promoter control was comparable to the values measured for the riboswitch plasmid (Figure 9B).

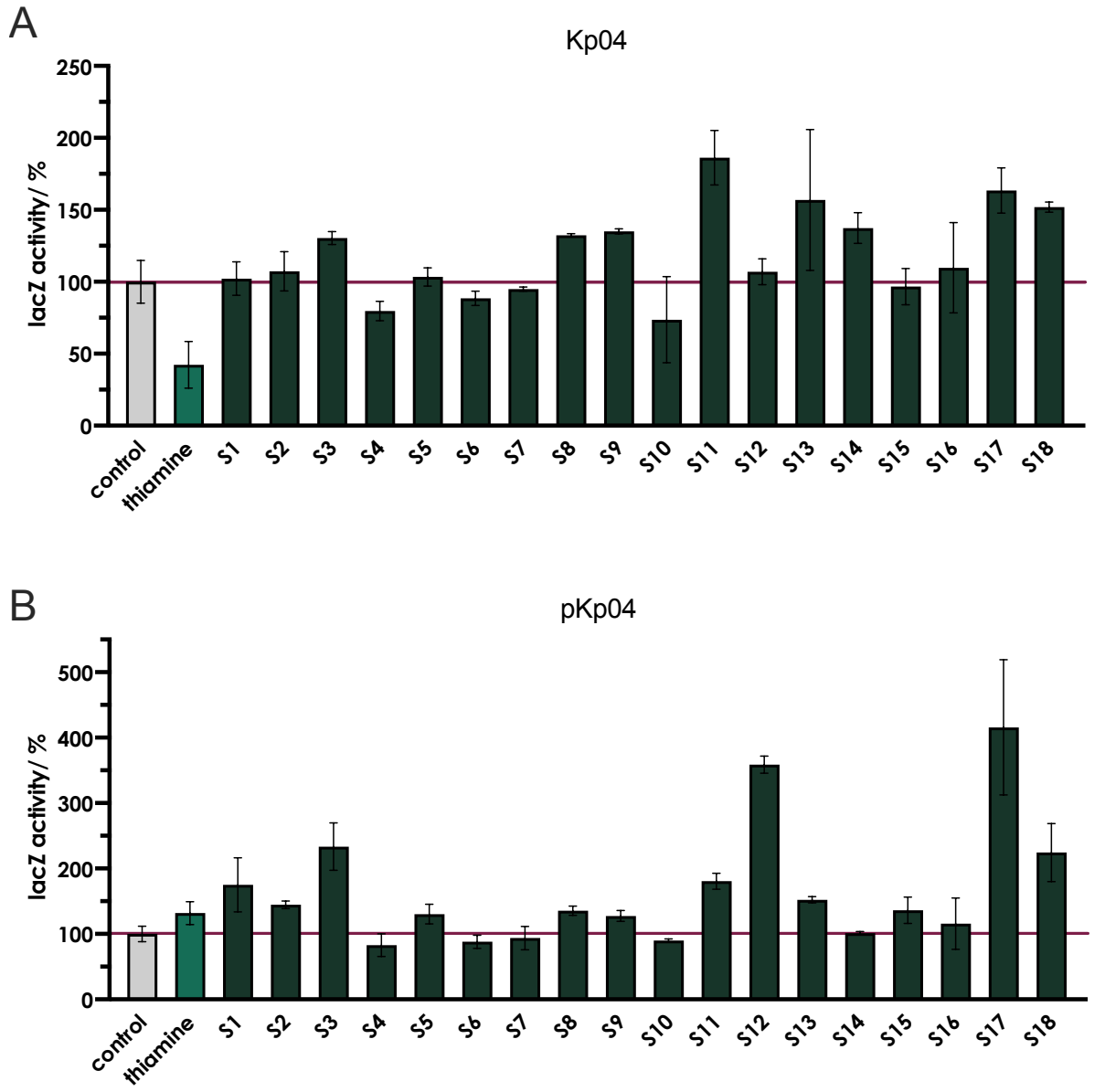

Figure 9: β-galactosidase reporter gene assays for (A) the *K. pneumoniae thiC* riboswitch Kp04 and (B) the promoter control strain pKp04. *E. coli* DH5α strains transformed with the pHA191 reporter plasmids were grown in M9 minimal medium in the absence (control) or presence of 1 mM of thiamine or one of the 18 small compounds with structural similarities. LacZ activity was measured using *o*-nitrophenyl-β-D-galactopyranoside as a substrate. In strain Kp04 the native *K. pneumoniae* promoter *thiC* is coupled to the riboswitch *thiC* and thus expression of the *lacZ* reporter gene is controlled by the riboswitch. Accordingly, the reduced gene expression upon addition of thiamine indicates that thiamine turns the riboswitch off. In strain pKp04 the reporter gene is constitutively expressed from the *K. pneumoniae thiC* promoter as no riboswitch is present. LacZ activity is given as relative activity compared to the control. Cultures were grown in triplicates in a plate reader in a 96-well plate. Depicted are the mean values ± standard deviations of the data obtained from the triplicates.

4.3 Development of an improved dual-luciferase reporter assay for testing riboswitch activity in *E. coli*

With the β-galactosidase reporter gene assay, the TPP riboswitch from *E. coli* was successfully analyzed. In addition, the *thiC* riboswitch from *K. pneumoniae* was experimentally validated for the first time. However, when more putative TPP riboswitches from other pathogenic bacteria

were examined, some of them showed only weak responses and for some the results seemed to be not entirely reproducible (data not shown).

Therefore, a more sensitive reporter gene assay was developed, employing a specific, newly designed plasmid harboring two different luciferase reporter genes, pDluc. In this dual-luciferase assay, which so far has been mostly used in mammalian cells, one reporter gene originating from the firefly (*luc*^{F}) was used to probe the riboswitch activity, whereas the second luciferase gene from *Renilla reniformis* (*luc*^{R}) was placed under control of a constitutive promoter and served for normalization. The thiamine-auxotrophic strain *E. coli* DH5α was used again as a host for this reporter assay.

To validate the newly developed reporter gene assay based on the dual-luciferase reactions, the assay was first tested with the *E. coli thiC* riboswitch (Ec01) that is known to negatively affect expression of *thiC* at the transcriptional as well as at the translational level (Winkler, Nahvi, *et al.*, 2002). Notably, for *E. coli* a dual-luciferase reporter assay has not been described before. To differentiate between regulation at the transcriptional as well as at the translational level two different constructs were generated.

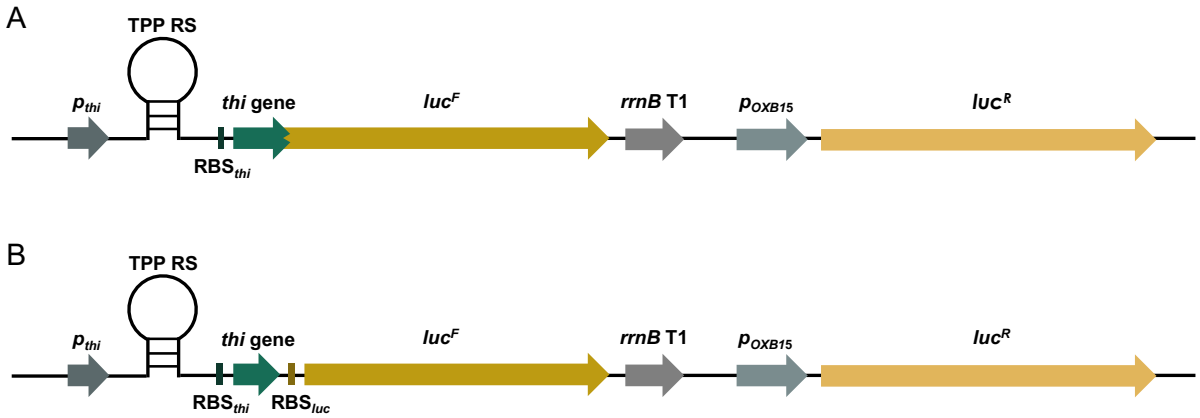

Figure 10: Schematic structure of (A) the translational reporter gene fusion plasmid pDluc and (B) the transcriptional fusion plasmids pDlucTC. On both plasmids the gene coding for the *Renilla* luciferase *luc*^{R} is controlled by the artificial, constitutive *E. coli* promoter p_{OXB15}. An *rrnB* T1 terminator sequence upstream of the p_{OXB15} promoter prevents interference of upstream transcription with *luc*^{R} expression. The firefly luciferase reporter gene *luc*^{F} is located downstream of the first few codons of the respective thiamine biosynthesis or transport gene (*thi* gene), the corresponding ribosomal binding site (RBS_{thi}), the TPP riboswitch (TPP-RS) and the employed promoter (p_{thi}). In the translational fusion plasmid pDluc (A) the firefly luciferase gene *luc*^{F} is directly fused to the *thiC* gene codons, while in the transcriptional fusion plasmid pDlucTC (B) an additional ribosomal binding site (RBS_{luc}) is placed between the *thi* gene and the *luc*^{F} coding sequence.

First, the translational riboswitch fusion was tested to validate the new reporter gene assay and to this end it was compared to the previously performed reporter gene assay based on the β-galactosidase reaction.

For the translational fusion the relative activity of the luciferase decreased significantly when 10 µM thiamine were added to the cultures, compared to the control without thiamine. This

effect was also more pronounced when compared to the β-galactosidase reporter assay, using the same riboswitch constructs (Figure 11).

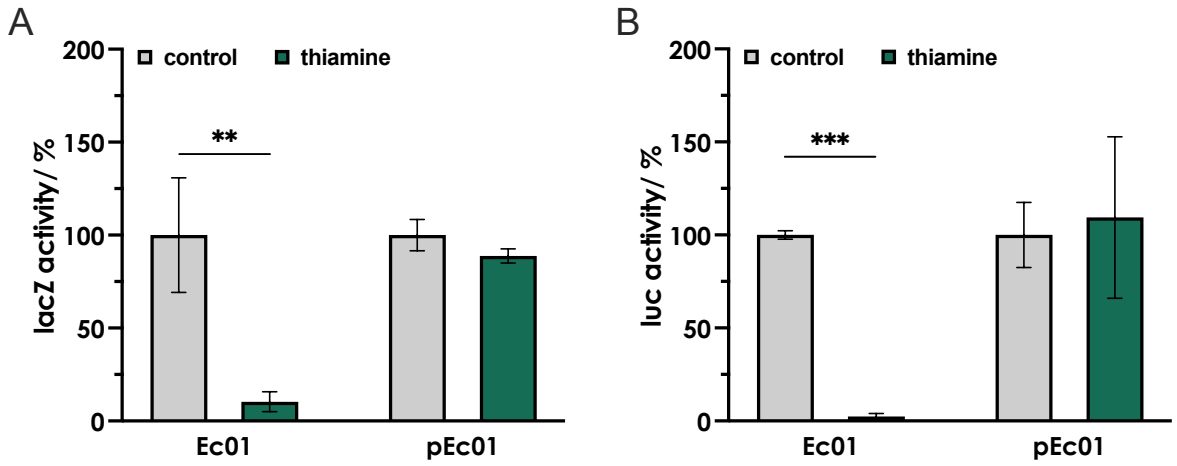

Figure 11: Comparison of the (A) β-galactosidase and (B) luciferase reporter gene assays for testing the *E. coli thiC* riboswitch activity in *E. coli* DH5α. Shown are the results from the β-galactosidase (LacZ)-based assay (A) and compared to the results of the novel dual-luciferase reporter gene assay (B) for the activity of the *E. coli thiC* riboswitch. *E. coli* DH5α strains transformed with the reporter plasmids were grown in M9 minimal medium in the absence (control) or presence of 10 µM thiamine. Firefly luciferase (Luc^F) activity was followed by measuring the light emission caused by the conversion of luciferin to oxyluciferin, whereas LacZ activity was measured using *o*-nitrophenyl-β-D-galactopyranoside as a substrate. In strain Ec01 the native *E. coli* promoter *thiC* is coupled to the riboswitch *thiC* and thus expression of the reporter gene is controlled by the riboswitch. In strain pEc01 the reporter gene is constitutively expressed from the *E. coli thiC* promoter as no riboswitch is present. Luciferase activity was normalized by the respective *Renilla* luciferase activity and Luc^F and LacZ activities are given as relative activities compared to the respective controls. Cultures were grown in triplicates in a plate reader in a 12-well plate. Depicted are the mean values ± standard deviations of the data obtained from the triplicates. Asterisks indicate statistically significant differences (** $p \leq 0.01$, *** $p \leq 0.001$).

To be able to determine the mode of action for a riboswitch, i. e. to distinguish between a translational and a transcriptional mechanism, a second plasmid was constructed. This plasmid is similar to the translational fusion plasmid, but additionally contains a second Shine-Dalgarno sequence upstream of the firefly luciferase gene. This allows reporter gene translation, even when the riboswitch sequesters the first ribosomal binding site of its downstream gene.

For the transcriptional fusion of the *E. coli thiC* riboswitch, as well as the promoter control, the reporter gene expression pattern is similar to the one of the translational fusion. Addition of thiamine decreased firefly luciferase activity significantly only in presence of the riboswitch (Figure 12).

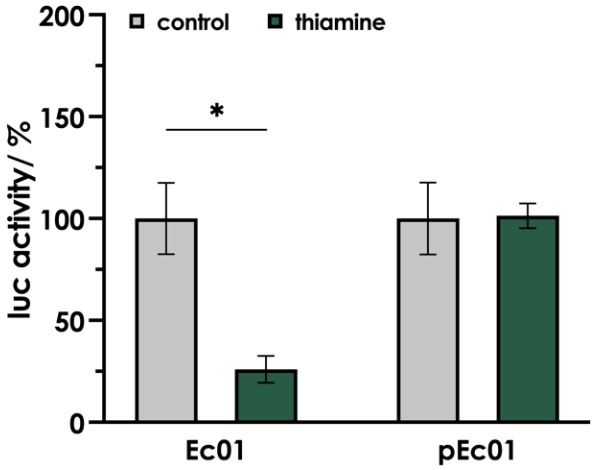

Figure 12: Thiamine decreases luciferase (Luc^F) activity in a transcriptional fusion with the *E. coli thiC* riboswitch Ec01, but not in the respective promoter control pEc01. *E. coli* strains transformed with the reporter plasmids based on pDlucTC were grown in M9 minimal medium in the absence (control) or presence of 10 µM thiamine. Firefly luciferase (Luc^F) activity was followed by measuring the light emission caused by the conversion of luciferin to oxyluciferin. Luc^F activity was normalized by the respective *Renilla* luciferase activity and is given as relative activity compared to the control. Cultures were grown in triplicates in a plate reader in a 12-well plate. Depicted are the mean values ± standard deviations of the data obtained from the triplicates. Asterisks indicate statistically significant differences (* $p \leq 0.05$).

4.4 Identification of new TPP riboswitches in ESKAPE pathogens, *Mammaliicoccus sciuri* and *Streptococcus pneumoniae*

After the assay was successfully established with the *E. coli thiC* riboswitch. Further putative TPP riboswitches from various pathogens were tested. Table 37 lists the potential riboswitch regions within the ESKAPE pathogens, as well as *M. sciuri a*nd *S. pneumoniae* that were investigated in this study. Riboswitch candidates were identified by searching the Rfam database for TPP riboswitches (performed by Dr. Vipul Panchal from the group of Prof. Dr. Ruth Brenk, University of Bergen, Norway), and their genomic localization was determined by matching the corresponding genome data in the NCBI database. The identified regions show sequence similarity to known TPP riboswitch sequences and are additionally located upstream of genes involved in thiamine synthesis or transport. The last column of Table 37 shows the PASIFIC web server prediction of the putative way of action of the riboswitch (also performed by Dr. Vipul Panchal from the group of Prof. Dr. Ruth Brenk, University of Bergen, Norway), based on the prognosticated presence of a transcriptional terminator-anti-terminator structure within the riboswitch sequence. A value above 0.5 was considered reliable for the prediction of such a structure. Riboswitches with a score below 0.5 were inversely assigned to the translational mode of action.

Table 37: Putative thiamine pyrophosphate riboswitches in ESKAPE pathogens and *Mammaliicoccus sciuri* and *Streptococcus pneumoniae*. Riboswitches (RS) are abbreviated with the initials of the species name and a number. The third column lists the respective gene, located downstream of the riboswitch. The mode of action, translational or transcriptional, was predicted with the PASIFIC web server (https://www.weizmann.ac.il/molgen/Sorek/PASIFIC/). A prediction score of over 0.5 for formation of a terminator structure was considered reliable.

Organism	RS	Gene	Gene product	Predicted type
Acinetobacter baumannii	**Ab01**	*thiC*	HMP-P synthase	Transcriptional
Enterobacter spp.	**Eb01**	*thiC*	HMP-P synthase	Transcriptional
	Eb03	*thiBPQ* operon	thiamine ABC transporter	Translational
Enterococcus faecium	**Ef02**	*thiT*	thiamine transporter	Translational
Klebsiella pneumoniae	**Kp01**	*thiBPQ* operon	thiamine ABC transporter	Translational
	Kp04	*thiC*	HMP-P synthase	Transcriptional
	Kp10	*tenA*	thiaminase II	Transcriptional
	Kp11	*thiM*	hydroxyethylthiazole kinase	Translational
Mammaliicoccus sciuri	**Ms01**	*tenA*	thiaminase II	Transcriptional
	Ms02	*thiE*	thiamine phosphate synthase	Transcriptional
Pseudomonas aeruginosa	**Pa01**	*thiC*	HMP-P synthase	Translational
Staphylococcus aureus	**Sa02**	*thiBPQ* operon	thiamine ABC transporter	Transcriptional
Streptococcus pneumoniae	**Sp06**	*thiD*	phosphomethylpyrimidine kinase	Translational

The first luciferase reporter gene assays with putative TPP riboswitches were performed employing a translational fusion plasmid with the *E. coli thiC* promotor that has been successfully used before. This was to ensure that the employed promoter was also functional in the *E. coli* host.

For the riboswitch sequences Pa01 from *P. aeruginosa* and the two sequences Eb01 and Eb03 from *Enterobacter* spp., as well as Ms02 from *M. sciuri*, a significant reduction in luciferase activity was observed upon addition of 10 µM thiamine to the bacterial cultures, compared to the control without thiamine (Figure 13C,D,E,G). For the riboswitch sequences Kp04 from *K. pneumoniae*, Ab01 from *A. baumannii* and Ms01 from *M. sciuri*, no effect of thiamine on the reporter activity was measured (Figure 13A,B,F). For the reporter plasmid with the putative *thiBPQ* riboswitch from *S. aureus* Sa02, no reporter gene activity was detected and therefore the response of this region to thiamine could not be determined with this assay.

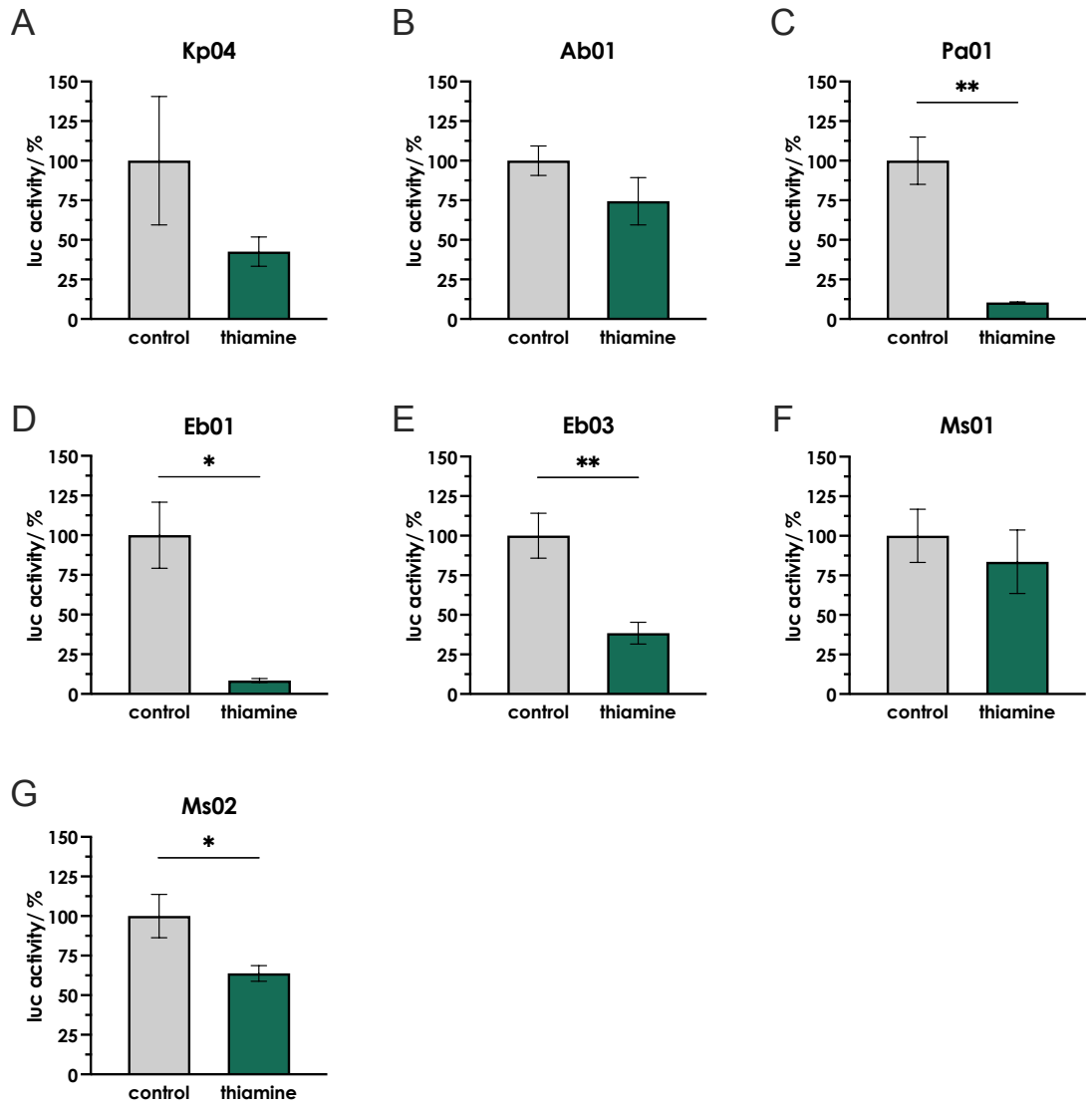

Figure 13: Reporter gene activity in translational fusions of putative riboswitches from pathogenic bacteria under control of the *E. coli thiC* promoter. *E. coli* DH5α strains transformed with the dual-luciferase reporter plasmids pDluc, for putative TPP riboswitches from **(A)** *K. pneumoniae*, *thi*C, Kp04 **(B)** *A. baumannii*, *thiC*, Ab01 **(C)** *P. aeruginosa, thiC*, Pa01 **(D)** *Enterobacte*r spp., *thiC*, Eb01 and **(E)** *Enterobacter thiBPQ* operon Eb03, as well as **(F)** *M. sciuri, tenA* Ms01 and **(G)** *M. sciuri, thiE*, Ms02 under control of the *E. coli thiC* promoter pEc01, were grown in M9 minimal medium without (control) and with 10 µM of thiamine. Luciferase activity was normalized by the respective *Renilla* luciferase activity and is given as relative activity compared to the control. Cultures were grown in triplicates in a 12-well plate. Depicted are the mean values ± standard deviations of the data obtained from the triplicates. Asterisks indicate statistically significant differences (* $p \leq 0.05$, ** $p \leq 0.01$).

Since the putative *thiC* riboswitch sequence Kp04 from *K. pneumoniae* shows a high sequence similarity to the *thiC* riboswitch sequence from *E. coli* and, moreover, was found to respond to thiamine in a previously performed *lacZ* reporter gene assay (see Figure 7), using the native *K. pneumonia*e promoter it was suspected that the employed *E. coli thiC* promotor was too strong and thus prevented Kp04 from functioning properly. Therefore, translational fusions of the riboswitches Kp04, Ab01, Ms01 and Ms02 were tested with their respective native promoters. In addition, sequences from *Enterococcus faecium* (Ef02) and *Streptococcus pneumoniae* were included (Sp06), which did not respond to thiamine in combination with the *E. coli thiC* promoter (Figure 14). A specific control plasmid was

constructed for each of these putative riboswitches, only containing the respective promotor and ribosomal binding site (RBS) but not the riboswitch sequence itself.

For none of the strains with a promoter-control plasmid, a reduction in luciferase activity was measured when thiamine was present. In all strains with a riboswitch plasmid reporter activity was significantly decreased (Figure 14), except for the *M. sciuri* Ms01 riboswitch (Figure 14D). While the Ms02 riboswitch in conjunction with its native promoter did not respond to thiamine to a greater extent than with the *E. coli thiC* promoter (Figure 14E, Figure 13G), the effect of thiamine was much more pronounced for the natural combination of promotor and riboswitch for the *A. baumannii* Ab01 and the *K. pneumoniae* Kp04 regions (Figure 14B,C).

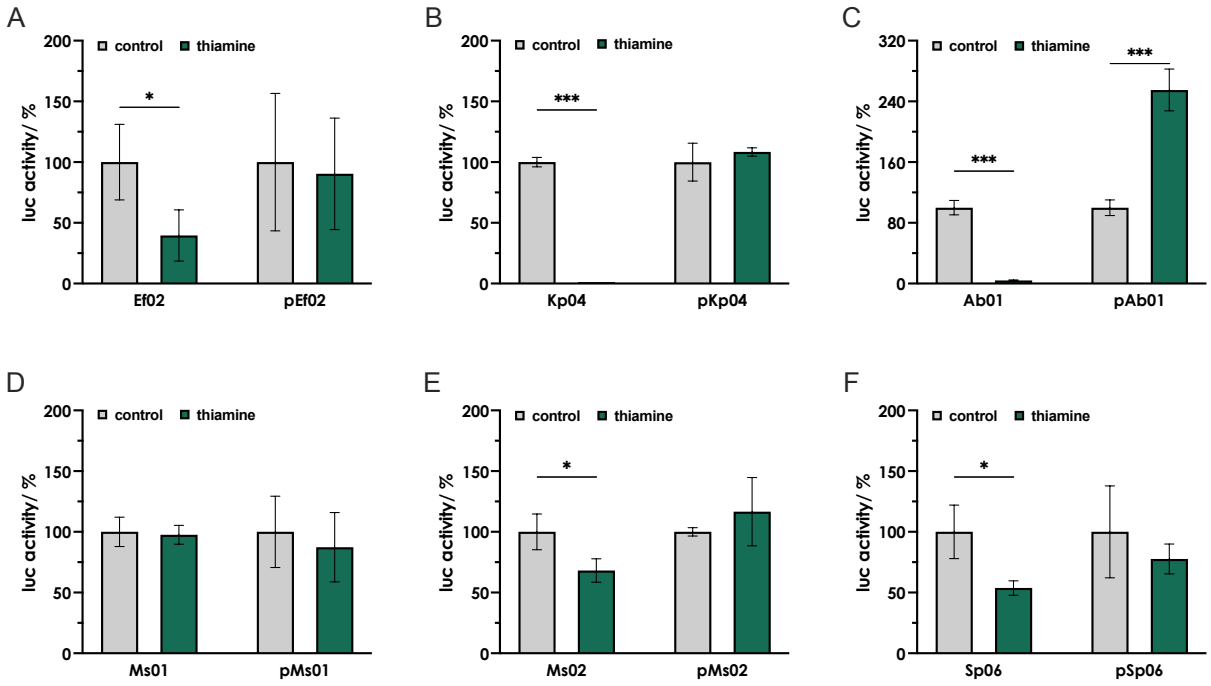

Figure 14: Reporter gene activity in translational fusions of putative riboswitches from pathogenic bacteria with their native promoters. *E. coli* DH5α strains transformed with the dual-luciferase reporter plasmids pDluc, for putative TPP riboswitches from **(A)** *E. faecium* (Ef02), **(B)** *K. pneumoniae* (Kp04), **(C)** *A. baumannii* (Ab01), **(D)** *M. sciuri tenA* (Ms01) and **(E)** *thiE* (Ms02) and **(F)** *S. pneumoniae* (Sp06) under control of their native promoters together with the respective promoter control plasmids pEf02, pKp04 pAb01, pMs01, pMs02 and pSp06 (not containing a RS) were grown in M9 minimal medium without (control) and with 10 µM of thiamine. Luciferase activity was normalized by the respective *Renilla* luciferase activity and is given as relative activity compared to the control. Cultures were grown in triplicates in a 12-well plate. Depicted are the mean values ± standard deviations of the data obtained from the triplicates. Asterisks indicate statistically significant differences (* $p \leq 0.05$, *** $p \leq 0.001$).

In total, the employment of the novel dual-luciferase assay identified eight new TPP riboswitches, at least one in each of the ESKAPE pathogen strains, excluding *S. aureus*, but including *M. sciuri* and *S. pneumoniae*.

4.4.1 Investigation of the mode of action for the newly identified TPP riboswitches

In the translational fusion plasmids, the putative riboswitch, the respective RBS and the first few codons of the downstream gene are directly fused to the firefly luciferase gene. This construct allows the detection of a regulation of downstream gene expression that can be achieved either by the sequestering of the RBS, as well as by the formation of a transcriptional terminator. This makes it a suitable construct to identify putative riboswitches. However, with this plasmid it is not possible to distinguish between the two modes of action. Therefore, a transcriptional fusion plasmid was assembled for all the riboswitches that were identified before. This plasmid contains an additional RBS for the *luc*^{F} gene, enabling a translation of mRNA even in case the first RBS has become inaccessible due to RNA folding. Hence, a reduction in luciferase activity only occurs, when a terminator structure is formed that already aborts transcription. For the transcriptional reporter gene fusions of the riboswitches from *K. pneumoniae*, *A. baumannii*, *P. aeruginosa* and the Eb01 riboswitch from *Enterobacter* spp., a significant reduction in luciferase activity was detected, when 10 µM of thiamine were added (Figure 15B,C,D,E).

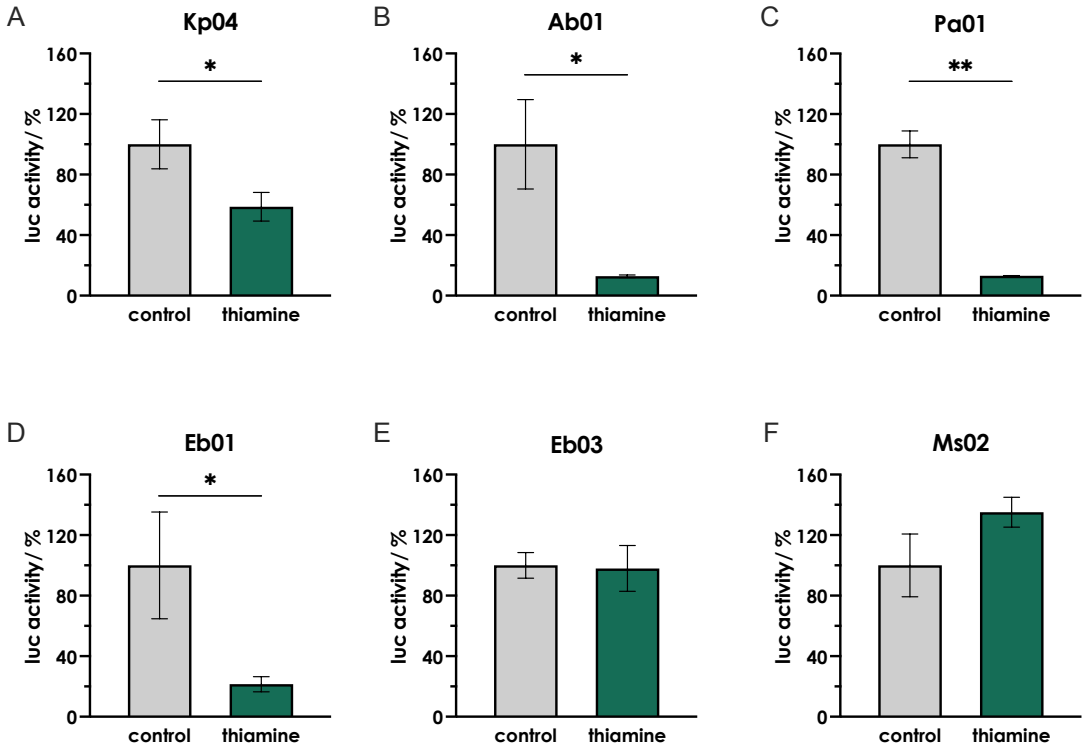

Figure 15: Reporter gene activity in transcriptional fusions of putative riboswitches from pathogenic bacteria under control of the *E. coli thiC* riboswitch. *E. coli* DH5α strains transformed with the dual-luciferase reporter plasmids pDlucTC, for putative TPP riboswitches from **(A)** *K. pneumoniae*, *thi*C, Kp04 **(B)** *A. baumannii*, *thiC*, Ab01 **(C)** *P. aeruginosa, thiC*, Pa01 **(D)** *Enterobacte*r spp., *thiC*, Eb01 and **(E)** *Enterobacter thiBPQ* operon Eb03, as well as **(F)** *M. sciuri, thiE* operon Ms02, under control of the *E. coli thiC* promoter pEc01, were grown in M9 minimal medium without (control) and with 10 µM of thiamine. Luciferase activity was normalized by the respective *Renilla* luciferase activity and is given as relative activity compared to the control. Cultures were grown in triplicates in a 12-well plate. Depicted are the mean values ± standard deviations of the data obtained from the triplicates. Asterisks indicate statistically significant differences (* $p \leq 0.05$, ** $p \leq 0.01$).

For the riboswitch regions of *M. sciuri* and the Eb03 region of *Enterobacter*, on the other hand, no reduction in reporter activity was measured (Figure 15E,F).

The riboswitches that have been identified before in a translational fusion in combination with their native promoter were examined again for their transcriptional function with the respective promoter region. This is to ensure that possible responses are not masked by some influence of the *E. coli* promoter. The riboswitch regions Kp04 and Ab01 were included as well, even though a significant effect of thiamine was already measured for these two when employing the Ec01 promoter. In contrast to the translational fusions for these regions, no stronger effect of thiamine is observed here on the reporter gene activity, when the native promoter is used (Figure 16C, D). For the riboswitch region Ef02 from *E. faecium*, a decrease in luciferase activity to 73% of the control was measured, when thiamine was added (Figure 16A).

The riboswitch region Sp06 from *S. pneumoniae* and the promoter control region pMs02 from *M. sciuri* could not be successfully tested in the transcriptional reporter gene assay. No firefly luciferase activity was detected in the cell-free extracts of the strains carrying the respective plasmids, although the reaction catalyzed by the control enzyme, the *Renilla* luciferase, was measurable and for the same riboswitch regions Luc^F activity could be measured for the translational fusion plasmid (Figure 14D,E).

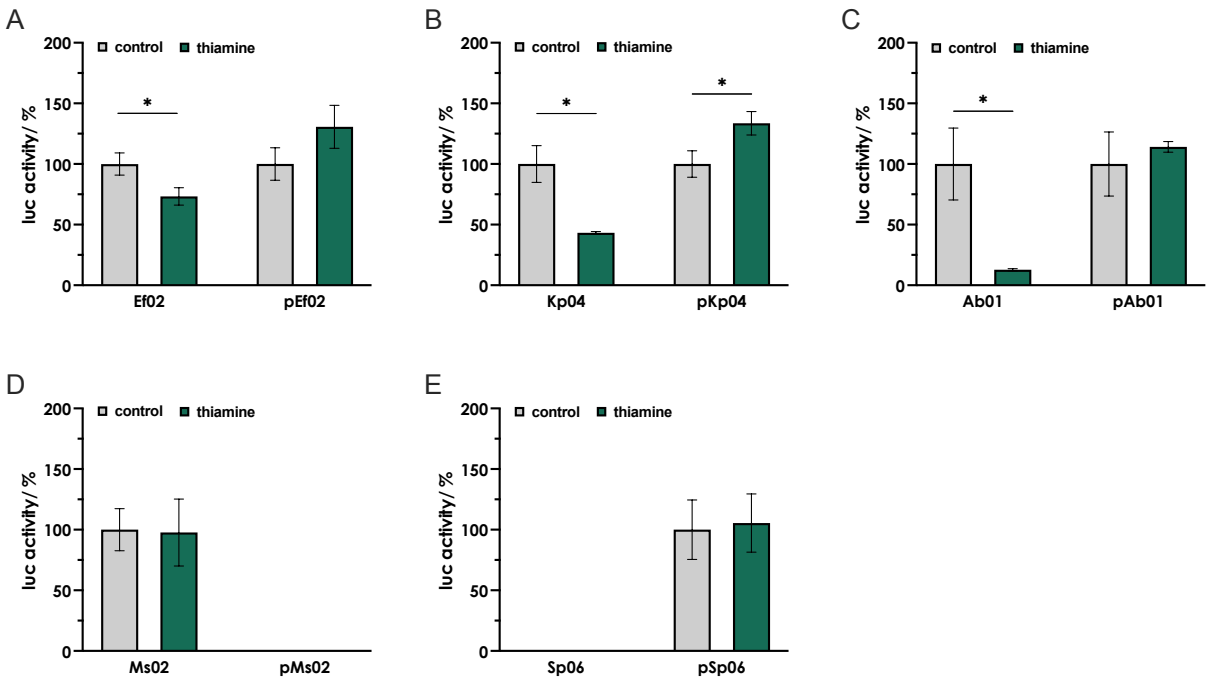

Figure 16: Reporter gene activity in transcriptional fusions of putative riboswitches from pathogenic bacteria with their native promoters. *E. coli* DH5α strains transformed with the dual-luciferase reporter plasmids pDlucTC, for putative TPP riboswitches from **(A)** *E. faecium* (Ef02), **(B)** *K. pneumoniae* (Kp04), **(C)** *A. baumannii* (Ab01), **(D)** *M. sciuri thiE* (Ms02) and **(E)** *S. pneumoniae* (Sp06) under control of their native promoters together with the respective promoter control plasmids pEf02, pKp04 pAb01, pMs02 and pSp06 (not containing a RS) were grown in M9 minimal medium without (control) and with 10 µM of thiamine. Luciferase activity was normalized by the respective *Renilla* luciferase activity and is given as relative activity compared to the control. Cultures were grown in triplicates in a 12-well plate. Depicted are the mean values ± standard deviations of the data obtained from the triplicates. Asterisks indicate statistically significant differences (* $p \leq 0.05$).

In total, eight different putative TPP riboswitch regions showed a response to thiamine in the reporter gene assay performed. Translational and transcriptional fusions were successfully tested for six of them. Table 38 lists all the riboswitch regions examined and provides a comparison of the *in silico* prediction of their mode of function with the results of the *in vivo* testing in this study.

Table 38: Identified thiamine pyrophosphate riboswitches in ESKAPE pathogens, including *M. sciuri* and *S. pneumoniae*. Listed are all the riboswitches that showed a decrease in reporter gene activity upon addition of thiamine. The *in silico* predicted mode of action (PASIFIC) is compared to the experimental outcome (exp.).

Organism	RS name	Gene	Predicted	Mode of action (exp.)
Acinetobacter baumannii	**Ab01**	*thiC*	Transcriptional	→ Transcriptional/(translational)
***Enterobacter* spp.**	**Eb01**	*thiC*	Transcriptional	→ Transcriptional
Enterobacter spp.	**Eb03**	*thiBPQ* operon	Translational	→ Translational
Enterococcus faecium	**Ef02**	*thiT*	Translational	→ Translational/transcriptional
Klebsiella pneumoniae	**Kp04**	*thiC*	Transcriptional	→ Translational/transcriptional
Pseudomonas aeruginosa	**Pa01**	*thiC*	Translational	→ Transcriptional
Mammaliicoccus sciuri	**Ms02**	*thiE* operon	Transcriptional	→ Translational
Streptococcus pneumoniae	**Sp06**	*thiD*	Translational	-

4.5 Test of identified riboswitches with the thiamine-analog pyrithiamine

4.5.1 Comparison of the reporter gene activity in a thiamine-auxotrophic and a prototrophic *E. coli* strain

The initial intention to investigate TPP-riboswitches from various pathogens as potential targets for new antibiotic substances. For that purpose, new structural analogs for thiamine should be synthesized and tested for their effects on TPP riboswitches. However, since no newly synthesized compounds have been available so far, the antibacterial thiamine-analog pyrithiamine (PT) and the HMP analog bacimethrin (BM) (Figure 17) were studied instead.

At first, the effect of pyrithiamine and bacimethrin was tested on the *E. coli thiC* riboswitch Ec01. When the thiamine-auxotrophic *E. coli* strain DH5α, for which 20 nM thiamine had to be added to the pre-cultures, was used as a host for the respective reporter plasmid, luciferase activity did not change upon addition of pyrithiamine (Figure S7).

The assay was therefore repeated using the prototrophic *E. coli* strain MG1655. A significant effect of pyrithiamine, but not bacimethrin, on luciferase activity was now observed for this strain (Figure 18A). However, the decrease in luciferase activity detected for growth with pyrithiamine was not as strong as that measured for the same TPP riboswitch with thiamine in DH5α (Figure 11B).

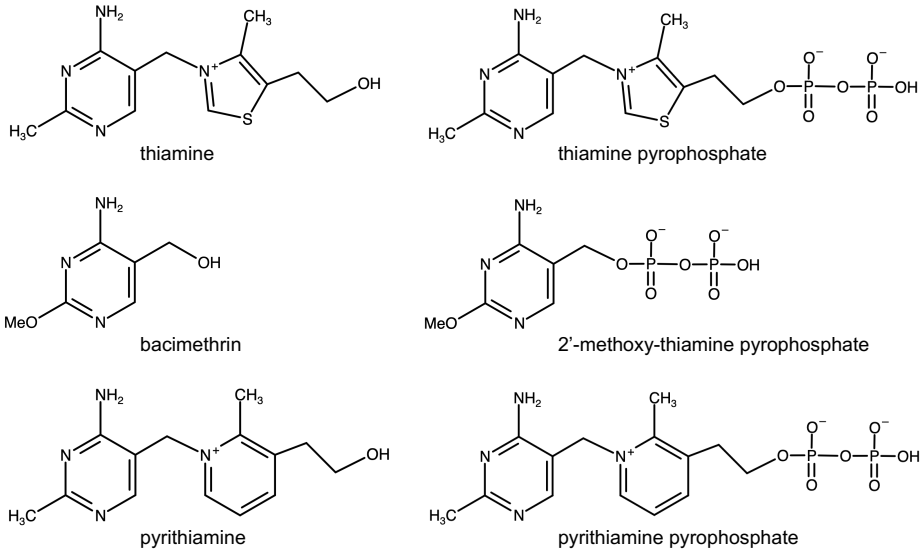

Figure 17: **Structures of thiamine pyrophosphate and its structural analogs 2'-methoxy-thiamine pyrophosphate and pyrithiamine pyrophosphate, together with the respective precursors thiamine, bacimethrin and pyrithiamine.**

To test whether the lack of response of the Ec01 riboswitch to pyrithiamine in DH5α is due to the addition of thiamine to the pre-cultures, an equivalent amount of thiamine was added to the MG1655 pre-cultures before performing the reporter assay. Under these conditions, addition of pyrithiamine did not result in a decrease in luciferase activity for the prototrophic strain as well (Figure 18B).

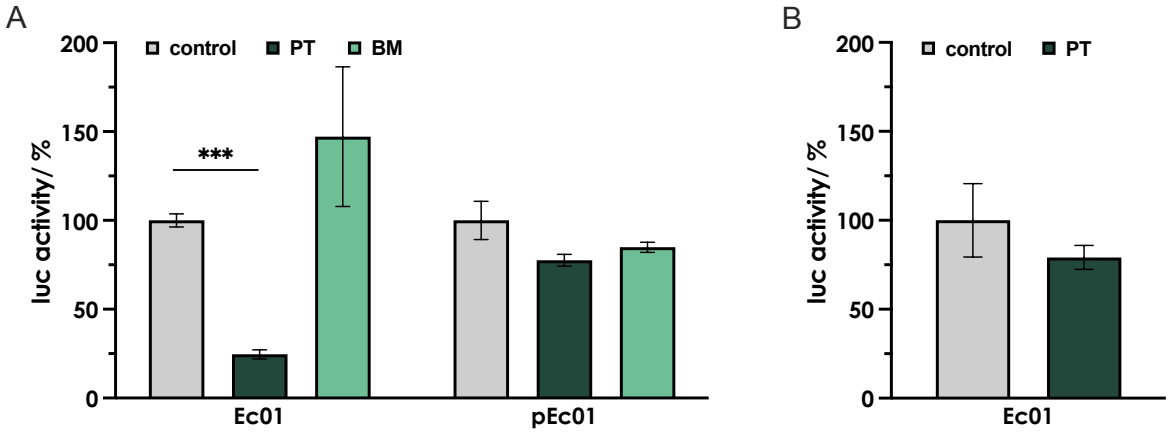

Figure 18: Effect of pyrithiamine on reporter gene activity testing a translational fusion of the *E.coli thiC* riboswitch (Ec01) and the reporter gene expressed from the natural promoter of *thiC* (pEc01). Luciferase activity (Luc^F) was determined for the prototrophic strain *E*. coli MG1655 **(A)** from M9 pre-cultures without thiamine and **(B)** from pre-cultures that contained 20 nM of thiamine. All *E. coli* main cultures for which the Luc^F activity was determined were grown in M9 minimal medium without thiamine and without (control) and with 10 µM of pyrithiamine (PT) or bacimethrin (BM). Luc^F activity was normalized by the respective *Renilla* luciferase activity and is given as relative activity compared to the control. Cultures were grown in triplicates in a 12-well plate. Depicted are the mean values ± standard deviations of the data obtained from the triplicates. Asterisks indicate statistically significant differences (*** $p \leq 0.001$).

4.5.2 Effect of pyrithiamine on TPP riboswitches from ESKAPE pathogens and *M. sciuri*

The previous results with the *E. coli thiC* riboswitch had shown that a thiamine-prototrophic strain has to be used to observe an effect of pyrithiamine on riboswitch activity. Thus, for the following experiments, the *E. coli* strain MG1655 was used to test the effect of pyrithiamine on other TPP riboswitches. For none of the tested TPP riboswitches from *M. sciuri*, *K. pneumoniae*, *A. baumannii*, *P. aeruginosa* and *Enterobacter* spp. that showed a response to thiamine, pyrithiamine had a significant effect on reporter gene activity.

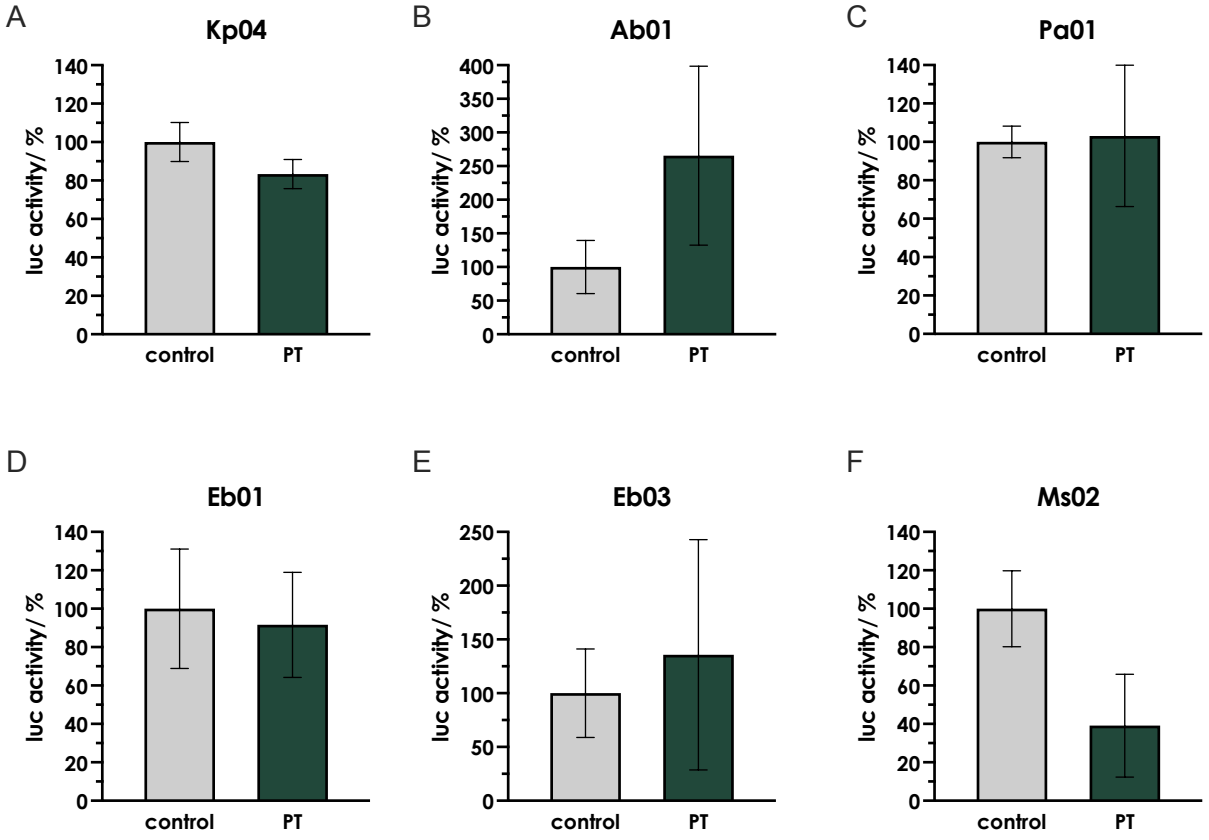

Figure 19: Effect of pyrithiamine on reporter gene activity in translational fusions with TPP-riboswitches from (A) *K. pneumoniae* Kp04, (B) *A. baumannii* Ab01, (C) *P. aeruginosa* Pa01 (D, E) *Enterobacter* spp. Eb01, Eb03 and (F) *M. sciuri* Ms01 expressed from the *thiC* promoter of *E. coli*. *E. coli* MG1655 strains were grown in M9 minimal medium without (control) and with 10 µM of pyrithiamine. Luc^F activity was normalized by the respective *Renilla* luciferase activity and is given as relative activity compared to the control. Cultures were grown in triplicates in a 12-well plate. Depicted are the mean values ± standard deviations of the data obtained from the triplicates.

Corresponding to the tests with thiamine, the riboswitch regions Ab01 and Kp04 were examined for their response to pyrithiamine in combination with their native promoter. However, no significant decrease in luciferase activity was observed for the treatment with pyrithiamine for these strains as well (Figure 20).

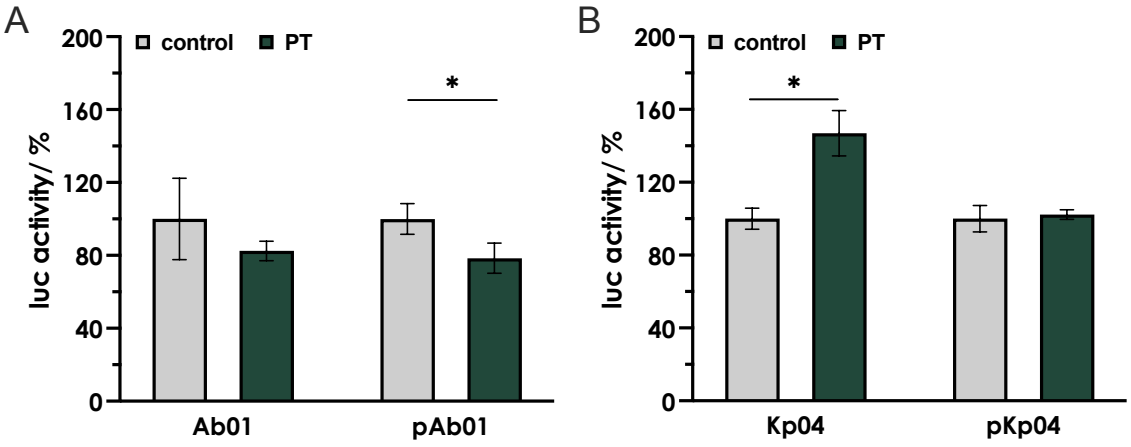

Figure 20: Effect of pyrithiamine on reporter gene activity in translational fusions with (A) the *A. baumannii thiC* riboswitch Ab01 and (B) the *K. pneumoniae thiC* riboswitch Kp04 under control of the respective native promoter. Promoter control plasmids were included for both riboswitches (pAb01, pKp04). *E. coli* MG1655 cultures were grown in M9 minimal medium without (control) and with 10 µM of pyrithiamine. Luc^F activity was normalized by the respective *Renilla* luciferase activity and is given as relative activity compared to the control. Cultures were grown in triplicates in a 12-well plate. Depicted are the mean values ± standard deviations of the data obtained from the triplicates. Asterisks indicate statistically significant differences (* $p \leq 0.05$).

4.5.3 Sequence and structural comparison of the *E. coli* and *K. pneumoniae thiC* riboswitches

Subsequently, differences in the primary and secondary structures of the *E. coli thiC* riboswitch and the *K. pneumoniae thiC* riboswitch were investigated to find possible reasons for their different responses to pyrithiamine. Generally, TPP riboswitches are quite conserved among different species. This also becomes evident, when the two sequences of the *thiC* riboswitches from *E. coli* and *K. pneumoniae* were compared (Figure 21A). For the *E. coli* riboswitch, the crucial nucleotides for binding of the thiamine pyrophosphate HMP moiety and the phosphate groups have already been identified (Serganov *et al.*, 2006). Especially in this aptamer domain responsible for the ligand binding, long continuous sequence segments are identical to the *K. pneumoniae thiC* riboswitch. However, two short additional sequence segments, nucleotides 21-37 and 42-48, as well as one differing nucleotide, A63, are present in the aptamer domain of the *K. pneumoniae* riboswitch (see Figure 21A).

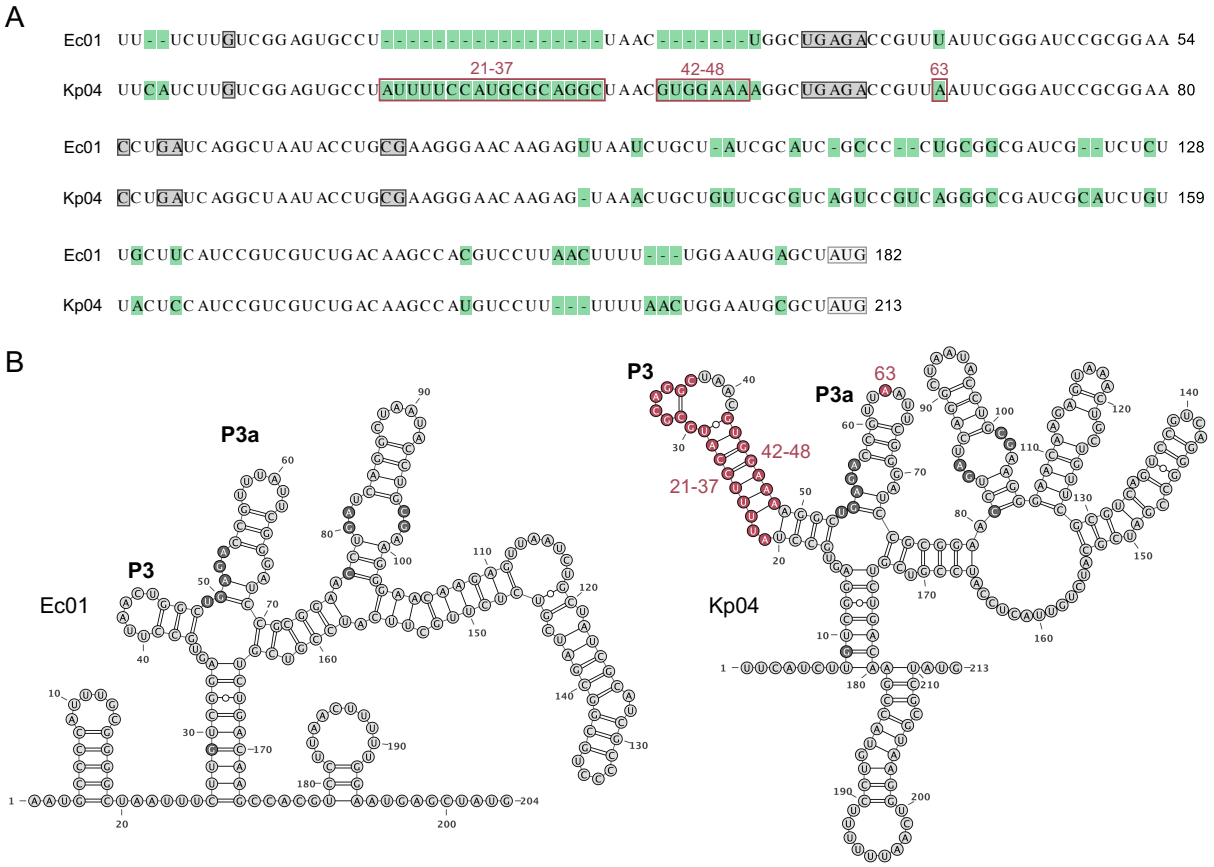

Figure 21: Alignment of the DNA sequences for the *E. coli* (Ec01) and the *K. pneumoniae* (Kp04) *thiC* riboswitches (A) and comparison of their secondary structures (B). (A) The sequence alignment was created using Emboss Needle employing the Needleman-Wunsch algorithm (Madeira *et al.*, 2022). Differences in the sequences are highlighted in green. **(B)** Folding of the riboswitch RNA sequences was performed with RNAfold. Sequence parts relevant for ligand binding are highlighted in gray. A light gray box marks the start codon of the *thiC* coding sequence. Relevant nucleotides (21-37, 42-48 and 63) that differ between the Kp04 sequence and the *E. coli thiC* riboswitch Ec01 are marked in red in the Kp04 sequence and structure.

In the expression platform of the riboswitches, on the other hand, the nucleotide sequences differ to a greater extent (Figure 21A). When the predicted secondary structures of the two riboswitch sequences generated by RNAfold were compared, similar pairings of the nucleotides become apparent, especially for the ligand binding sequences. However, some striking differences were also detected. Most notably the nucleotides 21-37 and 42-48 appear to form a prolonged P3 stem in the structure of the Kp04 riboswitch, which is absent in the Ec01 riboswitch (Figure 21B).

4.5.4 The effect of pyrithiamine on the activity of different mutants of the *K. pneumoniae thiC* riboswitch Kp04

To test whether these observed differences in the primary sequence of the *K. pneumoniae* Kp04 riboswitch in comparison to the *E. coli thiC* riboswitch are responsible for the lack of the Kp04 response to pyrithiamine, several Kp04 riboswitch mutants were generated. The adenine

at position 63 of the mRNA was replaced by uracil, resulting in the mutant Kp04^{A63U}, and both short inserts that form each side of the additional stem structure were deleted individually, creating the mutant riboswitches Kp04$^{\Delta 21\text{-}37}$ and Kp04$^{\Delta 42\text{-}48}$. For all three mutants the secondary structure was predicted *in silico* using RNAfold. The single nucleotide exchange in Kp04^{A63U} did not lead to any changes in the *in silico* folding of the Kp04 riboswitch (Figure 22A). This corresponds to the expectations since the nucleotide is positioned at the unpaired tip of the P3a helical arm. Nevertheless, the mutant Kp04^{A63U} was included in the further dual-luciferase assays with pyrithiamine Two differently shaped P3 stem structures are predicted for the two deletion mutants Kp04$^{\Delta 21\text{-}37}$ and Kp04$^{\Delta 42\text{-}48}$ (Figure 22B,C), with the Δ21-37 deletion showing the closest structural resemblance to the Ec01 riboswitch structure (Figure 21B).

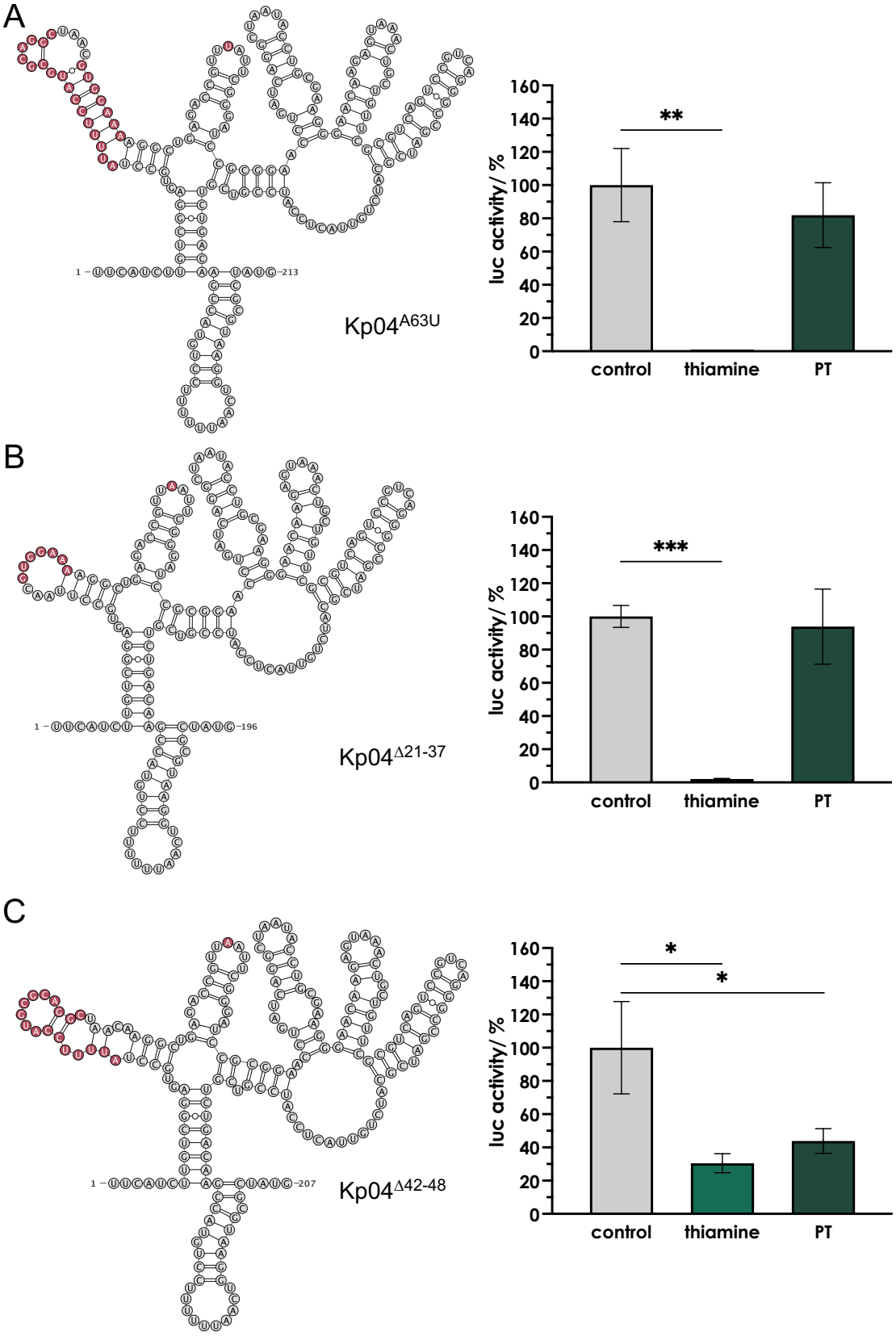

Figure 22: Effect of thiamine and pyrithiamine on luciferase activity for translational fusions with the *K. pneumoniae thiC* riboswitch mutants Kp04^{A63U} (A), Kp04$^{\Delta 21\text{-}37}$ (B) and Kp04$^{\Delta 42\text{-}48}$ (C). *E. coli* MG1655 strains were grown in M9 minimal medium without (control) and with 10 µM of thiamine or pyrithiamine (PT). Luciferase activity was normalized by the respective *Renilla* luciferase activity and is always given as relative activity compared to the control. Cultures were grown in triplicates in a 12-well plate. Depicted are the mean values ± standard deviations of the data obtained from the triplicates. Asterisks indicate statistically significant differences (* $p \leq 0.05$, (** $p \leq 0.01$, *** $p \leq 0.001$). The corresponding folded RNA structures are shown. Folding was performed with RNAfold. Relevant differences to the *E. coli thiC* riboswitch Ec01 are colored in red.

Thiamine still had a strong effect on luciferase activity in the riboswitch mutant strains Kp04^{A63U} and Kp04$^{\Delta 21\text{-}37}$, while pyrithiamine did not lead to a change in activity levels (Figure 22A,B). However, the deletion of the nucleotides 42 to 48 resulted in a significant reduction of luciferase activity compared to the control, when pyrithiamine was added. Notably, for this mutated riboswitch, thiamine reduced the luciferase activity to only about 30 % of the control (Figure 22C), compared to a reduction to less than 1% for the Kp04 WT (Figure 14B).

To further examine the influence of the nucleotides 42 to 48 of the Kp04 riboswitch on ligand binding, the nucleotides 42G, 43U, 44G and 46A were deleted individually from the reporter gene plasmid. The resulting riboswitch mutants were again tested for their responses to thiamine and pyrithiamine (Figure 23).

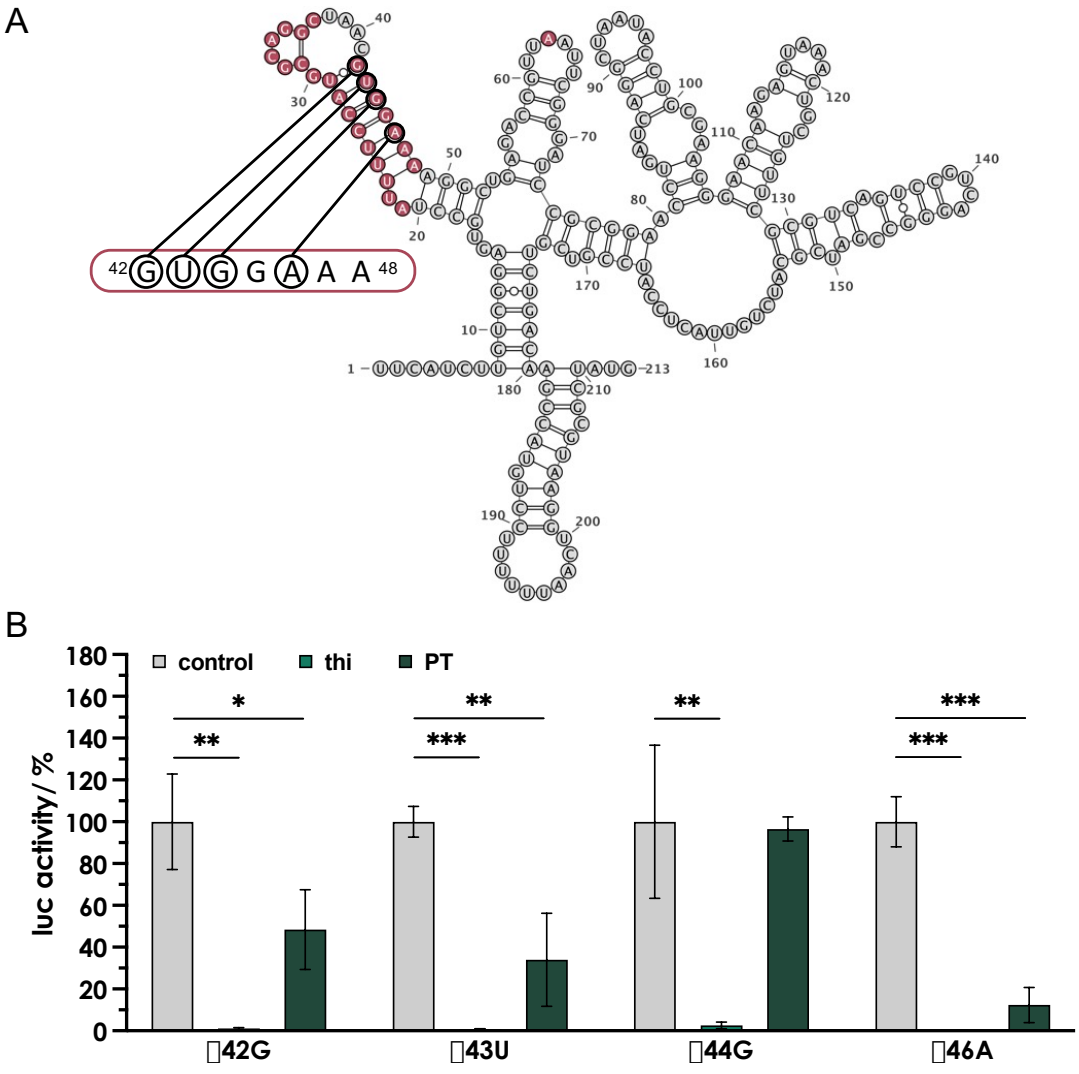

Figure 23: Effect of thiamine and pyrithiamine on luciferase activity for translational fusions with the *K. pneumoniae thiC* Kp04 riboswitch mutants Δ42G, Δ43U, Δ44G and Δ46A. (A) Folding of the Kp04 RS structure was performed with RNAfold. Relevant differences to the *E. coli thiC* riboswitch Ec01 are colored in red and individually deleted nucleotides from region 42-48 are marked with black circles. **(B)** *E. coli* MG1655 strains were grown in M9 minimal medium without (control) and with 10 µM of thiamine (thi) or pyrithiamine (PT). Luc^F activity was normalized by the respective *Renilla* luciferase activity and is always given as relative activity compared to the control. Cultures were grown in triplicates in a 12-well plate. Depicted are the mean values ± standard deviations of the data obtained from the triplicates. Asterisks indicate statistically significant differences (* $p \leq 0.05$, ** $p \leq 0.01$, *** $p \leq 0.001$).

Except for the G44 deletion, addition of pyrithiamine to the medium resulted in a repression of the luciferase gene for all the new riboswitch mutants, while the response of reporter activity to thiamine was always comparable to the Kp04 WT (Figure 23). The strongest decrease in reporter gene expression was observed when the luciferase gene was under control of the Kp04$^{\Delta 46A}$ riboswitch.

4.6 The effect of pyrithiamine on other *K. pneumoniae* TPP riboswitches

Pyrithiamine showed a strong antibacterial effect against *B. subtilis* and *E. coli* and inhibited growth of these two organisms in liquid media at concentrations of 140 µM and 200 µM, respectively (Sudarsan *et al.*, 2005). Since no effect of pyrithiamine was observed on the unmutated *thiC* riboswitch of *K. pneumoniae*, it was examined, whether pyrithiamine inhibited growth of this bacterium.

Therefore, growth experiments with *K. pneumoniae* were performed in a minimal medium that was either supplemented with 200 µM of thiamine or pyrithiamine (Figure 24A). Addition of thiamine did not affect growth of the strain, while pyrithiamine led to a slower growth and a lower final OD_{600}. However, this effect was not as pronounced as in *E. coli* or *B. subtilis*, even when 300 µM of pyrithiamine were added to the growth medium (Figure 24B).

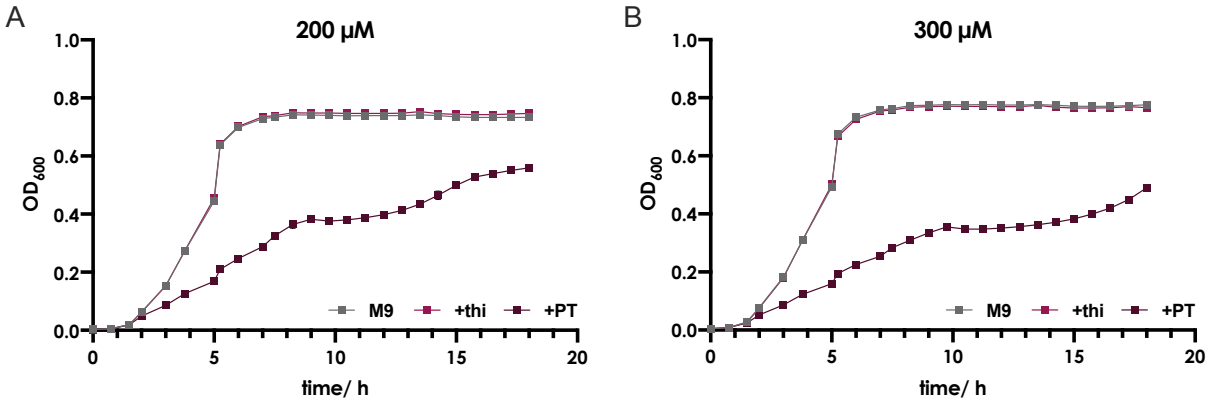

Figure 24: Growth of *K. pneumoniae* in M9 medium, supplemented with 200 µM (A) or 300 µM (B) of thiamine and pyrithiamine, respectively. Cultures were grown in triplicates in 1mL cultures in a 24-well plate. Depicted are the mean values of the data obtained from the triplicates. Standard deviations are too small to be visualized.

Still, the growth impairment of *K. pneumoniae* by pyrithiamine was obvious. Since it was already shown that this was not due to an influence on the Kp04 riboswitch activity, the other TPP riboswitches of *K. pneumoniae* were taken into focus. The bioinformatic analysis of the genome had revealed three more putative riboswitches Kp01, Kp10 and Kp11. Kp01 is located upstream of the *thiBPQ* operon (coding for the thiamine ABC transporter), Kp10 upstream of *tenA* (coding for thiaminase II) and Kp11 upstream of *thiMD* (coding for the bifunctional

hydroxyethylthiazole kinase/phosphomethylpyrimidine kinase). These putative riboswitches were first examined for their response to thiamine using the dual luciferase assay based on the test vector pDluc (Figure 25). For all of them, addition of thiamine to the medium resulted in a reduced expression of the luciferase reporter gene, while no repression was observed for the promoter control plasmids. For the Kp10 riboswitch this reduction in reporter activity was not statistically significant due to the high standard deviation of the control (Figure 25B).

These results validated that the three regions indeed contain functional riboswitches responding to TPP. Therefore, all three riboswitches were also tested for their response to pyrithiamine in the medium, i.e. the influence on reporter gene expression was analyzed again using the luciferase assay (Figure 25). In this setup, only the presence of the *thiMD* riboswitch Kp11 decreased luciferase activity significantly to around 60 % (Figure 25C). However, this effect was again not as pronounced as the one observed for the *E. coli thiC* riboswitch.

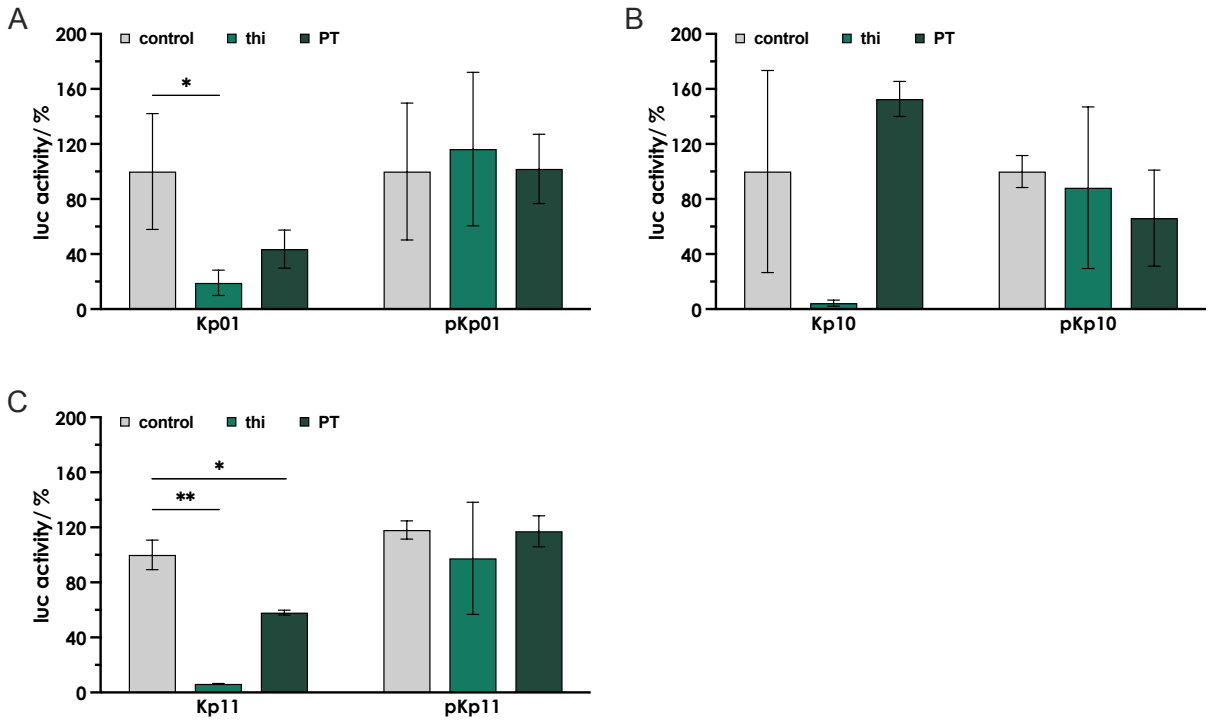

Figure 25: Effect of thiamine and pyrithiamine on luciferase activity for translational fusions with the *K. pneumoniae thiBPQ* (Kp01) (A), *tenA (*Kp10) (B) and *thiM* (Kp11) (C) riboswitches. *E. coli* MG1655 strains were grown in M9 minimal medium without (control) and with 10 µM of thiamine (thi) or pyrithiamine (PT). Luciferase activity was normalized by the respective *Renilla* luciferase activity and is always given as relative activity compared to the control. Cultures were grown in triplicates in a 12-well plate. Depicted are the mean values ± standard deviations of the data obtained from the triplicates. Asterisks indicate statistically significant differences (* $p \leq 0.05$, ** $p \leq 0.01$).

4.6.1 Generation of PT-resistant *K. pneumoniae* strains and sequencing of the TPP riboswitch regions

Growth of *K. pneumoniae* was only slightly reduced in the presence of pyrithiamine and no effect on riboswitch activity was observed for the riboswitches Kp01, Kp04 and Kp10. However, a significant effect of pyrithiamine was measured for the Kp11 riboswitch. Therefore, PT-resistant strains of *K. pneumoniae* were selected by growing cells in M9 minimal medium, supplemented with 1 mM of pyrithiamine. Saturated cultures were used to inoculate fresh medium with and without pyrithiamine, until the strains showed a similar growth curve in the cultures with pyrithiamine compared to the cultures without PT. Finally, cells passaged in medium with PT were plated on agar with pyrithiamine. Single colonies were checked for any possible changes in the sequences of all four TPP-riboswitches. However, none of the 13 individually selected strains had developed mutations in any of the TPP-riboswitch regions.

5 Discussion – Chapter I

Riboswitches are versatile genetic control elements, which regulate bacterial metabolic pathways. Binding of a small, specific ligand to the riboswitch RNA induces a change in secondary structure of the riboswitch and thereby alters expression of downstream genes (Mandal *et al.*, 2003). A variety of different mechanisms have been described so far by which riboswitches modulate gene expression in prokaryotes and eukaryotes (Bédard *et al.*, 2020). Due to their widespread distribution and the specific nature of the regulation of essential cellular processes, riboswitches have come into focus as new targets in antibiotics research (Aghdam *et al.*, 2016; Pavlova and Penchovsky, 2022; Ellinger *et al.*, 2023). Against this background, the aim of the first part of this study was to experimentally verify the functionality of TPP riboswitches in certain human pathogens.

5.1 TPP riboswitches

The TPP riboswitch has been described multiple times as a promising target for new antibiotic substances (Panchal and Brenk, 2021; Wakchaure and Ganguly, 2023). It is present in a wide range of pathogenic species and regulates essential genes involved in the thiamine metabolic pathway (Pavlova *et al.*, 2023). TPP riboswitch aptamers have been identified in a number of bacterial species by bioinformatic methods. This includes bacterial pathogens of the ESKAPE pathogen group, comprising *E. faecium*, *K. pneumoniae*, *A. baumannii*, *P. aeruginosa* and *Enterobacter* spp (Pavlova and Penchovsky, 2019; Panchal and Brenk, 2021). However, the actual functionality of these riboswitch sequences has not been validated experimentally.

5.1.1 Development of a dual-luciferase assay for *E. coli*

To test the functionality of the TPP riboswitches, a reporter assay was developed in which the riboswitch controls the expression of a reporter gene located downstream of the riboswitch sequence. At first, a reporter plasmid with the β-galactosidase gene *lacZ* was constructed and tested with the *E. coli thiC* riboswitch in *E. coli* DH5α. Compared to cells grown without thiamine supplementation, a significant reduction in reporter activity was observed for the cultures grown with 10 µM of thiamine, while reporter gene activity of the promoter control strain (not containing a riboswitch) remained unaffected by the addition of thiamine. This was a replication of the results obtained by Winkler *et al.* (2002), who first experimentally validated the response of the *E. coli thiC* riboswitch to thiamine. After the functionality of the newly constructed translational *lacZ* reporter plasmid was confirmed, it was used to test further putative TPP riboswitch sequences from ESKAPE pathogens, which had not yet been verified

experimentally. With this approach, a functional TPP riboswitch (Kp04) upstream of the *thiC* gene in *K. pneumoniae* was identified. The *E. coli thiC* riboswitch and the Kp04 riboswitch from *K. pneumoniae* not only control the expression of homologous genes, but their aptamer region also shows high sequence similarity. Analogous to the effect observed for the *E. coli* riboswitch, reporter gene activity was significantly reduced when thiamine was added to the cells carrying the Kp04 riboswitch plasmid. The *lacZ* reporter plasmid was then used to identify further TPP riboswitches in other ESKAPE strains. However, even though the results of the LacZ assay were reproducible for the *E. coli* and *K. pneumoniae thiC* riboswitch regions, the measured reporter activity showed high standard deviations for some of the constructs.

Therefore, another reporter gene plasmid was constructed, using the firefly luciferase gene luc^F as a reporter. Due to its activity as a monomer and the relatively short half-life of the protein, this luciferase exhibits a high sensitivity as a reporter (Thorne *et al.*, 2010). It has also been validated that the reporter assay based on the luciferase reaction represents a more sensitive reporter than the colorimetric assay used for the β-galactosidase (Jain and Magrath, 1991; Martin *et al.*, 1996; Schmid *et al.*, 1997). Additionally, the introduction of a second luciferase gene, constitutively expressed from the same reporter plasmid, allowed to normalize the data with regard to differences in cell lysis efficiency and plasmid copy numbers (Sherf *et al.*, 1996; Adams *et al.*, 2017), thereby making the reporter assay even more reliable. For this purpose, a new dual-luciferase plasmid was constructed based on the single luciferase plasmid pPrib-luc (Pedrolli, Kühm, *et al.*, 2015) by inserting the *Renilla* luciferase gene luc^R under control of the constitutive promoter OXB15.

The newly designed reporter plasmid for an *in vivo* reporter gene assay in *E. coli* was tested for its functionality, again using the *E. coli thiC* promoter and riboswitch. While thiamine addition decreased β-galactosidase activity to around 20 % of the activity of the control, the luciferase activity was consistently decreased to approximately 1 % of the control culture without thiamine. No decrease in activity was observed for the respective promoter control plasmid. Therefore, it was concluded that the dual-luciferase assay represents a more sensitive reporter assay to measure TPP riboswitch activity than the colorimetric β-galactosidase assay. To be able to also gain information about the mode of action of the riboswitches, a translational as well as a transcriptional fusion plasmid was constructed, allowing to determine the main way of function of the different riboswitches.

5.1.2 Identification and characterization of TPP riboswitches from ESKAPE pathogens

The main goal of this study was to test TPP riboswitches from various, potentially multiresistant bacterial strains as targets for new antibiotic substances. The first step was to experimentally

validate the functionality of the riboswitch candidates. The TPP riboswitch has been extensively studied and well characterized, especially in *E. coli* but also in other bacteria, as well as plants and fungi (Bu *et al.*, 2023). The crystal structures of eukaryotic and prokaryotic TPP riboswitches were solved (Serganov *et al.*, 2006; Thore *et al.*, 2006), as well as the crystal structures of TPP riboswitches from *E. coli* and *A. thaliana*, bound to different TPP analogs (Edwards and Ferré-D'Amaré, 2006; Thore *et al.*, 2008). However, as mentioned before, TPP riboswitch sequences have been bioinformatically identified in the genomes of various resistant pathogenic bacteria (Traykovska *et al.*, 2022), but to our knowledge, except for the TPP riboswitch from the human pathogen *Neisseria meningitidis* (Righetti *et al.*, 2020), no actual *in vivo* tests have been used to prove their response to TPP and further characterize their function. Therefore, tests with putative antibiotic substances targeting TPP riboswitches have so far been performed only with the already characterized TPP riboswitches from *E. coli* (Chen *et al.*, 2012; Lünse *et al.*, 2014; Wakchaure and Ganguly, 2021).

By using the dual-luciferase reporter assay, it was possible to experimentally validate the activity of TPP riboswitches from various ESKAPE pathogens. The riboswitch candidates were identified by an Rfam search (Burge *et al.*, 2013) and a first indication about the respective mode of action was obtained by an analysis with the PASIFIC web server (https://www.weizmann.ac.il/molgen/Sorek/PASIFIC/), which searches for possible transcriptional terminators within the sequence.

Putative TPP riboswitch sequences from *Enterobacter* spp*., P. aeruginosa, K. pneumoniae, A. baumannii* and *M. sciuri* were tested in combination with the *E. coli thiC* promoter. This approach only required one promoter control plasmid (not containing a riboswitch sequence) and was also chosen to ensure that the promoter employed was functional in the *E. coli* host that was used in the assay. For the *thiC* riboswitch Pa01 of *P. aeruginosa*, the *thiC* (Eb01) and *thiB* (Eb03) riboswitches of *Enterobacter* sp. and the *tenI* riboswitch Ms02 of *M. sciuri*, a significant decrease in luciferase activity was observed, when the respective recombinant *E. coli* strain was grown with 10 µM of thiamine. These riboswitches were thereby experimentally validated as TPP responsive elements, regulating downstream gene expression. However, no significant response to thiamine was measured for the *K. pneumoniae thiC* riboswitch Kp04 and the *A. baumannii thiC* riboswitch Ab01. When the Ec01 promoter of the translational reporter plasmid was replaced by the respective native promoter of the RS, a strong decrease in luciferase activity was measured for the Kp04 and Ab01 riboswitch regions, when thiamine was added to the *E. coli* cultures. This confirmed that these two elements are also functional riboswitches, responding to thiamine pyrophosphate. A significant reduction in reporter gene activity, though less pronounced as for the Kp04 and Ab01 elements, was determined for the Ef02 and Sp06 elements, confirming their function in

regulating downstream gene expression as well. In case of the Ms02 riboswitch, the replacement of the promoter did not affect the strength of its response to thiamine addition.
Taken together, the results obtained for these riboswitches indicate that the choice of promoter can be decisive for the influence of the riboswitch on downstream gene expression. To the best of my knowledge, there is no reports about the type of promoter region being of existential importance for the riboswitch to function at all. A study on theophylline riboswitch activity tested with mycobacterial promoters of varying strengths found no correlation between promoter strength and reporter gene activity of different specific promoter-riboswitch combinations (Van Vlack and Seeliger, 2015). For the *Bacillus methanolicus* lysine riboswitch, on the other hand, the use of different promoters of varying strength also influenced the relative decrease in reporter activity (Irla *et al.*, 2021). However, a complete absence of a response to addition of the riboswitch ligand when a specific promoter was used has not been observed.
Since the exact transcriptional start sites of the riboswitches are unknown, an explanation for the lack of response to thiamine of the pEc01-Kp04 and pEc01-Ab01 constructs might be that the cloned riboswitch regions were missing a part of the 5' sequence due to an incorrect assignment, which impaired their functionality. Therefore, it could be necessary to perform a transcriptional start site analysis for the riboswitch regions used to determine the actual start of the riboswitch transcript. For example, this was done for the *E. coli thiC* riboswitch, revealing a different transcript version with an elongated P1 stem (Chauvier *et al.*, 2017), compared to the originally described transcript (Winkler, Nahvi, *et al.*, 2002).
Interestingly, the putative *tenA* riboswitch Ms01 from *M. sciuri* did not respond to thiamine at all, neither with the *E. coli* thiC promoter nor with its native promoter. This strongly suggests that the tested sequence, despite the *in silico* annotation as a riboswitch aptamer, is not a functional TPP riboswitch. However, it is unclear whether the conserved aptamer part of the riboswitch is still able to bind TPP, but this binding event is not transmitted into a regulation of downstream gene expression. This possibility was also discussed for a similar example where an *in silico* prediction of a regulatory TPP riboswitch in diatoms could not be confirmed experimentally (Llavero-Pasquina *et al.*, 2022). This recent study identified riboswitch aptamer sequences in the 3'-untranslated region of putative thiamine biosynthesis and uptake genes in *Phaeodactylum tricornutum*. The function of these genes could be experimentally verified, but although the putative riboswitch aptamer of the *P. tricornutum THIC* gene shows high sequence similarity to validated eukaryotic riboswitches from *Chlamydomonas reinhardtii* and *Neurospora crassa*, the putative riboswitch aptamer in *P. tricornutum* and also in the diatom *Thalassiosira pseudonana* did not respond to external thiamine supplementation, even though thiamine was taken up by the cells (Llavero-Pasquina *et al.*, 2022). These results together with the current findings underline the necessity for experimental validation of riboswitch activity and since riboswitches represent promising new targets for antibiotic substances, further

investigations of their *in vivo* response to their putative ligand TPP in addition to the *in silico* analyses appear to be essential.

5.1.3 Determination of the mode of action for the identified riboswitches

To determine the mode of action for the riboswitches that were successfully validated, a second dual-luciferase reporter plasmid, allowing a transcriptional fusion of the riboswitch sequences to the *luc*^{F} gene, was used. Using the translational fusion plasmid, it is not possible to distinguish between transcription termination and translation inhibition. With the transcriptional fusion plasmid, however, a decrease in reporter activity will only be observed for riboswitches that suppress transcription.

A response to thiamine addition testing transcriptional fusions using the pEc01 promoter was only observed for the Pa01 and the Eb01 riboswitch, but not for the Eb03 and the Ms02 riboswitches. Thus, the latter two riboswitches regulate gene expression only via inhibiting translation. When the native promoter region was employed, a significant decrease in reporter activity was also measured for the Kp04 and the Ab01 riboswitch, but not for the Ef02 riboswitch, which is therefore thought to regulate at the translational level as well. No luciferase activity was detected with the transcriptional fusion plasmid of the Sp06 riboswitch, so in this case no conclusions can be drawn about the operating principle of the riboswitch.

From these results it can be concluded that the Pa01 riboswitch only functions via transcription termination since a similar reduction in activity to 10 and 13% was observed for both reporter plasmids in the presence of thiamine. For the Ab01 riboswitch, the reporter activity was reduced to 4% for the translational fusion, while the activity decreased to 13% for the transcriptional fusion. This small difference suggests a mainly transcriptional function, while an influence on translation cannot be excluded. In case of the Kp04 riboswitch, on the other hand, addition of thiamine reduced reporter activity to 0.5% of the control in the translational fusion, while the effect on the transcriptional riboswitch fusion was much smaller, with activity reduced to only 43% in the thiamine-grown cultures. This strongly suggests an involvement of a transcriptional as well as a translational termination mechanism for the *K. pneumoniae thiC* riboswitch. A similar observation was already made for the *thiC* riboswitch from *E. coli* and in this case, a similar conclusion about its mode of action has been drawn (Winkler, Nahvi, *et al.*, 2002; Chauvier *et al.*, 2017).

The reporter assay conducted here gives a first idea about the possible way of function for the riboswitches tested. However, to determine the exact mode of action, more experiments are needed. For example, the involvement of the Rho factor in the transcription termination mechanism of the transcriptional TPP riboswitches could be examined. The Rho factor, a DNA/RNA helicase, is involved in one of the major mechanisms of transcription termination

(Richardson, 2003). By using the Rho inhibitor bicyclomycin in a reporter gene assay (Chauvier *et al.*, 2017), it can be determined, whether the riboswitches regulate transcription *via* a Rho-dependent or Rho-independent mechanism.

5.1.4 The effect of putative antibiotic substances on TPP riboswitch activity

Following the experimental validation of the previously unrecognized riboswitches and the confirmation of their response to their natural ligand thiamine pyrophosphate, they were tested for their response to newly synthesized and pre-screened TPP analogs. However, the development and synthesis of these putative ligands to be tested as antibiotic substances was more complicated than expected. Therefore, 18 small commercially available compounds with structural similarities to thiamine were tested for their effect on the activity of the *thiC* TPP riboswitch of *K. pneumoniae* in a reporter gene assay, using the β-galactosidase gene *lacZ*. The different compounds were added to cultures of *E. coli* DH5α and reporter gene activity of the cell-free extracts was determined. However, none of the tested compounds reduced the reporter gene activity significantly. Addition of the substances 3, 11, 17 and 18 to the cultures even led to an increase of reporter gene activity, compared to the control. Since these compounds exhibited the same effect for the promoter control plasmid, it is likely that the observed increase in LacZ activity is not due to the activity of the riboswitch itself. It can rather be assumed that it is the result of a generally enhanced transcription rate or an increased copy number of the corresponding plasmid. The substances might induce a stress response in the *E. coli* strain that affects plasmid replication, for example by interfering with the RNase H1 or the RecG helicase. These two enzymes have been reported to influence R-loop formation, which plays an important role in replication of plasmids with a ColE1 origin (Harinarayanan and Gowrishankar, 2003), as it is present in the pHAt191l reporter plasmid. However, since many factors influence plasmid replication (Camps, 2010) and an increased copy number does not necessarily result in an enhanced translation rate, the exact mechanisms that led to elevated reporter gene activity upon treatment with certain TPP analogs remain unclear.
Altogether, these results emphasize the need to include a promoter control plasmid and show that a reporter gene assay that allows normalization to plasmid copy number is preferable. The newly adapted dual-luciferase assay provides this advantage and was therefore used for further experiments on the effect of the antibiotic compound pyrithiamine on riboswitch activity.

5.1.5 The effect of pyrithiamine on TPP riboswitches

As no novel thiamine analogs affecting TPP riboswitches could be provided during the time course of the project, the susceptibility of the newly identified TPP riboswitches to thiamine

analogs was tested with the previously described thiamine analogs pyrithiamine and bacimethrin. Pyrithiamine has already been established as a ligand for the TPP riboswitches. It can be taken up by *E. coli* via the thiamine transport system and is intracellularly pyrophosphorylated to pyrithiamine pyrophosphate (PTPP), the form in which it is recognized by the riboswitch (Kawasaki, 1969; Sudarsan *et al.*, 2005; Thore *et al.*, 2008). Bacimethrin is a naturally occurring analog of the HMP moiety of thiamine, in which a methoxy group replaces the 2-methyl group. It is processed *via* the thiamine biosynthesis pathway to generate 2'-methoxy thiamine and was shown to be toxic to bacteria and yeast grown in minimal medium (Reddick *et al.*, 2001). However, while bacimethrin shows antimicrobial activity, this effect was mainly attributed to an inhibition of TPP dependent enzymes upon binding of bacimethrin, not to it affecting the expression of thiamine biosynthetic genes (Zilles *et al.*, 2000; Rabe von Pappenheim *et al.*, 2020). In *E. coli*, only a very small impact of bacimethrin on the transcription of biosynthetic genes was observed, even though in this study a possible influence on translation was not investigated (Reddick *et al.*, 2001).

Since bacimethrin has to be further processed within the cell, the thiamine auxotrophic DH5α strain could not be used in these experiments. This strain carries a point mutation in the *thiE* gene (Song *et al.*, 2015), thereby preventing the successful synthesis of the 2'-methoxy thiamine from bacimethrin. Hence, the prototrophic *E. coli* strain MG1655 was used in the corresponding tests.

First, the response of the Ec01 riboswitch to bacimethrin and pyrithiamine was studied. While bacimethrin did not have a significant effect on reporter activity, addition of 10 µM of pyrithiamine to the medium decrease luciferase activity to around 25 % compared to the thiamine-free control. This effect was not observed when the same reporter plasmid was used in the thiamine auxotrophic strain DH5α and also for the strain MG1655, addition of 20 nM of thiamine to the pre-culture medium abolished the effect of pyrithiamine. This is in accordance with a similar observation made for the effect of pyrithiamine on riboswitch-regulated β-galactosidase reporter activity in an *E. coli* DH5αZ1 strain (Lünse *et al.*, 2014). Even though other compounds tested in this study, such as triazolethiamine, were found to have a significant effect on riboswitch activity also in the auxotrophic *E. coli* strain (Lünse *et al.*, 2014), the absence of an effect of PT suggests that other putative ligands of the TPP riboswitch should also be tested in a prototrophic strain,

In the present study, the response to pyrithiamine was tested for the previously identified riboswitches Kp04, Ab01, Pa01, Eb01, Eb03 and Ms02. Yet, none of these riboswitches showed a significant response to the ligand. This was surprising with regard to the high conservation of the RS aptamer region, and the fact that the central pyridine ring, which replaces the thiazolium ring in the pyrithiamine molecule, does not seem to be play a role in riboswitch binding (Chen *et al.*, 2012).

5.1.5.1 Effect of pyrithiamine on the *thiC* riboswitch of *K. pneumoniae*

To further examine the observed differences in the riboswitch response to pyrithiamine, the *thiC* riboswitch Kp04 from *K. pneumoniae* was investigated in more detail. The sequence alignment of the *E. coli thiC* RS Ec01 and the Kp04 riboswitch revealed that within the aptamer region, two short additional sequences are present in the Kp04 region (Figure 21). These show some complementarity and appear to form a extended P3 stem. Similar additional sequence parts were already found in TPP riboswitches from *Klebsiella aerogenes* and several *Serratia* species (Chauvier *et al.*, 2017, Supplement). Furthermore, a single nucleotide change from uracil to adenine was found at position 63 of the Kp04 sequence (Figure 21), when compared to Ec01. However, this mutation is positioned in a terminal loop and therefore most probably does not affect the overall structure of the riboswitch.

To test the hypothesis that the prolonged P3 stem might be responsible for the resistance of the riboswitch to pyrithiamine, site-directed mutagenesis was performed to alter the respective regions individually, resulting in the mutant riboswitches $Kp04^{A63U}$, $Kp04^{\Delta 21\text{-}37}$ and $Kp04^{\Delta 42\text{-}48}$. The exchange of the adenine at position 63 by uracil had no effect on the response to PT, neither did the deletion of nucleotides 21-37. The deletion of nucleotides 42-48, on the other hand, resulted in a significant decrease of reporter activity upon exposure to PT, while at the same time a reduced susceptibility to thiamine was observed for this mutated riboswitch. This outcome supported the hypothesis that the additional stem structure is responsible for the lack of influence of PT on the Kp04 RS. However, it is noteworthy that only the deletion of the 42-48 region but not the deletion of the nucleotides 21-37 altered the response of the riboswitch to PT and thiamine, since both complementary regions together form the additional P3 stem structure.

Based on the previous observations, four single nucleotides were deleted in order to more precisely identify the part of the sequence responsible for the differential binding of thiamine and pyrithiamine. Individual deletions of the nucleotides G42, U43 and A46 from the Kp04 sequence resulted in riboswitches that showed a similar susceptibility to thiamine as the wild type. All these mutations, however, led to different responses of the riboswitch to PT. Deletion of nucleotide G42 reduced reporter activity upon pyrithiamine treatment to 50% of the control, deletion of U43 to 35% and deletion of A46 to as little as 10% of the pyrithiamine-free cultures. These results reveal that a single nucleotide deletion within the riboswitch sequence can retain the normal riboswitch activity and response to the natural ligand but can make the riboswitch susceptible to other ligands as well, which are usually not accepted. In other words, the insertion of a single nucleotide can make the riboswitch resistant to other compounds while maintaining its affinity for the natural ligand. This is particularly interesting, since previous studies on TPP riboswitches have reported that single nucleotide changes within the riboswitch sequence usually eliminate the response of the riboswitch to both ligands PT and TPP at the

same time (Sudarsan *et al.*, 2005; Thore *et al.*, 2008). This was for example observed for the *E. coli* PT resistant mutant strain PT-R1 (Kawasaki and Nose, 1969). In this respect, the obtained results differ from previous findings for other TPP riboswitches and therefore may provide further information on the interaction of riboswitches with different ligands.

However, the exact reason for the effect of pyrithiamine observed for the different Kp04 mutants remains unclear. The present results indicate some involvement of the prolonged P3 stem although no direct connection of the P3 stem to a binding inhibition of pyrithiamine or another thiamine analog has been observed before. Interestingly, for eukaryotic TPP riboswitches a great variation in length and sequence of the P3 stem has been described (Sudarsan *et al.*, 2003; Wachter *et al.*, 2007). It was discussed that though the distal part of the P3 stem is not directly involved in ligand binding (Thore *et al.*, 2006, 2008), it might act as an anchor for the aptamer (Anthony *et al.*, 2012; Antunes *et al.*, 2019). A comparative study on the structural dynamics of the *E. coli* and *A. thaliana* TPP riboswitches suggests that the communication of the P3-L5 interaction may differ between the two species (Antunes *et al.*, 2019). However, the crystallization experiments this study was based on, which investigated the *A. thaliana* TPP riboswitch bound to TPP and PTPP, have worked with a riboswitch sequence in which the P3 stem was shortened for the co-crystallization (Thore *et al.*, 2006, 2008). Therefore, these studies do not allow to draw conclusions about an involvement of a prolonged P3 stem in binding – or prevention of binding – of PTPP to the TPP riboswitch.

5.1.6 Examination of TPP riboswitch regions in PT-resistant strains of *K. pneumoniae*

Pyrithiamine is a thiamine analog that exhibits antimicrobial activity against different bacterial species and it was shown that PT-resistant bacteria often carry mutations in the TPP riboswitch regions (Sudarsan *et al.*, 2005). Hence, the impact of pyrithiamine on the growth of the *K. pneumoniae* wildtype was investigated. This was to determine if despite the unresponsiveness of the Kp04 riboswitch to pyrithiamine there is an inhibitory effect of the substance on the growth of the strain. Indeed, high concentrations of pyrithiamine (200 µM) in a minimal medium impaired the growth of *K. pneumoniae*. However, even when the concentration was increased to 300 µM, growth was not further impaired, and no complete growth repression was achieved. Nevertheless, a visible inhibitory effect of pyrithiamine on the growth of *K. pneumoniae* was observed, so cells were passaged with high concentrations of pyrithiamine, similar to an approach by Sudarsan *et al.* (2005) for *B. subtilis* and *E. coli*. This led to the isolation of 13 different PT-resistant *K. pneumoniae* strains

Out of the four identified TPP riboswitches in *K. pneumoniae* located upstream of the *thiB* operon (Kp01), *thiC* (Kp04), *tenA* (Kp10) and *thiMD* (Kp11), pyrithiamine only triggered a

significant response of the Kp11 riboswitch. Nevertheless, for all 13 PT-resistant clones the four riboswitch regions were sequenced, but no mutations were found in any of the examined regions for these strains. Interestingly, Sudarsan *et al.* (2005) found that in *B. subtilis*, all PT-resistant clones screened had acquired mutations in the *tenA* riboswitch, while only 9 of the 23 PT-resistant *E. coli* clones carried mutations in one of the three TPP riboswitch regions. They concluded that these strains must have acquired resistance by some other mechanism, which is presumably the case as well for the *K. pneumoniae* strains tested here. This outcome was not unexpected, as none of the four *K. pneumoniae* riboswitches had previously shown a strong susceptibility to pyrithiamine in the reporter gene assays.

5.2 Outlook – The TPP riboswitch as a potential target for antimicrobial compounds

In the present study, several TPP riboswitches from ESKAPE pathogens were identified and tested for their responses to the thiamine analog pyrithiamine. In order to examine the *in vivo* suitability of the TPP riboswitch as a target for novel antibiotic compounds it is important to further characterize the identified riboswitches for their exact way of function. To validate their function as transcriptional or translational riboswitches, additional *in vitro* transcription/ translation assays should be performed (Bains *et al.*, 2023).

However, the present results also emphasize the importance of *in vivo* tests to verify riboswitch activity. Most striking is the insight that not all TPP riboswitches, despite their very high sequence conservation of the aptamer region, respond in the same way to ligands like pyrithiamine. Therefore, it seems inevitable to test all individual riboswitches from pathogens of interest for their responses to potential antibiotic substances. More studies are needed on sequence and structural comparisons of riboswitch sequences. A good tool for this would be crystallization studies like performed for the *thiC* riboswitch of *E. coli* bound to different ligands (Edwards and Ferré-D'Amaré, 2006; Serganov *et al.*, 2006). Bioinformatic tools on RNA structure prediction could be helpful for these tasks, but the small number of high-quality data sets of structures and alignment limit the usefulness and accuracy of these tools at the present time (Schneider *et al.*, 2023).

Regarding the differences observed in PTPP and TPP binding to the Kp04 riboswitch of *K. pneumoniae* more studies are needed on the effect of single nucleotide mutations altering the binding affinity to different ligands completely. It would also be interesting to modify the P3 stem of the *E. coli* TPP riboswitch and check for the susceptibility to pyrithiamine. With a CRISPR/Cas9 approach (Li *et al.*, 2015), these changes could also be introduced directly into the genome, to test if mutations confer resistance to pyrithiamine to the host cell. Thereby,

differences in the susceptibility of TPP riboswitches to thiamine analogs could be explored further.

CHAPTER II –

Regulation of flavin mononucleotide riboswitch activity by the RNA-binding protein RibR

6 Results – Chapter II

6.1 The RNA-binding protein RibR in *Bacillus subtilis*

The riboswitch regulator RibR has first been identified and characterized in *B. subtilis*. The bifunctional protein consists of two parts, whereby the N-terminal part was identified as a flavokinase and the RNA-binding (regulatory) activity was assigned to the C-terminal part. In the presence of $MgSO_4$ as the sole sulfur source, no expression of *ribR* is observed and FMN from extracellularly supplied riboflavin suppresses transcription of the riboflavin synthesis genes in the *ribDG* operon by binding to the *ribD* riboswitch (Figure 26A). However, when methionine and taurine are available as sulfur sources, expression of the *snaA* operon, including the *ribR* gene, is induced. The C-terminal part of the RibR protein then binds to the FMN riboswitch, allowing transcription of the riboflavin synthesis genes, even when the riboswitch ligand FMN is present (Figure 26B).

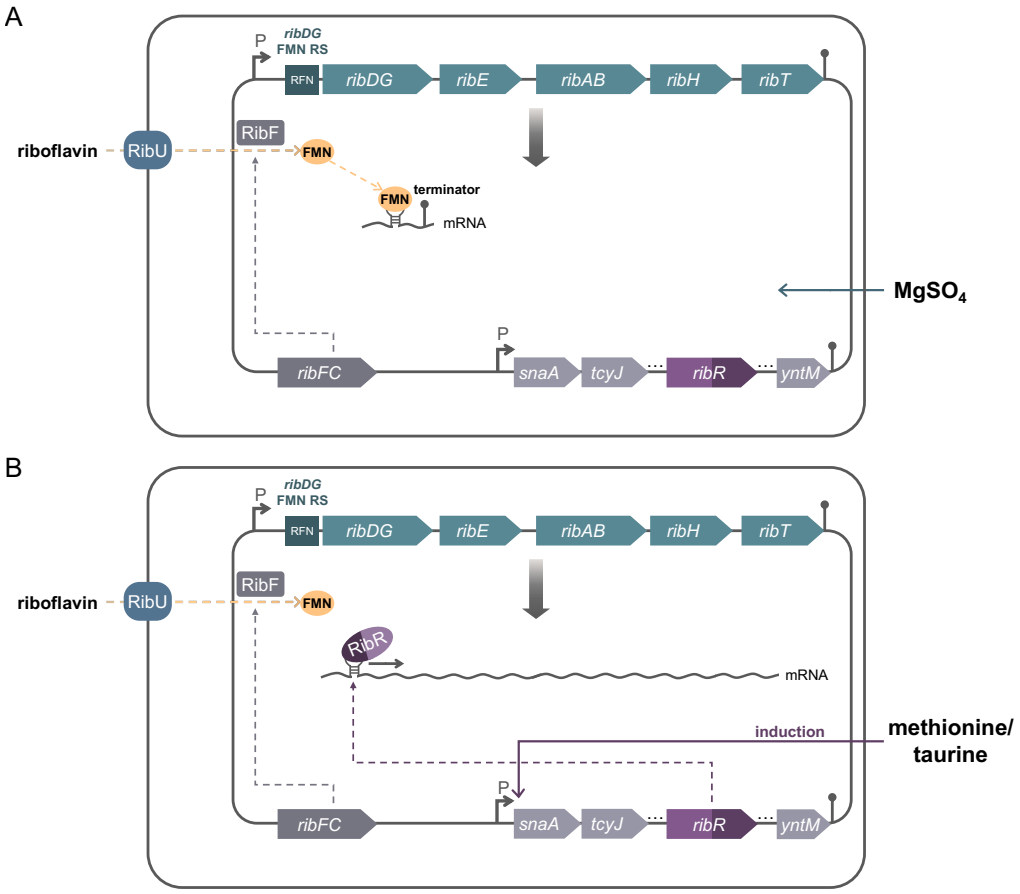

Figure 26: Schematic overview of the FMN riboswitch regulated expression of *rib* genes in *B. subtilis* in the presence of $MgSO_4$ (A) or methionine/taurine (B) as a sulfur source. Extracellular riboflavin is transported into the cell by the riboflavin transporter RibU and RibF catalyzes the conversion to FMN. **A)** In the presence of $MgSO_4$ as a sulfur source, intracellular FMN binds to the FMN riboswitch (RFN) upstream of the *ribDG* operon (encoding proteins involved in riboflavin synthesis), thereby downregulating the expression of these *rib* genes by preventing transcription. **B)** Providing methionine and taurine as the sole sulfur sources results in the induction of the *snaA* operon, including the *ribR* gene. The protein RibR binds to the *ribD* FMN RS, thus counteracting the effect of the ligand FMN and allowing transcription of the *rib* operon even at high concentrations of FMN.

To monitor the activity of the *ribD* FMN riboswitch, the gene product of *ribE*, which is part of the *ribDG* operon, can be used as an internal reporter. The riboflavin synthase RibE catalyzes the conversion of 6,7-dimethyl-8-ribityllumazine to riboflavin (Figure 27), so by measuring the riboflavin production in cell-free extracts of *B. subtilis* provided with the substrate 6,7-dimethyl-8-ribityllumazine, conclusions can be drawn about the activity of the *ribD* FMN riboswitch.

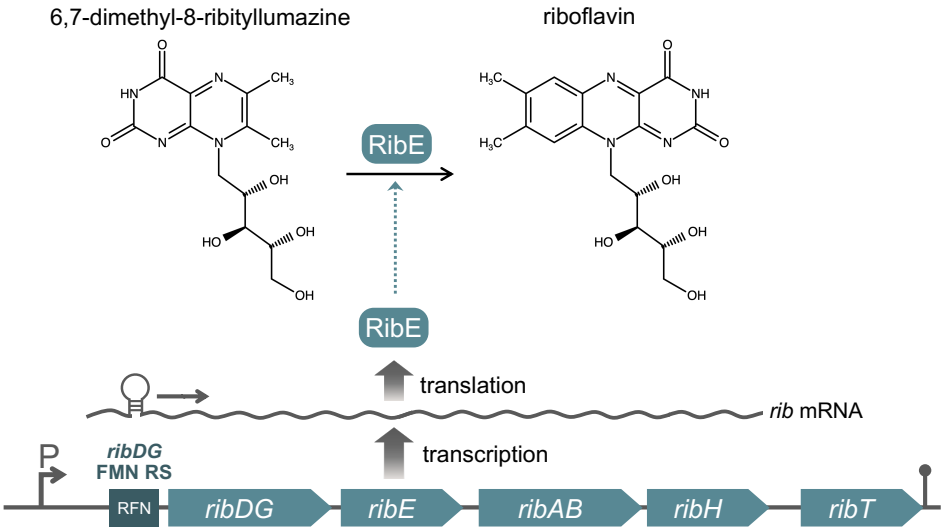

Figure 27: The riboflavin synthase (RFS) RibE of *B. subtilis* catalyzes the conversion of 6,7-dimethyl-8-ribityllumazine to riboflavin. The gene *ribE* is part of the *ribDG* operon and therefore its transcription is controlled by the *ribD* FMN riboswitch (RFN).

When *B. subtilis* was grown with $MgSO_4$ as a sulfur source, RibE activity in the cell-free extracts of cultures supplemented with 5 µM of the FMN precursor riboflavin was significantly decreased compared to cultures grown without riboflavin supplementation (Figure 28).

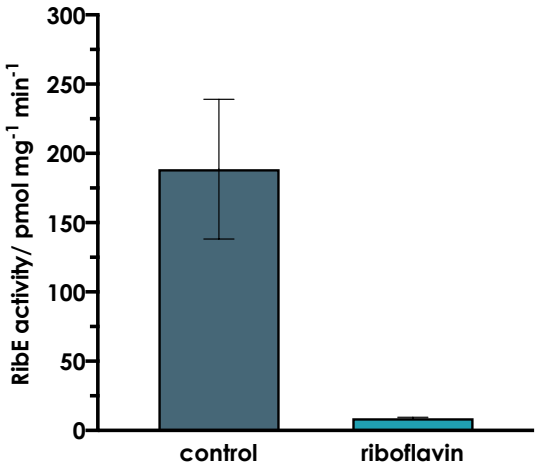

Figure 28: Riboflavin synthase (RibE) activity in a *B. subtilis* 168 wild-type strain changes upon addition of riboflavin to the culture medium. *B. subtilis* 168 was grown in shake flasks in a minimal medium containing $MgSO_4$ as the sole sulfur source (control). When riboflavin (5 µM) is added to the cultures (riboflavin) RibE activity decreases. RibE activity was determined in cell-free extracts of harvested cells using 6,7-dimethyl-8-ribityllumazine as a substrate. Enzyme activity assays were performed in duplicates with cell-free extracts of two independent cultures. Depicted are the mean values ± standard deviations of the data obtained from the duplicates. Riboflavin formation was measured via HPLC.

This indicates that *ribE* expression is downregulated by FMN binding to the *ribD* riboswitch, thereby preventing transcription of the *ribDG* operon.

For the further investigation of RibR function and the validation the previous results of RibR activity tested in a luciferase reporter gene assay (Pedrolli, Kühm, *et al.*, 2015), marker-free deletions of *ribR* and the individual C- and N-terminal coding parts of the gene were generated using a CRISPR/Cas9 system developed for *B. subtilis* (Altenbuchner, 2016). The riboflavin synthase (RFS) activity in cell-free extracts of the *B. subtilis* WT 168 was then compared to the *B. subtilis* mutant strains Δ*ribR*, Δ*C-ribR* and Δ*N-ribR* (Figure 29).

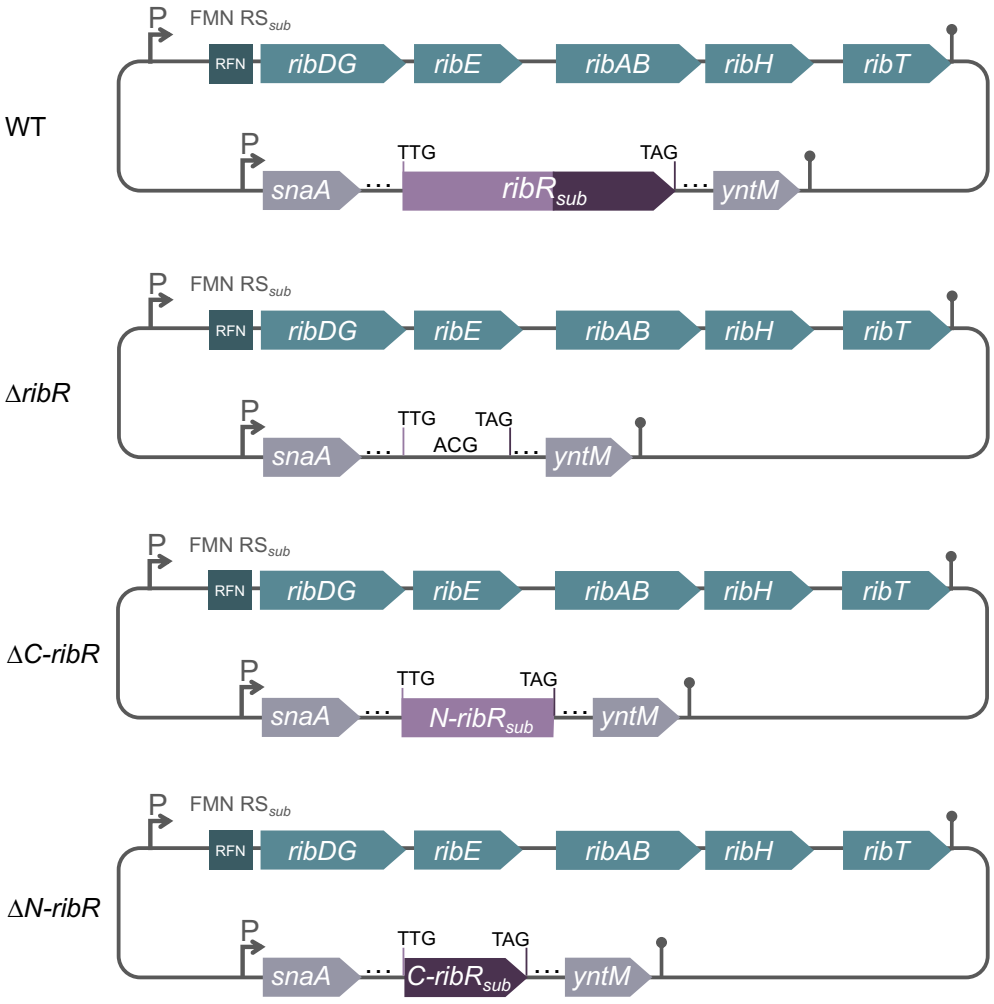

Figure 29: Schematic overview over the genomic modifications in the *B. subtilis* mutants Δ*ribR*, Δ*C-ribR* and Δ*N-ribR* compared to the *B. subtilis* WT. In the mutant strain Δ*ribR*, the entire *ribR* coding sequence (*ribR*$_{sub}$) was deleted, keeping only the original start (TTG) and stop (TAG) codon with the first base triplet (ACG) in between. In the strain Δ*C-ribR*, only the coding sequence for the C-terminal part of RibR (nucleotides 268-687) was deleted, keeping the last two codons of the complete coding region. In the strain Δ*N-ribR*, the coding sequence for the N-terminal part of RibR (nucleotides 7-267) was deleted, keeping the start codon and C-terminal coding part.

In the *B. subtilis* WT, induction of RibR by the addition of methionine and taurine leads to an increase in RibE activity compared to the $MgSO_4$ control (uninduced), despite the presence of riboflavin (Figure 30). An increase in RibE activity in the presence of methionine and taurine is

also detected in the Δ*N-ribR* mutant strain with only the C-terminal coding part of *ribR,* confirming the previous observations that the C-terminal RibR domain is sufficient to regulate FMN riboswitch activity. For the Δ*ribR* strain and the Δ*C-ribR* strain, carrying only the N-terminal coding region of *ribR*, RibE activity was not upregulated upon RibR induction. On the contrary, it was even lower for the methionine/taurine induced samples (Figure 30).

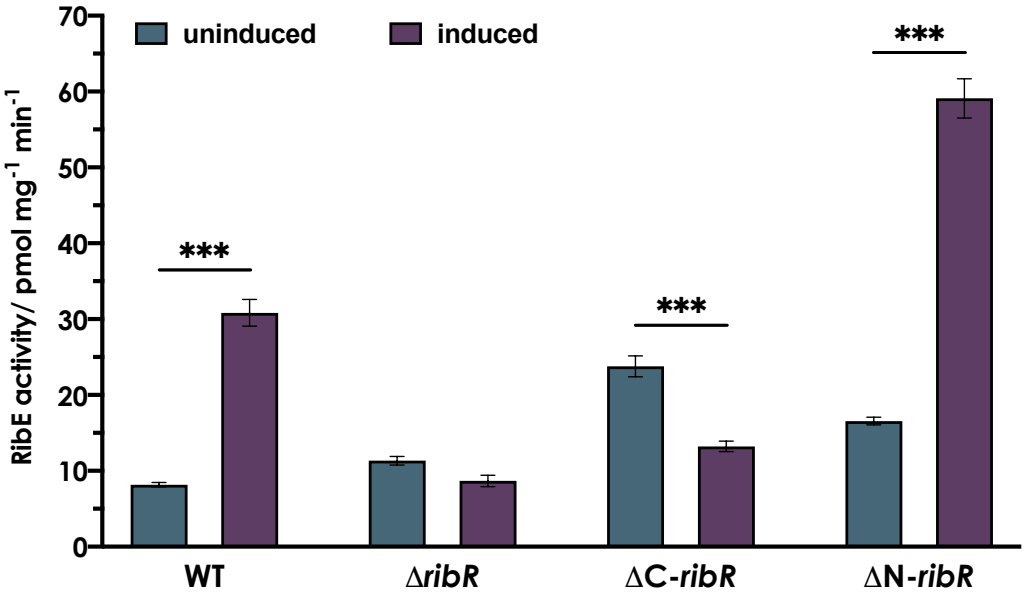

Figure 30: Riboflavin synthase activity for the RibR wildtype and different *ribR* deletion strains. *B. subtilis* 168 strains were grown in shake flasks in a minimal medium with 5 µM of riboflavin and $MgSO_4$ (uninduced) or methionine and taurine (induced) as sulfur sources in triplicates. RibE activity was determined in cell-free extracts of harvested cells using 6,7-dimethyl-8-ribityllumazine as a substrate. Enzyme activity assays were performed in triplicates with cell-free extracts of three independent cultures. Depicted are the mean values ± standard deviations of the data obtained from the triplicates. Asterisks indicate statistically significant differences (*** $p \leq 0.001$). Riboflavin formation was measured via HPLC.

6.2 RibR-like proteins in other *Bacillus* species

So far, the riboswitch-binding protein RibR had only been described in *Bacillus subtilis*. However, a comparison of the C-terminal RNA-binding part of RibR with the NCBI database revealed some similar protein sequences, mainly in other *Bacillus* species (Figure 31). While some of the detected proteins span the full length of the RibR sequence, interestingly in some organisms, the RibR sequence completely lacks the flavokinase domain. This truncated RibR-like protein, encoding only the putative RNA-binding part, is found for example *in Bacillus benzoevorans*, *Bacillus methanolicus*, *Bacillus smithii* and *Bacillus amyloliquefaciens*, a close relative of *B. subtilis*.

The alignment of the C-terminal part of the proteins reveals some conserved amino acid residues, such as a two-arginine motif (positions 179 and 180 of the *B. subtilis* amino acid sequence) that is present in all of the protein sequences compared (Figure 31).

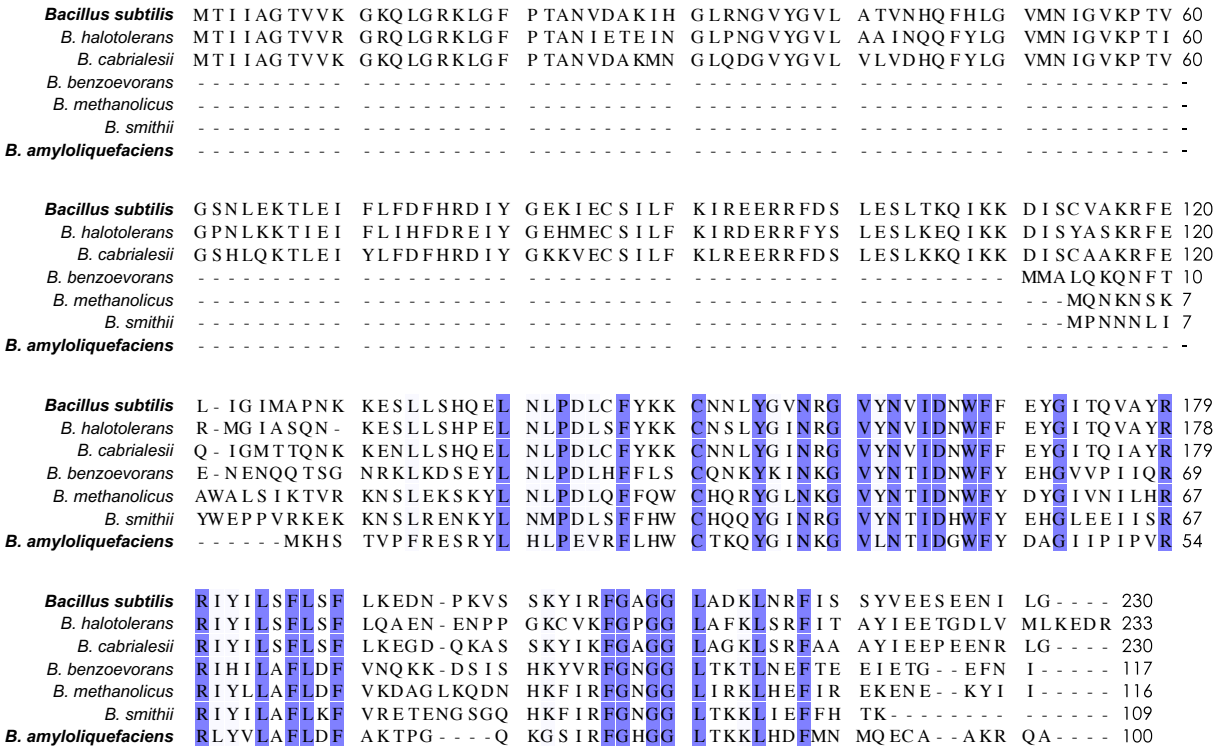

Figure 31: Alignment of RibR from *B. subtilis* with similar protein sequences from other *Bacillus* species. The Multiple Sequence Alignment was created with Clustal Omega. Conserved amino acid residues of the C-terminal parts are highlighted in blue.

6.3 The RibR-like protein RibR$_{amy}$ in *Bacillus amyloliquefaciens*

A sequence comparison of the RibR-like protein from *B. amyloliquefaciens* with RibR from *B. subtilis* reveals a rather low sequence similarity of 46% identity in the aligned parts (Figure 31), compared to sequence similarities of 78% to 95% for other proteins involved in riboflavin synthesis and transport in these two organisms (Table 39). However, the motif of two adjacent arginine residues is also present in the *B. amyloliquefaciens* RibR-like protein as well at positions 54 and 55 of the amino acid sequence.

Table 39: Sequence identity comparison for proteins of riboflavin synthesis and transport in *Bacillus subtilis* 168 and *Bacillus amyloliquefaciens* DSM7. Identity values were determined by a sequence comparison of the respective proteins using blastp.

Protein	Function	Identity [%] *B. subtilis*/ *B. amyloliquefaciens*
RibDG	bifunctional deaminase/reductase	78.49
RibE	riboflavin synthase	80.47
RibAB	bifunctional GTP cyclohydrolase II (A)/3,4-DHBP synthase	91.46
RibH	6,7-dimethyl-8-ribityllumazine synthase	92.86
RibT	GCN5-related N-acetyltransferase	94.35
RibU	riboflavin transmembrane transporter	87.37
RibFC	bifunctional riboflavin kinase/FAD synthetase	83.65

When the genomic environment of the two *ribR* genes is taken into focus it becomes evident that the genes are located in different parts of the genome, despite the close relationship of the two *Bacillus* species and the otherwise similar arrangement of the genes.
The *ribR* gene from *B. subtilis* is found in a gene cluster consisting of the twelve genes *snaA, tcyJ, tcyK, tcyL, tcyM, tcyN, cmoO, cmoI, cmoJ, ribR, sndA* and *ytnM* (Figure 32). Except for *ribR* this gene cluster comprises genes, which are involved in sulfur uptake and metabolism and the expression of this transcriptional unit is strongly increased in the presence of methionine and taurine as the sole sulfur sources (Coppée *et al.*, 2001; Burguière *et al.*, 2005b).

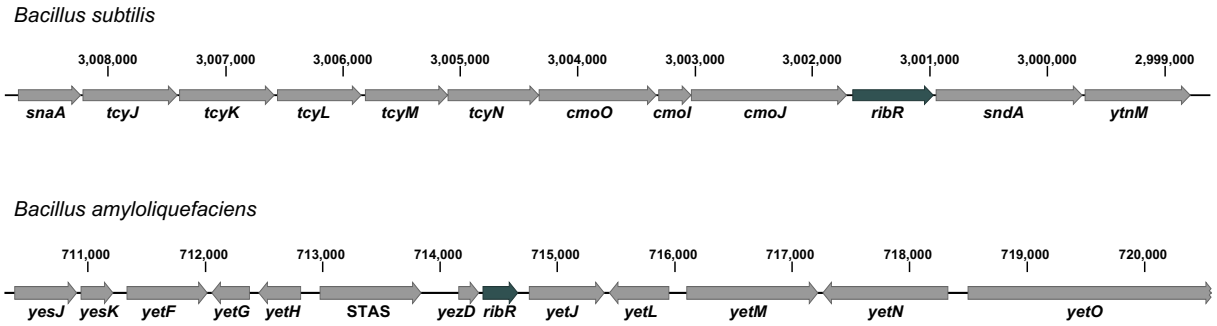

Figure 32: Schematic representation of the neighboring genes of *ribR* in *B. subtilis* and *B. amyloliquefaciens*. The respective *ribR* gene is highlighted in dark green. The genes from *snaA* to *ytnM* in *B. subtilis* form an operon, while *ribR* from *B. amyloliquefaciens* is in a putative transcription unit with *yezD*.

In *B. amyloliquefaciens* on the other hand, the *ribR*-like gene is found in a putative transcriptional unit with the small, uncharacterized gene *yezD* (Figure 32), of which a homolog is also present in the genome of *B. subtilis*.

6.4 Influence of $RibR_{amy}$ on the *ribD* FMN riboswitches from *B. subtilis* and *B. amyloliquefaciens*

To test whether $RibR_{amy}$ has the same effect on FMN riboswitch activity as observed for the *B. subtilis* RibR, the same enzyme assay was employed as before. The *ribR* gene in the *B. subtilis* host cell was replaced by the *ribR* gene from *B. amyloliquefaciens* ($ribR_{amy}$) while keeping the original start and stop codon. Additionally, the *B. subtilis ribDG* FMN riboswitch upstream of the riboflavin synthesis operon was exchanged for the *ribDG* riboswitch sequence of *B. amyloliquefaciens* in the *ribR* wildtype strain as well as the $ribR_{amy}$ strain. A comparison of the two FMN riboswitch sequences is presented below (Figure 33).

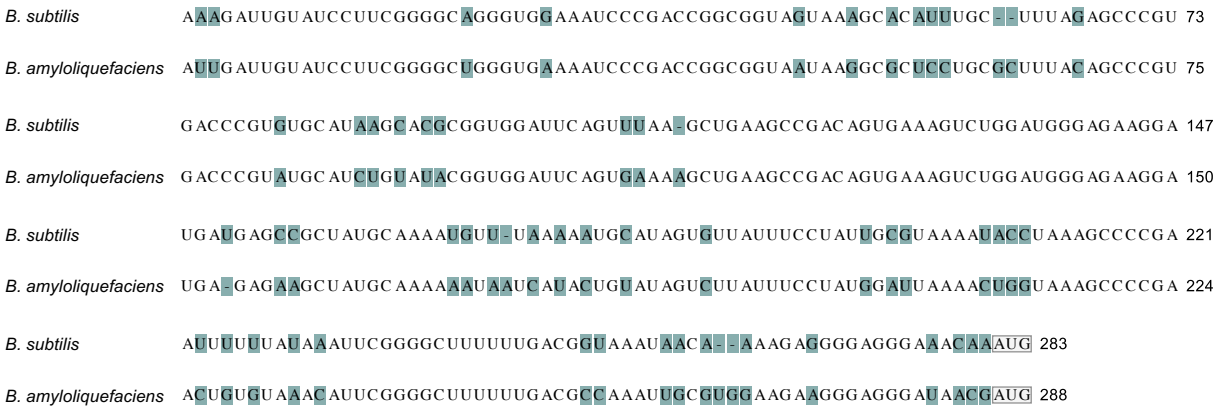

Figure 33: Alignment of the *ribD* FMN-binding riboswitch sequences from *B. subtilis* and *B. amyloliquefaciens* reveals that the sequences are highly similar. The sequences were aligned with the alignment tool from CLC Main Workbench. Nucleotide mismatches are highlighted in green-gray. A light gray box marks the start codon of the *ribD* coding sequence.

In total, three new *B. subtilis* strains (*ribR*$_{amy}$/*ribD*-RS$_{amy}$; *ribR*$_{amy}$/*ribD*-RS$_{sub}$; *ribR*$_{sub}$/*ribD*-RS$_{amy}$) with different combinations of *ribR* genes and *ribD* FMN riboswitches from *B. subtilis* and *B. amyloliquefaciens* were generated (Figure 34). These strains were again grown in minimal medium, containing 5 µM of riboflavin and either $MgSO_4$ or methionine and taurine as sulfur sources. The riboflavin synthase activity was determined from the cell-free extracts of these cultures.

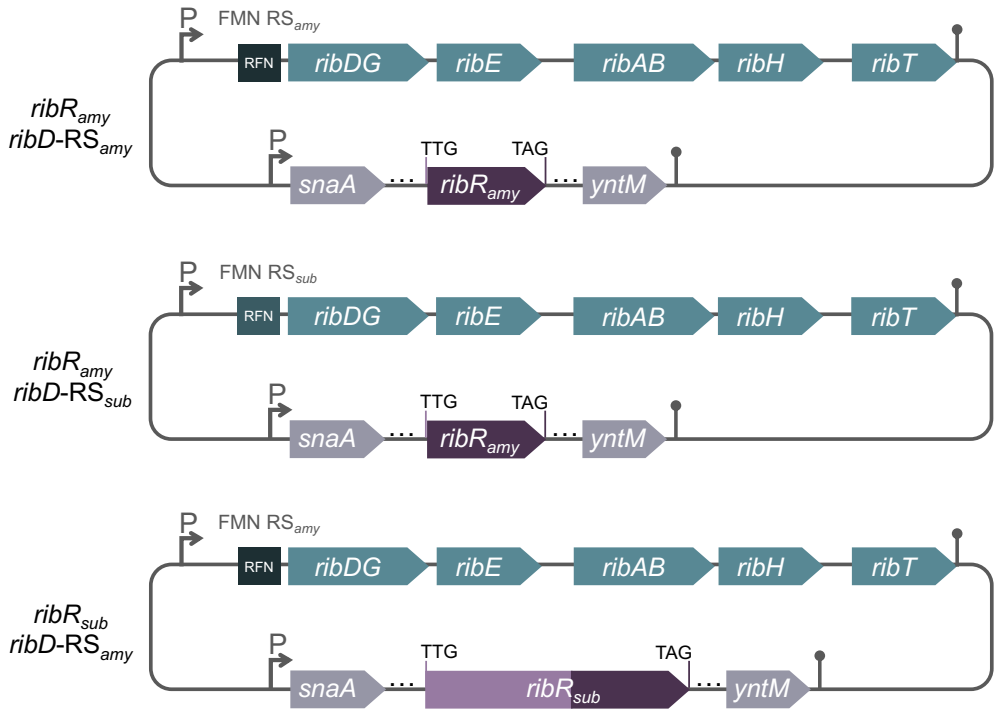

Figure 34: Schematic overview over the genomic modifications in the *B. subtilis* mutants *ribR*$_{amy}$/*ribD*-RS$_{amy}$, *ribR*$_{amy}$/*ribD*-RS$_{sub}$ and *ribR*$_{sub}$/*ribD*-RS$_{amy}$. In the mutant strain ribR$_{amy}$/ribD-RS*amy*, the *ribR*$_{sub}$ gene was replaced with the *B. amyloliquefaciens* homolog *ribR*$_{amy}$, keeping the original start (TTG) and stop (TAG) codon of *ribR*$_{sub}$. Additionally, the *ribD* FMN RS sequence (RFN) upstream of the *ribDG* operon was replaced with the *ribD* riboswitch from *B. amyloliquefaciens* (FMN RS$_{amy}$). In the strain *ribR*$_{amy}$/*ribD*-RS$_{sub}$, only the *ribR* coding sequence was replaced by *ribR*$_{amy}$. In the strain *ribR*$_{sub}$/*ribD*-RS$_{amy}$, only the FMN RS of *B. subtilis* was replaced by the FMN RS of *B. amyloliquefaciens*, keeping the native *ribR* sequence.

When methionine and taurine induced *ribR*$_{amy}$ expression in the *ribR*$_{amy}$ *ribD*-RS$_{amy}$ strain, a small but significant increase in riboflavin synthase activity was measured compared to the cell samples grown with sulfate (Figure 35). The same effect, with RibE activity in a similar range, was observed for the strain with *ribR*$_{amy}$ and the *ribD*-RS from *B. subtilis* (Figure 35). When only the *ribD*-RS was replaced by the riboswitch sequence from *B. amyloliquefaciens*, riboflavin synthase activity increased to a greater extent when methionine and taurine were present in the growth medium, compared to the strains with the *ribR*$_{amy}$ gene (Figure 35). Thus, the RibR protein from *B. subtilis* regulates the FMN riboswitch from *B. amyloliquefaciens* and vice versa.

However, compared to the RibR$_{sub}$ regulation of FMN riboswitch activity (Figure 30), the effect of the RibR protein from *B. amyloliquefaciens* on FMN riboswitch activity is considerably weaker, regardless of whether the FMN riboswitch of *B. subtilis* (Figure 30) or that of *B. amyloliquefaciens* (Figure 35) is observed.

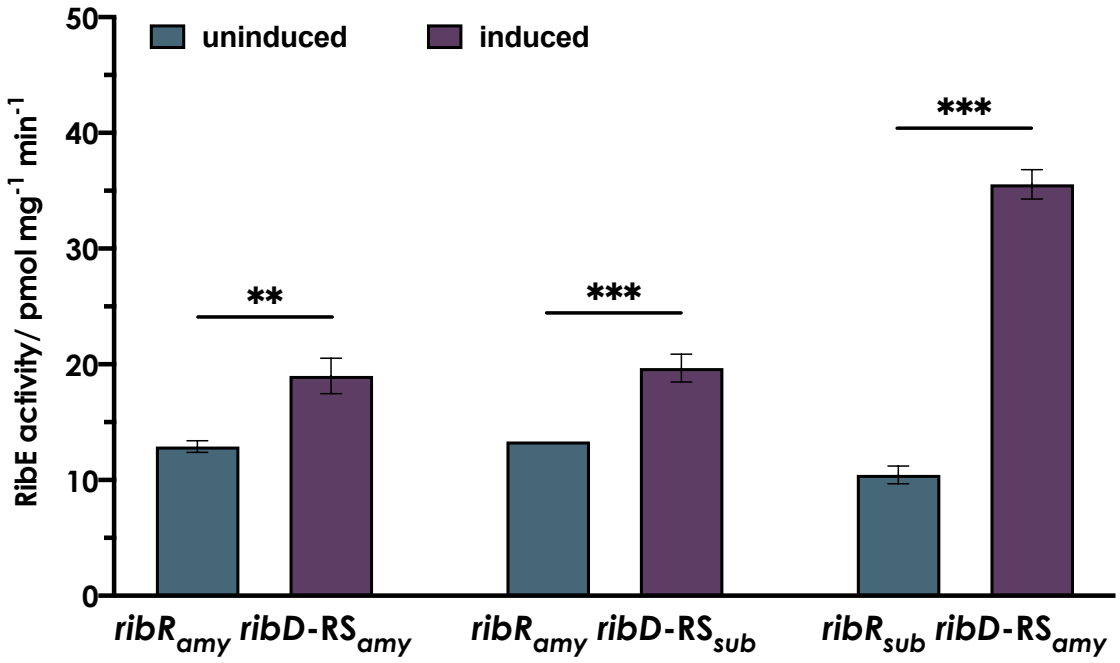

Figure 35: Riboflavin synthase activity in *B. subtilis* mutant strains with the *B. amyloliquefaciens ribR* gene and/or the *B. amyloliquefaciens ribD* FMN-riboswitch. *B. subtilis* 168 strains were grown in a minimal medium with 5 µM of riboflavin and $MgSO_4$ (uninduced) or methionine and taurine (induced) as sulfur sources in triplicates. RibE activity was determined in cell-free extracts of harvested cells using 6,7-dimethyl-8-ribityllumazine as a substrate. Enzyme activity assays were performed in triplicates with cell-free extracts of three independent cultures. Depicted are the mean values ± standard deviations of the data obtained from the triplicates. Asterisks indicate statistically significant differences (** $p \leq 0.01$, *** $p \leq 0.001$). Riboflavin formation was measured via HPLC.

6.4.1 Western Blot detection of a His-tagged version of RibR$_{amy}$

To check whether the observed effects on riboflavin synthase activity in *B. subtilis* can be attributed to the influence of RibR$_{amy}$, the induction of *ribR*$_{amy}$ and the presence of the RibR$_{amy}$

protein were analyzed using a His-tagged version of the protein. The respective coding region for *ribR*$_{amy}$-His$_6$ was introduced into *B. subtilis* genome via the CRISPR/Cas9 system and replaced the original *ribR*$_{sub}$ gene. The resulting strain *B. subtilis ribR*$_{amy}$*-his*$_6$ was grown in a minimal medium containing $MgSO_4$ or methionine and taurine as sulfur sources. Cells were harvested at an OD_{600} of 1.4 i.e. at a growth stage where the effect of RibR was found before. The cells were lysed and samples from the supernatants (S) and the pellets (P) were run on an SDS-PAGE gel. The protein bands were detected with a Western Blot, employing a 6-His antibody and visualized by a horseradish peroxidase (HRP) reaction. In the pellet sample from the methionine/taurine induced culture, a faint band could be detected that approximately matched the expected size for the RibR$_{amy}$-His$_6$ protein of 12.6 kDa. No bands at the same height became visible for the samples from the $MgSO_4$ cultures or the supernatant sample of the culture grown with methionine and taurine (Figure 36).

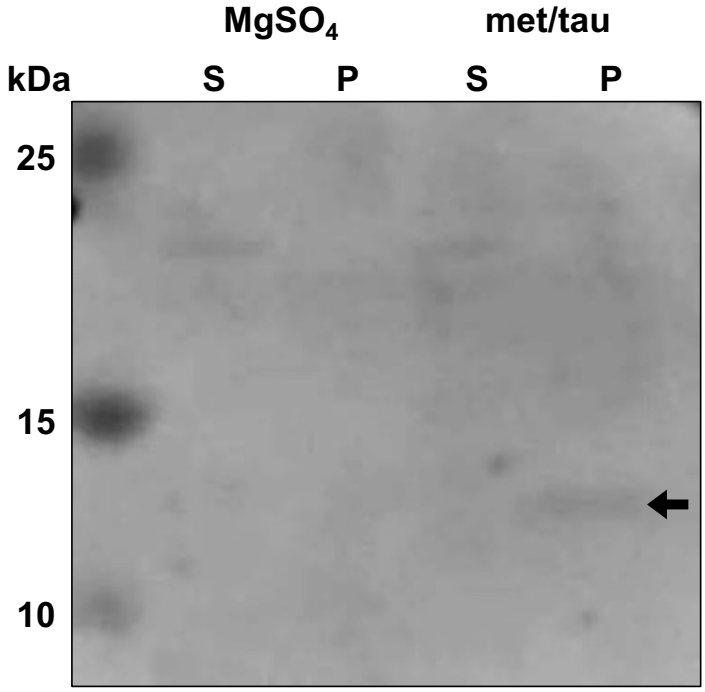

Figure 36: Western Blot detection of a His$_6$-tagged RibR$_{amy}$ in *B. subtilis* cultures induced with methionine/taurine. *B. subtilis ribR*$_{amy}$*-his*$_6$ was grown in Bacillus MM with $MgSO_4$ or methionine and taurine (met/tau) as sulfur sources. Cells were harvested at an OD_{600} of 1.4, lysed and samples of the supernatant (S) and the pellet (P) were prepared and run on an SDS-PAGE gel. Samples with a total protein amount of 20 µg were applied per lane. A protein ladder (M) was added for size comparison (PageRuler™ Plus Prestained Protein Ladder, Thermo Scientific). Proteins were blotted on a nitrocellulose membrane, incubated with a 1:700 solution of a horseradish peroxidase (HRP)-conjugated 6x-His tag monoclonal antibody (MA1-21315-HRP, Invitrogen). Bands were detected by horseradish peroxidase (HRP) driven conversion of DAB. The black arrow indicates the position of the His$_6$-tagged RibR$_{amy}$ (12.6 kDa).

6.5 Structural comparison of the RibR proteins from *B. subtilis* and *B. amyloliquefaciens*

Despite the low sequence similarity, the structures from the AlphaFold Protein Structure Database (https://alphafold.ebi.ac.uk/) for the two proteins align quite well with a root mean square deviation (rmsd) score of 0.529. Especially the two-arginine motif (R179/R180 in $RibR_{sub}$ and R54/R55 in $RibR_{amy}$) and the surrounding amino acids seem to form a similarly shaped pocket, with the two arginine residues positioned in the center (Figure 37). Since arginine residues are known to play a role in protein-RNA interactions by recognizing the RNA phosphate backbone and guanine bases (Chavali *et al.*, 2020a), the importance of these two adjoining arginines that are found in all compared RibR-like proteins, was examined.

To do so, *B. subtilis ribR* mutant strains were generated in which the coding sequence for the RR motif was replaced by nucleotides coding for two alanine residues instead ($RibR^{m}_{sub}$ R179A/R180A and $RibR^{m}_{amy}$ R54A/R55A). This was done for the *B. subtilis ribR* wild-type strain, as well as for the *ribR*$_{amy}$ strain and the strain with the combined exchange of the *ribR* and the *ribD* FMN riboswitch regions with the corresponding nucleotide sequences from *B. amyloliquefaciens*.

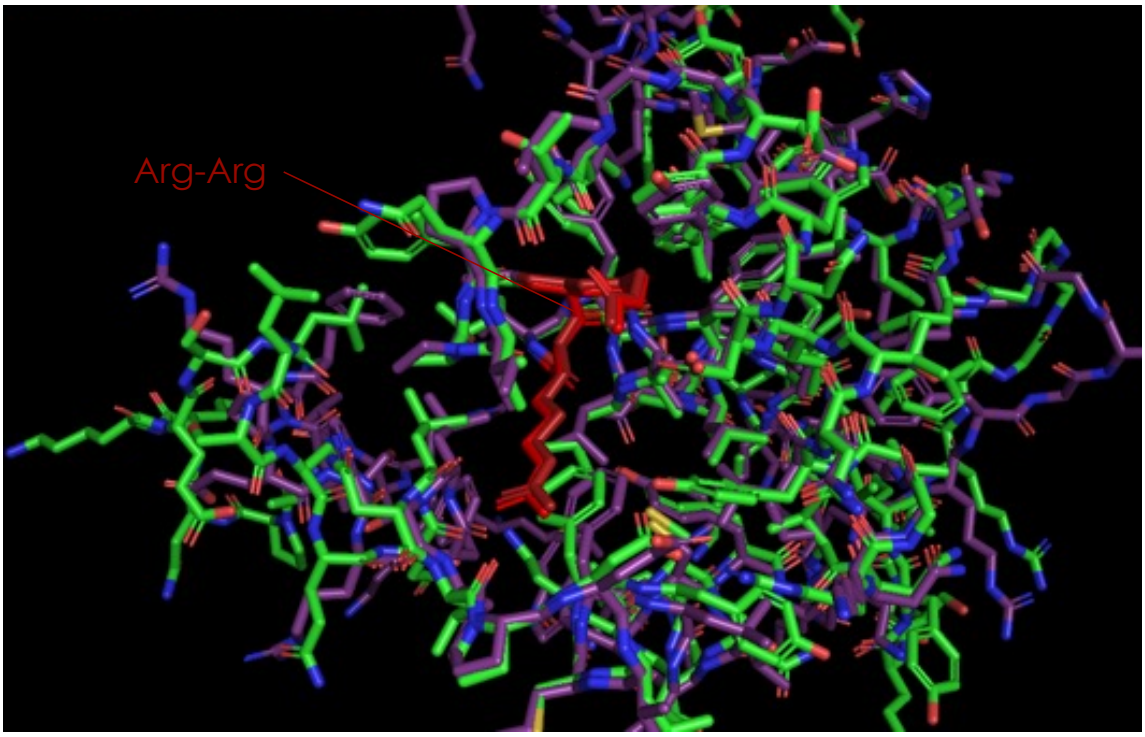

Figure 37: Structural alignment of the RibR-like protein $RibR_{amy}$ from *B. amyloliquefaciens* (green) and the C-terminal part of $RibR_{sub}$ from *B. subtilis* (violet). Both predicted protein structures were obtained from the AlphaFold Protein Structure Database. The structural alignment was obtained and visualized in PyMOL. The two-arginine motif Arg-Arg (RR) is colored in red for both proteins. Although the primary structures share only 46% identities the tertiary strucrures are similar (see Figure 31).

For these newly generated strains, another RFS assay was performed as before. In all three cases, in contrast to the strains with the unmodified RibR proteins (Figure 30, Figure 35), no increase in riboflavin synthase activity was observed when *ribR* expression was induced by methionine and taurine (Figure 38).

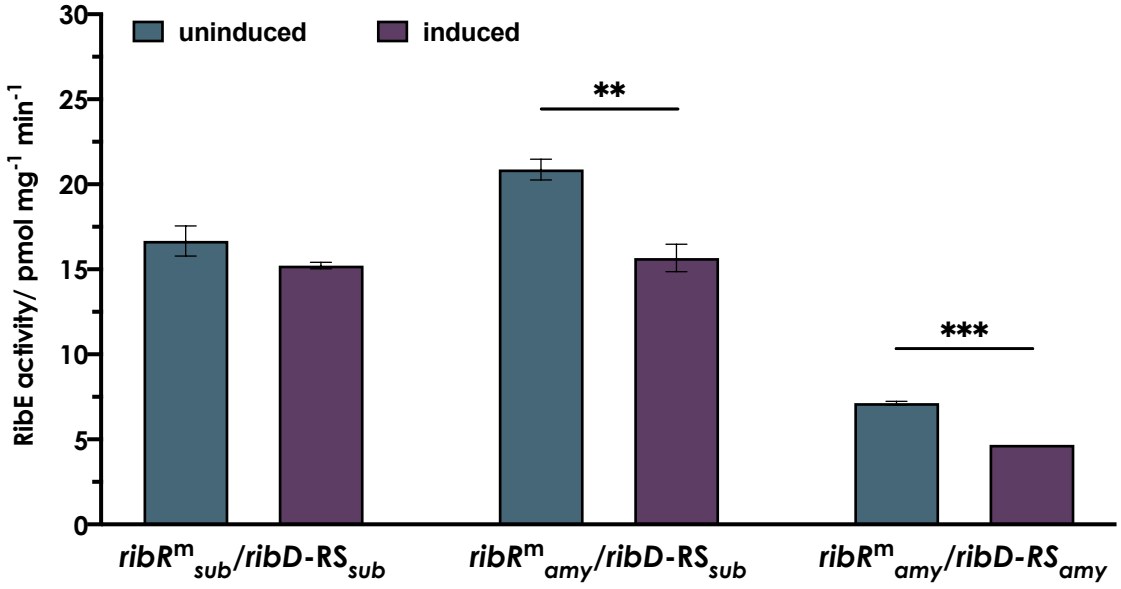

Figure 38: Riboflavin synthase activity in *B. subtilis* strains carrying the FMN *ribD*-RS versions of *B. subtilis* (*ribD*-RS$_{sub}$) or *B. amyloliquefaciens* (*ribD*-RS$_{amy}$) and producing the mutated RibR versions RibR$^{m}_{sub}$ and RibR$^{m}_{amy}$ with a mutation of the respective RR motif. *B. subtilis* 168 strains were grown in *Bacillus* MM with 5 µM of riboflavin and $MgSO_4$ (uninduced) or methionine and taurine (induced) as sulfur sources in triplicates. RibE activity was determined in cell-free extracts of harvested cells using 6,7-dimethyl-8-ribityllumazine as a substrate. Enzyme activity assays were performed in triplicates with cell-free extracts of three independent cultures. Depicted are the mean values ± standard deviations of the data obtained from the triplicates. Riboflavin formation was measured via HPLC.

6.6 Purification of the RibR-like protein from *B. amyloliquefaciens*

To further characterize RibR$_{amy}$ *in vitro* the recombinant protein was purified from an overproducing *E. coli* strain. The *E. coli* strains BL21 and BL21 pLysS were used as hosts to express the *ribR$_{amy}$* gene from a pET28a vector. While no distinct protein band of the expected size was observed in cell-free extracts when the BL21 strain was used as a host, expression of *ribR$_{amy}$* in BL21 pLys was successful. However, SDS-PAGE analysis of the proteome of the overproducing BL21 pLys strain showed that RibRamy was not present in the soluble fraction but mostly in the pellet (Figure 39). This suggests that RibR from *B. amyloliquefaciens*, just like RibR from *B. subtilis*, is not well water soluble.

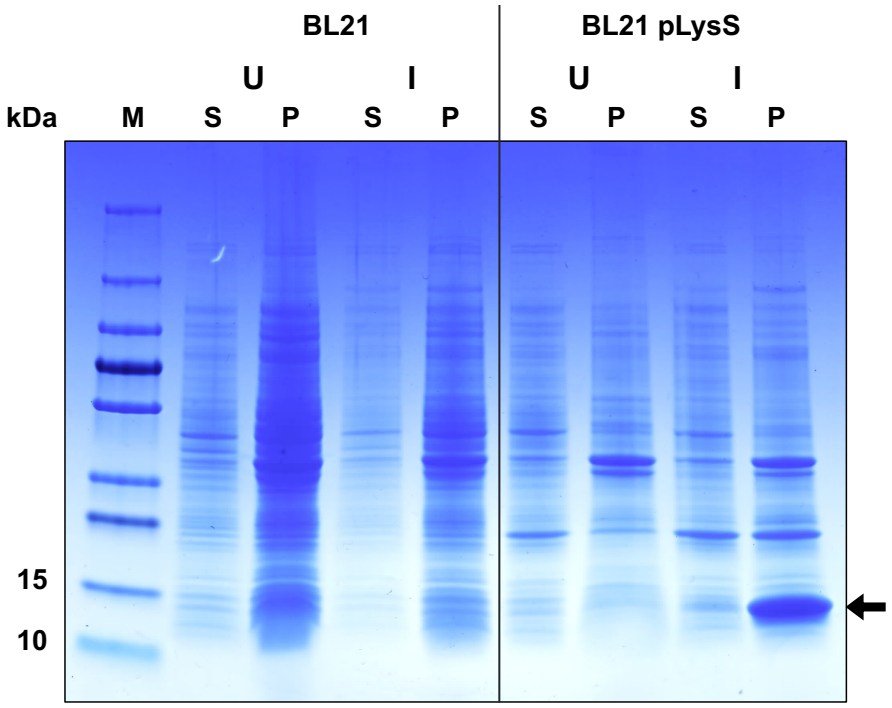

Figure 39: SDS-PAGE analysis of cell-free extracts from *E. coli* BL21 and BL21 pLysS strains overexpressing the *ribR*$_{amy}$ gene. *E. coli* BL21 and Bl21 pLys were transformed with a pET28a carrying the *ribR*$_{amy}$ gene under control of an IPTG-inducible T7 promoter. Cultures were grown at 37 °C in LB medium and were either kept uninduced (U) or were induced with 100 mM of IPTG (I). Cells were harvested 2h after induction. Cell-free extracts were prepared and samples from the supernatant (S) or the pellet (P) with a total protein amount of 8 µg were applied per lane. A protein ladder (M) was added for size comparison (PageRuler™ Plus Prestained Protein Ladder). The arrow indicates the position of the RibR$_{amy}$ protein (11.6 kDa). The gel was stained with Coomassie Brilliant Blue R-250.

6.6.1 Purification of RibR$_{sub}$ and RibR$_{amy}$ using a maltose-binding protein tag

To generate a soluble RibR derivative, a maltose-binding protein (MBP) tag was used. This 370 amino acid protein is a commonly employed tag, since it is known to significantly enhance the solubility of proteins. Fusion of a target protein to MBP allows a one-step purification using a dextrin sepharose resin.

The *B. amyloliquefaciens ribR* gene (*ribR*$_{amy}$) was ligated to pMAL-c6T carrying the *malE* gene to create an N-terminal fusion protein with MBP. The MBP-RibR$_{amy}$ fusion protein was overproduced using *E. coli* ER2523. As a control, the pure MBP protein was generated as well. Different expression times and temperatures were tested to optimize the conditions to produce these specific proteins. Figure 40 shows an exemplary SDS-PAGE gel for cell-free extracts of the expression strain cultures. It shows bands of the expected size for both MBP (45.5 kDa) and the MBP-RibR$_{amy}$ fusion protein in the respective supernatant fractions.

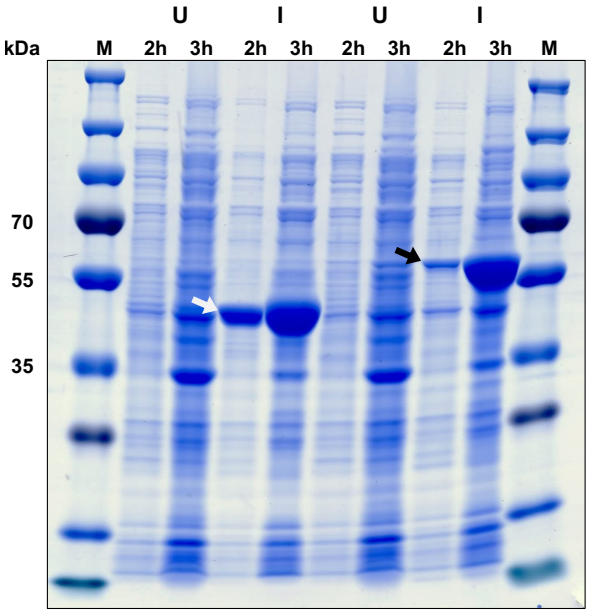

Figure 40: SDS-PAGE analysis of a test expression of maltose-binding protein (MBP) and MBP-RibR$_{amy}$ after 2h and 3h of induction in *E. coli* ER2325. *E. coli* ER2325 (NEBExpress) was transformed with the empty pMAL-c6T vector for producing MBP or pMAL-c6T::*ribR$_{amy}$* carrying the *malE*:*ribR$_{amy}$* gene fusion under control of an IPTG-inducible tac promoter. Cultures were grown at 37 °C in LB medium and were either left uninduced (U) or were induced with 0.3 mM of IPTG (I). Cells were harvested 2h or 3h after induction. Cell-free extracts were prepared and samples from the supernatant with a total protein amount of 8 µg were applied per lane. A protein ladder (M) was added for size comparison (PageRuler™ Plus Prestained Protein Ladder, Thermo Scientific). The white arrow indicates the position of MBP (45.5 kDa) and the black arrow the position of the MBP-RibR$_{amy}$ fusion protein (56.34 kDa). The gel was stained with Coomassie G-250 dye (PageBlue Protein Staining Solution, Thermo Scientific).

After the successful production of a soluble fusion protein for RibR$_{amy}$ as well as RibR$_{sub}$, both proteins and the sole MBP were purified via a chromatography column using a dextrin sepharose resin. An exemplary purification peak profile is presented for the MBP-tagged RibR$_{amy}$ (Figure 41). The sampled fractions from the protein elution were examined for their protein content with the Bradford assay (section 3.3.1). To ensure that the correct protein had been collected and that the purity was sufficient, samples of the eluted fractions were run on an SDS-PAGE gel.

For the purification of MBP, fractions nine to 19 were checked on a gel, together with the uninduced and induced samples of the unpurified cell-free extracts for comparison (Figure S8). The purified samples showed a concentrated protein of the expected size and only little background impurities. For further experiments, the fractions nine and 19 were used. Similar test gels were run for the purifications of the MBP-tagged versions of RibR from *B. subtilis* and *B. amyloliquefaciens.* Along with RibR$_{sub}$, its mutated version RibR$^{m}_{sub}$ with an exchange of the two arginine residues at positions 96/97 for two alanine residues was produced and purified. Here, the elution fractions seven to 17 and six to 16 were loaded onto a gel, respectively (Figure 42). There were still some impurities visible, but overall, the purification was effective and the protein bands corresponding to the size of the RibR proteins were the most prominent. For further analyses, the RibR$_{sub}$ fractions 16 and 17 and the fractions 15 and 16 from the RibR$^{m}_{sub}$ purification were used.

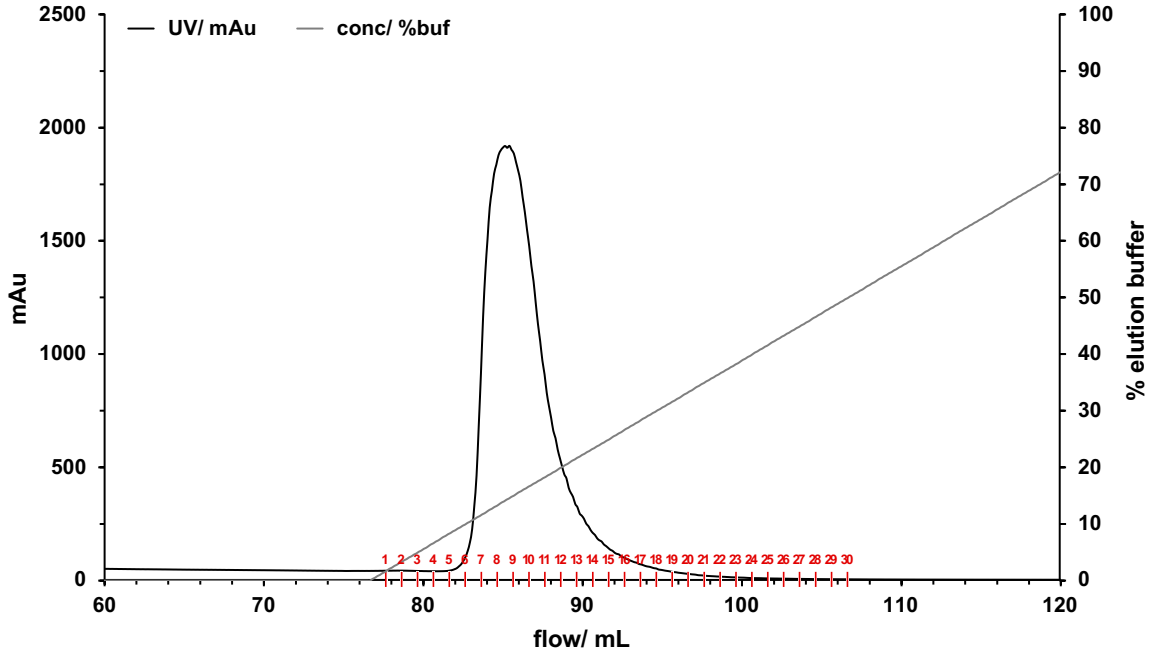

Figure 41: Chromatographic purification of the MBP-tagged RibR from *B. amyloliquefaciens*. Purification was performed with the ÄKTApurifier system, using a 5 mL MBPTrap HP column with a dextrin sepharose resin (Merck KGaA). The column was loaded with cell-free extracts of the *E. coli* ER2523 production strain for $RibR_{amy}$ in MBP column buffer. Elution was performed with an increasing concentration (conc) of MBP elution buffer (gray line). Elution fractions of 1 mL were collected over 30 minutes as indicated by the numbered red markers. Elution of the protein was followed by UV detection (black line).

Corresponding to the procedure for $RibR_{sub}$, the MBP-tagged version of the RibR protein from *B. amyloliquefaciens* was produced as well as the respective two-alanine mutant $RibR^{m}_{amy}$. Here, the fractions eight to 15 were checked for $RibR_{amy}$ and fractions seven to 17 for $RibR^{m}_{amy}$ (Figure 43). For the $RibR_{amy}$, unpurified fractions were additionally applied to the gel.

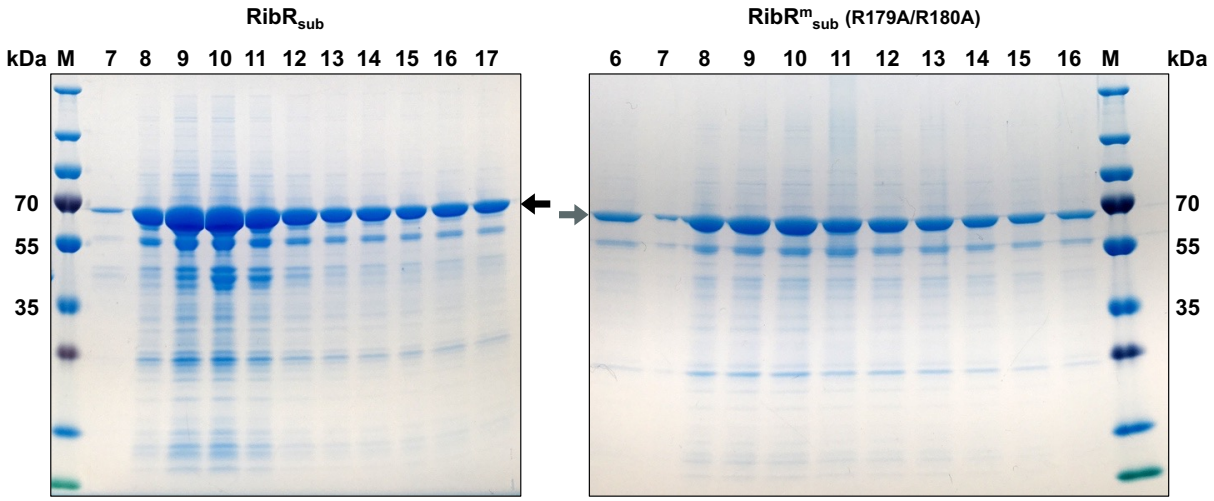

Figure 42: SDS-PAGE gel for sample fractions from the purification of MBP-$RibR_{sub}$ and MBP-$RibR^{m}_{sub}$. Cultures of *E. coli* ER2325 pMAL-c6T::*ribR*$_{sub}$ and pMAL-c6T::*ribR*$^{m}_{sub}$_RR>AA were grown at 37 °C in LB medium and were induced with 0.3 mM of IPTG. Cells were harvested 3h after induction. Cell-free extracts were prepared and purified with the ÄKTApurifier system. Samples with a total protein amount of 8 µg were applied per lane. A protein ladder (M) was added for size comparison (PageRuler™ Plus Prestained Protein Ladder, Thermo Scientific). The black arrow indicates the position of MBP-$RibR_{sub}$ (70.96 kDa) in the fractions 7-17 and the gray arrow the position of MBP-$RibR^{m}_{sub}$ (70.79 kDa) in the fractions 6-16. The gel was stained with Coomassie G-250 dye (PageBlue Protein Staining Solution, Thermo Scientific).

Some background bands are seen for the purified samples as well but compared to the unpurified samples (U and I) the impurities are minor and fractions eight and 15 were used for further experiments. For the RR mutant protein, fractions 16 and 17 were pooled and the protein contained was investigated further.

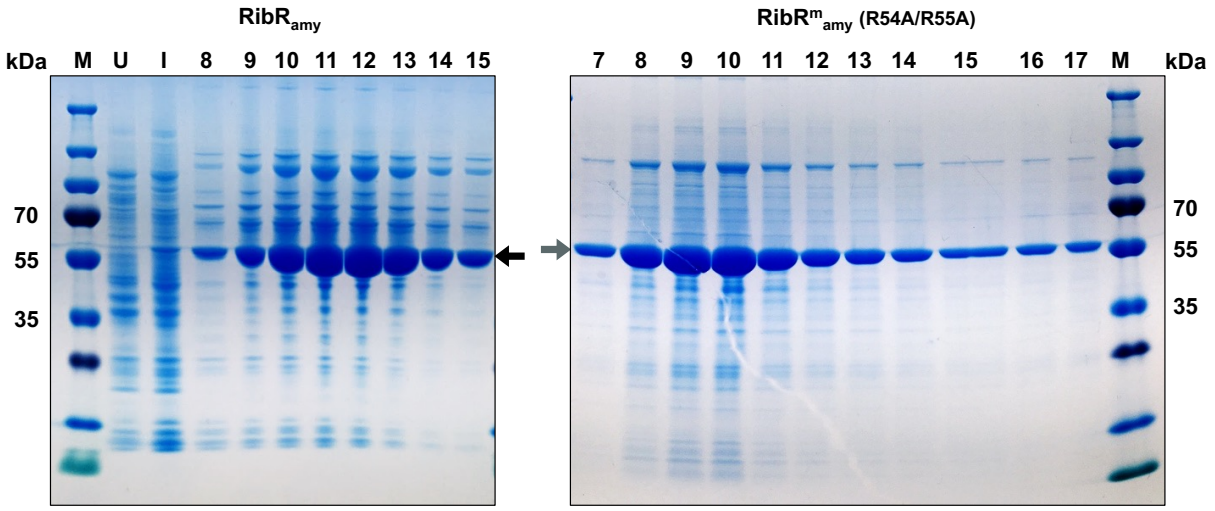

Figure 43: SDS-PAGE gel for sample fractions from the purification of MBP-RibR$_{amy}$ and MBP-RibR$^{m}_{amy}$. Cultures of *E. coli* ER2325 pMAL-c6T::*ribR$_{amy}$* and pMAL-c6T::*ribR$^{m}_{amy}$*_RR>AA were grown at 37 °C in LB medium and were either kept uninduced (U) or were induced with 0.3 mM of IPTG (I). Cells were harvested 3h after induction. Cell-free extracts were prepared and purified from induced samples with the ÄKTApurifier system. Samples with a total protein amount of 8 µg were applied per lane. A protein ladder (M) was added for size comparison (PageRuler™ Plus Prestained Protein Ladder, Thermo Scientific). The black arrow indicates the position of MBP-RibR$_{amy}$ (56.34 kDa) in the fractions 8-15 and the gray arrow the position of MBP-RibR$^{m}_{amy}$ (56.17 kDa) in the fractions 7-17. The gel was stained with Coomassie G-250 dye (PageBlue Protein Staining Solution, Thermo Scientific).

6.7 *In vitro* binding of RibR proteins to FMN riboswitch aptamers

An *in vivo* effect of RibR$_{sub}$ on riboswitch activity was shown before with the riboflavin synthase assay (Figure 30). Here, a similar effect was observed for RibR$_{amy}$. *B. subtilis* RibR$_{amy}$ cells that were induced with methionine and taurine had an increased riboflavin synthase activity compared to the uninduced cells grown with $MgSO_4$.

To further support the assumption that this observation is due to the influence of the RibR$_{amy}$ protein on FMN riboswitch activity, the predicted binding of the RibR proteins to the riboswitch aptamer RNAs was investigated using an electrophoretic mobility shift assay (EMSA). In this experimental setup, labeled RNA targets are incubated together with the potential RNA binding proteins and subsequently separated on a polyacrylamide gel. The different migration patterns of the labeled RNA in the gel reveal the formation of an RNA-protein complex, which slows down the movement of the RNA through the electrical field.

Both MBP-tagged RibR proteins, MBP-RibR$_{sub}$ and MBP-RibR$_{amy}$, were mixed with either of the *ribD* riboswitch aptamers of *B. subtilis* (Figure 44A) and *B. amyloliquefaciens* (Figure 44B)

and incubated in the absence or presence of $FMNH_2$. Additionally, the two mutated RibR versions $RibR^{m}_{sub}$ and $RibR^{m}_{amy}$ were included. While both wildtype proteins produced a gel shift with either of the two FMN riboswitch aptamers (samples 3 and 5, Figure 44A,B), no decelerated migration of the RNA was observed with the two proteins with a mutation of the two-arginine motif (samples 4 and 6). The addition of pure MBP (sample 2) to the mixture also did not change the movement of the two riboswitch aptamers compared to the control without any protein (sample 1).

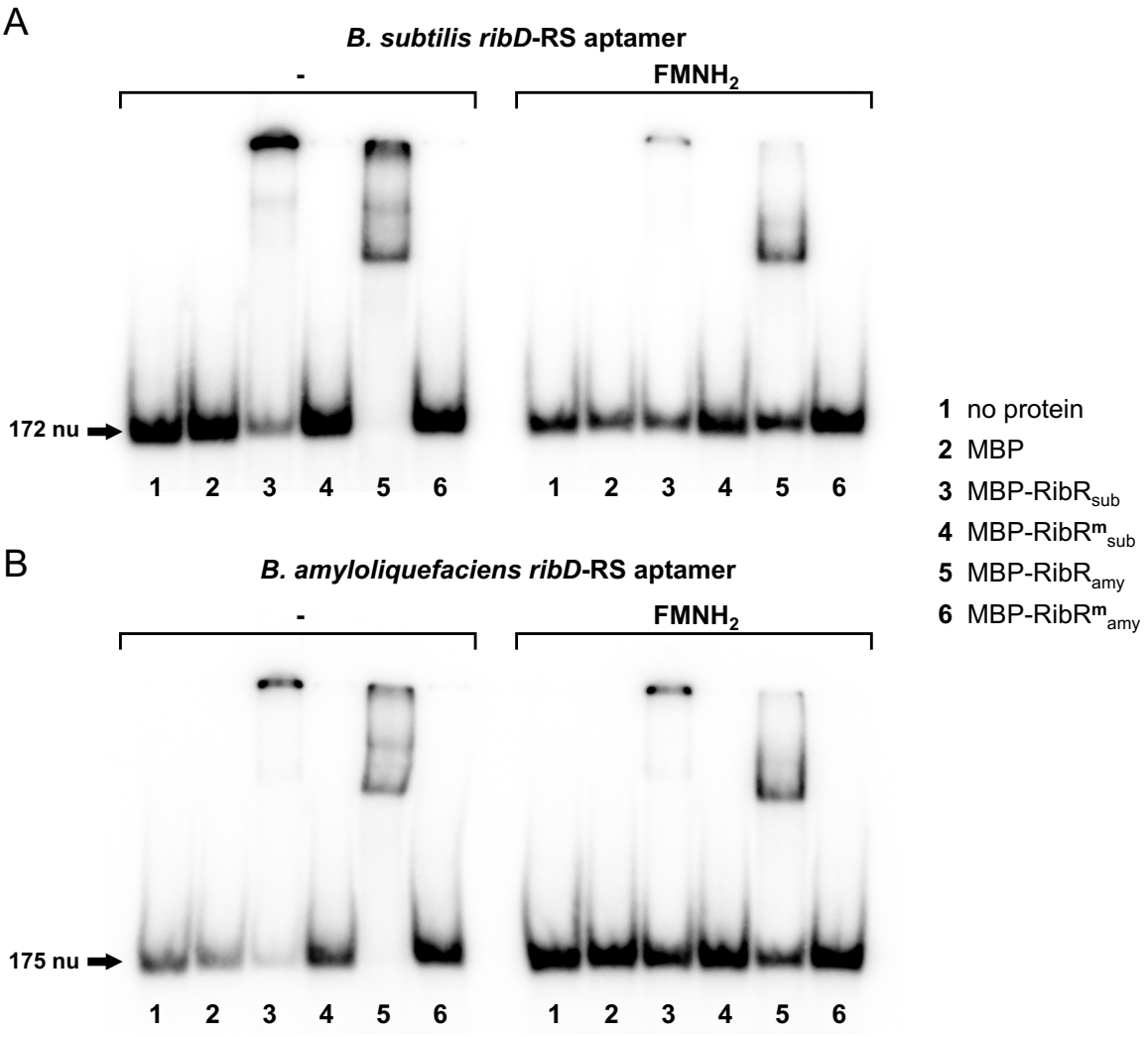

Figure 44: Electrophoretic mobility shift assay for *ribD* FMN riboswitch aptamers from *B. subtilis* (A) and *B. amyloliquefaciens* (B) in presence of purified MBP-RibR fusions. The FMN riboswitch RNA aptamer domains of *ribD*-RS from *B. subtilis* (172 nucleotides) and *B. amyloliquefaciens* (175 nucleotides) were produced via *in vitro* transcription, purified from a gel and 5'-labeled with [γ-^{32}P]ATP. The radiolabeled aptamers were incubated with or without 5 µM of $FMNH_2$ in the absence or presence of MBP or MBP-tagged RibR proteins including the RR mutants $RibR^{m}_{sub}$ and $RibR^{m}_{amy}$. The assay mixtures were separated on a polyacrylamide gel, with MBP-$RibR_{sub}$ and MBP-$RibR_{amy}$ producing a gel shift (samples 3 and 5) of the labeled RS aptamers.

6.8 Influence of RibR on riboflavin synthase activity and the putative connection to sulfur metabolism in *B. amyloliquefaciens*

For *B. subtilis*, a connection between the sulfur metabolism of the cell and the RibR regulation of FMN riboswitch activity has been discovered (Pedrolli, Kühm, *et al.*, 2015). Since the *ribR* gene is located in a cluster of genes involved in sulfur uptake and metabolism, this coherence could be suspected. The *ribR* gene of *B. amyloliquefaciens*, however, is found in a different genomic region in a transcriptional unit with the uncharacterized gene *yezD* (Figure 32).
To investigate the regulatory network of RibR in *B. amyloliquefaciens*, the riboflavin synthase assay was employed for this *Bacillus* species as well. First, the applicability of the assay was tested by comparing the RibE activity in *B. amyloliquefaciens* cells grown with and without riboflavin. When the emerging cell-free extracts were added to the assay mixture containing 6,7-dimethyl-8-ribityllumazine, riboflavin formation could be detected by HPLC analysis. Furthermore, the enzyme activity was significantly reduced, when riboflavin had been added to the bacterial cultures (Figure 45). This showed for the first time that the riboflavin synthase in this organism is a functional enzyme and that the upstream *ribD* riboswitch is responding to its ligand FMN, just like it has been documented for *B. subtilis*.

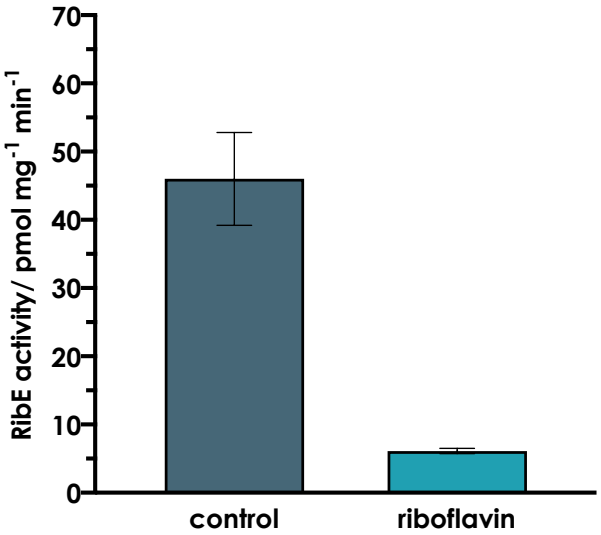

Figure 45: Riboflavin synthase (RibE) activity in the *B. amyloliquefaciens* WT changes upon addition of riboflavin to the medium. *B. amyloliquefaciens* was grown in shake flasks in a minimal medium containing $MgSO_4$ as the sole sulfur source (control). When riboflavin (2 µM) is added to the cultures (riboflavin) RibE activity decreases. RibE activity was determined in cell-free extracts of harvested cells using 6,7-dimethyl-8-ribityllumazine as a substrate. Enzyme activity assays were performed in triplicates with cell-free extracts of three independent cultures. Depicted are the mean values ± standard deviations of the data obtained from the triplicates. Riboflavin formation was measured via HPLC.

Based on these findings, the RFS assay was then used to test whether despite of the differing genomic localization compared to *B. subtilis*, there was a similar kind of regulatory connection between the presence of certain sulfur sources and the expression of *ribR* in

B. amyloliquefaciens. Therefore, consistent with the experimental design for *B. subtilis*, cultures of *B. amyloliquefaciens* were grown in the presence of either $MgSO_4$ or methionine and taurine as sulfur sources, with 2 µM of riboflavin added to the medium. When the riboflavin synthase activities of cell-free extracts from these cultures were compared, no increase in enzyme activity was detected for the cultures grown with methionine and taurine (Figure 46).

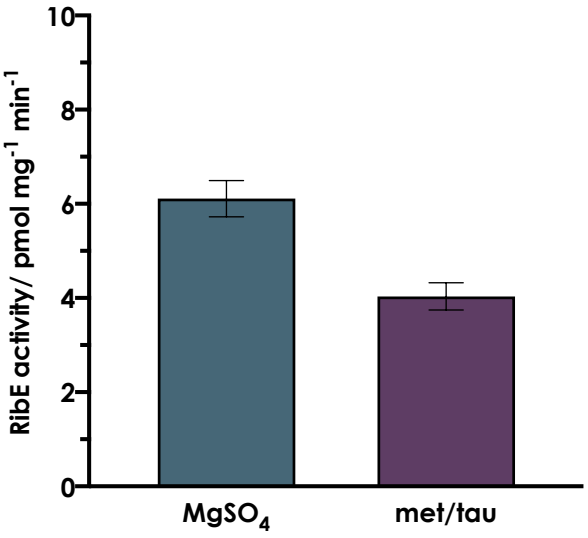

Figure 46: Riboflavin synthase (RibE) activity in the *B. amyloliquefaciens* WT grown with $MgSO_4$ or methionine/taurine as sulfur sources. *B. amyloliquefaciens* strains were grown in triplicates in shake flasks in a minimal medium with 2 µM of riboflavin and $MgSO_4$ or methionine and taurine (met/tau) as a sulfur source. RibE activity was determined in cell-free extracts of harvested cells using 6,7-dimethyl-8-ribityllumazine as a substrate. Enzyme activity assays were performed in triplicates with cell-free extracts of three independent cultures. Depicted are the mean values ± standard deviations of the data obtained from the triplicates. Riboflavin formation was measured via HPLC.

6.9 The influence of diamide-induced oxidative stress on riboflavin synthase activity in *B. amyloliquefaciens*

As stated earlier, the gene *yezD*, which appears to be in a transcriptional unit with $ribR_{amy}$, has not been characterized yet and nothing is known about its specific expression patterns. In *B. subtilis*, however, the homologue of *yezD* has been linked to cellular stress responses, since an elevating effect of the oxidative stressor diamide on *yezD* expression has been observed (Zhu and Stülke, 2018b).

A similar regulatory connection can be presumed for the close relative *B. amyloliquefaciens*. It was tested whether diamide really increases expression of *yezD* and thereby also the expression of $ribR_{amy}$. Based on this assumption, addition of a sublethal concentration of diamide to the bacterial cultures was expected to subsequently lead to an increase in riboflavin synthase activity through the interaction of $RibR_{amy}$ with the *ribD* FMN riboswitch.

The effect of diamide on riboflavin synthase activity was investigated both in the presence of $MgSO_4$ on the one hand and methionine/taurine on the other hand. Furthermore, cultures were

grown in either the absence or presence of riboflavin. For the cells grown in a medium containing methionine/taurine as the sulfur sources, addition of diamide led to an increase in RFS activity compared to the control without diamide (Figure 47A). However, this effect was only observed when no riboflavin had been added to the cultures. When riboflavin was present, cell-free extracts from diamide-induced cultures did not exhibit differences in riboflavin activity compared to the uninduced cells, whatsoever (Figure 47B). For the cultures grown with $MgSO_4$ but without riboflavin, diamide addition even led to a decrease in RibE activity compared to the control (Figure 47A,B).

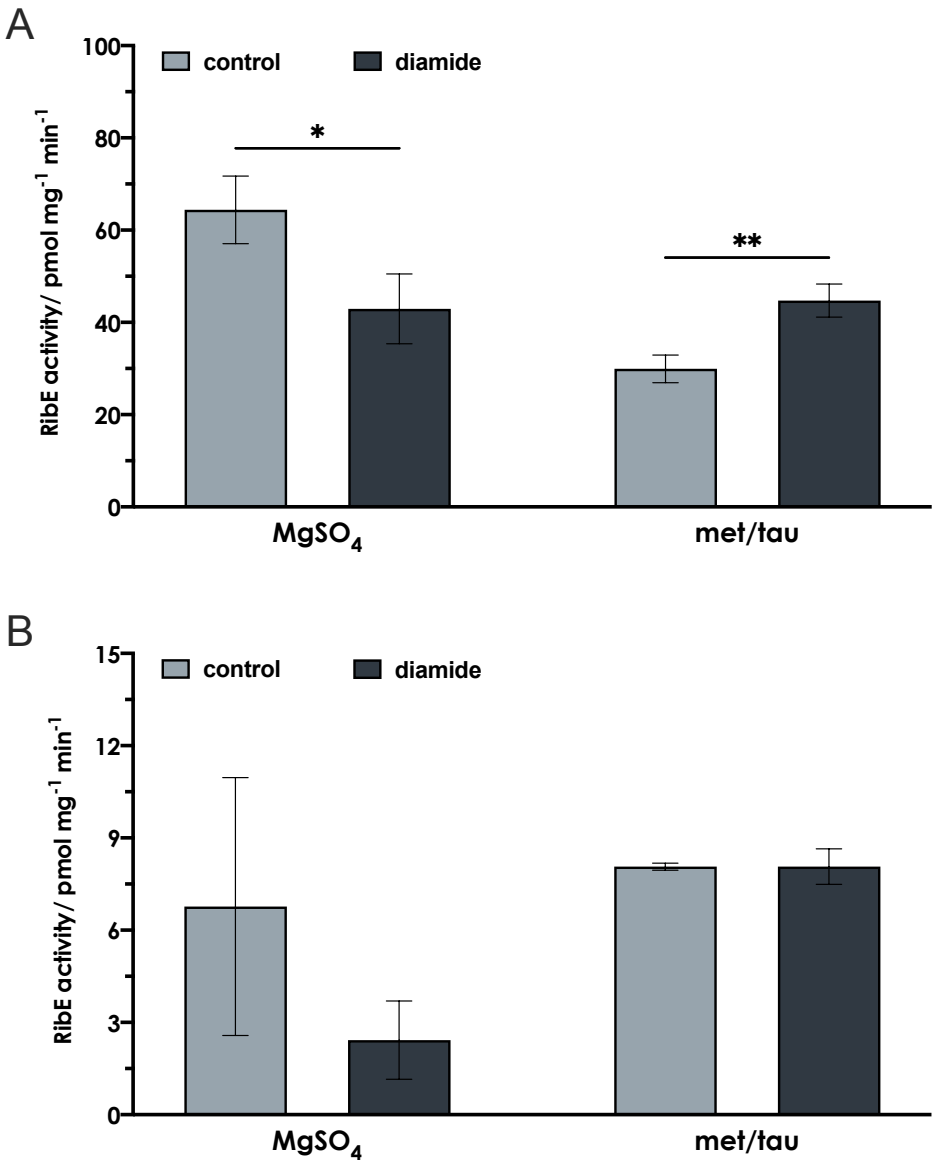

Figure 47: Effect of diamide on riboflavin synthase activity in *B. amyloliquefaciens* grown in the absence (A) or presence of riboflavin (B). *B. amyloliquefaciens* was grown in shake flasks in minimal medium with $MgSO_4$ or methionine and taurine (met/tau) as sulfur sources, either without (A) or with the addition of 5 µM of riboflavin (B) in triplicates. When cultures reached an OD_{600} of 0.8, 0.5 mM diamide was added to the cultures (diamide), while the control cultures (control) remained untreated. After the addition of diamide, all cultures were incubated for another 2 hours before harvesting. RibE activity was determined in cell-free extracts of harvested cells using 6,7-dimethyl-8-ribityllumazine as a substrate. Enzyme activity assays were performed in triplicates with cell-free extracts of three independent cultures. Depicted are the mean values ± standard deviations of the data obtained from the triplicates. Riboflavin formation was measured via HPLC.

6.9.1 Influence of diamide on transcription of *ribR*$_{amy}$ in *B. amyloliquefaciens*

To further substantiate the connection between diamide-induced expression of *ribR*$_{amy}$ and an increased activity of the riboflavin synthase, total RNA was extracted from *B. amyloliquefaciens* cells and mRNA levels for the *ribR* gene were checked via reverse transcription. The cultures were either grown with $MgSO_4$ or methionine and taurine as a sulfur source. Additionally, diamide was added to some cultures to check for its ability to induce the expression of the *ribR* gene. For that purpose, 0.5 mM of diamide were either added at the time of inoculation (+dia) and cells were harvested at an OD_{600} of 0.8, or diamide was added later when the cells had reached an OD_{600} of 0.8. In the latter case, cells were harvested two hours after the diamide had been added (+dia, 2h ind.), just as it had been done in the RibE assays with diamide. In both cases, cells grown under the same conditions, but without diamide, were harvested at the same time as the respective diamide-induced cultures for comparison of the transcript levels.

Total RNA was extracted from the harvested cells and transcribed back to DNA with the reverse transcriptase (RT). The *ribR*$_{amy}$ specific transcript, as well as the transcript for the housekeeping gene *citZ* as a positive control, were then detected with a second PCR reaction, using specific primers for the respective genetic region. Negative controls from an RT-PCR reaction without any reverse transcriptase were included to ensure that no genomic DNA contaminated the samples.

Even though both PCR reactions were generally successful, proven by the bands seen for the positive control with gDNA from *B. amyloliquefaciens* (Figure 48A,B), no bands for the housekeeping gene *citZ* were detected for any of the samples. For the *ribR* transcript on the other hand, bands of the respective size were visible for some of the samples. For the cultures that were grown with $MgSO_4$ as a sulfur source and harvested at an OD of 0.8, no band was detected, irrespective of the presence of diamide (Figure 48A, samples 4&5). For the equivalent samples of the cultures grown with methionine and taurine, a very faint band is found in the diamide-free sample (sample 8), while a prominent band shows for the sample of the culture that was incubated with diamide from the beginning (sample 9).

For the cultures to which diamide was added mid-growth and the respective negative controls, bands were visible in all samples. However, the bands from the samples of cultures grown with $MgSO_4$ (samples 6&7) are a little more pronounced than the ones from cultures grown with methionine and taurine (samples 10&11). For both sulfur sources, the addition of diamide did not influence the band intensity of the samples, hence, the transcription level of the *ribR* gene.

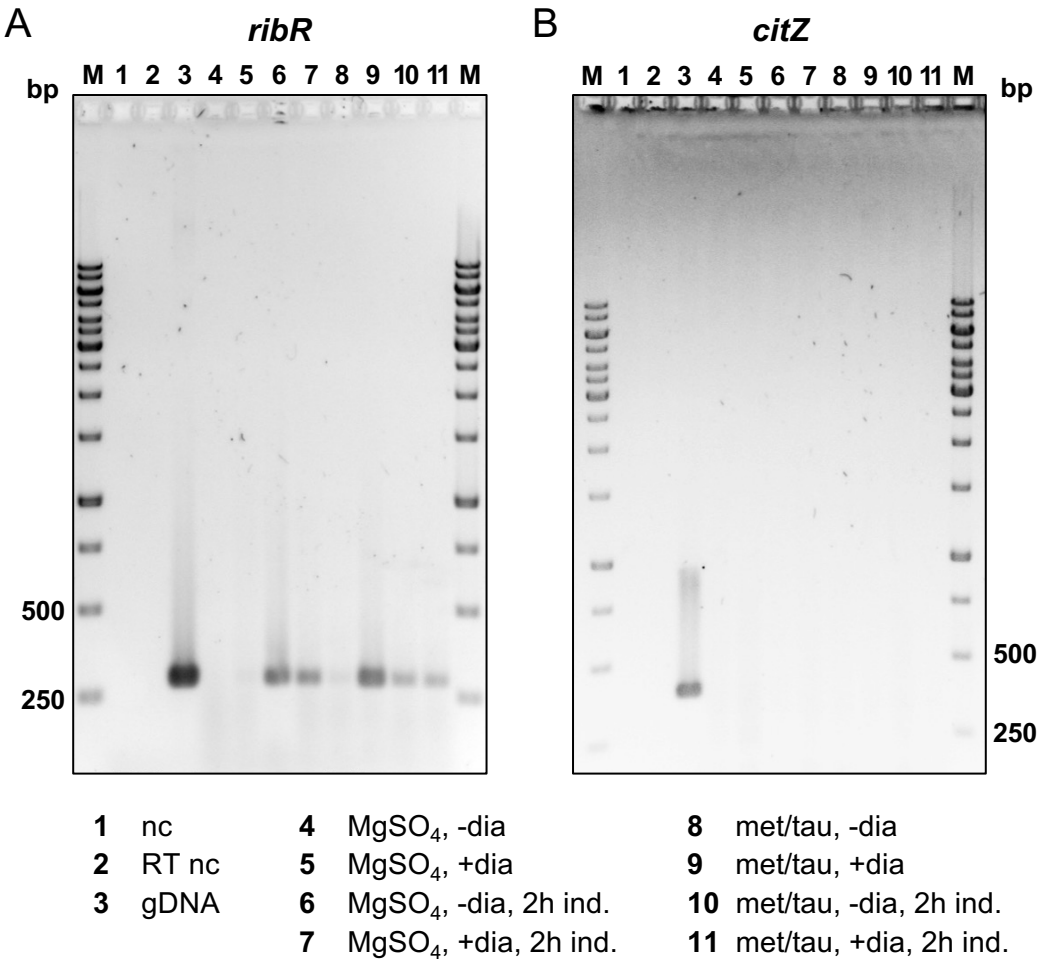

Figure 48: Detection of a *ribR* specific transcript in *B. amyloliquefaciens*. The gel shows amplified products of RT-PCR reactions for *ribR* **(A)** and the housekeeping gene *citZ* **(B)** from total RNA of *B. amyloliquefaciens* cultures. Cultures were grown in *Bacillus* MM with $MgSO_4$ (samples 2, 4-7) or methionine and taurine (met/tau, samples 8-11) as sulfur sources. Cultures were either grown without diamide (-dia), or with 0.5 mM of diamide (+dia) and harvested at an OD_{600} of 0.8, or diamide was added at an OD_{600} of 0.8 and cells were harvested 2h later (2h ind.) together with cells from the -dia control. Gels include a PCR negative control (nc) without any template, a control with a sample from the RT-PCR negative control reaction (RT nc) and a positive control with *B. amyloliquefaciens* gDNA (sample 3). A DNA ladder (M) was included for size comparison (GeneRuler 1 kb DNA ladder, Thermo Scientific). Band sizes are given in base pairs.

7 Discussion – Chapter II

7.1 The riboswitch binding protein RibR

The protein RibR from *B. subtilis* has been identified as a bifunctional protein with flavokinase activity that is additionally able to modulate FMN riboswitch activity through a regulatory RNA-binding part (Higashitsuji *et al.*, 2007; Pedrolli, Kühm, *et al.*, 2015). Furthermore, it was shown that expression of the operon, in which the *ribR* gene is located within the *B. subtilis* genome, is more strongly expressed in the presence of specific sulfur sources like methionine and taurine (Pedrolli, Kühm, *et al.*, 2015). In the present study, the RibR protein $RibR_{sub}$ from *B. subtilis* and the RibR-like protein $RibR_{amy}$ from the closely related strain *B. amyloliquefaciens* were further investigated and compared in their function.

7.1.1 Validation of RibR activity in *B. subtilis* by markerless deletion strains

Using CRISPR/Cas9 genome editing, different markerless *ribR*-deletion mutants were generated in *B. subtilis*, deleting either the whole gene or the individual parts coding for the N- and C-terminal part. To measure the influence of RibR on the *ribD* FMN riboswitch activity, which regulates the expression of the riboflavin biosynthetic operon, a reporter assay was used to measure the riboflavin synthase (RibE)-mediated conversion of 6,7-dimethyl-8-ribityllumazine to riboflavin. In the absence of RibR, addition of riboflavin to *B. subtilis* cultures leads to a reduction of *rib* gene expression due to formation of FMN, which turns the FMN riboswitch to the OFF state.

In previous studies, a yeast-three-hybrid system as well as a plasmid-based reporter gene assay in *E. coli* have assigned the flavokinase activity of RibR to the N-terminal part, while the C-terminal part was shown to be sufficient for FMN riboswitch regulation (Higashitsuji *et al.*, 2007; Pedrolli, Kühm, *et al.*, 2015).

The riboflavin synthase assay used in this study now confirms the previous attribution of the RibR riboswitch-regulating function to the C-terminal part of the protein also *in vivo* in *B. subtilis* cells. The results show that induction of $RibR_{sub}$ by methionine and taurine leads to an increase in RibE activity in the *B. subtilis* WT, even when cells are grown in the presence of 5 µM riboflavin. The same effect was observed when only the N-terminal coding region of $ribR_{sub}$ was deleted, but not when the whole *ribR* gene or only the C-terminal coding part was deleted (Figure 30). Thereby, the individual regulatory effect of the C-terminal part of $RibR_{sub}$ on FMN riboswitch function in the natural cellular environment was verified.

7.1.1.1 The individual character of RibR as a riboswitch-regulating protein

While the flavokinase activity of RibR seems to be negligible in the cellular context due to its low activity compared to the main flavokinase RibFC of *B. subtilis* (Mack *et al.*, 1998) and due to the fact that it does not significantly contribute to the increase of intracellular FMN levels (Pedrolli, Kühm, *et al.*, 2015), the uniqueness of the riboswitch-regulating capabilities of the C-terminal part of RibR must be emphasized.

Other riboswitch interacting enzymes have been described in bacteria before, like RNases (Spinelli *et al.*, 2008) and the k-turn binding protein YbxF (Baird *et al.*, 2012). But in all these examples, the proteins support the up- or downregulating mechanism initiated by the riboswitch ligand itself. RNases are directly involved in the riboswitch-mediated downregulation of transcript numbers by targeting the resulting mRNA for degradation (Spinelli *et al.*, 2008), YbxF induces additional folding of the *B. subtilis* glycine riboswitch and enhances binding of the ligand glycine (Baird and Ferré-D'Amaré, 2013). In *Vibrio vulnificus*, binding of adenine to the adenine riboswitch is not sufficient to enable translation, but additional binding of the ribosomal protein rS1 is required for folding into the ON-state (de Jesus *et al.*, 2021).

RibR, on the other hand, actually counteracts the effect of the natural ligand FMN. While binding of FMN to the riboswitch aptamer prevents transcription of the downstream operon in a negative feedback loop, RibR enables expression of the riboflavin synthase genes even in the presence of high levels of FMN (Pedrolli, Kühm, *et al.*, 2015).

7.1.2 The RibR-like protein of *B. amyloliquefaciens* regulates FMN riboswitch activity

To examine the existence of RibR-like proteins in other bacterial species, a BLASTp search (Altschul *et al.*, 1990) was conducted, using the complete amino acid sequence of $RibR_{sub}$. However, this produced a large number of hits in the database for the N-terminal flavokinase part of RibR, since flavokinases are enzymes which occur in all organisms. Therefore, a database comparison with just the C-terminal part (AA 90-230) of $RibR_{sub}$ was more promising and revealed only few RibR homologs in other species. Remarkably, these proteins only occur in the order of the *Bacillales* (Harirchi *et al.*, 2022) with most of them being part of the families *Bacillaceae* and *Paenibacillaceae*. While some strains like *Bacillus halotolerans* and *B. cabrialesii* also possess a full RibR sequence with homologous sequences for the N- and C-terminal part of $RibR_{sub}$, the genomes of other *Bacillus* species like *B. benzoevorans*, *B. smithii* and *B. amyloliquefaciens* contain a truncated *ribR*-like gene, coding only for the putative RNA-binding part.

B. amyloliquefaciens is a very close relative of *B. subtilis.* The two species are part of a group that share a high degree of similarity in the 16S rRNA gene sequences and are referred to as the *B. subtilis* species complex (Rooney *et al.*, 2009). Despite this close relation, the

B. amyloliquefaciens ribR-like gene is located in a different genomic region than the *ribR* gene of *B. subtilis*. Although the other homologous genes of the *snaA* operon of *B. amyloliquefaciens* are organized in the same way as in the *B. subtilis* genome, the $ribR_{amy}$ gene is found downstream of and in a putative transcriptional unit with the gene *yezD*, coding for a small, uncharacterized protein (Figure 32).

To test, whether the encoded protein $RibR_{amy}$ (WP_013351322.1) still exhibits a similar regulatory function in the riboflavin biosynthetic pathway, the *B. subtilis* riboflavin synthase RibE was again used as an *in vivo* reporter. When the $ribR_{sub}$ gene was replaced by $ribR_{amy}$ in the *B. subtilis* genome, induction with methionine/taurine resulted in an increase in RibE activity, compared to the uninduced cultures with $MgSO_4$ as the sole sulfur source. The same effect was observed when, in addition to the exchange of the *ribR* gene sequence, the *ribD* riboswitch sequence was replaced with the corresponding sequence from *B. amyloliquefaciens*. These results suggest that the RibR-like protein from *B. amyloliquefaciens* plays a similar role in the regulation of riboflavin biosynthesis genes as observed for RibR from *B. subtilis*. Notably, the effect of $RibR_{sub}$ and N-$RibR_{sub}$ on the activity of both FMN riboswitches was much stronger than that of $RibR_{amy}$. The low amount of produced $RibR_{amy}$ detected in the Western blot, compared to the comparatively higher amount of *B. subtilis* RibR measured previously (Pedrolli, Kühm, *et al.*, 2015) may provide an explanation for the rather small effect $RibR_{amy}$ has on riboswitch activity.

Nevertheless, the experimental outcome proves for the first time that both RibR proteins are able to recognize riboswitch sequences from other, though closely related, species. A previous study on $RibR_{sub}$ has found no regulatory effect of this protein on the *ribE* FMN riboswitch of *Streptomyces davaonensis* (Pedrolli, Kühm, *et al.*, 2015). However, it is noteworthy that the two *ribD* FMN riboswitches from *B. subtilis* and *B. amyloliquefaciens* share a very high sequence similarity (78.5%) (see alignment Figure 33) compared to the FMN riboswitch from *S. davaonensis* (39%). Even the *ribU* riboswitch from *B. subtilis*, which is also regulated by $RibR_{sub}$ (Pedrolli, Kühm, *et al.*, 2015), has a much lower identity (57.8%) compared to the *ribD* RS from the same organism (Figure S9).

7.1.3 The two-arginine motifs of $RibR_{sub}$ and $RibR_{amy}$ are essential for aptamer binding and regulation of FMN riboswitch activity

Arginine-rich motifs play an important role in protein recognition of RNA molecules (Bayer *et al.*, 2005). Arginine residues have been found to be often involved in protein-RNA interactions and specifically contribute to stacking interactions, especially due to its ability to form salt-bridges, as well as multiple hydrogen bonds (Barik *et al.*, 2015; Krüger *et al.*, 2018). The arginine fork model explains that and how a single arginine can recognize a specific RNA

backbone (Chavali *et al.*, 2020b). Furthermore, arginine residues have been shown to be involved in binding to the RNA k-turn motifs (Gagnon *et al.*, 2010; Huang and Lilley, 2013), which are also found in riboswitch structures (Lilley, 2014).

Therefore, the conserved two-arginine motif found in the RibR proteins of different species was of special interest. An alignment of the Alphafold structures of $RibR_{sub}$ and $RibR_{amy}$ reveals that despite the intermediate sequence similarity, folding of the two proteins seems to be alike, with the two arginine residues positioned quite exposed in a pocket. Replacement of these two arginine residues with two alanine residues resulted in a loss of regulation of FMN riboswitch activity by RibR for both proteins from *B. subtilis* and *B. amyloliquefaciens*. From this it can be concluded that the RR motif is important for regulating riboswitch activity. Additionally, an EMSA assay showed that both $RibR_{sub}$ and $RibR_{amy}$ bind *ribD* FMN riboswitch aptamers from both organisms. Replacement of the RR motif by AA in both proteins prevented binding.

Of course, a replacement of the arginine residues with alanine residues will affect the charge of the putative binding pocket, which could be argued as a possible reason for the lack of binding when the arginine residues are exchanged. However, it has been shown that even a "more conservative" change, in terms of molecular charge, from arginine to lysine can impair the binding of a peptide sequence to a specific RNA molecule (Belashov *et al.*, 2018). However, it cannot be completely excluded that the observed effect is the result of a more general influence of the mutated residues on the protein structure.

Interestingly, in the EMSA assay, *in vitro* binding of the aptamer was seen in the presence and absence of $FMNH_2$, which contradicts the results of Pedrolli *et al.* (2015), who observed binding only in the presence of one of the riboswitch ligands, FMN and $FMNH_2$. On the contrary, in the present study, binding to the riboswitch aptamers was even weaker in the presence of $FMNH_2$. While the present results strongly suggest that binding of RibR to the riboswitch is independent of FMN/$FMNH_2$, the slightly weaker affinity in the presence of $FMNH_2$ might be explained by the FMN reducing agent sodium dithionite.

7.1.4 Induction of RibR and the effect on FMN riboswitch activity in *B. amyloliquefaciens*

For further examinations on RibR function in *B. amyloliquefaciens*, activity of the riboflavin synthase RibE was directly measured for the wildtype of this organism. Measurement of RibE activity for cells grown in the presence and absence of riboflavin provided proof of function for the assay. It showed that RibE activity can be successfully quantified for *B. amyloliquefaciens* and that expression of *ribE* is furthermore controlled by the FMN riboswitch, which downregulates expression when cells are exposed to riboflavin.

In contrast to *B. subtilis*, growth of *B. amyloliquefaciens* in the presence of riboflavin revealed no increase in riboflavin synthase activity in cells supplied with methionine and taurine compared to cells grown with $MgSO_4$ as the sole sulfur source. This was not entirely unexpected, since the $ribR_{amy}$ gene is found at a different genomic location than the *ribR* gene of *B. subtilis* and so far, no connection of *ribR* expression to different available sulfur sources has been shown for *B. amyloliquefaciens*.
Interestingly, in cultures grown without riboflavin, RibE activity was decreased, when only methionine and taurine were available to the cells as a sulfur source. This finding might hint to another unknown regulatory pathway in *B. amyloliquefaciens*, connecting sulfur metabolism to riboflavin biosynthesis.

7.1.5 The oxidant stressor diamide induces transcription of *ribR* in *B. amyloliquefaciens*

The *ribR* gene of *B. amyloliquefaciens* is probably co-transcribed with the upstream gene *yezD*, which codes for a small, uncharacterized protein. Only very little is known about a possible function of this protein. However, some hints about YezD function can be drawn from a study on the *yezD* homolog *oscA* in *Pseudomonas corrugata* (Viti *et al.*, 2009). This gene was found to be located upstream of genes encoding a putative sulfate ABC transporter. An *oscA* mutant strain of *P. corrugata* was unable to utilize certain sulfur compounds, including S-methyl-L-cysteine, methionine and taurine, which the WT is normally able to metabolize. The genes located downstream of *oscA* homologs in other Gram-positive and Gram-negative bacteria, including several *Bacillus* species, were furthermore found to be involved in sulfur metabolism. This includes genes coding for other putative sulfate ABC transporters, e.g. in *B. halodurans*, genes involved in metabolism and transport of sulfonates in *Methylobacillus flagellates* and *B. clausii* and genes coding for enzymes involved in a sulfate reduction pathway resulting in cysteine production in other *Bacillus* strains (Viti *et al.*, 2009). Interestingly, the only described exception was the *B. subtilis* WT 168 in which the gene product of the downstream gene *yetJ* was characterized as a procaryotic BAX-inhibitor protein, involved in maintaining the Ca^{2+} homeostasis of the cell (Chang *et al.*, 2014). However, the findings for other *Bacillus* species make it plausible that also the *ribR* gene downstream of *yezD* in *B. amyloliquefaciens* is somehow involved in sulfur metabolism in this organism.
In *B. amyloliquefaciens*, the truncated *ribR* gene is positioned between the *yezD* gene and the *yetJ* homolog. Transcriptome data suggests that *yezD* from *B. subtilis* is upregulated in the presence of the oxidant diamide (Rochat *et al.*, 2012; Zhu and Stülke, 2018a) and in *Shewanella oneidensis*, transcription and translation of the *oscA* homolog was upregulated by chromate induced oxidative stress (Brown *et al.*, 2006). Therefore, it was expected that

diamide might also induce *yezD* expression in *B. amyloliquefaciens.* However, only in the absence of riboflavin a slight increase in RibE activity was measured for cells grown with methionine and taurine, but the effect was not visible for $MgSO_4$ as the sole sulfur source. For cultures grown with riboflavin no increase in riboflavin synthesis activity was observed for any of the sulfur sources. These results do not provide a consistent picture of the effect of diamide on *ribR* expression and FMN riboswitch activity, and until it is not clear whether *ribR* expression is actually induced by diamide, no deductions can be made about the influence of $RibR_{amy}$ on the FMN riboswitch in *B. amyloliquefaciens* itself.

Unfortunately, the results of a performed RT-PCR for detection of $ribR_{amy}$ transcripts did not clarify the results with regard to diamide-altered transcription levels of *ribR* affecting RibE activity. Moreover, the RT-PCR for the housekeeping gene *citZ* was not successful, even though the control PCR with gDNA produced a visible band for this gene. While diamide induced *ribR* transcription in the early exponential phase of cells grown with methionine/taurine but not with $MgSO_4$, *ribR* transcription in the later exponential phase was independent of diamide addition. The presence of an equivalent amount of *ribR* transcript in the later exponential phase may explain, why no differences in FMN riboswitch activity in *B. amyloliquefaciens* were detected with the riboflavin synthase assay. However, since only the transcriptional level of *ribR* expression was examined, no conclusions can be drawn about the presence of the actual $RibR_{amy}$ protein.

Taken together, the results suggest that diamide can induce *yezD* expression in *B. amyloliquefaciens*, as also postulated for *B. subtilis* (Rochat *et al.*, 2012), and thus the expression of the putatively co-transcribed gene *ribR.* The fact that differences in *ribR* transcription upon diamide induction depend on the respective sulfur source provided suggests a further link between oxidative stress, riboflavin production and sulfur metabolism.

7.2 Outlook – The FMN riboswitch-binding protein RibR in *Bacillus amyloliquefaciens*

The RibR-like protein from *B. amyloliquefaciens* was shown to be a riboswitch binding protein that also appears to affect FMN riboswitch activity. Since the $RibR_{amy}$ protein did not exhibit a strong effect on *ribD* riboswitch activity, compared to the regulation seen for RibR from *B. subtilis*, a confirmation of its effect on FMN riboswitches will need to be supported by further experiments. For that reason, *in vivo* reporter gene assay could be used, as done for the RibR protein from *B. subtilis* (Pedrolli, Kühm, *et al.*, 2015). Alternatively, *in vitro* transcription assays can be employed to validate the influence of RibR on FMN riboswitch activity.

In the present study, $RibR_{amy}$ function was only tested in a *B. subtilis* host. To gain more information about the behavior and RibR-regulated mechanisms in the natural host, genome

editing of *B. amyloliquefaciens* should be employed. A CRISPR/Cas9 based method developed for *B. amyloliquefaciens* could be used for this purpose (Xin *et al.*, 2022).

To further explore the connection between riboflavin metabolism, sulfur metabolism and oxidative stress responses, *B. amyloliquefaciens* cultures grown in presence of the oxidative stressor diamide should be examined for riboflavin synthase activity with simultaneous RT-PCR detection of *ribR* transcripts at different time points. Additional focus should be put on the gene *yezD* and the function of the corresponding gene product in oxidative stress responses and how this is connected to sulfur metabolism and riboflavin production. A first step to that would be the characterization of Δ*yezD* mutants of *B. subtilis* and *B. amyloliquefaciens*.

8 References

Abushaheen, M.A., Muzaheed, Fatani, A.J., Alosaimi, M., Mansy, W., George, M., *et al.* (2020) Antimicrobial resistance, mechanisms and its clinical significance. *Disease-a-Month* **66**: 1000971.

Adams, P.P., Avile, C.F., and Jewett, M.W. (2017) A dual luciferase reporter system for *B. burgdorferi* measures transcriptional activity during tick-pathogen interactions. *Front Cell Infect Microbiol* **7**: 1–13.

Aghdam, E.M., Hejazi, M.S., and Barzegar, A. (2016) Riboswitches: From living biosensors to novel targets of antibiotics. *Gene* **591**: 244–259.

Aghdam, E.M., Sinn, M., Tarhriz, V., Barzegar, A., Hartig, J.S., and Hejazi, M.S. (2017) TPP riboswitch characterization in *Alishewanella tabrizica* and *Alishewanella aestuarii* and comparison with other TPP riboswitches. *Microbiol Res* **195**: 71–80.

Aljeldah, M.M. (2022) Antimicrobial Resistance and Its Spread Is a Global Threat. *Antibiotics* **11**: 1–14.

Altenbuchner, J. (2016) Editing of the *Bacillus subtilis* genome by the CRISPR-Cas9 system. *Appl Environ Microbiol* **82**: 5421–5427.

Altschul, S.F., Gish, W., Miller, W., Myers, E.W., and Lipman, D.J. (1990) Basic Local Alignment Search Tool. *J Mol Biol* **215**: 403–410.

Anthony, P.C., Perez, C.F., García-García, C., and Block, S.M. (2012) Folding energy landscape of the thiamine pyrophosphate riboswitch aptamer. *PNAS* **109**: 1485–1489.

Antunes, D., Jorge, N.A.N., Garcia de Souza Costa, M., Passetti, F., and Caffarena, E.R. (2019) Unraveling RNA dynamical behavior of TPP riboswitches: a comparison between *Escherichia coli* and *Arabidopsis thaliana*. *Sci Rep* **9**: 1–13.

Averianova, L.A., Balabanova, L.A., Son, O.M., Podvolotskaya, A.B., and Tekutyeva, L.A. (2020) Production of Vitamin B_2(Riboflavin) by Microorganisms: An Overview. *Front Bioeng Biotechnol* **8**: 1–23.

Babitzke, P. (1997) Regulation of tryptophan biosynthesis: Trp-ing the TRAP or how *Bacillus subtilis* reinvented the wheel. *Mol Microbiol* **26**: 1–9.

Bacher, A., Eberhardt, S., Fischer, M., Kis, K., and Richter, G. (2000) Biosynthesis of Vitamin B_2 (Riboflavin). *Annu Rev Nutr* **20**: 153–167.

Bae, S., Park, J., and Kim, J.S. (2014) Cas-OFFinder: A fast and versatile algorithm that searches for potential off-target sites of Cas9 RNA-guided endonucleases. *Bioinformatics* **30**: 1473–1475.

Bains, J.K., Qureshi, N.S., Ceylan, B., Wacker, A., and Schwalbe, H. (2023) Cell-free transcription-translation system: a dual read-out assay to characterize riboswitch function. *Nucleic Acids Res* **51**: E82–E82.

Baird, N.J. and Ferré-D'Amaré, A.R. (2013) Modulation of quaternary structure and enhancement of ligand binding by the K-turn of tandem glycine riboswitches. *RNA* **19**: 167–176.

Baird, N.J., Zhang, J., Hamma, T., and Ferré-D'Amaré, A.R. (2012) YbxF and YlxQ are bacterial homologs of L7Ae and bind K-turns but not K-loops. *RNA* **18**: 759–770.

Barik, A., Nithin, C., Pilla, S.P., and Bahadur, R.P. (2015) Molecular architecture of protein-RNA recognition sites. *J Biomol Struct Dyn* **33**: 2738–2751.

Barrick, J.E. and Breaker, R.R. (2007) The distributions, mechanisms, and structures of metabolite-binding riboswitches. *Genome Biol* **8**: R239.1-R239.19.

Bastet, L., Chauvier, A., Singh, N., Lussier, A., Lamontagne, A.M., Prévost, K., *et al.* (2017) Translational control and Rho-dependent transcription termination are intimately linked in riboswitch regulation. *Nucleic Acids Res* **45**: 7474–7486.

Batey, R.T. (2011) Recognition of S-adenosylmethionine by riboswitches. *Wiley Interdiscip Rev RNA* **2**: 299–311.

Bayer, T.S., Booth, L.N., Knudsen, S.M., and Ellington, A.D. (2005) Arginine-rich motifs present multiple interfaces for specific binding by RNA. *RNA* **11**: 1848–1857.

Bédard, A.S.V., Hien, E.D.M., and Lafontaine, D.A. (2020) Riboswitch regulation mechanisms: RNA, metabolites and regulatory proteins. *Biochim Biophys Acta Gene Regul Mech* **1863**: 1–9.

Begley, T.P., Downs, D.M., Ealick, S.E., McLafferty, F.W., Van Loon, A.P.G.M., Taylor, S., *et al.* (1999) Thiamin biosynthesis in prokaryotes. *Arch Microbiol* **171**: 293–300.

Belashov, I.A., Crawford, D.W., Cavender, C.E., Dai, P., Beardslee, P.C., Mathews, D.H., *et al.* (2018) Structure of HIV TAR in complex with a Lab-Evolved RRM provides insight into duplex RNA recognition and synthesis of a constrained peptide that impairs transcription. *Nucleic Acids Res* **46**: 6401–6415.

Blouin, S. and Lafontaine, D.A. (2007) A loop-loop interaction and a K-turn motif located in the lysine aptamer domain are important for the riboswitch gene regulation control. *RNA* **13**: 1256–1267.

Blount, K., Puskarz, I., Penchovsky, R., and Breaker, R. (2006) Development and application of a high-throughput assay for *glmS* riboswitch activators. *RNA Biol* **3**: 77–81.

Blount, K.F. and Breaker, R.R. (2006) Riboswitches as antibacterial drug targets. *Nat Biotechnol* **24**: 1558–1564.

Bonner, E.R., D'Elia, J.N., Billips, B.K., and Switzer, R.L. (2001) Molecular recognition of *pyr* mRNA by the *Bacillus subtilis* attenuation regulatory protein PyrR. *Nucleic Acids Res* **29**: 4851–4865.

Bradford, M.M. (1976) A rapid and sensitive method for the quantitation of microgram quantities of protein utilizing the principle of protein-dye binding. *Anal Biochem* **72**: 248–254.

Breaker, R.R. (2011) Prospects for Riboswitch Discovery and Analysis. *Mol Cell* **43**: 867–879.

Brown, S.D., Thompson, M.R., VerBerkmoes, N.C., Chourey, K., Shah, M., Zhou, J., *et al.* (2006) Molecular dynamics of the *Shewanella oneidensis* response to chromate stress. *Molecular and Cellular Proteomics* **5**: 1054–1071.

Bu, F., Lin, X., Liao, W., Lu, Z., He, Y., Luo, Y., *et al.* (2023) Ribocentre-switch: a database of riboswitches. *Nucleic Acids Res*.

Bunik, V.I., Tylicki, A., and Lukashev, N. V. (2013) Thiamin diphosphate-dependent enzymes: From enzymology to metabolic regulation, drug design and disease models. *FEBS Journal* **280**: 6412–6442.

Burge, S.W., Daub, J., Eberhardt, R., Tate, J., Barquist, L., Nawrocki, E.P., *et al.* (2013) Rfam 11.0: 10 years of RNA families. *Nucleic Acids Res* **41**: D226–D232.

Burguière, P., Fert, J., Guillouard, I., Auger, S., Danchin, A., and Martin-Verstraete, I. (2005a) Regulation of the *Bacillus subtilis ytmI* operon, involved in sulfur metabolism. *J Bacteriol* **187**: 6019–6030.

Burguière, P., Fert, J., Guillouard, I., Auger, S., Danchin, A., and Martin-Verstraete, I. (2005b) Regulation of the Bacillus subtilis ytmI operon, involved in sulfur metabolism. *J Bacteriol* **187**: 6019–6030.

Camps, M. (2010) Modulation of ColE1-like Plasmid Replication for Recombinant Gene Expression. *Recent Pat DNA Gene Seq* **4**: 54–73.

Chan, C.M., Danchin, A., Marlière, P., and Sekowska, A. (2014) Paralogous metabolism: S-alkyl-cysteine degradation in *Bacillus subtilis*. *Environ Microbiol* **16**: 101–117.

Chang, Y., Bruni, R., Kloss, B., Assur, Z., Kloppmann, E., Rost, B., *et al.* (2014) Structural basis for a pH-sensitive calcium leak across membranes. *Science (1979)* **344**: 1131–1135.

Chauvier, A., Picard-Jean, F., Berger-Dancause, J.C., Bastet, L., Naghdi, M.R., Dubé, A., *et al.* (2017) Transcriptional pausing at the translation start site operates as a critical checkpoint for riboswitch regulation. *Nat Commun* **8**: 1–12.

Chavali, S.S., Cavender, C.E., Mathews, D.H., and Wedekind, J.E. (2020a) Arginine Forks Are a Widespread Motif to Recognize Phosphate Backbones and Guanine Nucleobases in the RNA Major Groove. *J Am Chem Soc* **142**: 19835–19839.

Chavali, S.S., Cavender, C.E., Mathews, D.H., and Wedekind, J.E. (2020b) Arginine Forks Are a Widespread Motif to Recognize Phosphate Backbones and Guanine Nucleobases in the RNA Major Groove. *J Am Chem Soc* **142**: 19835–19839.

Cheah, M.T., Wachter, A., Sudarsan, N., and Breaker, R.R. (2007) Control of alternative RNA splicing and gene expression by eukaryotic riboswitches. *Nature* **447**: 497–500.

Chen, L., Cressina, E., Dixon, N., Erixon, K., Agyei-Owusu, K., Micklefield, J., *et al.* (2012) Probing riboswitch-ligand interactions using thiamine pyrophosphate analogues. *Org Biomol Chem* **10**: 5924–5931.

Choi, S.Y., Reyes, D., Leelakriangsak, M., and Zuber, P. (2006) The global regulator Spx functions in the control of organosulfur metabolism in *Bacillus subtilis*. *J Bacteriol* **188**: 5741–5751.

Coppée, J.Y., Auger, S., Turlin, E., Sekowska, A., Le Caer, J.P., Labas, V., *et al.* (2001) Sulfur-limitation-regulated proteins in *Bacillus subtilis*: A two-dimensional gel electrophoresis study. *Microbiology (N Y)* **147**: 1631–1640.

Cressina, E., Chen, L., Abell, C., Leeper, F.J., and Smith, A.G. (2011) Fragment screening against the thiamine pyrophosphate riboswitch *thiM*. *Chem Sci* **2**: 157–165.

Croft, M.T., Moulin, M., Webb, M.E., and Smith, A.G. (2007) Thiamine biosynthesis in algae is regulated by riboswitches. *PNAS* **104**: 20770–20775.

DebRoy, S., Gebbie, M., Ramesh, A., Goodson, J.R., Cruz, M.R., Van Hoof, A., *et al.* (2014) A riboswitch-containing sRNA controls gene expression by sequestration of a response regulator. *Science (1979)* **345**: 937–940.

Deigan Warner, K., Homan, P., Weeks, K.M., Smith, A.G., Abell, C., and Ferré-D'Amaré, A.R. (2014) Validating fragment-based drug discovery for biological RNAs: Lead fragments bind and remodel the TPP riboswitch specifically. *Chem Biol* **21**: 591–595.

DeLano, W.L. (2002) PyMOL: An Open-Source Molecular Graphics Tool. *Newsletter on Protein Crystallography* **40**: 82–92.

Doench, J.G., Fusi, N., Sullender, M., Hegde, M., Vaimberg, E.W., Donovan, K.F., *et al.* (2016) Optimized sgRNA design to maximize activity and minimize off-target effects of CRISPR-Cas9. *Nat Biotechnol* **34**: 184–191.

Durand, G.A., Raoult, D., and Dubourg, G. (2019) Antibiotic discovery: history, methods and perspectives. *Int J Antimicrob Agents* **53**: 371–382.

Edwards, T.E. and Ferré-D'Amaré, A.R. (2006) Crystal Structures of the Thi-Box Riboswitch Bound to Thiamine Pyrophosphate Analogs Reveal Adaptive RNA-Small Molecule Recognition. *Structure* **14**: 1459–1468.

Ellinger, E., Chauvier, A., Romero, R.A., Liu, Y., Ray, S., and Walter, N.G. (2023) Riboswitches as therapeutic targets: Promise of a new era of antibiotics. *Expert Opin Ther Targets*.

Even, S., Burguière, P., Auger, S., Soutourina, O., Danchin, A., and Martin-Verstraete, I. (2006) Global control of cysteine metabolism by CymR in *Bacillus subtilis*. *J Bacteriol* **188**: 2184–2197.

Gagnon, K.T., Zhang, X., Qu, G., Biswas, S., Suryadi, J., Brown, B.A., and Maxwell, E.S. (2010) Signature amino acids enable the archaeal L7Ae box C/D RNP core protein to recognize and bind the K-loop RNA motif. *RNA* **16**: 79–90.

Garst, A.D., Edwards, A.L., and Batey, R.T. (2011) Riboswitches: Structures and mechanisms. *Cold Spring Harb Perspect Biol* **3**: 1–13.

Gelfand, M.S., Mironov, A.A., Jomantas, J., Kozlov, Y.I., and Perumov, D.A. (1999) A conserved RNA structure element involved in the regulation of bacterial riboflavin synthesis genes. *Trends in Genetics* **15**: 439–442.

Giarimoglou, N., Kouvela, A., Maniatis, A., Papakyriakou, A., Zhang, J., Stamatopoulou, V., and Stathopoulos, C. (2022) A Riboswitch-Driven Era of New Antibacterials. *Antibiotics* **11**: 1–27.

González-Zorn, B. and Escudero, J.A. (2012) Ecology of antimicrobial resistance: Humans, animals, food and environment. *International Microbiology* **15**: 101–109.

Hanahan, D. (1983) Studies on Transformation of Escherichia coli with Plasmids. *J Mol Biol* **166**: 557–580.

Harinarayanan, R. and Gowrishankar, J. (2003) Host factor titration by chromosomal R-loops as a mechanism for runaway plasmid replication in transcription termination-defective mutants of *Escherichia coli*. *J Mol Biol* **332**: 31–46.

Harirchi, S., Sar, T., Ramezani, M., Aliyu, H., Etemadifar, Z., Nojoumi, S.A., *et al.* (2022) *Bacillales*: From Taxonomy to Biotechnological and Industrial Perspectives. *Microorganisms* **10**: 1–46.

Hazra, S., Bhandari, D.M., Krishnamoorthy, K., Sekowska, A., Danchin, A., and Begley, T.P. (2022) Cysteine Dealkylation in *Bacillus subtilis* by a Novel Flavin-Dependent Monooxygenase. *Biochemistry* **61**: 952–955.

Heppell, B. and Lafontaine, D.A. (2008) Folding of the SAM aptamer is determined by the formation of a K-turn-dependent pseudoknot. *Biochemistry* **47**: 1490–1499.

Hickey, S.F. and Hammond, M.C. (2014) Structure-guided design of fluorescent S-adenosylmethionine analogs for a high-throughput screen to target SAM-I riboswitch RNAs. *Chem Biol* **21**: 345–356.

Higashitsuji, Y., Angerer, A., Berghaus, S., Hobl, B., and Mack, M. (2007) RibR, a possible regulator of the *Bacillus subtilis* riboflavin biosynthetic operon, *in vivo* interacts with the 5′-untranslated leader of *rib* mRNA. *FEMS Microbiol Lett* **274**: 48–54.

Hobl, B. and Mack, M. (2007) The regulator protein PyrR of *Bacillus subtilis* specifically interacts *in vivo* with three untranslated regions within *pyr* mRNA of pyrimidine biosynthesis. *Microbiology (N Y)* **153**: 693–700.

Hollands, K., Proshkin, S., Sklyarova, S., Epshtein, V., Mironov, A., Nudler, E., and Groisman, E.A. (2012) Riboswitch control of Rho-dependent transcription termination. *Proc Natl Acad Sci U S A* **109**: 5376–5381.

Howe, J.A., Wang, H., Fischmann, T.O., Balibar, C.J., Xiao, L., Galgoci, A.M., *et al.* (2015) Selective small-molecule inhibition of an RNA structural element. *Nature* **526**: 672–677.

Howe, J.A., Xiao, L., Fischmann, T.O., Wang, H., Tang, H., Villafania, A., *et al.* (2016) Atomic resolution mechanistic studies of ribocil: A highly selective unnatural ligand mimic of the *E. coli* FMN riboswitch. *RNA Biol* **13**: 946–954.

Huang, L. and Lilley, D.M.J. (2013) The molecular recognition of kink-turn structure by the L7Ae class of proteins. *RNA* **19**: 1703–1710.

Irla, M., Hakvåg, S., and Brautaset, T. (2021) Developing a riboswitch-mediated regulatory system for metabolic flux control in thermophilic *Bacillus methanolicus*. *Int J Mol Sci* **22**: 1–18.

Jain, V.K. and Magrath, I.T. (1991) A Chemiluminescent Assay for Quantitation of β-Galactosidase in the Femtogram Range: Application to Quantitation of β-Galactosidase in *lacZ*-Transfected Cells. *Anal Biochem* **199**: 119–124.

de Jesus, V., Qureshi, N.S., Warhaut, S., Bains, J.K., Dietz, M.S., Heilemann, M., *et al.* (2021) Switching at the ribosome: riboswitches need rProteins as modulators to regulate translation. *Nat Commun* **12**: 1–7.

Joosten, V. and van Berkel, W.J. (2007) Flavoenzymes. *Curr Opin Chem Biol* **11**: 195–202.

Jurgenson, C.T., Begley, T.P., and Ealick, S.E. (2009) The structural and biochemical foundations of thiamin biosynthesis. *Annu Rev Biochem* **78**: 569–603.

Kaempfer, R. (2003) RNA sensors: Novel regulators of gene expression. *EMBO Rep* **4**: 1043–1047.

Kavita, K. and Breaker, R.R. (2023) Discovering riboswitches: the past and the future. *Trends Biochem Sci* **48**: 119–141.

Kawasaki, T. (1969) Thiamine Uptake in *Escherichia coli* I. General Properties of Thiamine Uptake System in *Escherichia coli*. *Arch Biochem Biophys* **131**: 223–230.

Kawasaki, T. and Nose, Y. (1969) Thiamine Regulatory Mutants in *Escherichia coli**. *The Journal of Biochemistry* **65**: 417–425.

Kil, Y. V, Mironov, V.N., Yu Gorishin, I., Kreneva, R.A., and Perumov, D.A. (1992) Riboflavin operon of *Bacillus subtilis*: unusual symmetric arrangement of the regulatory region. *Molecular Genetics and Genomics* **233**: 483–486.

Kosower, N.S. and Kosower, E.M. (1995) Diamide: An oxidant probe for thiols. In *Methods in Enzymology*. Academic Press, pp. 123–133.

Krüger, D.M., Neubacher, S., and Grossmann, T.N. (2018) Protein-RNA interactions: structural characteristics and hotspot amino acids. *RNA* **24**: 1457–2465.

Kubodera, T., Watanabe, M., Yoshiuchi, K., Yamashita, N., Nishimura, A., Nakai, S., *et al.* (2003) Thiamine-regulated gene expression of *Aspergillus oryzae thiA* requires splicing of the intron containing a riboswitch-like domain in the 5′-UTR. *FEBS Lett* **555**: 516–520.

Kulshina, N., Edwards, T.E., and Ferré-D'Amaré, A.R. (2010) Thermodynamic analysis of ligand binding and ligand binding-induced tertiary structure formation by the thiamine pyrophosphate riboswitch. *RNA* **16**: 186–196.

Lang, K., Rieder, R., and Micura, R. (2007) Ligand-induced folding of the thiM TPP riboswitch investigated by a structure-based fluorescence spectroscopic approach. *Nucleic Acids Res* **35**: 5370–5378.

Larson, M.H., Mooney, R.A., Peters, J.M., Windgassen, T., Nayak, D., Gross, C.A., *et al.* (2014) A pause sequence enriched at translation start sites drives transcription dynamics in vivo. *Science (1979)* **344**: 1042–1047.

Lee, E.R., Baker, J.L., Zasha Weinberg, Sudarsan, N., and Breaker, R.R. (2010) An Allosteric Self-Splicing Ribozyme Triggered by a Bacterial Second Messenger. *Science (1979)* **329**: 845–848.

Lee Ventola, C. (2015) The Antibiotic Resistance Crisis Part 1: Causes and Threats.

Lemay, J.F., Desnoyers, G., Blouin, S., Heppell, B., Bastet, L., St-Pierre, P., *et al.* (2011) Comparative Study between Transcriptionally- and Translationally-Acting Adenine Riboswitches Reveals Key Differences in Riboswitch Regulatory Mechanisms. *PLoS Genet* **7**: 1001278.

Lenz, D.H., Mok, K.C., Lilley, B.N., Kulkarni, R. V, Wingreen, N.S., and Bassler, B.L. (2004) The Small RNA Chaperone Hfq and Multiple Small RNAs Control Quorum Sensing in *Vibrio harveyi* and *Vibrio cholerae*. *Cell* **118**: 69–82.

Leonardi, R. and Roach, P.L. (2004) Thiamine biosynthesis in *Escherichia coli*: *In vitro* reconstitution of the thiazole synthase activity. *Journal of Biological Chemistry* **279**: 17054–17062.

Li, Y., Lin, Z., Huang, C., Zhang, Y., Wang, Z., Tang, Y. jie, *et al.* (2015) Metabolic engineering of *Escherichia coli* using CRISPR-Cas9 meditated genome editing. *Metab Eng* **31**: 13–21.

Lilley, D.M.J. (2014) The K-turn motif in riboswitches and other RNA species. *Biochim Biophys Acta Gene Regul Mech* **1839**: 995–1004.

Llavero-Pasquina, M., Geisler, K., Holzer, A., Mehrshahi, P., Mendoza-Ochoa, G.I., Newsad, S.A., *et al.* (2022) Thiamine metabolism genes in diatoms are not regulated by thiamine despite the presence of predicted riboswitches. *New Phytologist* **235**: 1853–1867.

Lünse, C.E., Scott, F.J., Suckling, C.J., and Mayer, G. (2014) Novel TPP-riboswitch activators bypass metabolic enzyme dependency. *Front Chem* **2**: 1–8.

Lussier, A., Bastet, L., Chauvier, A., and Lafontaine, D.A. (2015) A kissing loop is important for btuB riboswitch ligand sensing and regulatory control. *Journal of Biological Chemistry* **290**: 26739–26751.

Macheroux, P., Kappes, B., and Ealick, S.E. (2011) Flavogenomics - A genomic and structural view of flavin-dependent proteins. *FEBS Journal* **278**: 2625–2634.

Mack, M., Van Loon, A.P.G.M., and Hohmann, H.-P. (1998) Regulation of Riboflavin Biosynthesis in *Bacillus subtilis* Is Affected by the Activity of the Flavokinase/Flavin Adenine Dinucleotide Synthetase Encoded by *ribC*. *J Bacteriol* **180**: 950–955.

Madeira, F., Pearce, M., Tivey, A.R.N., Basutkar, P., Lee, J., Edbali, O., *et al.* (2022) Search and sequence analysis tools services from EMBL-EBI in 2022. *Nucleic Acids Res* **50**: W276–W279.

Mandal, M., Boese, B., Barrick, J.E., Winkler, W.C., and Breaker, R.R. (2003) Riboswitches control fundamental biochemical pathways in *Bacillus subtilis* and other bacteria. *Cell* **113**: 577–586.

Mandal, M. and Breaker, R.R. (2004) Adenine riboswitches and gene activation by disruption of a transcription terminator. *Nat Struct Mol Biol* **11**: 29–35.

Mandal, M., Lee, M., Barrick, J.E., Weinberg, Z., Emilsson, G.M., Ruzzo, W.L., and Breaker, R.R. (2004) A glycine-dependent riboswitch that uses cooperative binding to control gene expression. *Science (1979)* **306**: 275–279.

Mansjö, M. and Johansson, J. (2011) The riboflavin analog roseoflavin targets an FMN-riboswitch and blocks *Listeria monocytogenes* growth, but also stimulates virulence gene-expression and infection. *RNA Biol* **8**: 674–680.

Martin, C.S., Wight, P.A., Dobretsova, A., and Bronstein, I. (1996) Dual Luminescence-Based Reporter Gene Assay for Luciferase and β-Galactosidase. *Biotechniques* **21**: 520–524.

Matzner, D. and Mayer, G. (2015) (Dis)similar analogues of riboswitch metabolites as antibacterial lead compounds. *J Med Chem* **58**: 3275–3286.

McCown, P.J., Corbino, K.A., Stav, S., Sherlock, M.E., and Breaker, R.R. (2017) Riboswitch diversity and distribution.

McCulloch, K.M., Kinsland, C., Begley, T.P., and Ealick, S.E. (2008) Structural studies of thiamin monophosphate kinase in complex with substrates and products. *Biochemistry* **47**: 3810–3821.

McDaniel, B.A., Grundy, F.J., and Henkin, T.M. (2005) A tertiary structural element in S box leader RNAs is required for S-adenosylmethionine-directed transcription termination. *Mol Microbiol* **57**: 1008–1021.

Mellin, J.R., Koutero, M., Dar, D., Nahori, M.-A., Sorek, R., and Riboswitches, al (2014) Riboswitches. Sequestration of a two-component response regulator by a riboswitch-regulated noncoding RNA. *Science (1979)* **345**: 940–943.

Miranda-Ríos, J. (2007) The THI-box Riboswitch, or How RNA Binds Thiamin Pyrophosphate. *Structure* **15**: 259–265.

Miranda-Ríos, J., Morera, C., Taboada, H., Dávalos, A., Encarnación, S., Mora, J., and Soberón, M. (1997) Expression of Thiamin Biosynthetic Genes (*thiCOGE*) and Production of Symbiotic Terminal Oxidase cbb_3 in *Rhizobium etli*. *J Bacteriol* **179**: 6887–6893.

Miranda-Ríos, J., Navarro, M., and Soberón, M. (2001) A conserved RNA structure (*thi* box) is involved in regulation of thiamin biosynthetic gene expression in bacteria. *Proc Natl Acad Sci U S A* **98**: 9736–9741.

Mironov, A.S., Gusarov, I., Rafikov, R., Lopez, L.E., Shatalin, K., Kreneva, R.A., *et al.* (2002) Sensing Small Molecules by Nascent RNA: A Mechanism to Control Transcription in Bacteria. *Cell* **111**: 747–756.

Motika, S.E., Ulrich, R.J., Geddes, E.J., Lee, H.Y., Lau, G.W., and Hergenrother, P.J. (2020) Gram-Negative Antibiotic Active through Inhibition of an Essential Riboswitch. *J Am Chem Soc* **142**: 10856–10862.

Murray, C.J., Ikuta, K.S., Sharara, F., Swetschinski, L., Robles Aguilar, G., Gray, A., *et al.* (2022) Global burden of bacterial antimicrobial resistance in 2019: a systematic analysis. *The Lancet* **399**: 629–655.

Nahvi, A., Sudarsan, N., Ebert, M.S., Zou, X., Brown, K.L., and Breaker, R.R. (2002) Genetic Control by a Metabolite Binding mRNA.

Nelson, J.W., Atilho, R.M., Sherlock, M.E., Stockbridge, R.B., and Breaker, R.R. (2017) Metabolism of Free Guanidine in Bacteria Is Regulated by a Widespread Riboswitch Class. *Mol Cell* **65**: 220–230.

Ontiveros-Palacios, N., Smith, A.M., Grundy, F.J., Soberon, M., Henkin, T.M., and Miranda-Ríos, J. (2008) Molecular basis of gene regulation by the THI-box riboswitch. *Mol Microbiol* **67**: 793–803.

Ott, E., Stolz, J., Lehmann, M., and Mack, M. (2009) The RFN riboswitch of *Bacillus subtilis* is a target for the antibiotic roseoflavin produced by *Streptomyces davawensis*. *RNA Biol* **6**: 67–71.

Panchal, V. and Brenk, R. (2021) Riboswitches as Drug Targets for Antibiotics. *Antibiotics* **10**: 45.

Pavlova, N., Kaloudas, D., and Penchovsky, R. (2019) Riboswitch distribution, structure, and function in bacteria. *Gene* **708**: 38–48.

Pavlova, N. and Penchovsky, R. (2022) Bioinformatics and Genomic Analyses of the Suitability of Eight Riboswitches for Antibacterial Drug Targets. *Antibiotics* **11**: 1–25.

Pavlova, N. and Penchovsky, R. (2019) Genome-wide bioinformatics analysis of FMN, SAM-I, glmS, TPP, lysine, purine, cobalamin, and SAH riboswitches for their applications as allosteric antibacterial drug targets in human pathogenic bacteria. *Expert Opin Ther Targets* **23**: 631–643.

Pavlova, N., Traykovska, M., and Penchovsky, R. (2023) Targeting FMN, TPP, SAM-I, and glmS Riboswitches with Chimeric Antisense Oligonucleotides for Completely Rational Antibacterial Drug Development. *Antibiotics* **12**: 1607.

Pedrolli, D.B., Kühm, C., Sévin, D.C., Vockenhuber, M.P., Sauer, U., Suess, B., and Mack, M. (2015) A dual control mechanism synchronizes riboflavin and sulphur metabolism in *Bacillus subtilis*. *PNAS* **112**: 14054–14059.

Pedrolli, D.B., Langer, S., Hobl, B., Schwarz, J., Hashimoto, M., and Mack, M. (2015) The *ribB* FMN riboswitch from *Escherichia coli* operates at the transcriptional and translational level and regulates riboflavin biosynthesis. *FEBS Journal* **282**: 3230–3242.

Penchovsky, R. and Stoilova, C.C. (2013) Riboswitch-based antibacterial drug discovery using high-throughput screening methods. *Expert Opin Drug Discov* **8**: 65–82.

Perkins, J.B. and Pero, J. (2001) Vitamin Biosynthesis. In *Bacillus subtilis and Its Closest Relatives: From Genes to Cells*. Sonenshein, A.L., Hoch, J.A., and Losick, R. (eds). Washington D.C.: ASM Press, pp. 271–286.

Petchiappan, A. and Chatterji, D. (2017) Antibiotic resistance: Current perspectives. *ACS Omega* **2**: 7400–7409.

Pöther, D.C., Liebeke, M., Hochgräfe, F., Antelmann, H., Becher, D., Lalk, M., *et al.* (2009) Diamide triggers mainly S thiolations in the cytoplasmic proteomes of *Bacillus subtilis* and *Staphylococcus aureus*. *J Bacteriol* **191**: 7520–7530.

Potter, K.D., Merlino, N.M., Jacobs, T., and Gollnick, P. (2011) TRAP binding to the *Bacillus subtilis trp* leader region RNA causes efficient transcription termination at a weak intrinsic terminator. *Nucleic Acids Res* **39**: 2092–2102.

Rabe von Pappenheim, F., Aldeghi, M., Shome, B., Begley, T., de Groot, B.L., and Tittmann, K. (2020) Structural basis for antibiotic action of the B1 antivitamin 2′-methoxy-thiamine. *Nat Chem Biol* **16**: 1237–1245.

Rapala-Kozik, M. (2011) Vitamin B1 (Thiamine): A Cofactor for Enzymes Involved in the Main Metabolic Pathways and an Environmental Stress Protectant. *Adv Bot Res* **58**: 37–91.

Reddick, J.J., Saha, S., Lee, J. ming, Melnick, J.S., Perkins, J., and Begley, T.P. (2001) The mechanism of action of bacimethrin, a naturally occurring thiamin antimetabolite. *Bioorg Med Chem Lett* **11**: 2245–2248.

Ren, A., Rajashankar, K.R., and Patel, D.J. (2012) Fluoride ion encapsulation by Mg2+ ions and phosphates in a fluoride riboswitch. *Nature* **486**: 85–89.

Rice, L.B. (2008) Federal funding for the study of antimicrobial resistance in nosocomial pathogens: No ESKAPE. *Journal of Infectious Diseases* **197**: 1079–1081.

Richardson, J.P. (2003) Minireview Loading Rho to Terminate Transcription.

Righetti, F., Materne, S.L., Boss, J., Eichner, H., Charpentier, E., and Loh, E. (2020) Characterization of a transcriptional TPP riboswitch in the human pathogen Neisseria meningitidis. *RNA Biol* **17**: 718–730.

Robbins, W.J. (1941) The Pyridine Analog of Thiamin and the Growth of Fungi. *Proceedings of the National Academy of Sciences* **27**: 419–422.

Rochat, T., Nicolas, P., Delumeau, O., Rabatinová, A., Korelusová, J., Leduc, A., *et al.* (2012) Genome-wide identification of genes directly regulated by the pleiotropic transcription factor Spx in *Bacillus subtilis*. *Nucleic Acids Res* **40**: 9571–9583.

Romeo, T. (1998) Global regulation by the small RNA-binding protein CsrA and the non-coding RNA molecule CsrB. *Mol Microbiol* **29**: 1321–1330.

Rooney, A.P., Price, N.P.J., Ehrhardt, C., Sewzey, J.L., and Bannan, J.D. (2009) Phylogeny and molecular taxonomy of the Bacillus subtilis species complex and description of *Bacillus subtilis* subsp. *inaquosorum* subsp. nov. *Int J Syst Evol Microbiol* **59**: 2429–2436.

Salvail, H. and Breaker, R.R. (2023) Riboswitches. *Current Biology* **33**: 343–348.

Sanger, F., Nicklen, S., and Coulson, A.R. (1977) DNA sequencing with chain-terminating inhibitors (DNA polymerase/nucleotide sequences/bacteriophage 4X174). *PNAS* **74**: 5463–5467.

Schmid, C., Reifferscheid, G., Zahn, R.K., and Bachmann, M. (1997) Increase of sensitivity and validity of the SOSrumu-test after replacement of the β-galactosidase reporter gene with luciferase. *Mutat Res* **394**: 9–16.

Schneider, B., Sweeney, B.A., Bateman, A., Cerny, J., Zok, T., and Szachniuk, M. (2023) When will RNA get its AlphaFold moment? *Nucleic Acids Res* **51**: 9522–9532.

Serganov, A., Huang, L., and Patel, D.J. (2009) Coenzyme recognition and gene regulation by a flavin mononucleotide riboswitch. *Nature* **458**: 233–237.

Serganov, A. and Nudler, E. (2013) A decade of riboswitches. *Cell* **152**: 17–24.

Serganov, A. and Patel, D.J. (2012) Metabolite recognition principles and molecular mechanisms underlying riboswitch function. *Annu Rev Biophys* **41**: 343–370.

Serganov, A., Polonskaia, A., Phan, A.T., Breaker, R.R., and Patel, D.J. (2006) Structural basis for gene regulation by a thiamine pyrophosphate-sensing riboswitch. *Nature Letters* **441**: 1167–1171.

Sherf, B.A., Navarro, S.L., Hannah, R.R., and Wood, K. V (1996) Dual-Luciferase TM Reporter Assay: An Advanced Co-Reporter Technology Integrating Firefly and *Renilla* Luciferase Assays. *Promega Notes Magazine Number* **57**: 2.

Sklyarova, S.A. and Mironov, A.S. (2014) *Bacillus subtilis ypaA* gene regulation mechanism by FMN riboswitch. *Russ J Genet* **50**: 319–322.

Solovieva, I.M., Kreneva, R.A., Errais Lopes, L., and Perumov, D.A. (2005) The riboflavin kinase encoding gene *ribR* of *Bacillus subtilis* is a part of a 10 kb operon, which is negatively regulated by the *yrzC* gene product. *FEMS Microbiol Lett* **243**: 51–58.

Solovieva, I.M., Kreneva, R.A., Leak, D.J., and Perumov', D.A. (1999) The *ribR* gene encodes a monofunctional riboflavin kinase which is involved in regulation of the *Bacillus subtilis* riboflavin operon. *Microbiology (N Y)* **145**: 67–73.

Song, Y., Lee, B.R., Cho, S., Cho, Y.B., Kim, S.W., Kang, T.J., *et al.* (2015) Determination of single nucleotide variants in *Escherichia coli* DH5α by using short-read sequencing. *FEMS Microbiol Lett* **362**: 1–7.

Speed, M.C., Burkhart, B.W., Picking, J.W., and Santangelo, T.J. (2018) An archaeal fluorideresponsive riboswitch provides an inducible expression system for hyperthermophiles. *Appl Environ Microbiol* **84**: e02306-17.

Spinelli, S. V., Pontel, L.B., García Véscovi, E., and Soncini, F.C. (2008) Regulation of magnesium homeostasis in *Salmonella*: Mg^{2+} targets the *mgtA* transcript for degradation by RNase E. *FEMS Microbiol Lett* **280**: 226–234.

Stülke, J., Martin-Verstraete, I., Zagorec, M., Rose, M., Klier, A., and Rapoport, G. (1997) Induction of the *Bacillus subtilis ptsGHI* operon by glucose is controlled by a novel antiterminator, GlcT. *Mol Microbiol* **25**: 65–78.

Sudarsan, N., Barrick, J.E., and Breaker, R.R. (2003) Metabolite-binding RNA domains are present in the genes of eukaryotes. *RNA* **9**: 644–647.

Sudarsan, N., Cohen-Chalamish, S., Nakamura, S., Emilsson, G.M., and Breaker, R.R. (2005) Thiamine pyrophosphate riboswitches are targets for the antimicrobial compound pyrithiamine. *Chem Biol* **12**: 1325–1335.

Tamura, K., Stecher, G., and Kumar, S. (2021) MEGA11: Molecular Evolutionary Genetics Analysis Version 11. *Mol Biol Evol* **38**: 3022–3027.

Thore, S., Frick, C., and Ban, N. (2008) Structural basis of thiamine pyrophosphate analogues binding to the eukaryotic riboswitch. *J Am Chem Soc* **130**: 8116–8117.

Thore, S., Leibundgut, M., and Ban, N. (2006) Structure of the Eukaryotic Thiamine Pyrophosphate Riboswitch with Its Regulatory Ligand. *Science (1979)* **312**: 1208–1211.

Thorne, N., Inglese, J., and Auld, D.S. (2010) Illuminating Insights into Firefly Luciferase and Other Bioluminescent Reporters Used in Chemical Biology. *Chem Biol* **17**: 646–657.

Tomšič, J., McDaniel, B.A., Grundy, F.J., and Henkin, T.M. (2008) Natural Variability in S-adenosylmethionine (SAM)-Dependent Riboswitches: S-Box Elements in *Bacillus subtilis* Exhibit Differential Sensitivity to SAM In Vivo and In Vitro. *J Bacteriol* **190**: 823–833.

Traykovska, M., Otcheva, L.A., and Penchovsky, R. (2022) Targeting TPP Riboswitches Using Chimeric Antisense Oligonucleotide Technology for Antibacterial Drug Development. *ACS Appl Bio Mater*.

Turner, B., Melcher, S.E., Wilson, T.J., Norman, D.G., and Lilley, D.M.J. (2005) Induced fit of RNA on binding the L7Ae protein to the kink-turn motif. *RNA* **11**: 1192–1200.

Uddin, T.M., Chakraborty, A.J., Khusro, A., Zidan, B.R.M., Mitra, S., Emran, T. Bin, *et al.* (2021) Antibiotic resistance in microbes: History, mechanisms, therapeutic strategies and future prospects. *J Infect Public Health* **14**: 1750–1766.

Viti, C., Decorosi, F., Mini, A., Tatti, E., and Giovannetti, L. (2009) Involvement of the *oscA* gene in the sulphur starvation response and in Cr(VI) resistance in *Pseudomonas corrugata* 28. *Microbiology (N Y)* **155**: 95–105.

Vitreschak, A.G., Rodionov, D.A., Mironov, A.A., and Gelfand, M.S. (2002) Regulation of riboflavin biosynthesis and transport genes in bacteria by transcriptional and translational attenuation. *Nucleic Acids Res* **30**: 3141–3151.

Van Vlack, E.R. and Seeliger, J.C. (2015) Using riboswitches to regulate gene expression and define gene function in mycobacteria. In *Methods in Enzymology*. Academic Press Inc., pp. 251–265.

Vogl, C., Grill, S., Schilling, O., Stülke, J., Mack, M., and Stolz, J. (2007) Characterization of riboflavin (vitamin B_2) transport proteins from *Bacillus subtilis* and *Corynebacterium glutamicum*. *J Bacteriol* **189**: 7367–7375.

Wachter, A., Tunc-Ozdemir, M., Grove, B.C., Green, P.J., Shintani, D.K., and Breaker, R.R. (2007) Riboswitch control of gene expression in plants by splicing and alternative 3′ end processing of mRNAs. *Plant Cell* **19**: 3437–3450.

Wakchaure, P.D. and Ganguly, B. (2023) Exploring the structure, function of thiamine pyrophosphate riboswitch, and designing small molecules for antibacterial activity. *Wiley Interdiscip Rev RNA*.

Wakchaure, P.D. and Ganguly, B. (2021) Molecular level insights into the inhibition of gene expression by thiamine pyrophosphate (TPP) analogs for TPP riboswitch: A well-tempered metadynamics simulations study. *J Mol Graph Model* **104**: 107849.

Wang, H., Mann, P.A., Xiao, L., Gill, C., Galgoci, A.M., Howe, J.A., *et al.* (2017) Dual-Targeting Small-Molecule Inhibitors of the *Staphylococcus aureus* FMN Riboswitch Disrupt Riboflavin Homeostasis in an Infectious Setting. *Cell Chem Biol* **24**: 576-588.e6.

Wickiser, J.K., Winkler, W.C., Breaker, R.R., and Crothers, D.M. (2005) The speed of RNA transcription and metabolite binding kinetics operate an FMN riboswitch. *Mol Cell* **18**: 49–60.

Winkler, W.C. and Breaker, R.R. (2003) Genetic control by metabolite-binding riboswitches. *ChemBioChem* **4**: 1024–1032.

Winkler, W.C., Cohen-Chalamish, S., and Breaker, R.R. (2002) An mRNA structure that controls gene expression by binding FMN. *PNAS* **99**: 15908–15913.

Winkler, W.C., Nahvi, A., and Breaker, R.R. (2002) Thiamine derivatives bind messenger RNAs directly to regulate bacterial gene expression. *Nature* **419**: 952–956.

Winkler, W.C., Nahvi, A., Roth, A., Collins, J.A., and Breaker, R.R. (2004) Control of gene expression by a natural metabolite-responsive ribozyme. *Nature* **428**: 281–286.

Woolley, D.W. and White, A.G.C. (1943) Selective reversible inhibition of microbial growth with pyrithiamine. *Journal of Experimental Medicine* **78**: 489–497.

World Health Organization (2022) 2021 Antibacterial agents in clinical and preclinical development: an overview and analysis.

Xin, Q., Chen, Y., Chen, Q., Wang, B., and Pan, L. (2022) Development and application of a fast and efficient CRISPR-based genetic toolkit in *Bacillus amyloliquefaciens* LB1ba02. *Microb Cell Fact* **21**: 1–13.

Xu, J., Hou, J., Ding, M., Wang, Z., and Chen, T. (2023) Riboswitches, from cognition to transformation. *Synth Syst Biotechnol* **8**: 357–370.

Zaman, G.J.R., Michiels, P.J.A., and van Boeckel, C.A.A. (2003) Targeting RNA: new opportunities to address drugless targets. *Drug Discov Today* **8**: 297–306.

Zhu, B. and Stülke, J. (2018a) SubtiWiki in 2018: From genes and proteins to functional network annotation of the model organism *Bacillus subtilis*. *Nucleic Acids Res* **46**: D743–D748.

Zhu, B. and Stülke, J. (2018b) SubtiWiki in 2018: From genes and proteins to functional network annotation of the model organism Bacillus subtilis. *Nucleic Acids Res* **46**: D743–D748.

Zilles, J.L., Croal, L.R., and Downs, D.M. (2000) Action of the Thiamine Antagonist Bacimethrin on Thiamine Biosynthesis. *J Bacteriol* **182**: 5606–5610.

9 Supplement

9.1 Abbreviations

Table S1: List of abbreviations.

AdoCbl	*adenosylcobalamin*
DAB	*3,3'-diaminobenzidine*
DMSO	*dimethyl sulfoxide*
DTT	*dithiothreitol*
EDTA	*ethylenediaminetetraacetic acid*
EMSA	*electrophoretic mobility shift assay*
ESKAPE	*group of pathogens, comprising Enterococcus faecium, Staphylococcus aureus, Klebsiella pneumoniae, Acinetobacter baumannii, Pseudomonas aeruginosa, Enterobacter spp.*
FAD	*flavin adenine dinucleotide*
FMN	*flavin mononucleotide*
$FMNH_2$	*flavin mononucleotide (reduced)*
FRET	*fluorescence resonance energy transfer*
HMP	*4-amino-5-hydroxymethyl-2-methylpyrimidine*
HMP-P	*4-amino-5-hydroxymethyl-2-methylpyrimidine phosphate*
HPLC	*high-performance liquid chromatography*
HRP	*horseradish peroxidase*
LacZ	*β-galactosidase*
Luc^F	*firefly luciferase*
Luc^R	*Renilla luciferase*
IVTT	*in vitro transcription/translation*
K_D	*dissociation constant*
MBP	*maltose-binding protein*
mRNA	*messenger RNA*
OD_{600}	*optical density at 600 nm*
PAA	*polyacrylamide*
PAGE	*polyacrylamide gel electrophoresis*
PCR	*polymerase chain reaction*
PNK	*polynucleotide kinase*
PT	*pyrithiamine*
PTPP	*pyrithiamine pyrophospate*
RBS	*ribosomal binding site*,
RFS	*riboflavin synthase*

rmsd	*root mean square deviation*
RNA	*ribonucleic acid*
RT	*reverse transcriptase*
SDS	*sodium dodecyl sulfate*
thi	*thiamine*
THZ	*4-methyl-5-(ß-hydroxyethyl) thiazole monophosphate*
TMP	*thiamine monophosphate*
TPP	Thiamine pyrophosphate
TRAP	*trp RNA-binding attenuation protein*
TT	*triazolethiamine*
UV	*ultraviolet*
WHO	*World Health Organization*
WT	*wild type*

9.2 Strains generated in this study

Table S2: List of strains generated in this study.

No.	Plasmid	Host strains	Description	Resistance	Source or reference
LacZ reporter plasmids					
1	pUC19del	*E. coli* DH5α	pUC19 vector with deletion of the *lac* promoter	AmpR	This study
2	pHA191	*E. coli* DH5α	pUC19 vector with deletion of the *lac* promoter, with *E. coli lacZ* gene (amplified from pDG268) for translational fusion,	AmpR	This study
3	pHAt191l	*E. coli* DH5α	pHA191 (2) vector with *rrnB* T1 terminator upstream and *lac* terminator downstream of *lacZ*	AmpR	This study
4	pHAt191l::pEc01	*E. coli* DH5α	pHAt191l (3) with *E. coli thiC* promoter and RBS region without RS (pEc01) fused to *lacZ*	AmpR	This study
5	pHAt191l::Ec01	*E. coli* DH5α	pHAt191l (3) with *E. coli thiC* RS region (Ec01) fused to *lacZ*	AmpR	This study
6	pHAt191l::pKp04	*E. coli* DH5α	pHAt191l (3) with *K. pneumoniae thiC* promoter and RBS region without RS (pKp04) fused to *lacZ*	AmpR	This study
7	pHAt191l::Kp04	*E. coli* DH5α	pHAt191l (3) with *K. pneumoniae thiC* RS region (Kp04) fused to *lacZ*	AmpR	This study
Dual-luciferase reporter plasmids					
8	pPrib-RibDG-RFN-luc	*E. coli* DH5α	pT7luc derived plasmid containing the *E.coli ribB* promoter and the firefly-luciferase gene controlled by the *ribDG* FMN riboswitch of *B.subtilis*	AmpR	Pedrolli, Kühm, *et al.* 2015
9	pPrib-RFN-luc-t	*E. coli* DH5α	pPrib-RibDG-RFN-luc (8) with rrnBT1 terminator	AmpR	This study

10	pPrib-RFN-luc-t _KpnI	*E. coli* DH5α	pPrib-RFN-luc-t (9) with KpnI restriction site inserted downstream of XhoI	AmpR	This study
11	pPrib-RFN-Dluc	*E. coli* DH5α	pPrib-RFN-luc-t _KpnI (10) with additional insertion of OXB15 promotor controlling *Renilla* luciferase gene (*luc*^{R})	AmpR	This study
12	pPrib-RFN-Dluc _NcoI	*E. coli* DH5α	pPrib-RFN-Dluc (11) plasmid for dual-luciferase assay with *Hin*dIII restriction site upstream of *B. subtilis ribDG* FMN-RS replaced by *Nco*I restriction site	AmpR	This study
13	pPrib-Dluc	*E. coli* DH5α	Plasmid pPrib-RFN-Dluc _NcoI (12) with *E. coli ribE* promoter but deletion of *ribDG* riboswitch	AmpR	This study
14	pDluc::pEc01	*E. coli* DH5α/ *E. coli* MG1655	Plasmid pDluc for dual-luciferase assay with *E. coli thiC* promoter pEc01 upstream of *luc*^{F} for translational fusion	AmpR	This study
15	pDluc::pEc01:Ab01	*E. coli DH5α*/ *E. coli* MG1655	Plasmid pDluc for dual-luciferase assay with *E. coli thiC* promoter pEc01 controlling *A. baumannii thiC* RS Ab01 translational fusion to *luc*^{F}	AmpR	This study
16	pDluc::pEc01:Kp04	*E. coli DH5α*/ *E. coli* MG1655	Plasmid pDluc for dual-luciferase assay with *E. coli thiC* promoter pEc01 controlling *K. pneumoniae thiC* RS Kp04 translational fusion to *luc*^{F}	AmpR	This study
17	pDluc::pEc01:Eb01	*E. coli DH5α*/ *E. coli* MG1655	Plasmid pDluc for dual-luciferase assay with *E. coli thiC* promoter pEc01 controlling *Enterobacter* spp. *thiC* RS Eb01 translational fusion to *luc*^{F}	AmpR	This study
18	pDluc::pEc01:Eb03	*E. coli DH5α*/ *E. coli* MG1655	Plasmid pDluc for dual-luciferase assay with *E. coli thiC* promoter pEc01 controlling *Enterobacter* spp. *thiB* RS Eb03 translational fusion to *luc*^{F}	AmpR	This study
19	pDluc::pEc01:Ms01	*E. coli* DH5α	Plasmid pDluc for dual-luciferase assay with *E. coli thiC* promoter pEc01 controlling *M. sciuri tenA* RS Ms01 translational fusion to *luc*^{F}	AmpR	This study
20	pDluc::pEc01:Ms02	*E. coli* DH5α/ *E. coli* MG1655	Plasmid pDluc for dual-luciferase assay with *E. coli thiC* promoter pEc01 controlling *M. sciuri thiE* RS Ms02 translational fusion to *luc*^{F}	AmpR	This study
21	pDluc::pEc01:Pa01	*E. coli* DH5α/ *E. coli* MG1655	Plasmid pDluc for dual-luciferase assay with *E. coli thiC* promoter pEc01 controlling *P. aeruginosa thiC* RS Pa01 translational fusion to *luc*^{F}	AmpR	This study
22	pDluc::pEc01:Sa02	*E. coli* DH5α	Plasmid pDluc for dual-luciferase assay with *E. coli thiC* promoter pEc01 controlling *S. aureus thiBPQ* RS Sa02 translational fusion to *luc*^{F}	AmpR	This study
23	pDlucTC::pEc01	*E. coli* DH5α	Plasmid pDlucTC for dual-luciferase assay with *E. coli thiC* promoter pEc01 upstream of *luc*^{F} for transcriptional fusion	AmpR	This study
24	pDlucTC::pEc01:Ab01	*E. coli* DH5α	Plasmid pDlucTC for dual-luciferase assay with *E. coli thiC* promoter pEc01 controlling *A. baumannii thiC* RS Ab01 transcriptional fusion to *luc*^{F}	AmpR	This study
25	pDlucTC::pEc01:Kp04	*E. coli* DH5α	Plasmid pDlucTC for dual-luciferase assay with *E. coli thiC* promoter pEc01 controlling *K. pneumoniae thiC* RS Kp04 transcriptional fusion to *luc*^{F}	AmpR	This study
26	pDlucTC::pEc01:Eb01	*E. coli* DH5α	Plasmid pDlucTC for dual-luciferase assay with *E. coli thiC* promoter pEc01 controlling *Enterobacter* spp. *thiC* RS Eb01 transcriptional fusion to *luc*^{F}	Amp	This study
27	pDlucTC::pEc01:Eb03	*E. coli* DH5α	Plasmid pDlucTC for dual-luciferase assay with *E. coli thiC* promoter pEc01 controlling *Enterobacter* spp. *thiB* RS Eb03 transcriptional fusion to *luc*^{F}	AmpR	This study

28	pDlucTC::pEc01:Ms02	*E. coli* DH5α	Plasmid pDlucTC for dual-luciferase assay with *E. coli thiC* promoter pEc01 controlling *M. sciuri thiE* RS Ms02 transcriptional fusion to luc^F	AmpR	This study
29	pDlucTC::pEc01:Pa01	*E. coli* DH5α	Plasmid pDlucTC for dual-luciferase assay with *E. coli thiC* promoter pEc01 controlling *P. aeruginosa thiC* RS Pa01 transcriptional fusion to luc^F	AmpR	This study
30	pDluc::Ec01	*E. coli* DH5α/ *E. coli* MG1655	Plasmid pDluc for dual-luciferase assay with *E. coli thiC* promoter and RS region Ec01 in translational fusion with luc^F	AmpR	This study
31	pDluc::pEf02	*E. coli* DH5α	Promoter control plasmid pDluc for dual-luciferase assay with *E. faecium thiT* promoter pEf02 and RBS in translational fusion with luc^F	AmpR	This study
32	pDluc::Ef02	*E. coli* DH5α	Plasmid pDluc for dual-luciferase assay with *E. faecium thiT* promoter and RS region Ef02 in translational fusion with luc^F	AmpR	This study
33	pDluc::pKp04	*E. coli* DH5α/ *E. coli* MG1655	Promoter control plasmid pDluc for dual-luciferase assay with *K. pneumoniae thiC* promoter pKp04 and RBS in translational fusion with luc^F	AmpR	This study
34	pDluc::Kp04	*E. coli* DH5α/ *E. coli* MG1655	Plasmid pDluc for dual-luciferase assay with *K. pneumoniae thiC* promoter and RS region Kp04 in translational fusion with luc^F	AmpR	This study
35	pDluc::pAb01	*E. coli* DH5α/ *E. coli* MG1655	Promoter control plasmid pDluc for dual-luciferase assay with *A. baumannii thiC* promoter pAb01 and RBS in translational fusion with luc^F	AmpR	This study
36	pDluc::Ab01	*E. coli* DH5α/ *E. coli* MG1655	Plasmid pDluc for dual-luciferase assay with *A. baumannii thiC* promoter and RS region Ab01 in translational fusion with luc^F	AmpR	This study
37	pDluc::pMs01	*E. coli* DH5α	Promoter control plasmid pDluc for dual-luciferase assay with *M.sciuri tenA* promoter pMs01 and RBS in translational fusion with luc^F	AmpR	This study
38	pDluc::Ms01	*E. coli* DH5α	Plasmid pDluc for dual-luciferase assay with *M. sciuri tenA* promoter and RS region Ms01 in translational fusion with luc^F	AmpR	This study
39	pDluc::pMs02	*E. coli* DH5α	Promoter control plasmid pDluc for dual-luciferase assay with *M.sciuri thiE* promoter pMs02 and RBS in translational fusion with luc^F	AmpR	This study
40	pDluc::Ms02	*E. coli* DH5α	Plasmid pDluc for dual-luciferase assay with *M. sciuri thiE* promoter and RS region Ms02 in translational fusion with luc^F	AmpR	This study
41	pDluc::pSp06	*E. coli* DH5α	Promoter control plasmid pDluc for dual-luciferase assay with *S. pneumoniae tenA* promoter pSp06 and RBS in translational fusion with luc^F	AmpR	This study
42	pDluc::Sp06	*E. coli* DH5α	Plasmid pDluc for dual-luciferase assay with *S. pneumoniae* promoter and RS region Sp06 in translational fusion with luc^F	AmpR	This study
43	pDluc::pKp01	*E. coli* DH5α/ *E. coli* MG1655	Promoter control plasmid pDluc for dual-luciferase assay with *K. pneumoniae thiBPQ* promoter pKp01 and RBS in translational fusion with luc^F	AmpR	This study
44	pDluc::Kp01	*E. coli* DH5α/ *E. coli* MG1655	Plasmid pDluc for dual-luciferase assay with *K. pneumoniae thiBPQ* promoter and RS region Kp01 in translational fusion with luc^F	AmpR	This study

45	pDluc::pKp10	*E. coli* DH5α/ *E. coli* MG1655	Promoter control plasmid pDluc for dual-luciferase assay with *K. pneumoniae tenA* promoter pKp10 and RBS in translational fusion with luc^F	AmpR	This study
46	pDluc::Kp10	*E. coli* DH5α/ *E. coli* MG1655	Plasmid pDluc for dual-luciferase assay with *K. pneumoniae tenA* promoter and RS region Kp10 in translational fusion with luc^F	AmpR	This study
47	pDluc::pKp11	*E. coli* DH5α/ *E. coli* MG1655	Promoter control plasmid pDluc for dual-luciferase assay with *K. pneumoniae thiM* promoter pKp11 and RBS in translational fusion with luc^F	AmpR	This study
48	pDluc::Kp11	*E. coli* DH5α/ *E. coli* MG1655	Plasmid pDluc for dual-luciferase assay with *K. pneumoniae thiM* promoter and RS region Kp11 in translational fusion with luc^F	AmpR	This study
49	pDluc::Kp04_A63U	*E. coli* DH5α/ *E. coli* MG1655	Plasmid pDluc for dual-luciferase assay with *K. pneumoniae thiC* promoter and mutated RS region Kp04_A63U in translational fusion with luc^F	AmpR	This study
50	pDluc::Kp04_Δ21-37	*E. coli* DH5α/ *E. coli* MG1655	Plasmid pDluc for dual-luciferase assay with *K. pneumoniae thiC* promoter and mutated RS region Kp04_Δ21-37 in translational fusion with luc^F	AmpR	This study
51	pDluc::Kp04_Δ42-48	*E. coli* DH5α/ *E. coli* MG1655	Plasmid pDluc for dual-luciferase assay with *K. pneumoniae thiC* promoter and mutated RS region Kp04_Δ42-48 in translational fusion with luc^F	AmpR	This study
52	pDluc::Kp04_Δ42G	*E. coli* DH5α/ *E. coli* MG1655	Plasmid pDluc for dual-luciferase assay with *K. pneumoniae thiC* promoter and mutated RS region Kp04_Δ42G in translational fusion with luc^F	AmpR	This study
53	pDluc::Kp04_Δ43U	*E. coli* DH5α/ *E. coli* MG1655	Plasmid pDluc for dual-luciferase assay with *K. pneumoniae thiC* promoter and mutated RS region Kp04_Δ43U in translational fusion with luc^F	AmpR	This study
54	pDluc::Kp04_Δ44G	*E. coli* DH5α/ *E. coli* MG1655	Plasmid pDluc for dual-luciferase assay with *K. pneumoniae thiC* promoter and mutated RS region Kp04_Δ44G in translational fusion with luc^F	AmpR	This study
55	pDluc::Kp04_Δ46A	*E. coli* DH5α/ *E. coli* MG1655	Plasmid pDluc for dual-luciferase assay with *K. pneumoniae thiC* promoter and mutated RS region Kp04_Δ46A in translational fusion with luc^F	AmpR	This study
56	pDlucTC::pEf02	*E. coli* DH5α	Promoter control plasmid pDlucTC for dual-luciferase assay with *E. faecium thiT* promoter pEf02 and RBS in transcriptional fusion with luc^F	AmpR	This study
57	pDlucTC::Ef02	*E. coli* DH5α	Plasmid pDlucTC for dual-luciferase assay with *E. faecium thiT* promoter and RS region Ef02 in transcriptional fusion with luc^F	AmpR	This study
58	pDlucTC::pKp04	*E. coli* DH5α	Promoter control plasmid pDlucTC for dual-luciferase assay with *K. pneumoniae thiC* promoter pKp04 and RBS in transcriptional fusion with luc^F	AmpR	This study
59	pDlucTC::Kp04	*E. coli* DH5α	Plasmid pDlucTC for dual-luciferase assay with *K. pneumoniae thiC* promoter and RS region Kp04 in transcriptional fusion with luc^F	AmpR	This study
60	pDlucTC::pAb01	*E. coli* DH5α	Promoter control plasmid pDlucTC for dual-luciferase assay with *A. baumannii thiC* promoter pAb01 and RBS in transcriptional fusion with luc^F	AmpR	This study
61	pDlucTC::Ab01	*E. coli* DH5α	Plasmid pDlucTC for dual-luciferase assay with *A. baumannii thiC* promoter and RS region Ab01 in transcriptional fusion with luc^F	AmpR	This study

62	pDlucTC::pMs02	*E. coli* DH5α	Promoter control plasmid pDlucTC for dual-luciferase assay with *M.sciuri thiE* promoter pMs02 and RBS in transcriptional fusion with luc^F	AmpR	This study
63	pDlucTC::Ms02	*E. coli* DH5α	Plasmid pDlucTC for dual-luciferase assay with *M. sciuri thiE* promoter and RS region Ms02 in transcriptional fusion with luc^F	AmpR	This study
64	pDlucTC::pSp06	*E. coli* DH5α	Promoter control plasmid pDlucTC for dual-luciferase assay with *S. pneumoniae tenA* promoter pSp06 and RBS in transcriptional fusion with luc^F	AmpR	This study
65	pDlucTC::Sp06	*E. coli* DH5α	Plasmid pDlucTC for dual-luciferase assay with *S. pneumoniae* promoter and RS region Sp06 in transcriptional fusion with luc^F	AmpR	This study
CRISPR/Cas9 plasmids for *B. subtilis*					
66	pJOEs1	*E. coli DH5α*	Plasmid for CRISPR/Cas9 in *B. subtilis* with spacer sequence (spacer1: CATTTAGGGGTTATGAATAT) for targeting the *B. subtilis ribR* gene	KanR	This study
67	pJOEs1:HRT-Δ*ribR*	*E. coli DH5α*	Plasmid for CRISPR/Cas9 in *B. subtilis* with spacer1 sequence for targeting B. subtilis *ribR* gene and Homology Repair Template for deletion of the *ribR* gene	KanR	This study
68	pJOEs1::HRT-ΔN-*ribR*	*E. coli* DH5α	Plasmid for CRISPR/Cas9 in *B. subtilis* with spacer1 sequence for targeting *B. subtilis ribR* gene and Homology Repair Template for deletion of N-terminal (bp 7-267) part of *ribR* gene	KanR	This study
69	pJOEs2	*E. coli* DH5α	Plasmid for CRISPR/Cas9 in B. subtilis with second spacer sequence (spacer2: CGGAAGATTTAACTCCTGAT) for targeting *B. subtilis ribR* gene	KanR	This study
70	pJOEs2::HRT-ΔC-*ribR*	*E. coli* DH5α	Plasmid for CRISPR/Cas9 in *B. subtilis* with spacer2 sequence for targeting *B. subtilis ribR* gene and Homology Repair Template for deletion of C-terminal part (bp 268-693) of *ribR* gene	KanR	This study
71	pJOEs2::HRT-$ribR_{amy}$	*E. coli* DH5α	Plasmid for CRISPR/Cas9 in *B. subtilis* with spacer2 sequence for targeting *B. subtilis ribR* gene and Homology Repair Template for replacing $ribR_{sub}$ with $ribR_{amy}$	KanR	This study
72	pJOEs2::HRT-$ribR^{m}_{sub}$	*E. coli* DH5α	Plasmid for CRISPR/Cas9 in *B. subtilis* with spacer2 sequence for targeting *B. subtilis ribR* gene and Homology Repair Template for replacing $ribR_{sub}$ with mutated $ribR_{sub}$ coding for RR>AA mutation (Pos. 179/180)	KanR	This study
73	pJOEs2::HRT-$ribR^{m}_{amy}$	*E. coli* DH5α	Plasmid for CRISPR/Cas9 in *B. subtilis* with spacer2 sequence for targeting *B. subtilis ribR* gene and Homology Repair Template for replacing $ribR_{sub}$ with mutated $ribR_{amy}$ coding for RR>AA mutation (Pos. 54/55)	KanR	This study
74	pJOEs2::HRT-his_6-$ribR_{amy}$	*E. coli* DH5α	Plasmid for CRISPR/Cas9 in *B. subtilis* with spacer2 sequence for targeting *B. subtilis ribR* gene and Homology Repair Template for replacing $ribR_{sub}$ with his_6-tagged $ribR_{amy}$	KanR	This study
75	pJOEs3	*E. coli* DH5α	Plasmid for CRISPR/Cas9 in *B. subtilis* with spacer3 sequence (spacer: ACATCACCCTTCGATCCGAA) for targeting *B. subtilis ribD*-RS	KanR	This study
76	pJOEs3::HRT-*ribD*-RS_{amy}	*E. coli* DH5α	Plasmid for CRISPR/Cas9 in B. subtilis with spacer sequence for targeting *B. subtilis ribD-RS* and Homology Repair Template for replacing *B. subtilis* ribD-RS *with B. amyloliquefaciens ribD*-RS	KanR	This study

Expression plasmids					
77	pET28a::*ribR*$_{amy}$	*E. coli* DH5α/ *E. coli* BL21/ *E. coli* BL21 pLysS	pET28a vector with putative *ribR* gene from *Bacillus amyloliquefaciens*	KanR	This study
78	pMAL-c5X::*ribR*$_{sub}$	*E. coli DH5α/* *E. coli NEBExpress*	pMAL-c5T vector for expression of MBP-tagged RibR$_{sub}$	AmpR	Pedrolli, Kühm *et al.*, 2015
79	pMAL-c6T::*ribR*$_{amy}$	*E. coli DH5α/* *E. coli NEBExpress*	pMAL-c6T vector for expression of MBP-tagged RibR$_{amy}$	AmpR	This study
80	pMAL-c5X::*ribR*$^{m}_{sub}$	*E. coli* DH5α/ *E. coli* NEBExpress	pMAL-c5X vector for expression of MBP-tagged mutated RibR$_{sub}^{R179A/R180A}$	AmpR	This study
81	pMAL-c6T::*ribR*$^{m}_{amy}$	*E. coli* DH5α/ *E. coli* NEBExpress	pMAL-c6T vector for expression of MBP-tagged mutated RibR$_{amy}^{R54A/R55A}$	AmpR	This study
***In vitro* transcription plasmids**					
82	pSP64::*ribD*RSapt$_{sub}$	*E. coli* DH5α	pSP64 plasmid for transcription of the *ribD* FMN-RS aptamer of *B. subtilis*, controlled by T7 promoter	AmpR	This study
83	pSP64::*ribD*RSapt$_{amy}$	*E. coli* DH5α	pSP64 plasmid for transcription of the *ribD* FMN-RS aptamer of *B. amyloliquefaciens*, controlled by T7 promoter	AmpR	This study

9.3 Plasmid maps

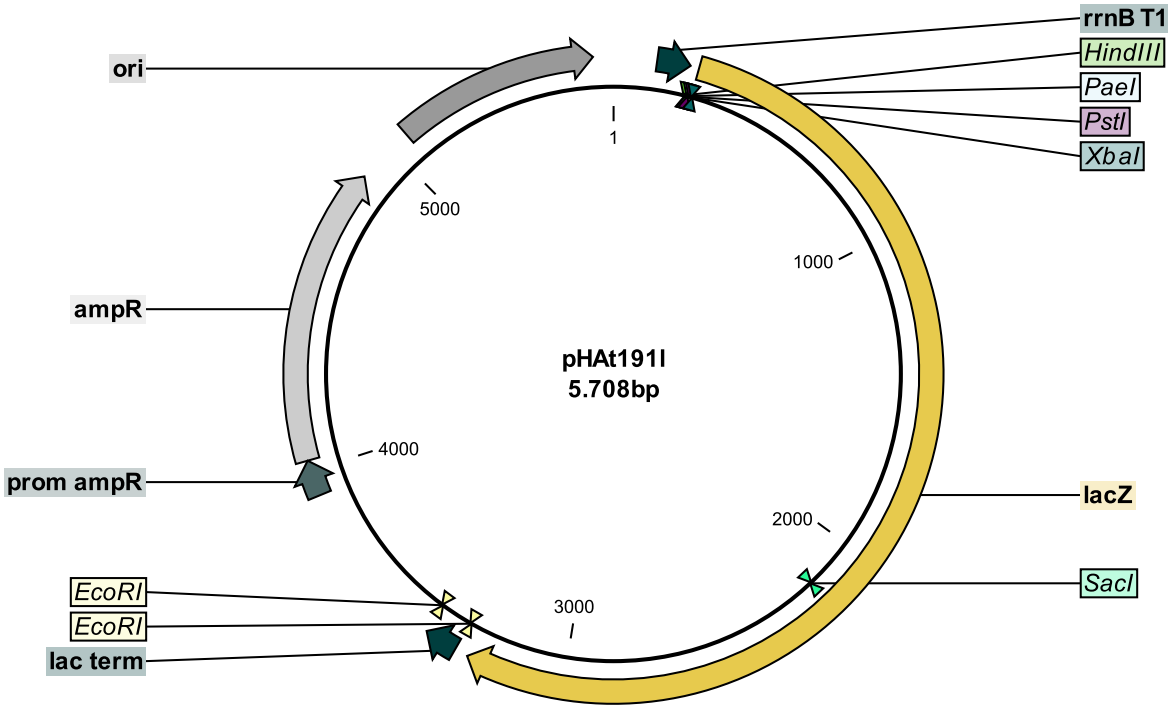

Figure S1: Plasmid map of pHAt191I. Depicted are the β-galactosidase coding sequence (*lacZ*), the origin of replication (ori), the ampicillin resistance gene (*ampR*) and its promoter (prom *ampR*), the *rrnB* T1 terminator (*rrnB* T1), the lac terminator (lac term) and the relevant restriction sites.

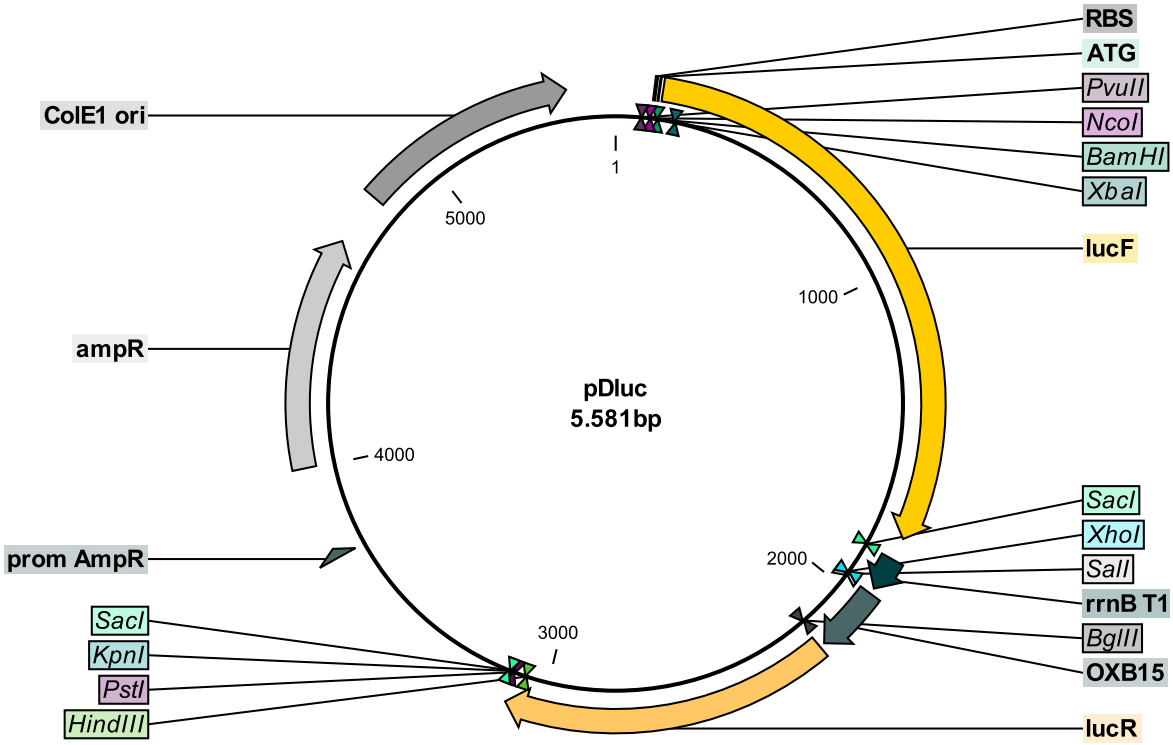

Figure S2: Plasmid map of pDluc. Depicted are the firefly luciferase coding sequence (*luc*^{F}) with the upstream ribosomal binding site (RBS) and additional start codon (ATG), the Renilla luciferase coding sequence (*luc*^{R}) the origin of replication (ColE1 ori), the ampicillin resistance gene (*ampR*) and its promoter (prom *ampR*), the *rrnB* T1 terminator (*rrnB* T1), the OXB15 promoter (OXB15) and the relevant restriction sites.

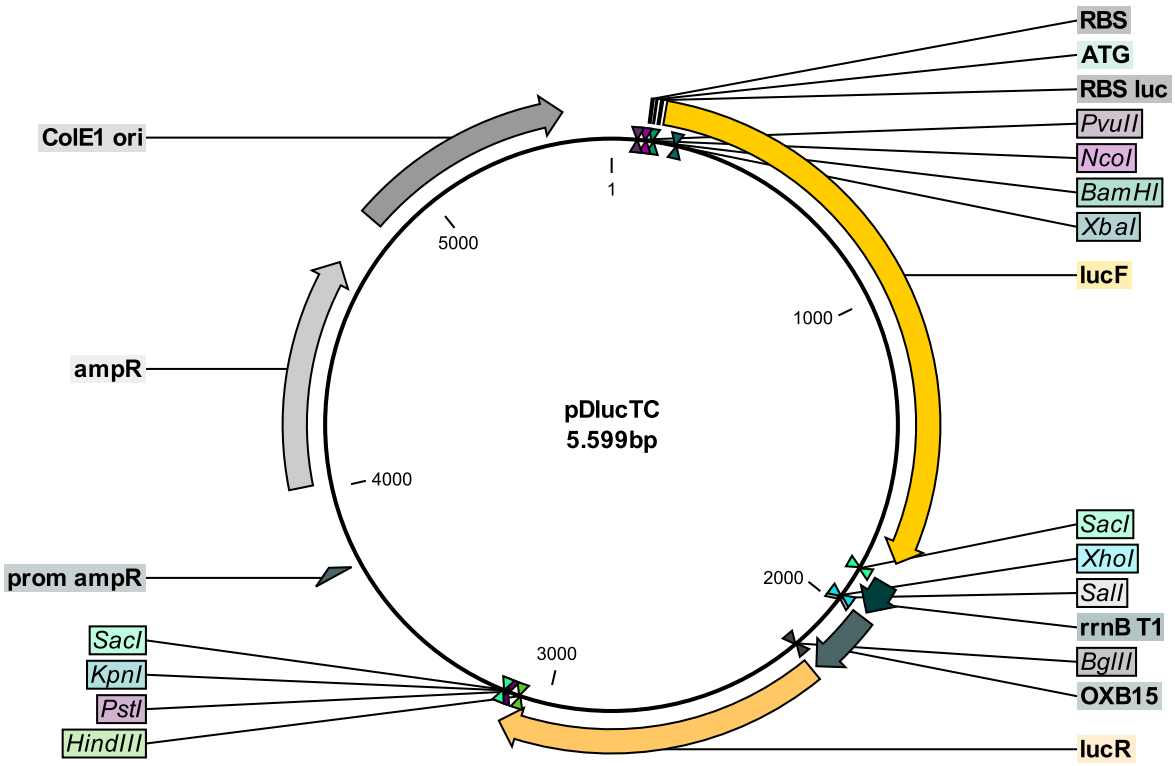

Figure S3: Plasmid map of pDlucTC. Depicted are the firefly luciferase coding sequence (*luc*^{F}) with the upstream ribosomal binding site (RBS), the *luc*^{F} RBS (RBS *luc*) and additional start codon (ATG), the Renilla luciferase coding sequence (*luc*^{R}) the origin of replication (ColE1 ori), the ampicillin resistance gene (*ampR*) and its promoter (prom *ampR*), the *rrnB* T1 terminator (*rrnB* T1), the OXB15 promoter (OXB15) and the relevant restriction sites.

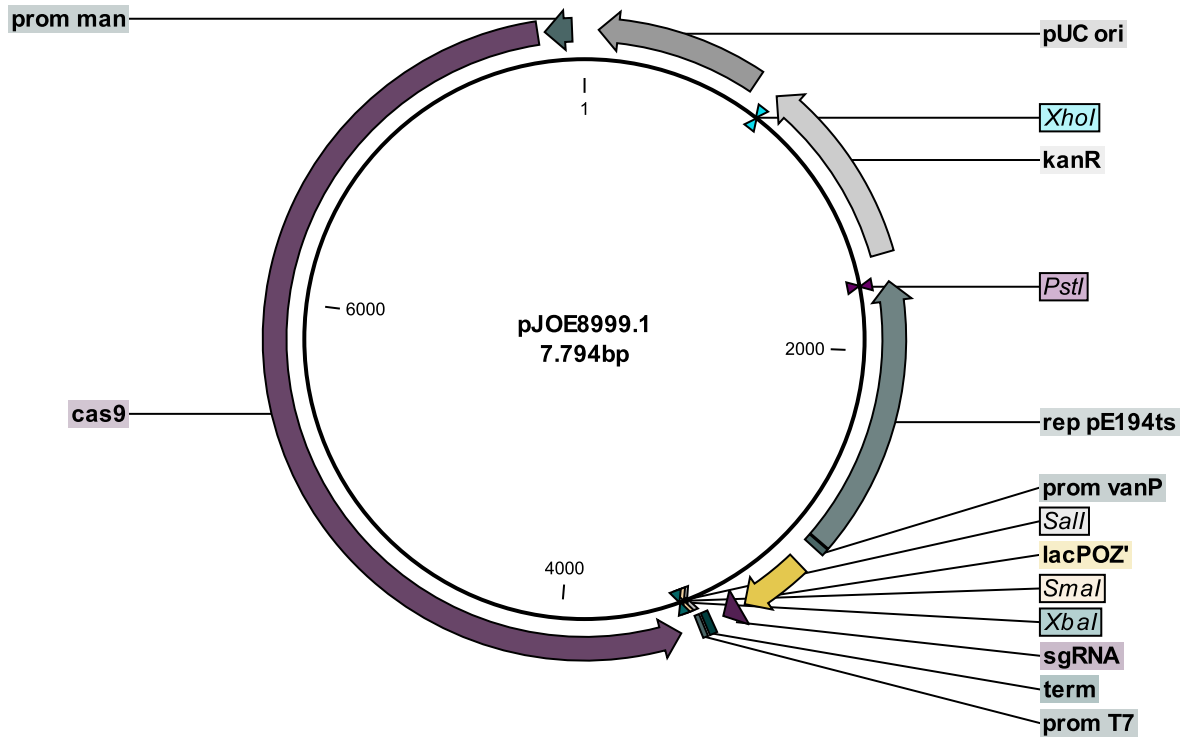

Figure S4: Plasmid map of pJOE8999.1. Depicted are the Cas9 coding sequence (*cas9*) with the mannose-inducible promoter (prom man), the temperature-sensitive replication origin (rep pE194^{ts}), the pUC origin of replication (pUC ori), the kanamycin resistance gene (*kanR*), the single guide RNA (sgRNA) transcribed from the semi-synthetic promoter (prom vanP), the *lacZ* α-fragment (*lac*POZ'), the T7 promoter (prom T7), the λ *oop* terminator (term) and the relevant restriction sites.

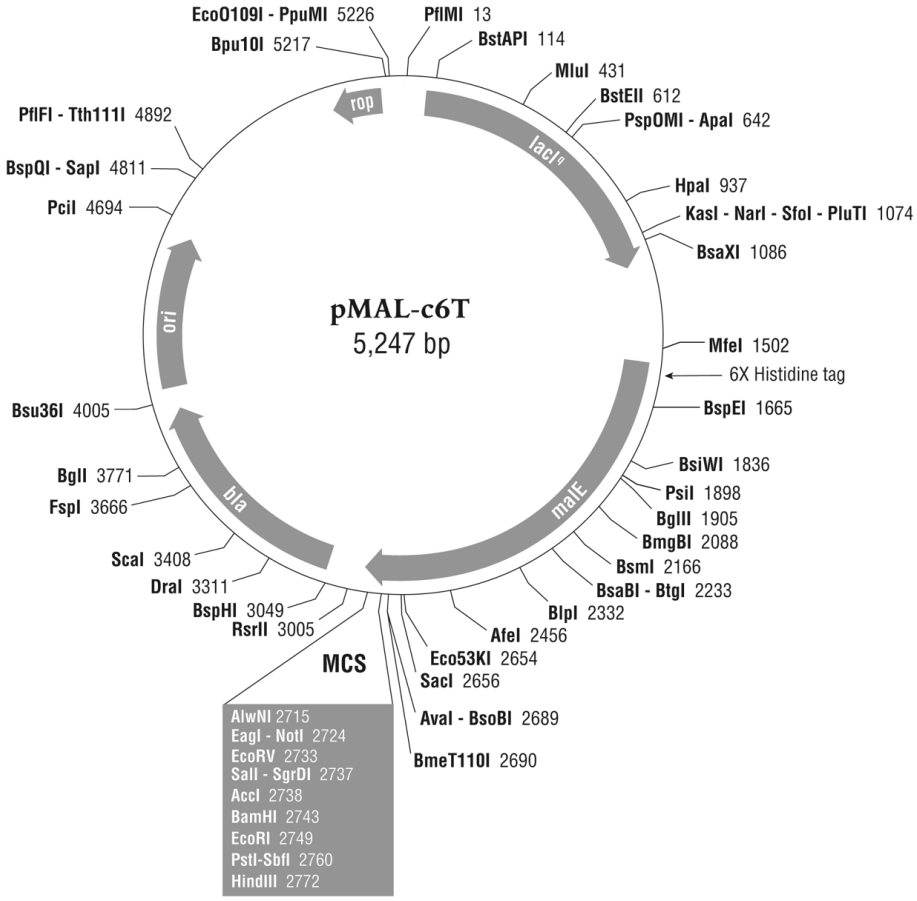

Figure S5: MBP-fusion vector pMAL-c6T. The image was taken from the instruction manual for the NEBExpress® MBP Fusion and Purification System from New England Biolabs GmbH (Frankfurt a. M., Germany).

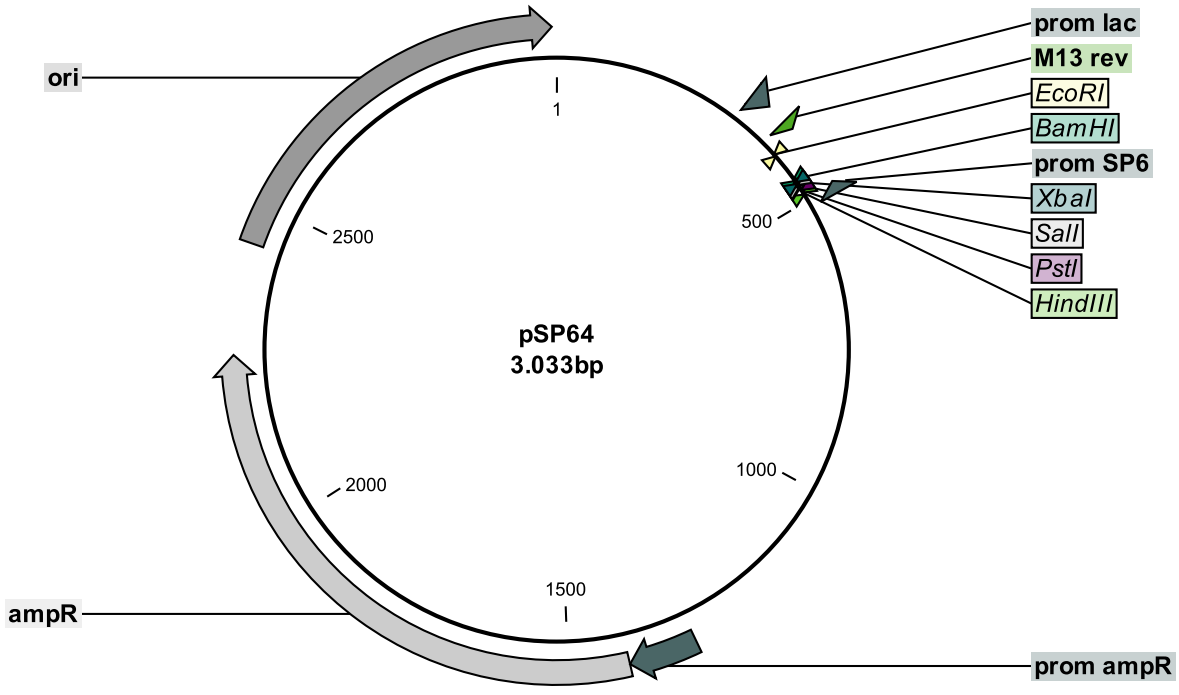

Figure S6: Plasmid map of pSP64. Depicted are the origin of replication (ori), the ampicillin resistance gene (*ampR*) and its promoter (prom *ampR*), the SP6 promoter (prom SP6) the lac promoter (prom lac) and the relevant restriction sites.

9.4 Promoter and terminator regions

Table S3: Nucleotide sequences of promoter regions, terminator regions and reporter gene sequences used in plasmid constructions. The BglII restriction site is printed in bold, the gene sequence coding for the *Renilla* luciferase (*luc*^{R}) is shown in gray.

lac terminator	GCCTGATACGCTGCGCTTATCAGGCCTACAAGTTCAGCGATCTACATTAGCCGCATCCGGCATGAACAAAGCG CAGGAACAAGCGTCGCATCATGCCTCTT
rrnB T1 terminator	GAAGAGCTAGGGAACTGCCAGGCATCAAATAAAACGAAAGGCTCAGTCGAAAGACTGGGCCTTTCGTTTTATCT GTTGTTTGTCGGTGAACGCTCTCCTGAGTA
T7 promoter	TAATACGACTCACTATAGG
OXB15	AAGCTGTTGTGACCGCTTGCTCTAGCCAGCTATCGAGTTGTGAACCGATCCATCTAGCAATTGGTCTCGATCTA GCGATAGGCTTCGATCTAGCTATGTAGAAACGCCGTGTGCTCGATCGCTTGATAAGGTCCACGTAGCTGCTATA GTTGCTTCAACAGAACATATTGACTATCCGGTATTACCCGGC
OXB15-*luc*^{R}	AAGCTGTTGTGACCGCTTGCTCTAGCCAGCTATCGAGTTGTGAACCGATCCATCTAGCAATTGGTCTCGATCTA GCGATAGGCTTCGATCTAGCTATGTAGAAACGCCGTGTGCTCGATCGCTTGATAAGGTCCACGTAGCTGCTATA GTTGCTTCAACAGAACATATTGACTATCCGGTATTACCCGGC**AGATCT**TTGTCGATC ATGACCAGCAAAGTTTA TGATCCGGAACAGCGTAAACGCATGATTACCGGTCCGCAGTGGTGGGCGCGTTGTAAACAAATGAATGTTCTG GATAGCTTCATCAACTATTACGACAGCGAAAAACATGCCGAAAACGCCGTTATTTTTCTGCATGGTAATGCAGC AAGCAGCTATCTGTGGCGTCATGTTGTTCCGCATATTGAACCGGTTGCGCGTTGTATTATTCCGGATCTGATTG GTATGGGTAAAAGCGGTAAATCAGGTAATGGTAGCTATCGTCTGCTGGATCATTACAAATATCTGACCGCATGG TTTGAACTGCTGAATCTGCCGAAAAAAATCATCTTTGTGGGTCATGATTGGGGTGCATGTCTGGCATTTCATTAT AGCTACGAACACCAGGACAAAATCAAAGCCATTGTTCATGCGGAAAGCGTTGTTGATGTTATTGAAAGCTGGGA TGAATGGCCTGACATCGAAGAAGATATTGCCCTGATTAAAAGCGAAGAGGGTGAAAAAATGGTGCTGGAAAAC AACTTTTTCGTGGAAACCATGCTGCCGAGCAAAATTATGCGTAAACTGGAACCGGAAGAATTTGCAGCATATCT GGAACCGTTTAAAGAAAAAGGTGAAGTTCGTCGTCCGACACTGAGCTGGCCTCGTGAAATTCCGCTGGTTAAA GGTGGTAAACCGGATGTTGTTCAGATTGTGCGTAACTATAATGCATATCTGCGTGCAAGTGATGACCTGCCTAA AATGTTTATCGAAAGCGATCCGGGTTTTTTTAGCAATGCAATTGTTGAAGGTGCCAAGAAATTTCCGAATACCGA ATTCGTTAAAGTGAAAGGCCTGCACTTTAGCCAAGAGGATGCACCGGATGAAATGGGCAAATATATCAAAAGCT TTGTGGAACGCGTGCTGAAAAACGAACAGTAA
lacZ	GTGGAAGTTACTGACGTAAGATTACGGGTCGACCGGGAAAACCCTGGCGTTACCCAACTTAATCGCCTTGCAG CACATCCCCCTTTCGCCAGCTGGCGTAATAGCGAAGAGGCCCGCACCGATCGCCCTTCCCAACAGTTGCGCA GCCTGAATGGCGAATGGCGCTTTGCCTGGTTTCCGGCACCAGAAGCGGTGCCGGAAAGCTGGCTGGAGTGCG ATCTTCCTGAGGCCGATACTGTCGTCGTCCCCTCAAACTGGCAGATGCACGGTTACGATGCGCCCATCTACAC CAACGTGACCTATCCCATTACGGTCAATCCGCCGTTTGTTCCCACGGAGAATCCGACGGGTTGTTACTCGCTCA CATTTAATGTTGATGAAAGCTGGCTACAGGAAGGCCAGACGCGAATTATTTTTGATGGCGTTAACTCGGCGTTT CATCTGTGGTGCAACGGGCGCTGGGTCGGTTACGGCCAGGACAGTCGTTTGCCGTCTGAATTTGACCTGAGC GCATTTTTACGCGCCGGAGAAAACCGCCTCGCGGTGATGGTGCTGCGCTGGAGTGACGGCAGTTATCTGGAA GATCAGGATATGTGGCGGATGAGCGGCATTTTCCGTGACGTCTCGTTGCTGCATAAACCGACTACACAAATCA GCGATTTCCATGTTGCCACTCGCTTTAATGATGATTTCAGCCGCGCTGTACTGGAGGCTGAAGTTCAGATGTGC GGCGAGTTGCGTGACTACCTACGGGTAACAGTTTCTTTATGGCAGGGTGAAACGCAGGTCGCCAGCGGCACC GCGCCTTTCGGCGGTGAAATTATCGATGAGCGTGGTGGTTATGCCGATCGCGTCACACTACGTCTGAACGTCG AAAACCCGAAACTGTGGAGCGCCGAAATCCCGAATCTCTATCGTGCGGTGGTTGAACTGCACACCGCCGACG GCACGCTGATTGAAGCAGAAGCCTGCGATGTCGGTTTCCGCGAGGTGCGGATTGAAAATGGTCTGCTGCTGCT GAACGGCAAGCCGTTGCTGATTCGAGGCGTTAACCGTCACGAGCATCATCCTCTGCATGGTCAGGTCATGGAT GAGCAGACGATGGTGCAGGATATCCTGCTGATGAAGCAGAACAACTTTAACGCCGTGCGCTGTTCGCATTATC CGAACCATCCGCTGTGGTACACGCTGTGCGACCGCTACGGCCTGTATGTGGTGGATGAAGCCAATATTGAAAC CCACGGCATGGTGCCAATGAATCGTCTGACCGATGATCCGCGCTGGCTACCGGCGATGAGCGAACGCGTAAC GCGAATGGTGCAGCGCGATCGTAATCACCCGAGTGTGATCATCTGGTCGCTGGGGAATGAATCAGGCCACGG CGCTAATCACGACGCGCTGTATCGCTGGATCAAATCTGTCGATCCTTCCCGCCCGGTGCAGTATGAAGGCGGC GGAGCCGACACCACGGCCACCGATATTATTTGCCCGATGTACGCGCGCGTGGATGAAGACCAGCCCTTCCCG GCTGTGCCGAAATGGTCCATCAAAAAATGGCTTTCGCTACCTGGAGAGACGCGCCCGCTGATCCTTTGCGAAT ACGCCCACGCGATGGGTAACAGTCTTGGCGGTTTCGCTAAATACTGGCAGGCGTTTCGTCAGTATCCCCGTTT ACAGGGCGGCTTCGTCTGGGACTGGGTGGATCAGTCGCTGATTAAATATGATGAAAACGGCAACCCGTGGTCG GCTTACGGCGGTGATTTTGGCGATACGCCGAACGATCGCCAGTTCTGTATGAACGGTCTGGTCTTTGCCGACC GCACGCCGCATCCAGCGCTGACGGAAGCAAAACACCAGCAGCAGTTTTTCCAGTTCCGTTTATCCGGGCAAAC CATCGAAGTGACCAGCGAATACCTGTTCCGTCATAGCGATAACGAGCTCCTGCACTGGATGGTGGCGCTGGAT GGTAAGCCGCTGGCAAGCGGTGAAGTGCCTCTGGATGTCGCTCCACAAGGTAAACAGTTGATTGAACTGCCTG AACTACCGCAGCCGGAGAGCGCCGGGCAACTCTGGCTCACAGTACGCGTAGTGCAACCGAACGCGACCGCAT GGTCAGAAGCCGGGCACATCAGCGCCTGGCAGCAGTGGCGTCTGGCGGAAAACCTCAGTGTGACGCTCCCC GCCGCGTCCCACGCCATCCCGCATCTGACCACCAGCGAAATGGATTTTTGCATCGAGCTGGGTAATAAGCGTT GGCAATTTAACCGCCAGTCAGGCTTTCTTTCACAGATGTGGATTGGCGATAAAAAACAACTGCTGACGCCGCTG CGCGATCAGTTCACCCGTGCACCGCTGGATAACGACATTGGCGTAAGTGAAGCGACCCGCATTGACCCTAACG CCTGGGTCGAACGCTGGAAGGCGGCGGGCCATTACCAGGCCGAAGCAGCGTTGTTGCAGTGCACGGCAGAT ACACTTGCTGATGCGGTGCTGATTACGACCGCTCACGCGTGGCAGCATCAGGGGAAAACCTTATTTATCAGCC GGAAAACCTACCGGATTGATGGTAGTGGTCAAATGGCGATTACCGTTGATGTTGAAGTGGCGAGCGATACACC GCATCCGGCGCGGATTGGCCTGAACTGCCAGCTGGCGCAGGTAGCAGAGCGGGTAAACTGGCTCGGATTAG GGCCGCAAGAAAACTATCCCGACCGCCTTACTGCCGCCTGTTTTGACCGCTGGGATCTGCCATTGTCAGACAT GTATACCCCGTACGTCTTCCCGAGCGAAAACGGTCTGCGCTGCGGGACGCGCGAATTGAATTATGGCCCACAC CAGTGGCGCGGCGACTTCCAGTTCAACATCAGCCGCTACAGTCAACAGCAACTGATGGAAACCAGCCATCGCC ATCTGCTGCACGCGGAAGAAGGCACATGGCTGAATATCGACGGTTTCCATATGGGGATTGGTGGCGACGACTC CTGGAGCCCGTCAGTATCGGCGGAATTACAGCTGAGCGCCGGTCGCTACCATTACCAGTTGGTCTGGTGTCAA AAATAATAATAACCGGGCAGGCCATGTCTGCCGTATTTC

9.5 TPP riboswitch regions and promoter control regions

Table S4: Sequences of TPP riboswitch regions (including promoter, RS, RBS and the first few codons of the downstream gene) and the respective promoter control regions (promoter + RBS and start of coding sequence). Important sequences are highlighted in different colors according to the following color code: Start codon, (put.) promoter region, RS region, (put.) RBS, *thi* gene. Restriction sites are displayed in bold.

Ec01 (pHAt191l)	**AAGCTT**GCTGGAAGATAAGCTGATTCTGCTGGTGCTTGACGCCGCCCGCGTCAAACATCCTGCT TGAGTTCTGCGCTGTTAACGCGTAATTTACATTCAATGCCCCATTTGCGGGGCTAATTTCTTGTCG GAGTGCCTTAACTGGCTGAGACCGTTTATTCGGGATCCGCGGAACCTGATCAGGCTAATACCTGC GAAGGGAACAAGAGTTAATCTGCTATCGCATCGCCCCTGCGGCGATCGTCTCTTGCTTCATCCGT CGTCTGACAAGCCACGTCCTTAACTTTTTGGAATGAGCTATGTCTGCAACAAAACTGACCCGCCG CGAACAACGC**TCTAGA**
pEc01 (pHAt191l)	**AAGCTT**GCTGGAAGATAAGCTGATTCTGCTGGTGCTTGACGCCGCCCGCGTCAAACATCCTGCT TGAGTTCTGCGCTGTTAACGCGTAATTTACATTCAATGCCCC**CTGCAG**TTTTGGAATGAGCTATGT CTGCAACAAAACTGACCCGCCGCGAACAACGC**TCTAGA**
Kp04 (pHAt191l)	**AAGCTT**GATAATATTGCGCCGACCGCTTGAGTTGTGAACCGTTAACGCGTAATTTACGTACATTATC CCTCTGCGGAGGGATTTCATCTTGTCGGAGTGCCTATTTTCCATGCGCAGGCTAACGTGGAAAAG GCTGAGACCGTTAATTCGGGATCCGCGGAACCTGATCAGGCTAATACCTGCGAAGGGAACAAGA GTAAACTGCTGTTCGCGTCAGTCCGTCAGGGCCGATCGCATCTGTTACTCCATCCGTCGTCTGAC AAGCCATGTCCTTTTTTTAACTGGAATGCGCTATGTCTACTACCAAACTAACCCGT**TCTAGA**
pKp04 (pHAt191l)	**AAGCTT**GATAATATTGCGCCGACCGCTTGAGTTGTGAACCGTTAACGCGTAATTTACGTACATTATC CCTCTGCGGAGGGATTTCAT**CTGCAG**GCCATGTCCTTTTTTAACTGGAATGCGCTATGTCTACTAC CAAACTAACCCGT**TCTAGA**
pEc01 (pDluc)	**CAGCTG**GCTGGAAGATAAGCTGATTCTGCTGGTGCTTGACGCCGCCCGCGTCAAACATCCTGCT TGAGTTCTGCGCTGTTAACGCGTAATTTACATTCAATGCCCC**CCATGG**GGGAGGGAAACAAATGT **GGATCC**
Ec01 (pDluc)	**CAGCTG**GCTGGAAGATAAGCTGATTCTGCTGGTGCTTGACGCCGCCCGCGTCAAACATCCTGCT TGAGTTCTGCGCTGTTAACGCGTAATTTACATTCAATGCCCCATTTGCGGGGCTAATTTCTTGTCG GAGTGCCTTAACTGGCTGAGACCGTTTATTCGGGATCCGCGGAACCTGATCAGGCTAATACCTGC GAAGGGAACAAGAGTTAATCTGCTATCGCATCGCCCCTGCGGCGATCGTCTCTTGCTTCATCCGT CGTCTGACAAGCCACGTCCTTAACTTTTTGGAATGAGCTATGTCTGCAACAAAACTGACCCGCCG CGAACAACGCT**GGATCC**
Kp04 (pDluc)	**CAGCTG**GATAATATTGCGCCGACCGCTTGAGTTGTGAACCGTTAACGCGTAATTTACGTACATTAT CCCTCTGCGGAGGGATTTCATCTTGTCGGAGTGCCTATTTTCCATGCGCAGGCTAACGTGGAAAA GGCTGAGACCGTTAATTCGGGATCCGCGGAACCTGATCAGGCTAATACCTGCGAAGGGAACAAG AGTAAACTGCTGTTCGCGTCAGTCCGTCAGGGCCGATCGCATCTGTTACTCCATCCGTCGTCTGA CAAGCCATGTCCTTTTTTAACTGGAATGCGCTATGTCTACTACCAAACTAACCCGTT**GGATCC**
pKp04 (pDluc)	**CAGCTG**GATAATATTGCGCCGACCGCTTGAGTTGTGAACCGTTAACGCGTAATTTACGTACATTAT CCCTCTGCGGAGGGATTTCAT**CTGCAG**GCCATGTCCTTTTTTAACTGGAATGCGCTATGTCTACTA CCAAACTAACCCGTT**GGATCC**
pEc01-Ab01	**CAGCTG**GCTGGAAGATAAGCTGATTCTGCTGGTGCTTGACGCCGCCCGCGTCAAACATCCTGCT TGAGTTCTGCGCTGTTAACGCGTAATTTACATTCAATGCCCC**CCATGG**TTAAATCGCTTGACGGAG CGCGAGTAATAGCTCGCTGAGATTGTGTAAATTTCGTGTTATCGCAACACCAGTTTGATCACAAGT ACCGTTGAACCTGATCAGGTTAAGACCTGCGTAGGAATCAAGCCATCTGAAAACCTAAGCCCTCA ATTTATCTAGTTCAAGATAAATCCGCCATCGTTTTTGGTCGTGCTTGATTCGTTGATGTTATTCATAA GGATCATGTGATGAACCAATTAACGAATCTCTCTT**GGATCC**
Ab01	**CAGCTG**GTATAGATACAAATTGACAATGCCAGCCAACCTAAAACATGTTAGTCTTTAAATCGCTTGA CGGAGCGCGAGTAATAGCTCGCTGAGATTGTGTAAATTTCGTGTTATCGCAACACCAGTTTGATCA CAAGTACCGTTGAACCTGATCAGGTTAAGACCTGCGTAGGAATCAAGCCATCTGAAAACCTAAGC CCTCAATTTATCTAGTTCAAGATAAATCCGCCATCGTTTTTGGTCGTGCTTGATTCGTTGATGTTATT CATAAGGATCATGTGATGAACCAATTAACGAATCTCTCTT**GGATCC**
pAc01	**CAGCTG**GTATAGATACAAATTGACAATGCCAGCCAACCTAAAACATGTTAGTCTTTAAATCGCTTGA CGGAGCGCGAGTAATA**CTGCAG**GTGCTTGATTCGTTGATGTTATTCATAAGGATCATGTGATGAACC CAATTAACGAATCTCTCTT**GGATCC**
Ef02	**CAGCTG**CCAGTTAGTCCATTGTTTGAAACAAAAAATAAATAATAAATAAACTCACAAAGGGGAGTC CAATTGGGCTGAGATTGAATCTATTTCTAAACCCTTCGTACCTGTATCGGTTATGCGAGCGTAGGA ATTGTGAATAAACAGCTGTTTGACTATTTTCGAAAGCTGCTTCCTCCTTTGTGACTTTTTTATTCAAA GGAGGAAGTTTTTTTATGGGAAAAAATAGAGTTTGGGTAGAAC**GGATCC**
pEf02	**CAGCTG**CCAGTTAGTCCATTGTTTGAAACAAAAAATAAATAATAAATAAACTCACAAAGGGGAGTC CAACTTCCTCCTTTGTGACTTTTTTATTCAAAGGAGGAAGTTTTTTTATGGGAAAAAATAGAGTTTG GGTAGAAC**GGATCC**
pEc01-Eb01	**CAGCTG**GCTGGAAGATAAGCTGATTCTGCTGGTGCTTGACGCCGCCCGCGTCAAACATCCTGCT TGAGTTCTGCGCTGTTAACGCGTAATTTACATTCAATGCCCC**CCATGG**AAATTTCTTGTCGGAGTG CCCAGTGCGTAAGCCGGGCTGAGACCGTTAATTCGGGATCCGCGGAACCTGATCAGGCTAATAC CTGCGAAGGGAACAAGAGTCAATCTGCTGTTGTATCGCCTCTGGGCGATCACCTCTTGCTTCATC CGTCGTCTGACAAGCCACTTCCTTTACTATTTTGGAATGAGCTATGTCTGCAAAATTGACCCGCCG CA**GGATCC**

pEc01-Eb03

CAGCTGGCTGGAAGATAAGCTGATTCTGCTGGTGCTTGACGCCGCCCGCGTCAAACATCCTGCT
TGAGTTCTGCGCTGTTAACGCGTAATTTACATTCAATGCCCC**CCATGG**GCTGTTCTCAACGGGGT
GCTGCATCAACGATGTGCGCTGAGATAATACCCGTCGAACCTGATCCGGATAACGCCGGCGAAG
GGATTTGAGGCTGTCGCTCAAAATCCTTTGCCACTCAACTTTGAGGTGCAAAGTGTTAAAAAAAG
TTCTCCCCCTGCTGGCGA**GGATCC**

pEc01-Ms01

CAGCTGGCTGGAAGATAAGCTGATTCTGCTGGTGCTTGACGCCGCCCGCGTCAAACATCCTGCT
TGAGTTCTGCGCTGTTAACGCGTAATTTACATTCAATGCCCC**CCATGG**TTAAACCACTGGAAGTGC
CTTGATAAAGGCTGAGATTAAAGTGATACCTTTAAAATTCCTTGAACCTGATCCAGCTTATACTGGC
GTAGGAAAGTGGCGTATTGATTTTAAGGTACTCATGACGCTATTTTCTTAATGAAAATAGCGTTTTTT
TAATTATAACGGATCC

Ms01

CAGCTGATTTTATTTGCAATCCTAGGATAAAACAGATATGTTGAAAGAGTATAGAAATTAAATAATTTT
AAACCACTGGAAGTGCCTTGATAAAGGCTGAGATTAAAGTGATACCTTTAAAATTCCTTGAACCTG
ATCCAGCTTATACTGGCGTAGGAAAGTGGCGTATTGATTTTAAGGTACTCATGACGCTATTTTCTTA
ATGAAAATAGCGTTTTTTTAATTATAACGGATCC

pMs01

CAGCTGATTTTATTTGCAATCCTAGGATAAAACAGATATGTTGAAAGAGTATAGAAATTAAATAATT**C**
TGCAGTAAGGTACTCATGACGCTATTTTCTTAATGAAAATAGCGTTTTTTTAATTATAACGGATCC

pEc01-Ms02

CAGCTGGCTGGAAGATAAGCTGATTCTGCTGGTGCTTGACGCCGCCCGCGTCAAACATCCTGCT
TGAGTTCTGCGCTGTTAACGCGTAATTTACATTCAATGCCCC**CCATGG**AATGTCCACTGGAAGTG
CCTTATTATAGGCTGAGACTGAAGTAGTGACTTCGGGATTCCTTGAACCTGATCCAGTTCATACTG
GCGTAGGAAAGTGGCGTATATAAGCTTACTTATACTTATAATTAAATTTTTACGCTATTTTTCTATCCA
GAAAAATAGCGTTTTTTATTTGGAGTGATTTCATTGTTTATTGCTGTTACACCGTATAAATGGATCC

Ms02

CAGCTGTTCTGCAATCATCTGAGCAACATATAAATTTGAACATTCTTACTTTTATATGTACAATGGAT
GTAATAACTGAATAAATGTCCACTGGAAGTGCCTTATTATAGGCTGAGACTGAAGTAGTGACTTCG
GGATTCCTTGAACCTGATCCAGTTCATACTGGCGTAGGAAAGTGGCGTATATAAGCTTACTTATACT
TATAATTAAATTTTTACGCTATTTTTCTATCCAGAAAAATAGCGTTTTTTATTTGGAGTGATTTCATTGT
TTATTGCTGTTACACCGTATAAATGGATCC

pMs02

CAGCTGTTCTGCAATCATCTGAGCAACATATAAATTTGAACATTCTTACTTTTATATGTACAATGGAT
GTAATAACTGAATAAATGTCCACTG**CTGCAG**CGTTTTTTATTTGGAGTGATTTCATTGTTTATTGCTG
TTACACCGTATAAATGGATCC

pEc01-Pa01

CAGCTGGCTGGAAGATAAGCTGATTCTGCTGGTGCTTGACGCCGCCCGCGTCAAACATCCTGCT
TGAGTTCTGCGCTGTTAACGCGTAATTTACATTCAATGCCCC**CCATGG**GGGTTCTTGTCGGGGTG
CCCTATACGAGGGGCTGAGATCGGATAGTTCCGGATCCCGTTGAACCTGATCGGGCTAGCGTCC
GGTTCCGCCTCGCGCGGACCGCAGCAACCCGCGTAGGGAACAAGATGTCCGCGCCATGCCTGC
CTTGCCGGCGCGTCCTTCTCGCCACCAGTCCCGGTGGCCCCGCGTGCCAGGTTCTCCCGACAA
TCACCCAGGAGAGCCATCGATGAGCGCAACGCAGAAGAACAACATCACCCGCCTTGAGCAGCTC
GACCGCCAGTCGACGCAGCCTTTCCCGAACTCGCGCAAGGTCTACCTGACCGGCTCGCGCCCG
GACATCCGCG**GGATCC**

pEc02-Sa02

CAGCTGGCTGGAAGATAAGCTGATTCTGCTGGTGCTTGACGCCGCCCGCGTCAAACATCCTGCT
TGAGTTCTGCGCTGTTAACGCGTAATTTACATTCAATGCCCC**CCATGG**AAATCGCACACACTAGG
GGTGTTTTATACTGAGATGAGGCTTGCCCTCAAACCCTTTGAACCTGATCTAGCTTGAACTAGCGT
AGGAAAGTGTTACTATACATATGTTTTACTAATATATATTGTGAACGCATAACTTTCCTATGGATGGTT
GTGCGTTTTTTTATTAGGAGGATGTAAAAATGTCAAAAGGTTTAAAGCTATCTGAACGGATCC

Sp06

CAGCTGAATCATTTGAAAAACGATTTGCAGTCAAATATTACTATATAAACAATAAAAATATGCTATACT
AAAGAAAAAAGAAAACAACCACTAGGGGTGCGTAAAGCTGAGATTAACGACTGTTAGATCCCTCT
GACTCAATCTAGGTAATGCTAGCTGATGGAAGTGGAAATGATAATGGGGACTAGCAGTCTTCTATT
GCCTTTCTAAAACAGACTAGCTTGTTCTTAAGAATACAAACTTCAGTTGGTTGGGAGGTTTTAGAT
GACTTATTTACCCGTTGCTTTGACCATTGCAGGGACTGACCCTAGTGGTGGTGCTGGCATTATGG
CAGATTTAA**GGATCC**

pSp06

CAGCTGAATCATTTGAAAAACGATTTGCAGTCAAATATTACTATATAAACAATAAAAATATGCTATACT
AAAGAAAAAAGAAAACAACCACTAGGG**CTGCAG**AACTTCAGTTGGTTGGGAGGTTTTAGATGACT
TATTTACCCGTTGCTTTGACCATTGCAGGGACTGACCCTAGTGGTGGTGCTGGCATTATGGCAGA
TTTAA**GGATCC**

Kp01

CAGCTGCATGGTTTGCGCCGCCGGAGCCGTAAGCGCTTTCCGTCATCTGACAAAATCATTACACT
AAGGCCGTTCTCAACGGGGTGCTAATAAACATACGCAATATCATTCAAGTTGCATCAAGGCAGCAA
GCGGGTGAATCCCCTGGAGCATAGATAACTATGTGACTGGGGTGAACGCGCGAAGCTAACGCAG
ATGCGGCTTGAAGGATGAAGCGCATGGGCTGAGAAAATACCCGTCGAACCTGATCCGGATAACG
CCGGCGAAGGGATTTGAGGCTCACTCAAAATCCTTTGCCACCCCTTTTTTCTGAGGTGCAAAGTG
TTGAAAAAATTACTCCCGCTGCTGGCGT**GGATCC**

pKp01

CAGCTGCATGGTTTGCGCCGCCGGAGCCGTAAGCGCTTTCCGTCATCTGACAAAATCATTACACT
AAGGCCG**CTGCAG**TCTGAGGTGCAAAGTGTTGAAAAAATTACTCCCGCTGCTGGCGT**GGATCC**

Kp10

CAGCTGTTCTTGCGCGGAAAAGCGCTGGCTATCCCCCATTACCATCATCCTGCGTCAAGGTGGC
GCGGTGATTGTATTCAAAAGGTGAATGTCGTATAACATAGCGCTACCGAGGGGTGTCCCGTGAGG
GCTGAGATGGCGCAAGCCGAACCCTTTGAACCTGATCTGGGTCATGCCAGCGAAGGGACGGGT
CGGCAATTTTGCCAGCATTACCGCCATTGCCTGTTCACACCCCTGCACGCCCGGATCTCCCCTGA
ATAAATGGAGGTCCTGTGATCGTTCCCGCTTTTAGCCAAGGTCTTTACT**GGATCC**

pKp10

CAGCTGTTCTTGCGCGGAAAAGCGCTGGCTATCCCCCATTACCATCATCCTGCGTCAAGGTGGC
GCGGTGATTGTATTCAAAAGGTGAATGTCGTATAACATAGCGC**CTGCAG**AAATGGAGGTCCTGTG
ATCGTTCCCGCTTTTAGCCAAGGTCTTTACT**GGATCC**

Kp11	**CAGCTG**GGCCGCGAAGGTGTCGTATCCAGGGCTAAAGGCTTGTTGTATGAACCGGTGAGTTGCG GTAAATTCCACAACGCTTAACAATTTCACTATTTTGACTCGGGGTGCCCTTCTTCGTTGAAGGCTG AGAAATACCCGTACCACCTGATCTGGATAATGCCAGCGTAGGGAAGTCAGAGACCGCAGGGTCAT TGCTTCTACCTCGTCTGGCGGGAGCAAACTATGCCTGAGCTGTTGAATCCCGCGCCTGTC**TGGA TCC**
pKp11	**CAGCTG**GGCCGCGAAGGTGTCGTATCCAGGGCTAAAGGCTTGTTGTATGAACCGGTGAGTTGCG GTAAATTCCACAACGCTTAACAATTTCACTATTT**CTGCAG**TGGCGGGAGCAAACTATGCCTGAGCT GTTGAATCCCGCGCCTGTCT**GGATCC**

9.6 Homology repair templates for CRISPR/Cas9 plasmids

Table S5: Homology repair templates used for the CRISPR-Cas9 based genome editing of *B. subtilis.* Important sequences are highlighted in different colors according to the following color code: Start codon, stop codon, N-term *ribR*$_{sub}$, C-term *ribR*$_{sub}$, altered PAM sequence, mutated sequence (RR→AA), *ribR*$_{amy}$, His$_6$-tag, *ribD* FMN RS$_{amy}$. Restriction sites are displayed in bold.

HRT-ΔribR

GTCGACTTGCTGCTAAAAATGCGGATGCGATTTTTACCCATTCCAATTCATTAGAAGAGACAAAAGCGT
TTTATGCGGATGTGAAAAGCCGAGCTGCTGATGAAGGGCGTGATCCTTCAAGTGTGCGGATTTTTCCA
GGGATCAGCCCGATTGTGGCAGATACGGAAGAAGAGGCGGAAAAGAAGTATCGTGAATTTGCAGAATT
GATACCGATTGAAAATGCTGTTACTTATTTGGCCCGTTTTTTTGATGATTATGATCTGAGTGTTTACCCGT
TGGATGAGCCATTTCCCGATATTGGCGATGTGGGAAAGAATGCGTTTCAAAGCACAACAGACCGGATT
AAGAGAGAAGCAAAAGCCAGAAATCTGACATTGCGGGAGGTAGCACAGGAAATGGCTTTTCCACGGA
CTCTATTCATCGGAACACCAGAGCGTGTCGCATCCTTAATTGAAACTTGGTTCAACGCTGAGGCGGCG
GATGGGTTTATCGTTGGGTCGGATATACCGGGAACACTTGATGCTTTTGTAGAAAAGGTGATTCCGATT
CTTCAAGAAAGAGGGCTTTATCGTCAAGATTATCGCGGCGGGACATTGCGGGAAAATCTCGGTCTTGG
CATTCCGCAGCATCAATCCGTTTTACATTCATCACATCATTAGGTTTCGTCTGATCGAATGCGGAAGCTG
AGAGAGGAGGCTGACTTTTTTGACGTAGGGAAAGGAGCGGAACATATGTCTTTGGATTATTGGAGAAA
TATAGAAGGCTCCTATCCATATCAGACTACAGGAAATGACATCCTGACGTTGAAAGAGGAGTCTAATCC
CGTAAATCTCTCAACGCTAGAAAAGCAGCTCATCGGCATTCGCCGGCACCTGCACCAATATCCTGAAC
TGTCAAAAGAAGAATTTGAAACAACTGCTTTTATAAAAAAATGCCTTAAAGAAAAGGGGATACAGATTCG
CCCTACTGCTCTAAAAACGGGTGTGTTCGCAGACATAGCAGGGGAGTCAGAAGGTCCGGCGATTGCT
TTGAGGGCTGATATTGACGCCTTGCCAATTGAAGAAAAAACAGGATTGCCTTATGCGTCTAAACATAAA
GGGATCATGCATGCGTGCGGTCATGATTTTCATACGGCAGCGCTTCTTGGTGCGGCCTTTTTATTGAAG
GAAAATCAAGACAGTCTGAAAGGAAAGATTCGTTTATTATTTCAGCCAGCAGAGGAAGCGGGTGCAGG
CGCTACAAAAGTGATAGAGGACGGCCAACTGGATGGCATTGATGCGGTTATTGGCCTTCACAATAAAC
CGGATATCGCGGTTGGGACTGTAGGGTTAAAAACAGGCCCGCTTATGGCTGCTGTTGACCGATTTAAA
GTAGAGATAGAAGGGAAAGGTGCTCATGCAGCATTGCCGCATAA**TCTAGA**

HRT-ΔC-ribR

GTCGACACCCGTTGGATGAGCCATTTCCCGATATTGGCGATGTGGGAAAGAATGCGTTTCAAAGCACA
ACAGACCGGATTAAGAGAGAAGCAAAAGCCAGAAATCTGACATTGCGGGAGGTAGCACAGGAAATGG
CTTTTCCACGGACTCTATTCATCGGAACACCAGAGCGTGTCGCATCCTTAATTGAAACTTGGTTCAACG
CTGAGGCGGCGGATGGGTTTATCGTTGGGTCGGATATACCGGGAACACTTGATGCTTTTGTAGAAAAG
GTGATTCCGATTCTTCAAGAAAGAGGGCTTTATCGTCAAGATTATCGCGGCGGGACATTGCGGGAAAA
TCTCGGTCTTGGCATTCCGCAGCATCAATCCGTTTTACATTCATCACATCATTAGGTTTCGTCTGATCGA
ATGCGGAAGCTGAGAGAGGAGGCTGACTTTTTTGACGATCATTGCCGGTACGGTTGTGAAAGGAAAA
CAATTAGGCAGAAAGCTTGGATTCCCCACGGCAAATGTAGATGCAAAAATACATGGGCTGCGTAATGGA
GTTTATGGGGTTCTGGCGACAGTCAATCATCAATTTCATTTAGGGGTTATGAATATCGGTGTGAAACCGA
CGGTGGGCTCTAACCTTGAAAAGACATTGGAGATTTTTTTGTTTGACTTTCATAGAGACATTTATGGAGA
AAAAATCGAATGCAGCATTCTCGGATAGGGAAAGGAGCGGAACATATGTCTTTGGATTATTGGAGAAAT
ATAGAAGGCTCCTATCCATATCAGACTACAGGAAATGACATCCTGACGTTGAAAGAGGAGTCTAATCCC
GTAAATCTCTCAACGCTAGAAAAGCAGCTCATCGGCATTCGCCGGCACCTGCACCAATATCCTGAACT
GTCAAAAGAAGAATTTGAAACAACTGCTTTTATAAAAAAATGCCTTAAAGAAAAGGGGATACAGATTCGC
CCTACTGCTCTAAAAACGGGTGTGTTCGCAGACATAGCAGGGGAGTCAGAAGGTCCGGCGATTGCTT
TGAGGGCTGATATTGACGCCTTGCCAATTGAAGAAAAAACAGGATTGCCTTATGCGTCTAAACATAAAG
GGATCATGCATGCGTGCGGTCATGATTTTCATACGGCAGCGCTTCTTGGTGCGGCCTTTTTATTGAAGG
AAAATCAAGACAGTCTGAAAGGAAAGATTCGTTTATTATTTCAGCCAGCAGAGGAAGCGGGTGCAGGC
GCTACAAAAGTGATAGAGGACGGCCAACTGGATGGCATTGATGCGGTTATTGGCCTTCACAATAAACC
GGATATCGCGGTTGGGACTGTAGGGTTAAAAACAGGCCCGCTTATGGCTGCTGTTGACCGATTTAAAG
TAGAGATAGAAGGGAAAGGTGCTCATGCAGCATTGCCGCATAA**TCTAGA**

HRT-ΔN-ribR

GTCGACTTGCTGCTAAAAATGCGGATGCGATTTTTACCCATTCCAATTCATTAGAAGAGACAAAAGCGT
TTTATGCGGATGTGAAAAGCCGAGCTGCTGATGAAGGGCGTGATCCTTCAAGTGTGCGGATTTTTCCA
GGGATCAGCCCGATTGTGGCAGATACGGAAGAAGAGGCGGAAAAGAAGTATCGTGAATTTGCAGAATT
GATACCGATTGAAAATGCTGTTACTTATTTGGCCCGTTTTTTTGATGATTATGATCTGAGTGTTTACCCGT
TGGATGAGCCATTTCCCGATATTGGCGATGTGGGAAAGAATGCGTTTCAAAGCACAACAGACCGGATT
AAGAGAGAAGCAAAAGCCAGAAATCTGACATTGCGGGAGGTAGCACAGGAAATGGCTTTTCCACGGA
CTCTATTCATCGGAACACCAGAGCGTGTCGCATCCTTAATTGAAACTTGGTTCAACGCTGAGGCGGCG
GATGGGTTTATCGTTGGGTCGGATATACCGGGAACACTTGATGCTTTTGTAGAAAAGGTGATTCCGATT
CTTCAAGAAAGAGGGCTTTATCGTCAAGATTATCGCGGCGGGACATTGCGGGAAAATCTCGGTCTTGG
CATTCCGCAGCATCAATCCGTTTTACATTCATCACATCATTAGGTTTCGTCTGATCGAATGCGGAAGCTG
AGAGAGGAGGCTGACTTTTTTGACGTTTAAAATTAGAGAAGAAAGAAGGTTTGATTCTTTGGAGTCTTT
AACAAAGCAAATTAAAAAGGATATTTCGTGCGTTGCAAAACGCTTTGAGCTGATTGGGATTATGGCACC
AAACAAAAAAGAAAGCCTTCTTTCCCATCAGGAGTTAAATCTTCCGGATCTCTGCTTTTACAAGAAATGT
AATAACCTATATGGCGTCAACCGAGGCGTATACAATGTCATTGATAACTGGTTTTTTGAGTACGGAATTA
CACAAGTAGCTTACAGGCGCATTTATATTTTATCTTTTTTAAGCTTTTTGAAAGAAGATAATCCGAAAGTT
TCCAGCAAGTATATAAGATTTGGGGCGGGCGGTCTTGCTGATAAATTGAACCGATTTATTTCATCTTATG
TTGAAGAGTCTGAAGAAAATATATTGGGATAGGGAAAGGAGCGGAACATATGTCTTTGGATTATTGGAG
AAATATAGAAGGCTCCTATCCATATCAGACTACAGGAAATGACATCCTGACGTTGAAAGAGGAGTCTAAT
CCCGTAAATCTCTCAACGCTAGAAAAGCAGCTCATCGGCATTCGCCGGCACCTGCACCAATATCCTGA
ACTGTCAAAAGAAGAATTTGAAACAACTGCTTTTATAAAAAAATGCCTTAAAGAAAAGGGGATACAGATT
CGCCCTACTGCTCTAAAAACGGGTGTGTTT**TCTAGA**

HRT-ribR_RR>AA

GTCGACATTCCGATTCTTCAAGAAAGAGGGCTTTATCGTCAAGATTATCGCGGCGGGACATTGCGGGA
AAATCTCGGTCTTGGCATTCCGCAGCATCAATCCGTTTTACATTCATCACATCATTAGGTTTCGTCTGAT
CGAATGCGGAAGCTGAGAGAGGAGGCTGACTTTTTTGACGATCATTGCCGGTACGGTTGTGAAAGGA
AAACAATTAGGCAGAAAGCTTGGATTCCCCACGGCAAATGTAGATGCAAAAATACATGGGCTGCGTAAT
GGAGTTTATGGGGTTCTGGCGACAGTCAATCATCAATTTCATTTAGGGGTTATGAATATCGGTGTGAAA
CCGACGGTGGGCTCTAACCTTGAAAAGACATTGGAGATTTTTTTGTTTGACTTTCATAGAGACATTTATG
GAGAAAAAATCGAATGCAGCATTCTCTTTAAAATTAGAGAAGAAAGAAGGTTTGATTCTTTGGAGTCTTT
AACAAAGCAAATTAAAAAGGATATTTCGTGCGTTGCAAAACGCTTTGAGCTGATTGGGATTATGGCACC
AAACAAAAAAGAAAGCCTTCTTAGTCATCAGGAGTTAAATCTTCCGGATCTCTGCTTTTACAAGAAATGT
AATAACCTATATGGCGTCAACCGAGGCGTATACAATGTCATTGATAACTGGTTTTTTGAGTACGGAATTA
CACAAGTAGCTTACGCAGCGATTTATATTTTATCTTTTTTAAGCTTTTTGAAAGAAGATAATCCGAAAGTT
TCCAGCAAGTATATAAGATTTGGGGCGGGCGGTCTTGCTGATAAATTGAACCGATTTATTTCATCTTATG
TTGAAGAGTCTGAAGAAAATATATTGGGATAGGGAAAGGAGCGGAACATATGTCTTTGGATTATTGGAG
AAATATAGAAGGCTCCTATCCATATCAGACTACAGGAAATGACATCCTGACGTTGAAAGAGGAGTCTAAT
CCCGTAAATCTCTCAACGCTAGAAAAGCAGCTCATCGGCATTCGCCGGCACCTGCACCAATATCCTGA
ACTGTCAAAAGAAGAATTTGAAACAACTGCTTTTATAAAAAAATGCCTTAAAGAAAAGGGGATACAGATT
CGCCCTACTGCTCTAAAAACGGGTGTGTTCGCAGACATAGCAGGGGAGTCAGAAGGTCCGGCGATTG
CTTTGAGGGCTGATATTGACGCCTTGCCAATTGAAGAAAAAACAGGATTGCCTTATGCGTCTAAACATA
AAGGGATCATGCATGCGTGCGGTCATGATTTTCATACGGCAGCGCTTCTTGGTGCGGCCTTTTTATTGA
AGGAAAATCAAGACAGTCTGAAAGGAAAGATTCGTTTATTATTTCAGCCAGCAGAGGAAGCGGGTGCA
GGCGCTACAAAAGTGATAGAGGACGGCCA**TCTAGA**

HRT-ribR$_{amy}$

GTCGACTTGCTGCTAAAAATGCGGATGCGATTTTTACCCATTCCAATTCATTAGAAGAGACAAAAGCGT
TTTATGCGGATGTGAAAAGCCGAGCTGCTGATGAAGGGCGTGATCCTTCAAGTGTGCGGATTTTTCCA
GGGATCAGCCCGATTGTGGCAGATACGGAAGAAGAGGCGGAAAAGAAGTATCGTGAATTTGCAGAATT
GATACCGATTGAAAATGCTGTTACTTATTTGGCCCGTTTTTTTGATGATTATGATCTGAGTGTTTACCCGT
TGGATGAGCCATTTCCCGATATTGGCGATGTGGGAAAGAATGCGTTTCAAAGCACAACAGACCGGATT
AAGAGAGAAGCAAAAGCCAGAAATCTGACATTGCGGGAGGTAGCACAGGAAATGGCTTTTCCACGGA
CTCTATTCATCGGAACACCAGAGCGTGTCGCATCCTTAATTGAAACTTGGTTCAACGCTGAGGCGGCG
GATGGGTTTATCGTTGGGTCGGATATACCGGGAACACTTGATGCTTTTGTAGAAAAGGTGATTCCGATT
CTTCAAGAAAGAGGGCTTTATCGTCAAGATTATCGCGGCGGGACATTGCGGGAAAATCTCGGTCTTGG
CATTCCGCAGCATCAATCCGTTTTACATTCATCACATCATTAGGTTTCGTCTGATCGAATGCGGAAGCTG
AGAGAGGAGGCTGACTTTTATGAAGCATTCAACTGTCCCTTTCCGGGAGAGCCGGTATCTGCACTTGC
CTGAAGTGCGCTTTCTGCATTGGTGCACGAAGCAATACGGCATTAACAAAGGAGTGCTGAACACAATT
GACGGCTGGTTTTATGATGCGGGCATCATTCCCATTCCCGTCAGGCGTCTTTATGTGCTGGCGTTTCT
CGATTTTGCGAAAACGCCGGGACAGAAGGGGAATATCCGATTCGGGCACGGGGGATTGACGAAAAAA
CTGCATGATTTCATGGATATGCAGGAGTGCGCAGCAAAACGCCAGGCTTGAGGAAAGGAGCGGAACA
TATGTCTTTGGATTATTGGAGAAATATAGAAGGCTCCTATCCATATCAGACTACAGGAAATGACATCCTGA

CGTTGAAAGAGGAGTCTAATCCCGTAAATCTCTCAACGCTAGAAAAGCAGCTCATCGGCATTCGCCGG
CACCTGCACCAATATCCTGAACTGTCAAAAGAAGAATTTGAAACAACTGCTTTTATAAAAAAATGCCTTA
AAGAAAAGGGGATACAGATTCGCCCTACTGCTCTAAAAACGGGTGTGTTCGCAGACATAGCAGGGGA
GTCAGAAGGTCCGGCGATTGCTTTGAGGGCTGATATTGACGCCTTGCCAATTGAAGAAAAAACAGGAT
TGCCTTATGCGTCTAAACATAAAGGGATCATGCATGCGTGCGGTCATGATTTTCATACGGCAGCGCTTC
TTGGTGCGGCCTTTTTATTGAAGGAAAATCAAGACAGTCTGAAAGGAAAGATTCGTTTATTATTTCAGCC
AGCAGAGGAAGCGGGTGCAGGCGCTACAAAAGTGATAGAGGACGGCCAACTGGATGGCATTGATGC
GGTTATTGGCCTTCACAATAAACCGGATATCGCGGTTGGGACTGTAGGGTTAAAAACAGGCCCGCTTAT
GGCTGCTGTTGACCGATTTAAAGTAGAGATAGAAGGGAAAGGTGCTCATGCAGCATTGCCGCATAA**TC**
TAGA

HRT-ribR$_{amy}$_RR>AA

GTCGACTTGCTGCTAAAAATGCGGATGCGATTTTTACCCATTCCAATTCATTAGAAGAGACAAAAGCGT
TTTATGCGGATGTGAAAAGCCGAGCTGCTGATGAAGGGCGTGATCCTTCAAGTGTGCGGATTTTTCCA
GGGATCAGCCCGATTGTGGCAGATACGGAAGAAGAGGCGGAAAAGAAGTATCGTGAATTTGCAGAATT
GATACCGATTGAAAATGCTGTTACTTATTTGGCCCGTTTTTTTGATGATTATGATCTGAGTGTTTACCCGT
TGGATGAGCCATTTCCCGATATTGGCGATGTGGGAAAGAATGCGTTTCAAAGCACAACAGACCGGATT
AAGAGAGAAGCAAAAGCCAGAAATCTGACATTGCGGGAGGTAGCACAGGAAATGGCTTTTCCACGGA
CTCTATTCATCGGAACACCAGAGCGTGTCGCATCCTTAATTGAAACTTGGTTCAACGCTGAGGCGGCG
GATGGGTTTATCGTTGGGTCGGATATACCGGGAACACTTGATGCTTTTGTAGAAAAGGTGATTCCGATT
CTTCAAGAAAGAGGGCTTTATCGTCAAGATTATCGCGGCGGGACATTGCGGGAAAATCTCGGTCTTGG
CATTCCGCAGCATCAATCCGTTTTACATTCATCACATCATTAGGTTTCGTCTGATCGAATGCGGAAGCTG
AGAGAGGAGGCTGACTTTTATGAAGCATTCAACTGTCCCTTTCCGGGAGAGCCGGTATCTGCACTTGC
CTGAAGTGCGCTTTCTGCATTGGTGCACGAAGCAATACGGCATTAACAAAGGAGTGCTGAACACAATT
GACGGCTGGTTTTATGATGCGGGCATCATTCCCATTCCCGTCAGGCGTCTTTATGTGCTGGCGTTTCT
CGATTTTGCGAAAACGCCGGGACAGAAGGGGAATATCCGATTCGGGCACGGGGGATTGACGAAAAAA
CTGCATGATTTCATGGATATGCAGGAGTGCGCAGCAAAACGCCAGGCTTGAGGAAAGGAGCGGAACA
TATGTCTTTGGATTATTGGAGAAATATAGAAGGCTCCTATCCATATCAGACTACAGGAAATGACATCCTGA
CGTTGAAAGAGGAGTCTAATCCCGTAAATCTCTCAACGCTAGAAAAGCAGCTCATCGGCATTCGCCGG
CACCTGCACCAATATCCTGAACTGTCAAAAGAAGAATTTGAAACAACTGCTTTTATAAAAAAATGCCTTA
AAGAAAAGGGGATACAGATTCGCCCTACTGCTCTAAAAACGGGTGTGTTCGCAGACATAGCAGGGGA
GTCAGAAGGTCCGGCGATTGCTTTGAGGGCTGATATTGACGCCTTGCCAATTGAAGAAAAAACAGGAT
TGCCTTATGCGTCTAAACATAAAGGGATCATGCATGCGTGCGGTCATGATTTTCATACGGCAGCGCTTC
TTGGTGCGGCCTTTTTATTGAAGGAAAATCAAGACAGTCTGAAAGGAAAGATTCGTTTATTATTTCAGCC
AGCAGAGGAAGCGGGTGCAGGCGCTACAAAAGTGATAGAGGACGGCCAACTGGATGGCATTGATGC
GGTTATTGGCCTTCACAATAAACCGGATATCGCGGTTGGGACTGTAGGGTTAAAAACAGGCCCGCTTAT
GGCTGCTGTTGACCGATTTAAAGTAGAGATAGAAGGGAAAGGTGCTCATGCAGCATTGCCGCATAA**TC**
TAGA

HRT-his$_6$-ribR$_{amy}$

GTCGACTTGCTGCTAAAAATGCGGATGCGATTTTTACCCATTCCAATTCATTAGAAGAGACAAAAGCGT
TTTATGCGGATGTGAAAAGCCGAGCTGCTGATGAAGGGCGTGATCCTTCAAGTGTGCGGATTTTTCCA
GGGATCAGCCCGATTGTGGCAGATACGGAAGAAGAGGCGGAAAAGAAGTATCGTGAATTTGCAGAATT
GATACCGATTGAAAATGCTGTTACTTATTTGGCCCGTTTTTTTGATGATTATGATCTGAGTGTTTACCCGT
TGGATGAGCCATTTCCCGATATTGGCGATGTGGGAAAGAATGCGTTTCAAAGCACAACAGACCGGATT
AAGAGAGAAGCAAAAGCCAGAAATCTGACATTGCGGGAGGTAGCACAGGAAATGGCTTTTCCACGGA
CTCTATTCATCGGAACACCAGAGCGTGTCGCATCCTTAATTGAAACTTGGTTCAACGCTGAGGCGGCG
GATGGGTTTATCGTTGGGTCGGATATACCGGGAACACTTGATGCTTTTGTAGAAAAGGTGATTCCGATT
CTTCAAGAAAGAGGGCTTTATCGTCAAGATTATCGCGGCGGGACATTGCGGGAAAATCTCGGTCTTGG
CATTCCGCAGCATCAATCCGTTTTACATTCATCACATCATTAGGTTTCGTCTGATCGAATGCGGAAGCTG
AGAGAGGAGGCTGACTTTTATGAAGCATTCAACTGTCCCTTTCCGGGAGAGCCGGTATCTGCACTTGC
CTGAAGTGCGCTTTCTGCATTGGTGCACGAAGCAATACGGCATTAACAAAGGAGTGCTGAACACAATT
GACGGCTGGTTTTATGATGCGGGCATCATTCCCATTCCCGTCAGGCGTCTTTATGTGCTGGCGTTTCT
CGATTTTGCGAAAACGCCGGGACAGAAGGGGAATATCCGATTCGGGCACGGGGGATTGACGAAAAAA
CTGCATGATTTCATGGATATGCAGGAGTGCGCAGCAAAACGCCAGGCTCATCACCATCACCATCAGTG
AGGAAAGGAGCGGAACATATGTCTTTGGATTATTGGAGAAATATAGAAGGCTCCTATCCATATCAGACTA
CAGGAAATGACATCCTGACGTTGAAAGAGGAGTCTAATCCCGTAAATCTCTCAACGCTAGAAAAGCAG
CTCATCGGCATTCGCCGGCACCTGCACCAATATCCTGAACTGTCAAAAGAAGAATTTGAAACAACTGCT
TTTATAAAAAAATGCCTTAAAGAAAAGGGGATACAGATTCGCCCTACTGCTCTAAAAACGGGTGTGTTC
GCAGACATAGCAGGGGAGTCAGAAGGTCCGGCGATTGCTTTGAGGGCTGATATTGACGCCTTGCCAA
TTGAAGAAAAAACAGGATTGCCTTATGCGTCTAAACATAAAGGGATCATGCATGCGTGCGGTCATGATT
TTCATACGGCAGCGCTTCTTGGTGCGGCCTTTTTATTGAAGGAAAATCAAGACAGTCTGAAAGGAAAG
ATTCGTTTATTATTTCAGCCAGCAGAGGAAGCGGGTGCAGGCGCTACAAAAGTGATAGAGGACGGCCA
ACTGGATGGCATTGATGCGGTTATTGGCCTTCACAATAAACCGGATATCGCGGTTGGGACTGTAGGGT

TAAAAACAGGCCCGCTTATGGCTGCTGTTGACCGATTTAAAGTAGAGATAGAAGGGAAAGGTGCTCAT
GCAGCATTGCCGCATAA**TCTAGA**

HRT-ribD-RS$_{amy}$

GTCGACGATTCATATTGGCTGGAGGTTTAGAAATGGGAAGAATAAAAACCAAGATTACCATTCTGTTAGT
GCTTTTGCTTTTACTTGCAGGCGGTTATATGTACATAAATGATATTGAGCTGAAGGATGTTCCGACAGCA
ATTGGACAAACCTTGTCCTCGGAAGAAGAGGAATACACCATCCAGGAATATAAAGTGACGAAAATTGAC
GGCTCAGAGTATCATGGAGTAGCAGAAAACGGAACGAAAATCATCTTCAACGGAAAAAAATTAAATCAG
GATTTATCTGATATAAAAGAAGGTGACAAGATTAAGGCTTACTTCAGCAAATCAAAGCGGATCGACGGAT
TAATCAAGGTTGCAAAAGTGAATGATTAAAAAACATCAGTTTTCGGATCGAAGGGTGATGTTTTGTTTTT
CTCAAATTGTAAGTTTATTTCATTGCGTACTTTAAAAAGGATCGCTATAATAACCAATAAGGACAAATGAAT
ATTGATTGTATCCTTCGGGGCTGGGTGAAAATCCCGACCGGCGGTAATAAGGCGCTCCTGCGCTTTAC
AGCCCGTGACCCGTATGCATCTGTATACGGTGGATTCAGTGAAAAGCTGAAGCCGACAGTGAAAGTCT
GGATGGGAGAAGGATGAGAGAAGCTATGCAAAAAATAATCATACTGTATAGTCTTATTTCCTATGGATTAA
AACTGGTAAAGCCCCGAACTGTGTAAACATTCGGGGCTTTTTTGACGCCAAATTGCGTGGAAGAAGGG
AGGGATAACGATGGAAGAGTATTATATGAAGCTGGCCTTAGATCTTGCGAAGCAGGGCGAAGGACAGA
CCGAATCCAATCCGCTCGTCGGCGCTGTTGTCGTAAAGGACGGACAAATTGTCGGAATGGGCGCCCA
TTTAAAATATGGTGAAGCTCATGCAGAAGTTCATGCCATCCATATGGCTGGAGCACATGCAGAGGGTGC
CGACATTTACGTTACACTCGAACCGTGCAGCCATTACGGAAAAACACCGCCATGTGCAGAATTGATTAT
CAACTCTGGTATCAAAAGAGTGTTCGTGGCGATGAGAGATCCTAATCCGCTTGTGGCTGGAAGAGGGA
TCAGCATGATGAAAGAAGCTGGCATTGAGGTAAGGGAAGGCATCCTGGCAGACCAGGCGGAGAGGC
TGAATGAAAAATTTCTGCACTTTATGAGGACAGGCCTTCCGTACGTCACGCTAAAAGCGGCTGCCAGC
CTTGACGGCAAGATAGCTACCAGCACGGGTGACAGCAAATGGAT**TCTAGA**

9.7 Effect of pyrithiamine on the *E. coli thiC* riboswitch in *E. coli* DH5α

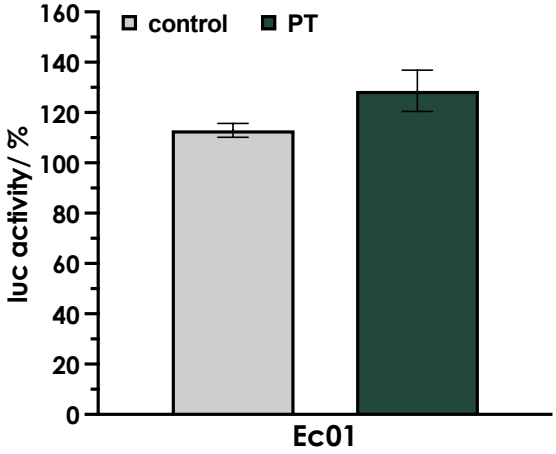

Figure S7: Effect of pyrithiamine on reporter gene activity testing a translational fusion of the *E.coli thiC* riboswitch (Ec01) in *E. coli* DH5α. Luciferase activity (Luc^F) was determined for the thiamine-auxotrophic strain *E*. coli DH5α from M9 pre-cultures that contained 20 nM of thiamine. *E. coli* main cultures for which the Luc^F activity was determined were grown in M9 minimal medium without thiamine and without (control) and with 10 µM of pyrithiamine (PT). Luc^F activity was normalized by the respective *Renilla* luciferase activity and is given as relative activity compared to the control. Cultures were grown in triplicates in a 12-well plate. Depicted are the mean values ± standard deviations of the data obtained from the triplicates.

9.8 Purification of the maltose-binding protein

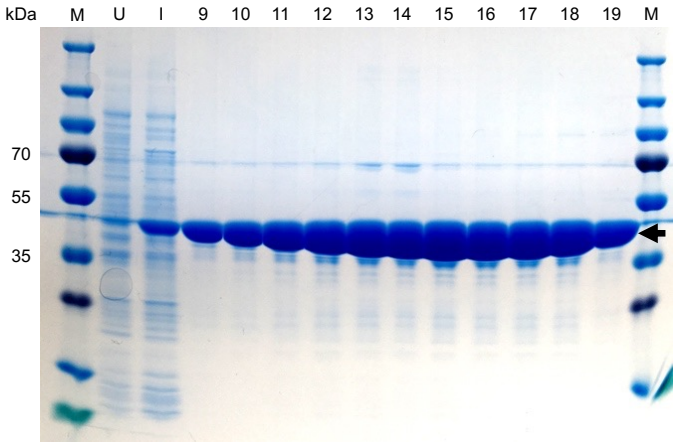

Figure S8: SDS-PAGE analysis of fractions 9-19 from the purification of the maltose-binding protein MBP (control protein). Cultures of *E. coli* ER2325 pMAL-c6T were grown at 37 °C in LB medium and were either kept uninduced (U) or were induced with 0.3 mM of IPTG (I). Cells were harvested 3h after induction. Cell-free extracts were prepared and purified from induced samples with the ÄKTApurifier system. Samples with a total protein amount of 8 µg were applied per lane. A protein ladder (M) was added for size comparison (PageRuler™ Plus Prestained Protein Ladder, Thermo Scientific). The black arrow indicates the position of MBP (45.5 kDa). The gel was stained with Coomassie G-250 dye (PageBlue Protein Staining Solution, Thermo Scientific).

9.9 Alignment of FMN riboswitch sequences from *Bacillus subtilis*, *Bacillus amyloliquefaciens* and *Streptomyces davaonensis*

```
S.davaonensis_ribE-RS           --------AAGCAGCGCACTCCGGGGTCGGTGAAAGTCCGAACCGGCGGTTACAGTCCGC   52
B.subtilis_ribU-RS              AATTTCATATGATCAATCTTCGGGGCAGGGTGAAATTCCCTACCGGCGGTGATGAGCCAA   60
B.subtilis_ribD-RS              --------GATTGTATCCTTCGGGGCAGGGTGGAAATCCCGACCGGCGGTAGTAAAGCAC   52
B.amyloliquefaciens_ribD-RS     -----ATTGATTGTATCCTTCGGGGCTGGGTGAAAATCCCGACCGGCGGTAATAAGGCGC   55
                                          ** ***   **** ** ***  *********       *

S.davaonensis_ribE-RS           GACCCGACCG--------------------CTTCCAGCGGCCGGTTGACCAGGTGAAATTC   93
B.subtilis_ribU-RS              TGGCTCTAAG---CCCGCGAGCTGTCTTTA---------CAGCAGGATTCGGTGAGATTC   108
B.subtilis_ribD-RS              A--TTTGCTTTAGAGCCCGTGACCCGTGTGCATAAGCACGCGGTGGATTCAGTT-TAAGC   109
B.amyloliquefaciens_ribD-RS     TCCTGCGCTTTACAGCCCGTGACCCGTATGCATCTGTATACGGTGGATTCAGTGAAAAGC   115
                                                                *   **    **   * *

S.davaonensis_ribE-RS           CTGGACCGACGGTTAAAGTCCGGATGGGAGGCAGTGCGCGGCGGGCGGGCATTCGTGCGC   153
B.subtilis_ribU-RS              CGGAGCCGACAGTA-CAGTCTGGATGGGAGAAGATGGAGGTTCATAAGCGTTTTGAAATT   167
B.subtilis_ribD-RS              TGAAGCCGACAGTGAAAGTCTGGATGGGAGAAGGATGATGAGCCGCTATGCAAAATGTTT   169
B.amyloliquefaciens_ribD-RS     TGAAGCCGACAGTGAAAGTCTGGATGGGAGAAGGATGAGAGAAGCTATGCAAAAAATAAT   175
                                     ***** **   **** *********

S.davaonensis_ribE-RS           GCCGCCGATGTGAGCTCGTTCCCTCGTGGGACGGGTCCTTCCGGCGTCGTTCC--CGGTG   211
B.subtilis_ribU-RS              GAATTTTTCAAACGTTTCTTTG-CCTAGCCTAATTTTCG-AAACCCCGCTTTTATATATG   225
B.subtilis_ribD-RS              AAAAATGCATAGTGTTATTTCC-TATTGCGTAAAATACCTAAAGCCCCGAATTTTTTATA   228
B.amyloliquefaciens_ribD-RS     CATACTGTATAGTCTTATTTCC-TATGGATTAAAACTGGTAAAGCCCCGAACTGTGTAAA   234
                                        *  **       *               *

S.davaonensis_ribE-RS           CCGCAGTCCGTGTTCTCTGTCGTCATCGACAGCCCCGGAGTCCGTGCCCCTATGAGGCAG   271
B.subtilis_ribU-RS              AAGCGGTTTTTTTATTGGCTGGAAAAGAACCTTTCCGTTTTCGAGTAAGATGTGATCGAA   285
B.subtilis_ribD-RS              AATTCGGGGCTTTTTTGACGGTAAATAAC-------------AAAAGAGG----------   265
B.amyloliquefaciens_ribD-RS     CATTCGGGGCTTTTTTGACGCCAAATTGC-------------GTGGAAGA----------   271
                                     *    * *  *        *

S.davaonensis_ribE-RS           GAGGACCC-GGGAAGTGTTCACCGGAATCGTCGAAG-------    306
B.subtilis_ribU-RS              AAGGAGAGAATGAAGTGAAAGTAAAAAAATTAGTTGTGG----    324
B.subtilis_ribD-RS              ----GGA--GGGAAACAAATGGAAGAGTATTATATGAAGCTGG    302
B.amyloliquefaciens_ribD-RS     ----AGGGAGGGATAACGATGGAAGAATATTATATGAATACGG    310
                                        **           *    *    *
```

Figure S9: Alignment of FMN riboswitch sequences from *B. subtilis*, *B. amyloliquefaciens* and *S. davaonensis.* The alignment was generated using EMBOSS needle **(Madeira *et al.*, 2022)**. Conserved nucleotides are marked with an asterisk.

9.10 Acknowledgements

Finally, I would like to thank all the people who have made this work possible.
First, I want to thank Prof. Matthias Mack for giving me the opportunity to work on these interesting and challenging projects in his group, for all the scientific input and support and for everything I was able to learn during my time in his lab in Mannheim.
I would also like to thank Prof. Matthias Mayer for taking over the supervision of my thesis and Prof. Andres Jäschke for being part of my advisory committee and examination commission. I would like to thank them both for all their support, the fruitful discussions during the committee meetings and all the helpful suggestions. Many thanks also go to Prof. F. Nina Papavasiliou for agreeing to be a member of my examination commission.
Furthermore, a special thanks goes to the Heidelberg Biosciences International Graduate School, namely to Dr. Rolf Lutz, Martina Galvan and Sandra Martini, for providing a great environment for doing a PhD and for a lot of support during these years.
I would also like to thank all my cooperation partners from the JPIAMR EXPLORE project, especially Prof. Ruth Brenk and Dr. Vipul Panchal for the lively exchange about the experiments. Furthermore, I want to thank Prof. Dr. Beatrix Süß for giving me the opportunity to perform the EMSA assays in her lab and Dr. Michael Vockenhuber for his kind support with these experiments.
Of course, I would also like to thank all the members of the MIB lab. A big thank you goes to all our technicians for running the lab and always helping out. Thanks to all the former members of my group, especially to Carmen, Ben and Ahmed, who helped me a lot at the beginning of my time here and who, together with Mischl, made the coffee breaks into a fun time of lively discourse. A big thank you also goes to all the members of the BIC group and all the bachelor and master students from our labs for all the great times and nice activities we had.
Many thanks go to my PhD colleagues, Guoxia, Lars and Johannes for being an awesome lab team and for all the fun we had in- and outside of the lab, and especially to Tanya, with whom I started my PhD journey. She has been a great friend in these past years and I could not have done this without her.
Furthermore, I want to thank all my friends for the great support outside of the lab and for always cheering me up when I needed it. I am very lucky that I can count on them at all times.
I would also like to thank my whole family. My warmest thanks go to my parents and my brother Samuel. They have always been there for me, and I am more than grateful for everything they have done for me to get me to where I am today.
Last but not least, I would like to thank Marco for always being at my side. I cannot thank him enough for always having my back, for celebrating every little success with me, for encouraging me and especially for helping me through every difficult time.
I would like to dedicate this work to Fabian. You always believed in me.